# Functional and molecular characterisation of the uterus and cervix in a mouse model of reproductive ageing

Patel, Rima Mafatlal

*Awarding institution:*
King's College London

# FUNCTIONAL AND MOLECULAR CHARACTERISATION OF THE UTERUS AND CERVIX IN A MOUSE MODEL OF REPRODUCTIVE AGEING

Rima Patel

Division of Women's Health
King's College London
Women's Health Academic Centre KHP
St. Thomas' Hospital
London, UK

A thesis submitted to King's College London for the degree of Doctor of Philosophy in the Women's Health Research

October 2013

## Abstract

**Background:** Advanced maternal age (≥35 years at delivery) is associated with increased rates of operative delivery, stillbirth, and post-term labour induction (Bewley et al., 2009). The physiological causes for such complications remain to be ascertained, although myometrial function has been implicated (Smith et al., 2008, Arrowsmith et al., 2012). To investigate the hypothesis that maternal age directly influences successful parturition, timing of birth and fetal outcome were assessed in a pregnant mouse model at three months (young) vs. eight months (older) of age using infra-red video recording. The impact of maternal age on the function of myometrium and cervix were also examined *ex vivo* using qPCR, isometric tension, immunohistochemistry, and measurement of the enzymatic activities of the mitochondrial electron transport chain complexes.

**Results:** Older pregnant mice compared to three month old mice had significantly longer mean gestation and labour durations ($p<0.001$), as well as reduced litter size ($p<0.01$). Cervical tissues from older mice demonstrated greater distension compared to younger mice ($p<0.05$). However, collagen content and matrix metalloproteinase-2 protein expression were similar in late pregnant cervical tissues from three, five and eight month old mice. Expression of oxytocin receptor and connexin-43 mRNA were significantly reduced in myometrium from eight month vs. three month old mice ($p<0.05$, $p<0.01$ respectively). Spontaneous myometrial contractions were more frequent but of shorter duration in older pregnant mice ($p<0.05$); tissues from these older mice also exhibited reduced contractile response to oxytocin. Mitochondrial copy number was reduced in myometrium from eight month old mice, but there were no age-induced changes to the enzymatic activities of the mitochondrial electron transport chain complexes.

**Conclusions:** In this mouse model of reproductive ageing, gestation and labour duration were prolonged. This is unlikely to be associated with delayed cervical softening. However, the alterations in spontaneous and oxytocin augmented contractions, coupled with a reduction in myometrial mitochondrial copy number in older mice, could potentially result in poorly coordinated myometrial contractions *in-vivo*. This study provided an insight into the reproductive ageing of myometrium in mice.

## Acknowledgements

Firstly, I would like to express my sincere gratitude to Dr. Rachel Tribe for her continued support, and guidance throughout my PhD. I am extremely grateful to her for always taking time out of her busy schedule to provide supervision whenever and wherever was needed. My heartfelt appreciation also goes to my second supervisor, Professor Lucilla Poston, who has always been there to provide direction and expertise throughout the more challenging periods of my PhD. Many of the techniques used for this thesis, were taught by talented scientists outside the Division of Women's Health to whom I owe endless thanks. I would like to start by thanking Dr James Moffat who kindly allowed me to invade his laboratory at St George's University of London for months on end while he patiently taught me histology. Thank you to him for explaining things carefully, and thoroughly and for being such a fabulous teacher. At the same time many thanks to Dr Tanya Shaw for also providing me with essential histology protocols and advice. My deep gratitude goes to both James and Tanya for agreeing for me to use their laboratory equipment and supplies (free of charge). Thank you also to Dr Anthea Rowlerson for offering use of her laboratory for never-ending tissue sectioning. I always appreciated that she would visit the lab to say hello and kindly offer her help.

My deepest appreciation and thanks goes to Dr Luc Demaison and particularly to Dr Evangelia Mourmoura at the Université Joseph Fourier, Grenoble, France for all of their help regarding mitochondrial respiratory chain complex activity assays. I am sincerely in debt to Evangelia for all of her help with teaching me how to perform the assays and helping me to set up every day so that I could get through my samples as quickly as possible. I feel truly honoured to have been able to visit their laboratory, and carry out some of my key PhD experiments with them. Evangelia made me feel very welcome during my visit, and I appreciate her patience with me regarding my minimal French speaking skills. Similarly, special thanks to Dr Afshan Malik and Ania Czajka, as without them I would not have been able to carry out my mitochondrial copy number experiments. Heartfelt thanks for the (unpublished) primer sequences, for the use of equipment in your laboratory, and limitless advice. Thank you also to Paul Seed for his help with complicated statistics, and for trying his best to explain them to me.

I would like to acknowledge all of the funding bodies that have contributed towards my PhD, allowing me to be able to buy consumables, present at international conferences and visit France for a laboratory visit. I feel extremely privileged; many thanks to the Biotechnology and Biological Sciences Research Council (BBSRC), Tommys charity, NIHR Biomedical Research Centre for the early career award, London Vascular Biology Forum, as well as King's College London Graduate School.

Without a doubt, the least favourite experience of my PhD would be the days spent in the BSU having to carry out mass murders. If it had not been for the support of exceptional BSU staff, in particular, Stuart Bradley, and for my dear friends Ksanthi Maragkoudaki-Georgiannakis, and Yosef Mansour, I know I would not have been able to make it this far. Speaking of support, I have been truly blessed to have worked with exceptional postdoctoral scientists namely Dr Hiten Mistry, Dr Laura McCallum and Dr Evonne Chin-Smith. Words cannot describe my gratitude for all that they have taught me and for their continued help, support and guidance. It leaves me to thank the "offcee". To all that I have been lucky enough to share an office with, thank you for the laughs and making work a fun place to be. I would like to express a particular heartfelt thank you to Hiten, Yosef, Ksanthi, May and Funso for getting me through these last few weeks, especially for your help with proof reading. I didn't think that I'd be fortunate enough to make such good friends whilst doing my PhD! Sincere apologies along with thanks go to my friends Krina, Meera, Annika, Roshni, Priya, Anjali, and Sarika for putting up with me over this past year. I am sorry for being distant, and not having the time to talk on the phone, or meet for dinner. Thank you to them all for being so understanding.

Thank you from the bottom of my heart to my family. Mum, Dad, Reena, Jij and my little loves Maahi and Ashni. I don't know where I would be without them all keeping me going. They have been particularly considerate to me over these past stressful months; I don't think I could've coped without their cuddles and constant supply of chocolate and for that I will always be grateful.

I would finally like to say a big thank you to Anish. Without him I wouldn't have been able to stay focused and get through some of my hardest days. Anish would be the person to make me smile after a bad day in the lab or writing my thesis. Not only was he there to provide emotional support, but I will forever be grateful to him for all of his help with my infra –red camera work. Without his assistance to source, buy and wire up the camera system I would never have been able to carry out this important part of my PhD.

***"Hard work and prayers equals success"***

***- Pujya Pramukh Swami Maharaj***

## Declaration

Unless specifically stated in the text, all work described in this thesis is my own, completed under the supervision of Dr Rachel Tribe and Professor Lucilla Poston. The following work was carried out in collaboration with external parties:

- Primer sequences to determine mitochondrial copy number were acquired from Dr Afshan Malik (King's College London, UK).
- Linear regression statistical analyses were performed by Mr Paul Seed, senior lecturer in Medical Statistics (King's College London, UK).
- Enzymatic activities of mitochondrial electron transport chain complexes were determined during a two week visit to Dr Luc Demaison's laboratory (Joseph Fourier University, France).

No part of this thesis has been previously accepted for, or is currently being submitted for another degree.

Rima Patel

October 2013

# Table of Contents

# Table of Figures

# Table of Tables

## Abbreviations

| | |
|---|---|
| ACTH | Adrenocorticotropic hormone |
| ATP | Adenosine-5'-triphosphate |
| BMI | Body mass index |
| CAP | Contractile associated protein |
| Cx43 | Connexin-43 |
| CR | Calorie restriction |
| CXCL1 | Chemokine (C-X-C motif) ligand 1 |
| DF | Dominant follicle |
| DHEA | Dehydroepiandrosterone |
| DHEAS | Dehydroepiandrosterone sulphate |
| DNA | Deoxyribonucleic acid |
| ECM | Extracellular matrix |
| ETC | Electron transport chain |
| FSH | Follicle stimulating hormone |
| GAG | Glycosaminoglycans |
| GnRH | Gonadotropin-releasing hormone |
| HPA | Hypothalamic-pituitary-adrenal |
| IGF | Insulin-like growth factor |
| IL | Interleukin |
| IP3 | Inositol 1,4,5-trisphosphate |
| LH | Luteinising hormone |
| MIP2-α | Macrophage inflammatory protein 2-alpha |
| MIT | Mean integral tension |
| MLCK | Myosin light-chain kinase |
| MLCP | Myosin light-chain phosphatase |
| MR | Magnetic resonance |
| MtDNA | Mitochondrial DNA |

| | |
|---|---|
| Mt/N | Mitochondrial/nuclear ratio |
| mTOR | Mammalian target of rapamycin |
| NF-κβ | Nuclear factor kappa beta |
| NO | Nitric oxide |
| OT | Oxytocin |
| OTR | Oxytocin receptor |
| OXPHOS | Oxidative phosphorylation |
| PBS | Phosphate buffered saline |
| PG | Prostaglandin |
| PIP2 | Phosphatidylinositol 4,5-bisphosphate |
| PLC | Phospholipase C |
| PRA | Progesterone receptor isoform A |
| PRB | Progesterone receptor isoform B |
| PTGS2 | Prostaglandin-endoperoxide synthase 2 |
| PSS | Physiological saline solution |
| qPCR | Quantitative reverse transcription polymerase chain reaction |
| RNA | Ribonucleic acid |
| ROS | Reactive oxygen species |
| SOD | Superoxide dismutase |
| SPARC protein | Secreted protein acidic and rich in cysteine |
| TNF | Tumor necrosis factor |
| TGFβ | Transforming growth factor beta |
| 8-oxoG | 8-oxo-2′deoxyguanosine |

# Chapter 1

## General Introduction

# Chapter 1 : General Introduction

The global increase in life expectancy over recent years has led to an unprecedented rise in the ageing population (Bewley et al., 2009). This in turn has caused a myriad of clinical challenges and a considerable burden on society and healthcare providers. Life expectancy in women has risen from 42 years of age from 1838-54 to 82 years of age in 2006-10 (Table 1.1) and concurrent with this, there has been a trend for women to delay childbirth into their later years of fertility, with women who have babies at the age of 35 years and above being referred to as 'advanced maternal age' mothers (Kirz et al., 1985, Bewley et al., 2009, Bayrampour and Heaman, 2010).

**Table 1.1 Life expectancies at birth for England and Wales between 1838-2035**

| Years | Males | Females |
|---|---|---|
| 1838-54 | 40 | 42 |
| 1901-10 | 49 | 52 |
| 1950-52 | 66 | 72 |
| 1980-90 | 72 | 78 |
| 1991-2000 | 74 | 79 |
| 2001-05 | 76 | 81 |
| 2006-10 | 77 | 82 |
| 2015-25 (estimate) | 81 | 85 |
| 2026-35 (estimate) | 83 | 86 |

Data from the Office for National Statistics for England and Wales (Office for National Statistics for England and Wales, 2011a). Adapted from: Reproductive Ageing (Bewley et al., 2009).

Over recent decades, the average age of primigravid mothers in developed countries has risen steadily, with women (including multiparous women) over the age of 35 comprising a significant proportion of the pregnant population (Bewley et al., 2009). Such trends are reflected by a simultaneous rise in the reported incidence of complications in pregnancy and labour including preeclampsia, gestational diabetes mellitus, miscarriage, stillbirth, preterm labour, post-term inductions, increased Caesarean section and instrumental delivery rates, failure to progress in labour, and postpartum haemorrhage (Gilbert et al., 1999, Ecker et al., 2001, Ziadeh and Yahaya, 2001, Tough et al., 2006, Chan and Lao, 2008, Jahromi and Husseini, 2008, Smith et al., 2008, Bewley et al., 2009, Ludford et al., 2012, Karabulut et al., 2013, Khalil et al., 2013). Although maternal reproductive ageing has been well documented with loss of fertility, risk of multiple births and birth defects (Gindoff and Jewelewicz, 1986, Heffner, 2004, Bewley et al., 2009, Balasch and Gratacos, 2012, Weeg et al., 2012), much less is known about how reproductive ageing impacts on parturition especially that of the first child and in particular, how myometrial and cervical functions may be altered in labour.

Theoretically, there are three potential mechanisms that could explain why advanced maternal age mothers experience complications in the initiation of birth and progression in labour. Firstly, there may be a disruption of the complex maternal-fetal hormonal signalling cascade that is involved in the timing/initiation of labour; secondly, the physiological preparation of the myometrium (the smooth muscle of the uterus) and the cervix for labour could be altered or delayed; and thirdly, the ability of the myometrium to contract may be impaired due to age-related mitochondrial dysfunction.

To explore how these potential mechanisms could be altered in advanced maternal age mothers, an understanding of the biology of ageing is first required.

## 1.1 The Biology of Ageing

Ageing can be broadly described as the universal, intrinsic, progressive and deleterious inevitable biological changes that occur over the course of a lifetime. Questions remain at the most basic level about what triggers ageing in our cells and tissues, why it occurs and which biological processes underlie these age-related changes. More than 300 theories of ageing have been postulated to date and the number is still increasing (Vina et al., 2007). A detailed analysis of all of these theories of ageing is beyond the scope of this thesis, but the interlinking key areas of research within this field will now be discussed, with a particular focus on mitochondrial dysfunction.

### 1.1.1 Ageing and genetic influences

A fundamental focus of ageing research has been on the identification of genes, which may control or contribute to longevity. Most longevity genes identified to date influence one of the following cellular pathways: insulin/IGF-1, sirtuins, or mammalian target of rapamycin (mTOR). Friedman and Johnson (1988) discovered the first gene shown to limit lifespan in the nematode (worm) *Caenorhabditis elegans*, which they named age-1 (Friedman and Johnson, 1988). Further investigation revealed that when the activity of the age-1 gene was silenced, the insulin/IGF-1 pathway activity decreased and prolonged lifespan in *Caenorhabditis elegans* (Dorman et al., 1995, Tissenbaum and Ruvkun, 1998). The sirtuin pathway is another significant area of interest in ageing research. Sirtuin genes are present in all species and are involved in the regulation of metabolism, transcription, inflammation, apoptosis and mitochondrial biogenesis in the cell (Horio et al., 2011). Kaeberlein *et al*., (1999) confirmed that inserting an additional copy of the sirtuin gene, Sir2, increased the lifespan of *Saccharomyces cerevisiae* (yeast) (Kaeberlein et al., 1999).

The mTOR pathway is considered to regulate cell growth, proliferation, metabolism and survival (Johnson et al., 2013). The pathway has been linked to ageing of *Saccharomyces cerevisiae, Caenorhabditis elegans*, *Drosophila melanogaster* (flies), and mice (Powers et al., 2006, Jia et al., 2004, Kapahi et al., 2004, Harrison et al., 2009). It is commonly accepted that inhibiting the mTOR pathway in mice genetically, or pharmacologically using rapamycin, leads to increased longevity (National Institute on Aging, 2011).

Genetic ageing is also linked to the accumulation of genetic damage throughout life (López-Otín et al., 2013). The stability and integrity of DNA are continuously challenged by exogenous chemical, physical and biological agents as well as endogenous threats including DNA replication errors, spontaneous hydrolytic reactions, and reactive oxygen species (Hoeijmakers, 2009). Age-related genetic impairments include point mutations, translocations, chromosomal gains and losses, telomere shortening, and DNA copy number variation. To minimise these insults, organisms have evolved a complex network of DNA repair mechanisms that are collectively capable of dealing with most of the damage inflicted to nuclear DNA (Lord and Ashworth, 2012).

### *Telomere shortening*

Telomeres are regions of repetitive nucleotide structures located at the ends of linear eukaryotic chromosomes (Shawi and Autexier, 2008); they do not encode any proteins but instead protect the protein-encoding part of the DNA. Telomeres are most susceptible to the accumulation of DNA damage with age (Blackburn et al., 2006). During cell division, telomeres become shorter and in most cells, the telomeres eventually reach a critical length when they can no longer protect the cell's DNA. In most cells, telomere length cannot be restored. Extreme telomere shortening triggers one of the following responses: the cell stops replicating and becomes senescent; the cell stops replicating and apoptosis occurs, or the cell continues to proliferate. Telomere exhaustion explains the limited proliferative capacity of some types of *in vitro* cultured cells, as summarised by the Hayflick limit (replicative senescence) (Hayflick and Moorhead, 1961). Telomeres are bound by a characteristic multi-protein complex known as shelterin (Palm and de Lange, 2008). A central function of shelterin is to prevent the access of DNA repair proteins to the telomeres; otherwise, telomeres would be ‘‘repaired’’ as DNA breaks leading to chromosome fusions. Due to their restricted DNA repair, DNA damage at telomeres is particularly persistent and highly efficient in inducing cellular senescence and/or apoptosis (Fumagalli et al., 2012). In particular cells types, such as oocytes, the enzyme telomerase is able to restore telomeres to the ends of chromosomes. However, most mammalian somatic cells do not express telomerase. This telomere lengthening ensures that cells can continue to safely divide and multiply. Telomerase has been shown to be activated in most immortal cancer cells, since telomeres do not shorten when cancer cells divide (López-Otín et al., 2013).

Telomere shortening is observed during normal ageing, both in humans and mice (Blasco, 2007). The importance of telomere shortening is highlighted by genetically altered mice with shortened or lengthened telomeres that exhibit decreased or increased lifespans respectively (Armanios et al., 2009, Herrera et al., 1999, Tomas-Loba et al., 2008). Recent evidence also indicates that ageing can be reversed by telomerase activation. In particular, the premature ageing of telomerase-deficient mice can be reversed when telomerase is genetically reactivated in these aged mice (Jaskelioff et al., 2011). In humans, recent meta-analyses have reinforced the existence of a strong correlation between short telomeres and mortality risk, particularly at younger ages (Boonekamp et al., 2013). These observations have led to the proposal that telomere length is a biomarker of ageing.

### 1.1.2 Ageing and alterations in intercellular pathways

Ageing induces changes to intercellular communication, inclusive of endocrine, neuroendocrine and neuronal pathways (Russell and Kahn, 2007, Laplante and Sabatini, 2012, Rando and Chang, 2012, Zhang et al., 2013). Consequently, signalling cascades such as the renin-angiotensin-aldosterone, adrenergic and insulin-IGF1 pathways tend to be deregulated with increasing age as the incidence of inflammatory reactions become more frequent and immunity against pathogens declines.

### *Inflammation*

The immune system declines in reliability and efficiency as mammals age, resulting in greater susceptibility to infectious disease. These changes are further multiplied by reduced responsiveness and impaired communication between all cells of the immune system. The overall cellular exhaustion of the immune system with age is termed “immunosenescence” (Goronzy and Weyand, 2013). A large part of the ageing phenotype, including immunosenescence, is explained by an imbalance between inflammatory and anti-inflammatory signal networks, which results in the low grade, chronic pro-inflammatory status which accompanies ageing in mammals, termed “inflammaging” (Franceschi et al., 2007). “Inflammaging” is believed to be a consequence of cumulative lifetime exposure to antigenic load caused by both clinical and subclinical infections as well as exposure to non-infectious antigens (Baylis et al., 2013). The resultant inflammatory response, tissue damage, and production of reactive oxygen species that cause oxidative damage, trigger the secretion of additional proinflammatory cytokines from the innate immune system and also from the acquired immune response. This subsequently results in the failure of an ever more dysfunctional immune system (Salminen et al., 2012, Baylis et al., 2013).

All of these contribute to drive the immune system in favour of a chronic proinflammatory state where pathophysiological changes, tissue injury and healing occur simultaneously; production of IL-1β, tumor necrosis factor, and interferons are elevated and irreversible molecular and cellular damage that is not clinically evident gradually accumulates over decades (Baylis et al., 2013). “Inflammaging” is a complex cycle of progressive negative impact on the immune system, as summarised in Figure 1.1.

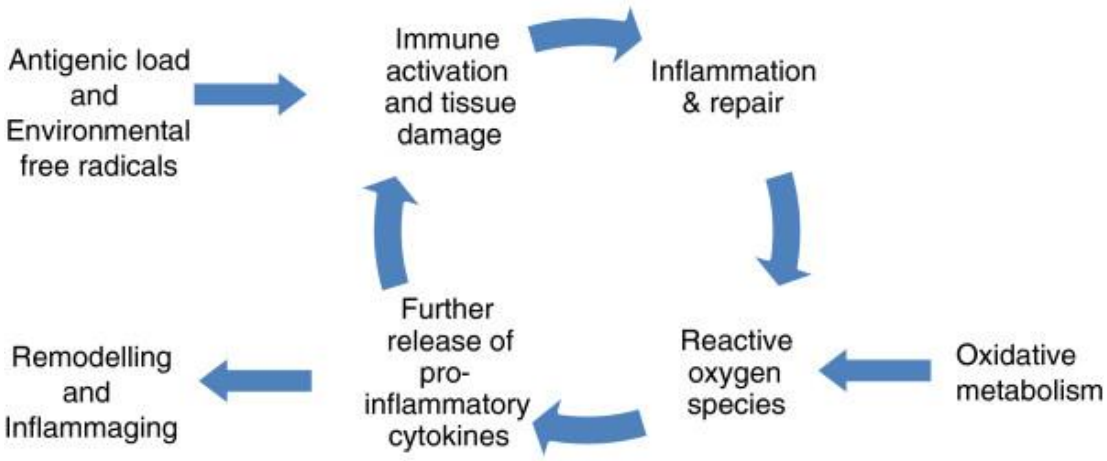


**Figure 1.1 The cycle of "inflammation"**

"Inflammaging" is a consequence of multiple contributors, leading to a chronic pro-inflammatory state. Figure from: Understanding how we age: insights into Inflammaging (Baylis et al., 2013).

Ageing studies have emphasised over activation of the NF-κB pathway as one of the key transcriptional signatures of "inflammaging". Genetic and pharmacological inhibition of NF-κB signalling has been shown to prevent age-associated features in different mouse models of ageing (Osorio et al., 2012, Tilstra et al., 2012). A recent study by Zhang *et al*. (2013) also highlights a link between inflammation and ageing. Inflammatory and stress responses activate NF-κB in the hypothalamus which triggers a signalling pathway that results in reduced production of gonadotropin-releasing hormone (GnRH) by neurons. This GnRH decline may contribute to age-related changes such as muscle weakness, bone fragility, skin atrophy, and diminished neurogenesis. Consistently, GnRH treatment in mice has been shown to prevent age-impaired neurogenesis and slow down ageing development (Zhang et al., 2013). These findings suggest that the hypothalamus may modulate systemic ageing by integrating NF-κB-driven inflammatory responses with GnRH-mediated neuroendocrine effects (López-Otín et al., 2013).

Anti-inflammaging is a mechanism considered to stabilise the “inflammaging” process by increasing blood cortisol concentrations. Cortisol is secreted via the activation of the hypothalamic-pituitary-adrenal (HPA) axis (Goncharova, 2013), and is considered to be an immunosuppressant. Neuronal cells within the HPA axis contain multiple cytokine receptors, particularly for IL-1, IL-6 and TNF and it has been demonstrated that injection of IL-6 or TNF in humans induces a marked upregulation in HPA axis. Therefore, a predictable physiological response to “inflammaging” is an elevation in the concentration of blood cortisol, which may also have a negative response of inducing systemic immunosuppression (Straub et al., 2000, Giunta, 2008, Baylis et al., 2013).

Dehydroepiandrosterone (DHEA) and its sulphated precursor, DHEA sulphate (DHEAS), have opposing actions to cortisol and may provide protection from the negative effects of anti-inflammaging. DHEA and DHEAS are mainly secreted from the adrenal cortex and in smaller amounts from the testis and ovary, where both are later converted to sex steroids; they account for 30% to 50% of testosterone in men and 100% of oestrogen in postmenopausal women. Like cortisol, DHEAS is also secreted in response to ACTH. Blood DHEAS concentrations reach a maximum level in early adulthood and subsequently decline with age to approximately 10 to 20% of maximal concentration levels by 70 years (Labrie, 2010). Phillips *et al.,* (2010) have described an immuno-modulating role for DHEAS; they proposed that low concentrations are associated with chronic inflammatory conditions and counteracts the effects of cortisol via glucocorticoid receptor antagonism. Further, DHEAS may directly inhibit glucocorticoid receptor production (Phillips et al., 2010, Baylis et al., 2013).

In summary, cortisol causes immune suppression and is increased in concentration with age. DHEA(S) is immune modulating, antagonises the effects of cortisol, and its concentration declines with age. Therefore, when considering the effects of the HPA axis on inflammaging, the ratio of cortisol to DHEAS is highly important.

### 1.1.3 Influence of environmental factors on ageing mechanisms

There have been numerous studies that examine the impact of the environment and lifestyle on the control of ageing. For example, exercise-induced stress has been linked to an apparent increase in life span (Marton et al., 2010, Sanchis-Gomar et al., 2011, Corbi et al., 2012). Similarly, life span is considered to be regulated by environmental conditions that may impact on circadian rhythms (Froy, 2011). However, the best-documented environmental/lifestyle theory related to ageing is that calorie/dietary restriction may prolong life span.

#### *Calorie Restriction*

Calorie restriction (CR) can extend the average and maximum life span and delay the onset of age-associated changes in many organisms. It is commonly defined by at least a 10-30 % decrease in calorie consumption compared to a regular calorific intake with a balanced amount of protein, fat, vitamins and minerals (National Institute on Aging, 2011). McCay *et al*., (1935) noted that restriction of intake by 40% in laboratory rats from the age of weaning dramatically extended lifespan (McCay et al., 1989). Further work confirming the success of calorie-restricted longevity in a wide range of other species has accumulated over the last decade.

Model organisms used to confirm calorie-restricted longevity include *Saccharomyces cerevisiae* (Fabrizio and Longo, 2007), *Caenorhabditis elegans* (Klass, 1977, Yuan et al., 2012), *Drosophila melanogaster* (Bross et al., 2005, Burger et al., 2010, Zeng et al., 2011), some but not all strains of mice (Weindruch, 1996), dogs (Lawler et al., 2008, Richards et al., 2013) and non-human primates (Kemnitz, 2011, Mattison et al., 2012).

Two prospective investigations designed to evaluate the effects of CR on general physiology, health, and lifespan in non-human primates began nearly 25 years ago and are still on going. The first study is being conducted by the National Institute on Aging of the National Institutes of Health (USA) and the other by the University of Wisconsin, through funding from the National Institute on Aging. These studies began in 1987 and 1989 respectively. Findings to date from these investigations have confirmed that CR is associated with an extension in lifespan of rhesus monkeys. Monkeys exhibited reduced body fat, slower rate of age-related muscle loss, and improved insulin sensitivity and glucose tolerance. The incidence of cardiovascular disease, type 2 diabetes mellitus and endometriosis were lower and there was no apparent adverse effect on bone health or on total energy expenditure. In addition, there are no reports of deleterious effects of CR on reproductive endpoints (Kemnitz, 2011).

Despite its apparent widespread acceptance, CR does not lengthen lifespan in all animal models as genetic influences seem to play a key role in the success of calorie-restricted longevity. In studies of wild mice, CR did not have any overall effect on lifespan; rather they showed higher mortality in CR wild mice compared to laboratory mice early in life. This may be due to differences in the genetic background of the wild mice (Harper et al., 2006). To attempt to answer the ultimate question of whether CR can influence human longevity, the Comprehensive Assessment of Long-Term Effects of Reducing Calorie Intake (CALERIE Phase1)

study was setup in 2002. Participants of this study after the first year on CR, had lowered their fasting glucose, total cholesterol, core body temperature, body weight, and fat. At the cellular level, they demonstrated improved mitochondrial function and reduced DNA damage (Fontana et al., 2010, National Institute on Aging, 2011).

In addition, many studies have focused on identifying the mechanisms and pathways by which CR works. CR is suggested to counteract age-associated changes by modulating the mTOR signalling pathway, IGF1/insulin signalling, adiponectin expression, DNA methylation, histone acetylation and deacetylation and reducing free radical production from the mitochondrial electron transport chain (Finley and Haigis, 2009, Fontana et al., 2010, Ribaric, 2012). Increased understanding of these pathways has contributed to the development of two drugs that may mimic effects of CR; namely resveratrol and rapamycin. Resveratrol (a natural phenol known to have antioxidant and anti-inflammatory properties) activates the sirtuin pathway and has been shown to increase the lifespan of *Saccharomyces cerevisiae*, *Caenorhabditis elegans, Drosophila melanogaster* and fish (Baur, 2010, Bass et al., 2007, Gualdoni et al., 2013). In mice, resveratrol appeared to diminish the negative effects of high fat and high calorie diet-induced disease and has been shown to prevent age-related decline in heart function. However, the compound did not have an impact on the overall survival or maximum lifespan of mice (Baur, 2010). Rapamycin acts on the mTOR pathway and its main clinical use is as an immunosuppressant. However, rapamycin has been shown to extend the median and maximum lifespan of mice, likely by inhibiting the mTOR pathway. Rapamycin exerted positive effects even when fed to the mice at very old age (600 days old), suggesting that an intervention started later in life may still be able to increase longevity (Harrison et al., 2009).

These examples of CR mimicking drugs highlight that the mechanisms and pathways underlying CR are key to the progression of future healthy ageing therapies. It is likely that control of the ageing process via calorie restriction works through a combination of the mechanisms listed earlier, and others yet to be identified. However, the mechanisms and pathways of CR mimicking drugs are yet to be confirmed in humans, and although model organisms have provided some insight they cannot be extrapolated directly to humans. Model organisms such as *Caenorhabditis elegans and Drosophila melanogaster*, are commonly used since they are well established, and a great proportion of human disease-causing genes are believed to have a functional homolog in such organisms (Pandey and Nichols, 2011). However, limitations of these models include the absence of some human molecular pathways, lack of a sophisticated immune system, and absence or structural differences in key organs such as the heart preventing them to model the complete physiology of humans (Kaletta and Hengartner, 2006). The most important drawback of such model organisms in relation to human ageing would be that all known experimental models have a considerably shorter life span than humans, for example, *Caenorhabditis elegans* has an extremely rapid life cycle of approximately four days (Kaletta and Hengartner, 2006). Therefore, the ageing processes between humans and model organisms are undoubtedly different.

### 1.1.4 Mitochondrial dysfunction

Whilst the above mechanisms have been implicated in ageing, one of the major foci of this thesis has been mitochondrial dysfunction, which is discussed here in more detail. The role of mitochondrial reactive oxygen species (ROS) generation and subsequent mitochondrial DNA (mtDNA) mutations have been of particular interest in the field of ageing. Mitochondria are double-membrane organelles located in the cytosol of most eukaryotic cells. They are responsible for maintaining cellular energy balance, specifically by carrying out oxidative phosphorylation (OXPHOS) energy production to produce adenosine-5'-triphosphate (ATP) (Malik and Czajka, 2012).

ROS are produced by various pathways of aerobic metabolism, however the major source of their production is in mitochondria (Van Remmen and Richardson, 2001) on the basis that more than 90% of the oxygen used by aerobic cells is metabolised in mitochondria by the electron transport chain (ETC) (Sastre et al., 2000, Van Remmen and Richardson, 2001). The generation of mitochondrial ROS is a normal consequence of OXPHOS, an essential process of mitochondria, which transfer electrons from nicotinamide adenine dinucleotide (NADH) or succinate to a series of electron carriers in order to generate ATP. The substrates NADH and succinate deliver electrons to the ETC, which is composed of four complexes (I, II, III and IV) that transfer electrons in a stepwise manner to finally reduce oxygen, forming water. Three of the four complexes (I, III and IV) couple the electron transfer to vectorial proton translocation outside the matrix space. Due to the low proton conductance of the inner mitochondrial membrane, protons accumulate and create an electrochemical gradient across the inner mitochondrial membrane. This osmotic energy is used to drive ATP synthesis as the protons re-enter the mitochondrial matrix through ATP synthase (Mitchell, 1961, Balaban et al., 2005, Larsson, 2010, Lagouge and Larsson, 2013).

At several sites along the ETC, electrons derived from NADH or succinate oxidation may escape and react with oxygen or other electron acceptors to generate free radicals. Complexes I and III are predicted to be the major sites for ROS production (Chance et al., 1979, Lee and Wei, 2007, Rigoulet et al., 2011). The reduction of oxygen by one electron generates the superoxide anion ($O_2^-$), which can then be further reduced to the hydroxyl radical ($OH^-$) and hydrogen peroxide ($H_2O_2$) (Murphy, 2009). These ROS can damage lipids, proteins and DNA. However, the cell is equipped with a variety of defence mechanisms to scavenge ROS. Catalysed by two intramitochondrial superoxide dismutase (SOD), Cu–Zn SOD (SOD1) and MnSOD (SOD2), the superoxide radical is converted to hydrogen peroxide ($H_2O_2$), which can then be transformed into water by catalase or glutathione peroxidase. Cells also contain non-enzymatic ROS scavengers such as ascorbate, flavonoids, carotenoids and glutathione, which may all contribute to the inactivation of otherwise damaging ROS. This low level of ROS production is an unavoidable by-product of ETC function, and therefore mitochondria are the major source of ROS in eukaryotic cells (Chen et al., 2003, Chan, 2006).

***Mitochondrial free radical theory***

In 1956, Denham Harman first proposed the free radical theory of ageing (Harman, 1956). The basis of this theory is that the production and accumulation of intracellular ROS over time has a damaging effect on numerous cellular components, contributing to the decline in physiological function of tissues with age. Since the discovery of the SOD enzymes in 1969, it became widely accepted that enzymatic scavenging systems have evolved to clear superoxide and other types of ROS (McCord and Fridovich, 1969). As explained above, the mitochondrial respiratory chain is a principal site of ROS production in cells and it has therefore

been proposed that mitochondria themselves are the prime targets for oxidative damage. This understanding has led to a modification of Harman's free radical theory into the mitochondrial free radical theory of ageing (Harman, 1972). The mitochondrial theory of ageing proposes that ageing is a consequence of mitochondrial ROS accumulation, which in turn causes progressive damage to mtDNA and other mitochondrial constituents during an individual's lifetime. Cumulative mtDNA mutations result in dysfunction of the mitochondrial respiratory chain, causing increased ROS production in mitochondria and subsequently more mtDNA mutations. This vicious cycle has been proposed to account for an increase in oxidative damage during ageing, which leads to the progressive decline of cellular and tissue functions as a result of an insufficient supply of energy and/or increased susceptibility to apoptosis (Lee and Wei, 2007, Lagouge and Larsson, 2013). This theory has provided a stable framework into the research of mitochondrial function and ageing; however, it has been extensively debated since there is a lack of conclusive experimental evidence to support it. New theories, like the one recently described by Hekimi *et al.* (2011) predict that mitochondrial ROS play a subtler role in ageing.

It is believed that ROS generation is not a direct cause of ageing, but rather represents a stress signal, activating compensatory homeostatic responses in response to age-dependent damage. As chronological age advances, cellular stress and damage increase and the numbers of ROS rise in parallel in an attempt to maintain survival. However, beyond a certain threshold, the increase ROS ceases to be homeostatic and eventually exaggerate, rather than alleviate, the age-associated damage. This new outlook on the mitochondrial free radical theory of ageing may help to balance the conflicting evidence regarding the effects of ROS on ageing (Hekimi et al., 2011, López-Otín et al., 2013).

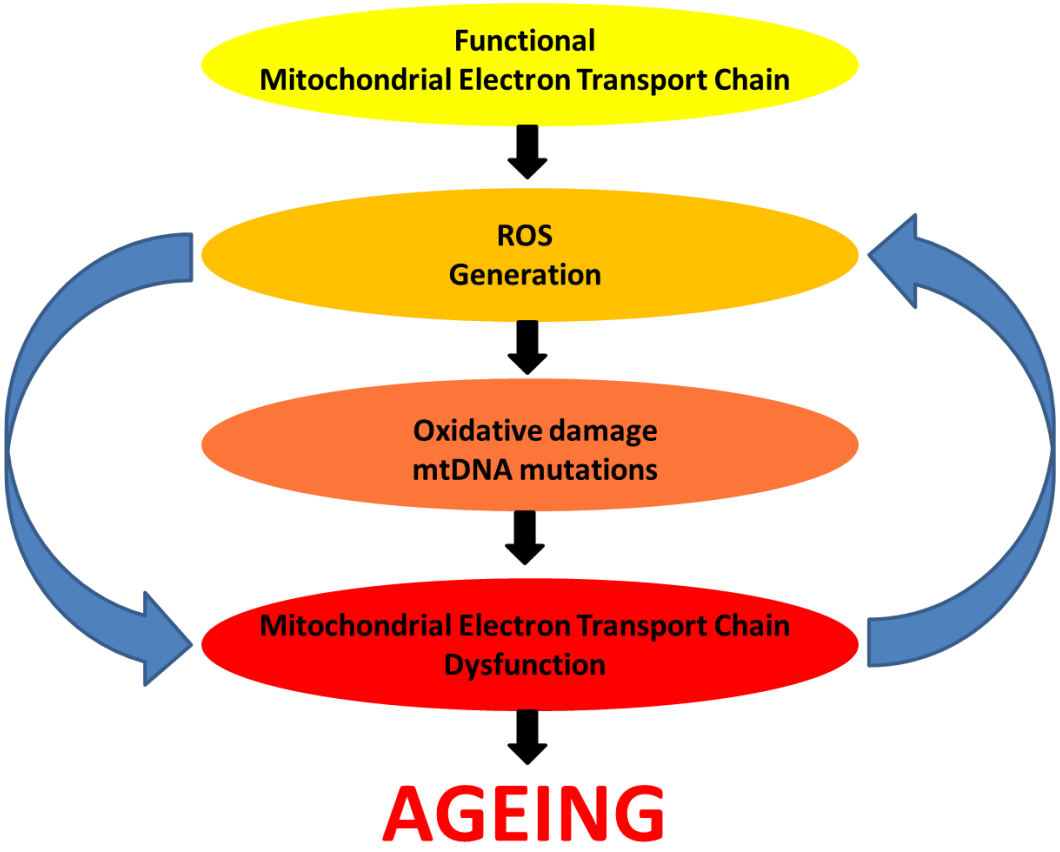


**Figure 1.2 The vicious cycle of the mitochondrial free radical theory of ageing**
Reactive oxygen species are normal by-products of the mitochondrial electron transport chain. ROS progressively damage the components of mitochondria, inducing the dysfunction of the electron transport chain (oxidative phosphorylation) and increased ROS production through a vicious cycle, ultimately leading to cellular dysfunction and ageing. Adapted from: The role of mitochondrial DNA mutations and free radicals in disease and ageing (Lagouge and Larsson, 2013).

### *Accumulation of mtDNA mutations with age*

Mutated mtDNA have been demonstrated to accumulate with age, this can be explained by two principles: replication errors and unrepaired damage. It has been suggested that the considerable mtDNA replication occurring during embryogenesis will result in replication errors due to the inherent error rate of the mtDNA polymerase (Larsson, 2010, Lagouge and Larsson, 2013). The mtDNA mutations formed during embryogenesis are then exposed to segregation and clonal expansion in postnatal life. Secondly, an alternative theory is that accumulated damage, for example caused by ROS, will overpower the repair machinery and result in accumulation of mtDNA mutations. There are mechanisms to maintain mtDNA integrity, such as base excision repair, but the number of available repair systems seems to be much more limited in mitochondria than in the nucleus. It should be highlighted that mtDNA is not unprotected but rather packaged into protein–mtDNA aggregates named nucleoids (Kukat et al., 2011). This is likely to physically protect mtDNA from chemical damage (Lagouge and Larsson, 2013). The mechanisms that impair the efficiency of the repair machinery with ageing remain unclear, but a decline in the mitochondrial import capacity with age could be one such mechanism. For example, it is considered that 8-oxo-2′deoxyguanosine (8-oxoG) is one of the most abundant oxidative lesions that accumulate in mtDNA over time. Of interest, it has been reported that accumulation of 8-oxoG in mtDNA occurs with age possibly because OGG1, a DNA glycosylase enzyme involved in base excision repair of 8-oxoG, accumulates in an uncontrolled manner in the mitochondrial intermembrane space and fails to be imported inside the mitochondrial matrix (Lagouge and Larsson, 2013).

Numerous studies have been published in which the level of mtDNA mutation accumulation has been correlated to life span. One such study by Barja and Herrero (2000) hypothesised that if oxidative damage to mtDNA is involved in ageing, long-lived animals which age slowly should show lower levels of mtDNA damage markers in comparison to short-lived animals. Levels of 8-oxodG were compared to deoxyguanosine (control for oxidative damage) using high performance liquid chromatography in the mtDNA and nuclear DNA from heart and brain samples of six mammalian species ranging in maximum life span from 3.5 to 46 years (Figure 1.3). Significantly higher 8-oxodG/dG values were found in mtDNA than in nuclear DNA in all the species studied in both tissues. The results support the hypothesis that mitochondrial free radicals cause damage to mtDNA in a way related to the ageing rate of each species, and provide evidence of a causative link between mtDNA mutations and induction of the ageing phenotype (Barja and Herrero, 2000).

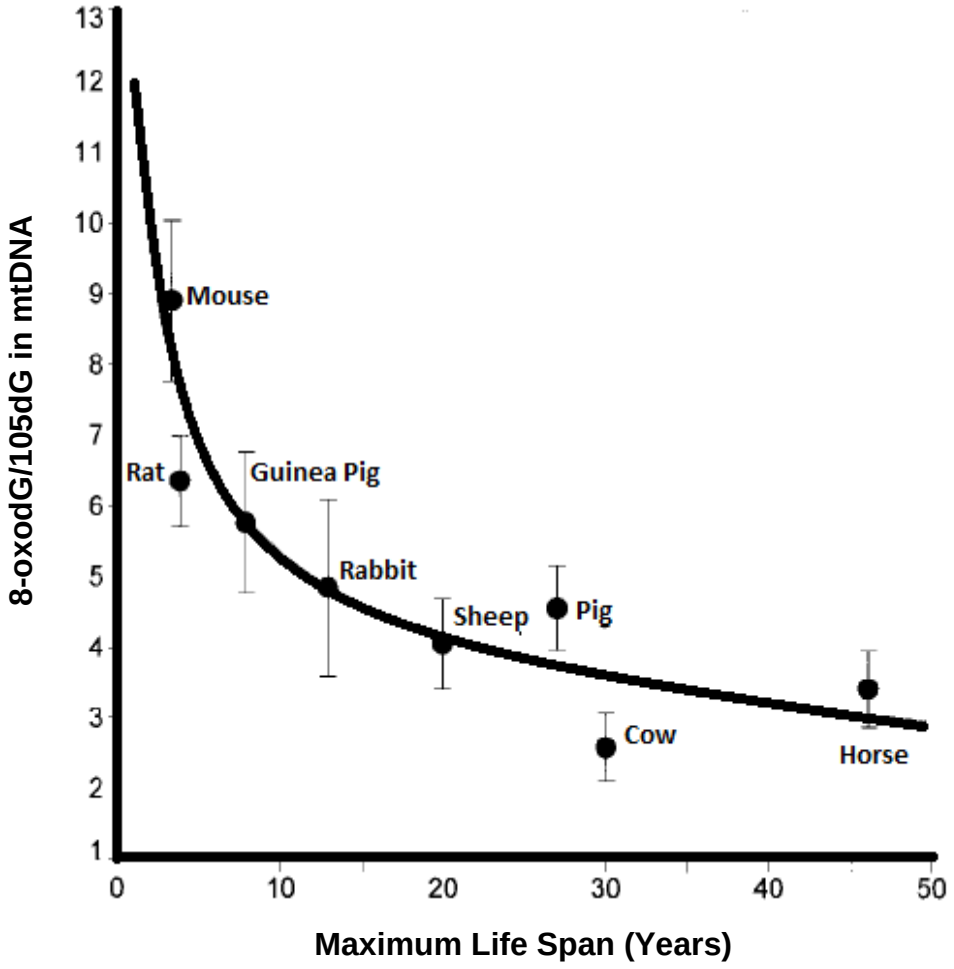


**Figure 1.3 Inverse correlation between 8-oxodG/105dG in heart mitochondrial DNA (mtDNA) and maximum life span in eight mammalian species.**
8-oxodG/105dG values were plotted as a function of maximum life span, and data were fitted to the power function $y = a \cdot x^b$, where b is the scaling exponent used to model the curve, y is 8-oxodG in mtDNA and x is maximum life span ($r = -0.92$, $P<0.001$). Values are means ± SEM. The number of animals per species was eight mice and rats, six guinea pigs and pigs, and seven rabbits, sheep, cows, and horses. Figure from: Oxidative damage to mitochondrial DNA is inversely related to maximum life span in the heart and brain of mammals (Barja and Herrero, 2000).

### *Mitochondrial OXPHOS Function Declines with Age*

Mitochondrial oxidative phosphorylation performance has been shown to decline with age. There is a reported age-related decrease in mitochondrial membrane potential and an increase in proton leakage of the ETC in tissues of old animals and humans. Given that the mitochondrial membrane potential is the driving force for OXPHOS, these were found to correlate with reduced ATP synthesis in these tissues (Harper et al., 1998, Sastre et al., 2000, Short et al., 2005, Lee and Wei, 2007). Acute oxidative stress causes inhibition of mitochondrial respiration, which affects the mitochondrial membrane potential. Mitochondrial morphology is important because changes in the ultrastructure of mitochondria can modulate their function. Enlargement, matrix vacuolisation and altered cristae have been found in mitochondria from old animals by electron microscopy and flow cytometry. Alterations of mitochondrial cristae in old mitochondria may be responsible for the age-related impairment in mitochondrial membrane potential (Sastre et al., 2000). Acute oxidative stress is well known to cause mitochondrial swelling. Therefore, age-associated chronic oxidative stress may be the cause, at least in part, of mitochondrial swelling seen with age (Kumaran et al., 2005, Yasuda et al., 2006).

Bioenergetic studies of humans and animals indicate that the respiratory function of mitochondria declines in ageing, post-mitotic tissues. The electron transport activities of respiratory enzyme complexes gradually decline with age in the brain, skeletal muscle and liver of normal human subjects (Cooper et al., 1992, Ojaimi et al., 1999, Yen et al., 1989, Muller et al., 2010, Short et al., 2005). Similar changes have been reported in various tissues including brain, heart and skeletal muscle of experimental animals (Torii et al., 1992, Sugiyama et al., 1993, Takasawa et al., 1993, Kwong and Sohal, 2000).

Lin *et al*. (2000) showed that bladders from aged rats (24 months old) fatigued faster than bladders from young rats (3 months old) following repeated contractions induced by electrostimulation. This correlated with a reduction in the mitochondrial enzyme activity (indicative of mitochondrial dysfunction) in bladder tissues from the older rats resulting in a lower energy-production capability, which might explain some of the voiding dysfunctions found in the elderly (Lin et al., 2000). In addition to the age-related decline in the activities of respiratory chain enzyme complexes, the respiratory control ratio, OXPHOS efficiency, and ATP synthesis of mitochondria all decline to varying degrees with age in human and animal tissues (Yen et al., 1989, Lee and Wei, 2007). The deterioration in mitochondrial respiratory function can result in lower ATP production and greater ROS generation in aged tissues, which provides evidence to support the mitochondrial free radical theory of ageing.

To summarise, chronological age progression is associated with a marked decline in mitochondrial function, characterised by an increase in mtDNA mutations, abnormal mitochondrial cristae structures and free radical production coupled with a decrease in oxidative phosphorylation and ATP synthesis (Bossy-Wetzel et al., 2003, Huang and Manton, 2004, Linford et al., 2006). There is a lack of evidence showing mitochondrial function in aged uterine tissue from pregnant women and animal models.

## 1.2 Obstetric Complications Related to Advanced Maternal Age

The average age of childbirth is rising in the UK. The percentage of women aged 35 years and older from the total numbers of UK live births has risen from 8% in 1985 to 20% in 2011 (Office for National Statistics for England and Wales, 2011c, Bewley et al., 2009). Statistics from England and Wales in 2011 indicate that the average age of a woman giving birth was 29.7 years, and the average age of a woman having her first birth was 27.9 years (Office for National Statistics for England and Wales, 2011c). By 2011, nearly a fifth of all births in England and Wales were to mothers aged 35 years and over (Figure 1.4). The overall percentage rise since 1973 suggests a general shift in the age of childbearing. Possible influences for delayed conception include increased participation in higher education, increased female participation in the labour force, the increasing importance of a career, the rising opportunity costs of childbearing, labour market uncertainty, housing factors and instability of partnerships (Benzies et al., 2006, Tough et al., 2006, Jefferies, 2008, Chan and Lao, 1999, Ziadeh and Yahaya, 2001, Fitzgerald et al., 1998). Parallel with delayed natural conceptions, there has also been a rise in women aged 35 and older being treated with assisted reproductive technologies to overcome fertility complications; the total number of women being treated in the UK has more than doubled between 1996 and 2007 (Human Fertilisation and Embryology Authority, 2011). Escalation in the employment of assisted reproductive technologies has also inevitably contributed the shift in the age of childbearing over the past decades. Women of advanced maternal age frequently experience adverse difficulties achieving and maintaining pregnancy and delivering a healthy baby in comparison to younger pregnant women (Chan and Lao, 2008, Chan and Lao, 1999, Jahromi and Husseini, 2008, Fitzgerald et al., 1998, Gilbert et al., 1999).

The impact of paternal age on the parturition process is unknown, but it is worth noting that nearly two-thirds of babies (65%) were fathered by men who were aged 30 and over in England and Wales in 2011(Office for National Statistics for England and Wales, 2011b).

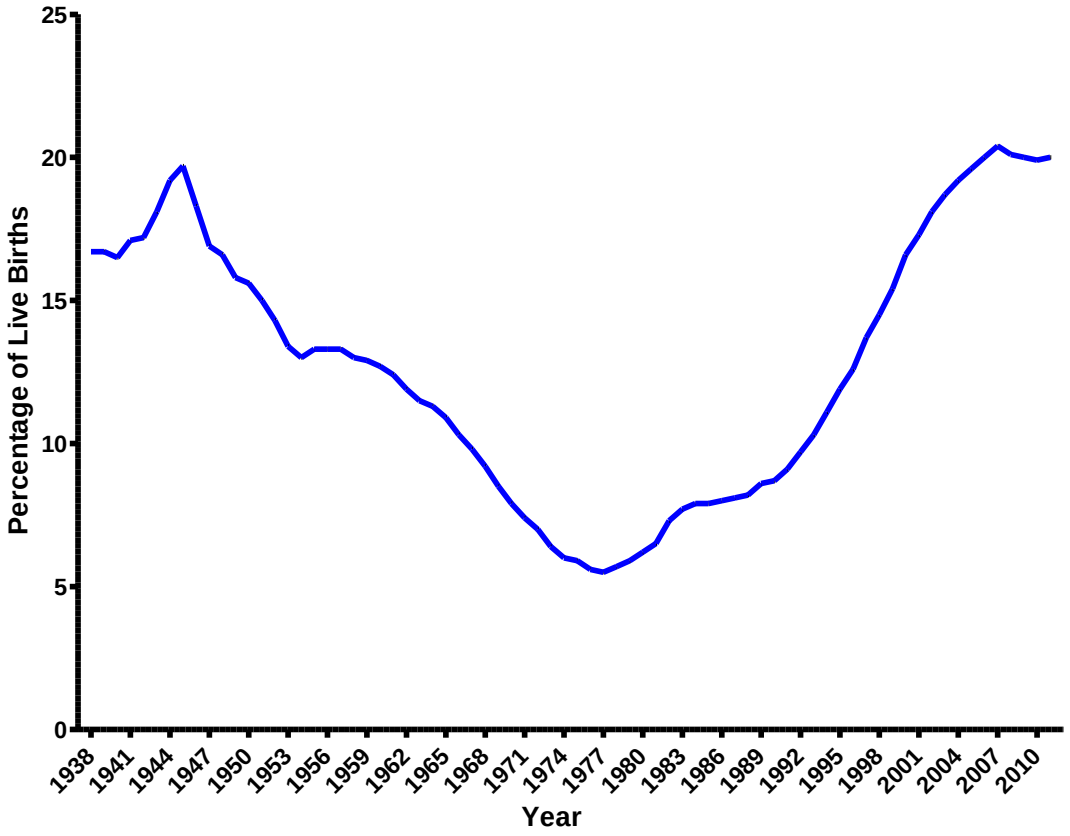


**Figure 1.4 Percentage of live births by mothers aged 35 and over, between 1938– 2011**
Data from the Office for National Statistics for England and Wales (Office for National Statistics for England and Wales, 2011c)

Women of advanced maternal age also exhibit a greater prevalence of fetal mortality during pregnancy and labour. Based on a European cohort of 634,272 women, it has been reported that approximately 20% of all wanted pregnancies in women aged 35 years result in fetal loss due to stillbirth, miscarriage or ectopic pregnancies; this figure rises to 54.5% in women aged 42 (Nybo Andersen et al.,

2000). The risk of miscarriage alone is a major concern for mothers of advanced maternal age, with a risk of 24.6% in women aged 35-39, 51% aged 40-44 and rising to 93.4% at 45 years and above (Nybo Andersen et al., 2000, Bewley et al., 2009).

Mothers above the age of 35 years also have a greater risk of Caesarean section delivery (Bewley et al., 2009, Ziadeh and Yahaya, 2001, Gilbert et al., 1999, Smith et al., 2008, Ecker et al., 2001, Mbugua Gitau et al., 2009, Main et al., 2000, Bayrampour and Heaman, 2010). Gilbert *et al*. (1999) report a 47% Caesarean section rate in nulliparous women aged 40 and over in comparison to 22.5% for women aged between 20-29, based on a cohort of 24,032 women in USA. They also highlight that 61% of the nulliparous women over the age of 40 require some form of operative delivery (Caesarean section, forceps, vacuum) (Gilbert et al., 1999). In a recent UK population cohort study looking at 215,344 births, it was confirmed that the risk ratios for Caesarean sections were considerably higher in mothers aged 40 and above [RR = 1.83, (95% CI: 1.77–1.90)] (Kenny et al., 2013). Other studies assessing labour characteristics report that length of labour and incidence of prolonged labour does vary with maternal age. In a retrospective cohort study of 31,976 births in USA, older nulliparous women aged 40 years and above were shown to persistently have higher rates of prolonged first and second stages of labour, compared to younger nulliparous women aged 20 years old and under. The second stage of labour was reported to be 97 minutes longer in older nulliparous women compared to the younger cohort ($p<0001$) (Greenberg et al., 2007).

## 1.3 The Reproductive Cycle and its Secession with Age

The reproductive life span in both humans and animal models is determined by regularity of the menstrual cycle (humans) or oestrous cycle (rodents). For all species, menstrual/oestrous cycling ceases at a defined age, normally mid-life; for humans this usually occurs between the late 40s and early 50s and for C57BL/6J mice between 11-16 months (Nelson et al., 1982, Felicio et al., 1984, Bromberger et al., 1997, Gold et al., 2013). The basic hormonal profiles of the menstrual/oestrous cycle are generally similar between most species.

Humans have a long reproductive lifespan of an average 36 years, from menarche at 8.5-13 years to menopause (defined as one year of anovulation) at around 50 years (Park et al., 2002, Aydos et al., 2005, Mihm et al., 2011). The 'textbook' menstrual cycle in young healthy women with proven fertility is 28 days. However, menstrual cycle length is highly variable, ranging from 25 to 34 days, and becomes noticeably shorter from 35 years of age with high variability, long cycle lengths and bleeding irregularities in the 5 years preceding menopause. Most of the cycle length variability is due to variability of the follicular phase, which shortens by three to seven days over time (Waller et al., 1998, Wilcox et al., 2000).

Since this present study investigates parturition in mice of advancing reproductive age, the oestrous cycle in mice will now be briefly discussed. Mouse oestrous cycle lasts between four to six days and is divided into four discrete but overlapping phases: pro-oestrous, oestrous, metoestrous and dioestrous (Nelson et al., 1982, Tan et al., 2003, Caligioni, 2009). Dioestrous is characterised by basal circulating concentrations of oestrogen and progesterone, atrophic endometrium and sexual inactivity.

Low concentrations of oestrogen and progesterone permit the synthesis of FSH by the pituitary gland. During pro-oestrous, uterine oedema and proliferation of endometrial cells occur, accompanied by gradually increasing oestrogen concentrations. Oestrous is when ovulation occurs and mice are sexually receptive, and the uterus becomes trophic under peak concentrations of oestrogen and other ovarian steroids. This is the critical period for sperm capacitation and the subsequent transition of the uterine environment toward the receptive stage after mating (Fata et al., 2001). In mice, there is a surge in circulating progesterone concentrations just prior to ovulation, which then drop during ovulation and rise marginally again during metoestrous. In the absence of successful fertilisation, degeneration of the corpus luteum occurs and the uterus undergoes regression, which is associated with cell apoptosis in all uterine cell types. This parallels the fall in serum oestrogen concentrations and the conversion of progesterone to less active 20$\alpha$-hydroxyprogesterone, resulting in the initiation of another follicular maturation cycle (Fata et al., 2001, Tan et al., 2003). Nelson *et al*., (1982) confirmed that peak oestrous cycling periods (defined by regularity of cycles) begin to decline by 9 months of age and can cease as early as 11 months of age in mice, meaning that the reproductive lifespan of mice is limited to as little as 11 months (Nelson et al., 1982, Felicio et al., 1984).

## 1.4 The Timing of Parturition

One of the principle components of this present study has been to address the mechanisms that underpin the impact of ageing on parturition. The hormonal processes involved in the timing of parturition in both humans and mice will now be discussed. Parturition is the process of giving birth or to be in labour, and requires ripening of the cervix and development of rhythmic myometrial contractions. In humans, the timing and triggers for these events have not been fully elucidated (Lopez Bernal, 2003, Smith, 2007, Kamel, 2010). However, it has been proposed, as a result of detailed *in vivo* animal studies and *in vitro* human investigations, that there is a cascade of hormonal signals driven by maternal-fetal interactions that prime the uterus and cervix, and induce labour (summarised in Figure 1.5) (Norwitz et al., 1999, Smith, 2007, Smith and Nicholson, 2007).

The hormonal cascade involves positive-feedback loops, which initiate an integrated series of changes within target reproductive tissues (the myometrium, decidua, fetal membranes and uterine cervix) over a period of days or weeks. Central to these are i) the development of the fetal hypothalamic adrenal axis (HPA) resulting in the secretion of fetal corsitol, dehydroepiandrosterone sulphate (DHEAS) and oestrogen (although the HPA is considered to play only a supportive role in human parturition) (Bernal, 2001, Mendelson, 2009, Kamel, 2010); ii) increased placental synthesis and release of corticotropin-releasing hormone (CRH) (Smith and Nicholson, 2007); iii) The process of a 'functional' progesterone withdrawal (Allport et al., 2001, Smith et al., 2012b). All of these events are believed to feed forward to enhance synthesis of uterotonins (agents that stimulate contractions) including prostaglandins and oxytocin, and upregulate the expression of contractile associated proteins including oxytocin receptor, connexin-43 and prostaglandin-endoperoxide synthase 2, resulting in the priming of the uterus, ripening of the cervix and rupture of fetal membranes (Norwitz et al., 1999, Bernal, 2001, Tribe,

2001, Smith, 2007, Smith and Nicholson, 2007, Vidaeff and Ramin, 2008, Mendelson, 2009). A slow and progressive shortening of the ripened cervix can then be mediated in labour by lower segment uterine contractions and strong expulsive contractions originating in the fundal region of the primed uterus allowing the cervix to fully dilate and resulting in the delivery of the baby. A more detailed summary of how these hormonal changes directly impact the target tissues (cervix and myometrium) are discussed in sections 1.5 and 1.6.

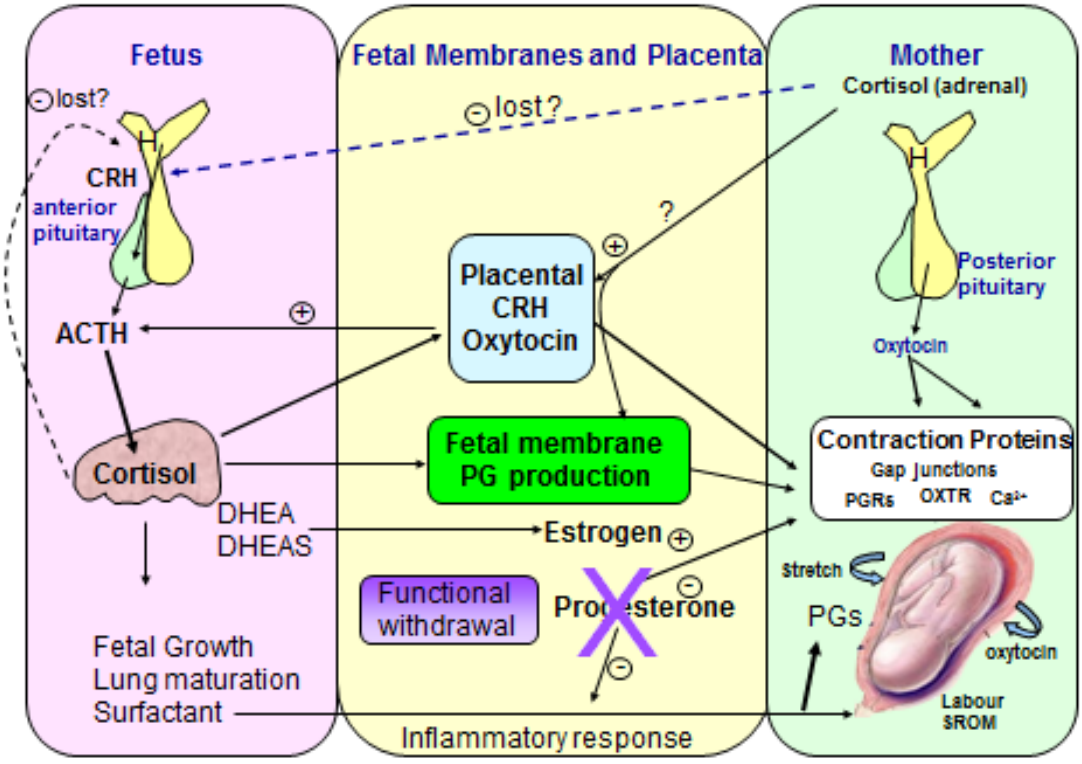


**Figure 1.5 Proposed mechanism of labour induction at term**
The major hormones and paracrine/autocrine factors responsible for promoting uterine contractions at term in an integrated parturition cascade are shown. Plus signs indicate activation or up-regulation. Minus signs indicate negative feedback mechanisms. ACTH: adrenocorticotrophic hormone, CRH: corticotropin-releasing hormone, DHEA: dehydroepiandrosterone, DHEAS: dehydroepiandrosterone sulfate, OXTR: oxytocin receptor, PGs: prostaglandins, PGRs: prostaglandin receptors, SROM: spontaneous rupture of the fetal membranes. Figure adapted from based on Norwitz *et al.*, (1999) and Smith *et al.,* (2007).

### 1.4.1 Fetal Signals and the Initiation of Parturition

There is increasing evidence to suggest that the fetus may generate signals that contribute to the initiation of labour in both human and animal models. These include cortisol release via the fetal HPA, CRH secretion from the placenta and the synthesis and secretion of pulmonary surfactant lipids and proteins by the fetal lung.

***The fetal hypothalamic-pituitary-adrenal axis***

As the fetus grows, the fetal HPA matures in preparation for the production and secretion of hormones such as CRH and adrenocorticotrophic hormone (ACTH), particularly during late gestation; the subsequent increased cortisol production by the fetal adrenal gland has been suggested to serve a role in the initiation of labour in humans and sheep (Liggins et al., 1973, Kamel, 2010). The major difference in the pregnant mouse model from sheep and humans is that the fetus does not appear to play such a dominant role and it is in fact the progesterone withdrawal ,as a result of luteolysis, which is considered to initiate labour (Mitchell and Taggart, 2009). The luteolytic mechanism does not relate to human parturition, as the corpus luteum is not required for the last two thirds of gestation. There is some belief that the fetal HPA appears only to have a supportive, rather than direct role in labour. This theory arises from observations in anencephalic pregnancies where there is little or no residual pituitary/adrenal function. Examination of the length of gestation in women carrying single anencephalic fetuses who went into spontaneous labour showed that the mean length of gestation was similar to that in women carrying normal singleton fetuses, but with a much wider scatter around the mean. This suggests that spontaneous labour can occur in anencephaly, but that a normal fetal pituitary adrenal function is required for the fine-tuning of the timing of parturition (Bernal, 2001).

### *Corticotrophin-releasing hormone secretion*

In the humans and non-human primates, it has been suggested that CRH, which is secreted in increasing amounts by the placenta near term, provides a fetal signal for the initiation of labour (Nathanielsz, 1998, Smith and Nicholson, 2007, Smith et al., 2012b). Such increased level of free active CRH near term not only triggers fetal cortisol production, which subsequently promotes fetal lung maturation via positive feedback mechanisms, but also increases placental oestrogen synthesis and prostaglandin release in fetal membranes, decidua and myometrium. Increased prostaglandin production is considered to potentially influence the upregulation of other contraction associated proteins in the myometrium such as gap junctions and oxytocin receptor (Smith, 2007, Kamel, 2010). The efficiency of CRH action is governed by the expression of its functional receptors (CRH-R), which are increased by 2 to 3-fold at the onset of labour (Markovic et al., 2007). Increased fetal CRH is proposed to up-regulate fetal pituitary secretion of ACTH, which enhances production of cortisol and dehydroepiandrosterone sulphate (DHEAS) by the fetal adrenal. DHEAS is subsequently metabolised to DHEA and then further converted by the placenta to oestrogen, which is necessary for spontaneous delivery (Smith and Nicholson, 2007, Smith et al., 2012b) (summarised in Figure 1.5).

In the mouse, CRH mRNA is developmentally induced to high levels in the bronchiolar epithelium of fetal lungs between days 13.5 and 17.5 days of gestation and is then depleted by day 18.5. This rise in CRH expression comes before the developmental induction of synthesis of the major surfactant protein, surfactant protein A (SP-A), by the fetal lung. Induction of *SP-A* expression was found to be delayed together with lung maturation in CRH-null murine fetuses from CRH-deficient mothers (Muglia et al., 1999). Therefore, CRH may contribute to the initiation of mouse labour by acting indirectly to stimulate fetal ACTH and adrenal

cortisol production and/or directly enhancing fetal lung maturation and the production of surfactant components (Mendelson, 2009).

***Fetal lung surfactant lipids and proteins***

The contribution of fetal lung surfactants to human parturition is debated, although it seems they may be more important in the mouse parturition. The synthesis and secretion of pulmonary surfactant by the fetal lung is initiated during the third trimester of human gestation. Surfactant, a glycerophospholipid-rich lipoprotein, is produced by alveolar type II pneumocytes and is secreted into amniotic fluid. Surfactant contains four principle lung-specific proteins, SP-A, SP-B, SP-C, and SP-D; SP-A is assumed to be the key signal for the initiation of labour (Mendelson, 2009, Yadav et al., 2011). Pulmonary surfactant isolated from human amniotic fluid has been shown to promote the synthesis of prostaglandin E in discs of human amnion. It is believed that surfactant phospholipids secreted by the fetal lung into amniotic fluid provide a source of arachidonic acid as a precursor for prostaglandin synthesis (Lopez Bernal et al., 1988). Mendelson and colleagues observed that SP-A gene expression is increased by proinflammatory stimuli such as IL-1 and NF-κB and by hormones and factors that increase cAMP in human fetal lung type II cells in culture (Islam and Mendelson, 2002, Condon et al., 2004).

In the mouse, SP-A mRNA and protein levels have been shown to be barely detectable in fetal lung on day 16 gestation, at day 17 there is an upregulation, followed by further rapid increase peaking at day 19 (Korfhagen et al., 1992, Alcorn et al., 1999, Condon et al., 2004). This gestational surge in SP-A secretion by the fetal lung is accompanied by a parallel increase in IL-1β protein expression in macrophages isolated from amniotic fluid, migration of activated macrophages to the pregnant uterus and activation of uterine NF-κB (Condon et al., 2004). Condon *et al*., (2004), directly assessed the ability of SP-A to initiate labour *in vivo*, by injecting

parallel groups of mice with purified SP-A or with a control (SP-A-depleted preparation). The majority of mice injected with SP-A on day 15 of gestation delivered prematurely on day 16-17 of gestation. Fetal macrophage migration and NF-κB activation were detected within the SP-A injected uterine horn but not in the control horn, suggesting a local inflammatory response (Condon et al., 2004). The authors went on to evaluate the role of endogenous SP-A in the initiation of labour. Pregnant mice on day 15 of gestation were intra-amniotically injected with an antibody raised against SP-A to deplete endogenous levels of the surfactant protein in amniotic fluid. All of the injected mice delivered viable pups 1 day later than normal gestational length, whereas the control group (pregnant mice intra-amniotically injected with non-immune rabbit antibody on day 15 of gestation) delivered at term; suggesting that the depletion of surfactant protein in amniotic fluid was able to considerably delay parturition by 5% of the normal gestation length in this model. However, the size of control group (n=3), was half of that of the test group (n=6); for a more conclusive outcome, authors should have matched sample sizes in both test and control groups. Condon and colleagues concluded that increased production of SP-A by the maturing fetal lung towards term provides a hormonal stimulus for the activation of an inflammatory cascade within the maternal uterus that results in enhanced myometrial contractility leading to parturition (Condon et al., 2004, Mendelson and Condon, 2005).

### 1.4.2 Role of progesterone in the onset of parturition

Secretion of progesterone during pregnancy prevents the secretion of FSH, which stops the selection and growth of a dominant follicle from the pool of follicles in the ovary. In the human, the initial site of progesterone production during gestation is the corpus luteum. However, five to six weeks after conception, the placenta is the major source of progesterone thereafter. Removal of the corpus luteum before this period of "luteal-placental shift" can result in abortion. In most experimental animal models, concentrations of maternal plasma progesterone remain relatively elevated throughout gestation, with an abrupt withdrawal of progesterone from the maternal circulation at the onset of parturition; this is paired with a simultaneous elevation in oestrogen concentrations (Mitchell and Taggart, 2009). Only in the guinea pig and human are circulating progesterone levels maintained at high concentrations throughout gestation and parturition (summarised in Figure 1.6). Progesterone is considered to act mainly to suppress the induction of pro-contractile pathways, whereas oestrogen, the other primary steroid hormone released by the placenta, is considered to be responsible for the upregulation of genes associated with labour, particularly the oxytocin receptor and connexin-43 (Nissenson et al., 1978, Lefebvre et al., 1995).

Mice depend on an active corpus luteum for progesterone synthesis throughout pregnancy. The onset of labour is triggered by luteolysis, which is mediated by activation of prostanoid FP receptors in the corpus luteum by prostaglandin $F_{2\alpha}$ released from the endometrium. Luteolysis induces a rapid fall in maternal progesterone levels, which triggers the onset of labour (Mitchell and Taggart, 2009, Lopez Bernal, 2003). This rapid decline in progesterone levels prompted the progesterone block theory by Csapo (1956), where it was proposed that a withdrawal of progesterone from the maternal circulation was necessary to cause the required uterine and cervical changes resulting in parturition.

According to this theory, progesterone promotes uterine quiescence by stimulation of relaxant pathways and suppression of stimulatory pathways, for example by reducing myometrial oestrogen sensitivity through inhibiting the expression of oestrogen receptor alpha (ER$\alpha$) in human myometrium. In animal models, parturition occurs only after a withdrawal of progesterone. It has been shown that progesterone suppressed the expression of several pro-contractile pathways in the pregnant uterus and stimulated expression of relaxant systems; at the onset of labour, the fall in progesterone triggers uterine activation (Csapo, 1956, Zakar and Hertelendy, 2007, Mitchell and Taggart, 2009, Kamel, 2010). In mice, these changes are also associated with a sharp increase in uterine oxytocin receptor levels, leading to the assumption that oxytocin has a physiological role in the activation of uterine contractions in labour (Lopez Bernal, 2003).

Similar to the mouse, circulating progesterone concentrations are altered at term and at labour onset in humans; progesterone concentrations are still high but stop increasing and have a tendency to plateau. There is also a change in progesterone receptor subtype that mediates a functional progesterone withdrawal (Smith, 2007, Kamel, 2010).

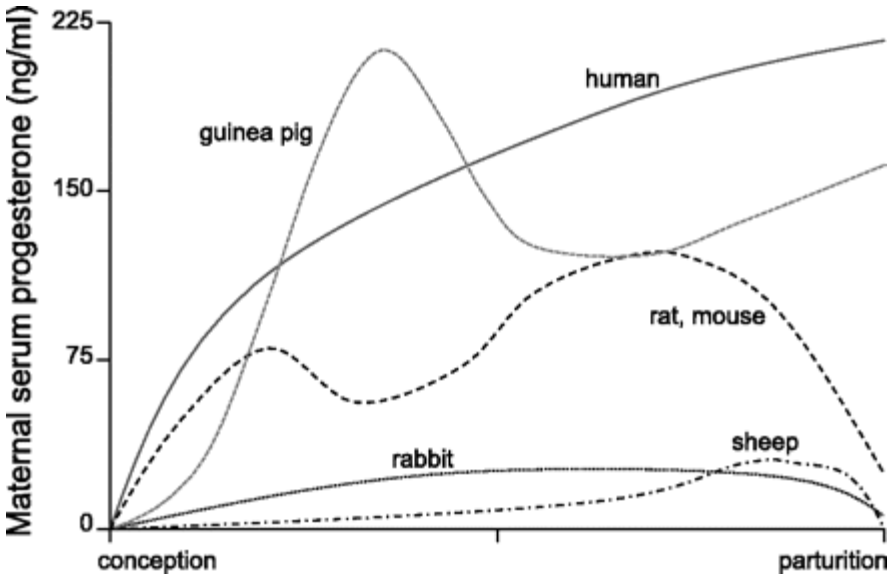


**Figure 1.6 Maternal serum concentrations of progesterone through gestation**
In most experimental animal models, there is an abrupt withdrawal of progesterone from the maternal circulation before parturition. Only in the guinea pig and human are progesterone levels maintained at a high and increasing concentration throughout parturition. Figure from: Are animal models relevant to key aspects of human parturition? (Mitchell and Taggart, 2009)

The mechanism(s) through which progesterone block/withdrawal triggers onset of parturition still remain to be fully elucidated. It has been suggested that the actions of progesterone in target cells are complicated and are mediated by multiprotein complexes that include progesterone-binding components (receptors) that modify components (coregulators and adaptors) and effector proteins (RNA-polymerase, chromatin remodelling proteins, and RNA-processing factors) (Zakar and Hertelendy, 2007). From all of the existing work published to date, Mitchell and Taggart (2009) have summarised two major models that could explain what could be taking place.

The first mechanism, for which most experimental evidence exists, is the “paracrine hypothesis”. Progesterone is synthesised within a local intrauterine network, including the fetal membranes (amnion and chorion) and maternal decidua, which controls progesterone concentrations in the underlying myometrium. Significant changes in progesterone production or metabolism could occur in this network and this could affect myometrial progesterone concentrations and contractility without changes occurring in the maternal systemic circulation. It has been shown that both oestrogen and progesterone are produced and metabolised by human fetal membranes and decidua (Khan-Dawood, 1987, Mitchell et al., 1987, Mitchell and Taggart, 2009). In addition, this intrauterine paracrine network produces other potentially important hormones such as oxytocin, endothelin (ET)-1, prostaglandin $F_{2\alpha}$ ($PGF_{2\alpha}$), prostacyclin ($PGI_2$) and nitric oxide (NO). It is now considered that paracrine interactions within the pregnant uterus are physiological regulators of uterine contractility and play a key role in human parturition onset (Mitchell and Taggart, 2009).

The second mechanism of functional progesterone withdrawal is linked to the expression of progesterone receptor (PR) isoforms. The full-length isoform, PR-B, is the primary mediator through which progesterone exerts its effects. However, there is an alternate transcription start site that codes for a protein, PR-A, that is identical to PR-B apart from missing the NH2-terminal 163 amino acids that contain one of the activating functional domains (AF3) of PR-B (Hovland et al., 1998). PR-A tends to have opposing effects to those of PR-B through the actions of an inhibitory function due to the absence of AF3. In both rat and human uterus, mRNA for PR-A appears to increase significantly before labour onset at term, and in the human, this also is true at protein level. The possibility of an alteration of PR-A:PR-B ratio causing functional progesterone withdrawal has been widely published (Pieber et

al., 2001, Fang et al., 2002, Mesiano et al., 2002, Merlino et al., 2007, Zakar and Hertelendy, 2007).

Other recently postulated mechanisms are the catabolism of progesterone into inactive metabolites, changes in the cofactor protein levels affecting PR activation and regulation of PR responsive genes through the competitive blocking by NF-κB at promoter sites. In addition, progesterone has been shown to directly inhibit binding of oxytocin to its receptor, potentially interfering with the effects of this potent contractile agonist. This explains why disruption of progesterone alone could trigger the full parturition cascade (Mesiano et al., 2011, Allport et al., 2001, Zakar and Hertelendy, 2007, Dunlap and Stormshak, 2004, Lindstrom and Bennett, 2004).

### 1.4.3 The immune system control on the onset of parturition

The relationship between the immune system and parturition remains unclear, but for many decades it has been postulated that labour is associated with an inflammatory cascade. The process of a 'functional' progesterone withdrawal is proposed to modulate the influx of inflammatory cells and release of inflammatory mediators. Two major components of this pathway are cytokines and prostaglandins. Romero and his colleagues have documented concentrations of proinflammatory cytokines in the amniotic fluid of women in the presence and absence of positive amniotic fluid bacterial cultures. They found that IL-1β, IL-6 and TNF concentrations were all significantly increased at term and with the onset of human labour (Romero et al., 1992b, Romero et al., 1992c, Romero et al., 2006). Expression of cytokines in the fetal membranes and the decidua suggests an inflammatory reaction occurs at term. These inflammatory cytokines regulate the release of uterotonins such as prostaglandins (Romero et al., 2006).

Many proinflammatory cytokines initiate signalling pathways that include transcription factors such as NF-κB, CAAT-enhancer binding protein β-isoform (CEBPβ), activator protein-1 (AP-1) and specificity protein-1 (Sp-1). Response elements for these transcription factors are commonly found in the regulatory regions of genes that are considered to be important in the cascade leading to parturition such as oxytocin receptor , prostaglandin FP, prostaglandin-endoperoxide synthase 1 and 2, and Cx-43. Many more studies have investigated the roles of proinflammatory cytokines on the expression of, and signalling pathways associated with, these factors. The results have been mixed, with many positive and some negative conclusions. One downstream effect of several proinflammatory cascades is the generation of $PGF_{2\alpha.}$ Whereas this causes luteolysis and subsequent progesterone withdrawal in mouse models, the role of $PGF_{2\alpha}$ in the human is much less clear. Lastly, one of the more consistent findings in microarray experiments investigating molecular events of parturition is an increase in expression of genes associated with an immune response (Tan et al., 2012, Havelock et al., 2005).

Prostaglandins are vital in the initiation of parturition in the mouse, and are also considered to play a key role in the human parturition pathway (Winchester et al., 2002). Prostaglandins are formed from arachidonic acid that is converted to prostaglandin H2 by the enzyme prostaglandin H synthase, also known as cyclooxygenase (Kota et al., 2013). Amniotic fluid concentrations of prostaglandin E2 (PGE2) and prostaglandin $F_{2\alpha}$ ($PGF_{2\alpha}$) have been shown to be increased before the onset of human labour (Lee et al., 2008). Similarly, the peak in uterine $PGF_{2\alpha}$ levels occurs at day 19.0 of gestation in mice, correlating with the onset of labour (Winchester et al., 2002). Allport et al., (2001) have demonstrated that human parturition is related to an up-regulation of prostaglandins within the uterus, synthesiszed by PTGS2. This leads to remodelling of the fetal membranes and

cervix and stimulation of myometrial contractions (Allport et al., 2001). Furthermore, myometrial contractions are shown to be mediated by PGE2, $PGF_{2\alpha}$ and thromboxane through targeting prostanoid EP, FP and TP receptors, respectively (Fischer et al., 2008).

There is much data suggesting a role of NF-κB, which is classically linked to inflammation, in the pathophysiology of labour. NF-κB activity increases with onset of labour, which in turn up-regulates expression of PTGS2 which contributes to the functional progesterone withdrawal and synthesis of prostaglandins (Lappas and Rice, 2007). An array of receptors, pro-inflammatory cytokines and inducible factors connected with the onset of human parturition have been shown to be regulated by NF-κB including TNF, IL-1β, IL-8, PTGS2, oxytocin receptor and phospholipase-A2.

These have been examined in gestational tissues including the amnion, decidua, cervix and myometrium. Additionally, inhibitors of NF-κB activity such as IL-10 have been shown to suppress both LPS-induced pre-term labour in rodents in rodents (Schottelius et al., 1999, Dudley and Dangerfield, 1996, Terrone et al., 2001) and IL-1β induced uterine contractions in Rhesus monkeys (Sadowsky et al., 2003, Cookson and Chapman, 2010). These findings suggest that NF-κB is a key regulator of pro-inflammatory agents during parturition. However, it is not clear whether the role of NF-κB is a cause or effect of the parturition process.

In summary, these studies reinforce the association between immune activation and mechanisms of parturition in both mouse and human, however full understanding of the association still remains unclear.

## 1.5 The Cervix in Pregnancy and Labour

### 1.5.1 Structure of the cervix

One of the proposed mechanisms investigated in this thesis are the potential delays in cervical softening and/or ripening in ageing mice. The following section describes the preparation of the cervix for labour. The cervix is a structure that allows attachment of the uterus to the vagina. It is approximately four centimetres long in the human and five millimetres long in the mouse. Human and mouse basic anatomy are similar as shown in Figure 1.7. The cervix can be divided into the ectocervix and the endocervical canal. The ectocervix is the portion of the cervix that projects into the vagina. It is lined by stratified squamous non-keratinised epithelium. The opening in the ectocervix, the external *os*, marks the transition from the ectocervix to the endocervical canal. The endocervical canal is the 'inner' portion of the cervix. It is lined by a mucus-secreting simple columnar epithelium. In the human cervix, the endocervical canal ends and the uterine cavity begins at the internal *os*. It is principally composed of connective tissue, the majority of which is collagen arranged in fibres and embedded in proteoglycans. There is a small amount of smooth muscle (<10%) and fibroblast cells(Leppi, 1964, Graham, 1966, Norman, 2007, Thompson, 2013).

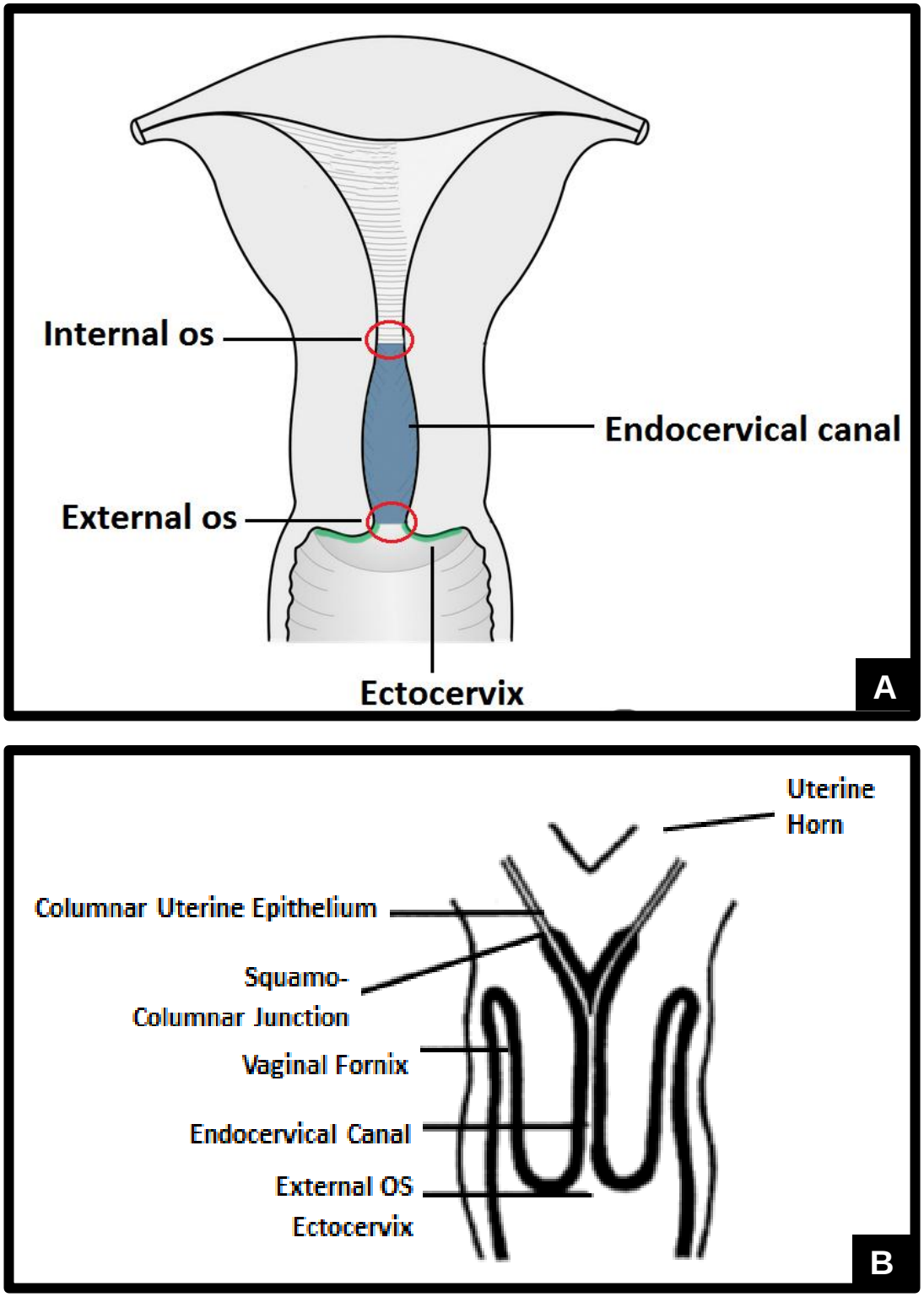


**Figure 1.7 Schematic frontal section through human and mouse cervix**
The cervix is the structure that allows attachment of the uterus to the vagina. The structure of the cervix is similar in both human and mouse. In both, it can broadly be divided into two components: the ectocervix (lined by stratified squamous epithelium) and the endocervical canal (lined by a mucus-secreting columnar epithelium). **A:** Human cervix; figure from (Thompson, 2013); **B:** Mouse cervix; figure from (Graham, 1966).

### 1.5.2 Distinct phases of cervical ripening

The non-pregnant cervix is a fibrous organ with a high connective tissue content that undergoes extensive remodelling throughout gestation and the postpartum period (Maul et al., 2006, Yu and Leppert, 1991). Early in gestation, the cervix increases in volume as its primary function is to maintain rigidity, termed physical integrity. This physical integrity is critical so that the developing fetus can remain in the uterus until the appropriate time for delivery. The secondary function is to provide a physical and chemical barrier (the cervical epithelia produce cytokines and antimicrobial peptides) to prevent infection ascending up into the uterus via the vagina (Critchley et al., 2004, Timmons et al., 2007, Timmons et al., 2010, Frew and Stock, 2011, Miessen et al., 2012). Towards term, the structure of the cervix softens and becomes more distensible through a process known as cervical ripening; this subsequently facilitates cervical dilation promoted by myometrial contractions during labour.

Cervical remodelling in both human and mouse, can be divided into four separate but overlapping stages defined as softening, ripening, dilation and postpartum repair (Leppert, 1995, Word et al., 2007, Timmons et al., 2010) (Figure 1.8). Hegar (1985) was the first to report that the human lower uterine segment felt softer in pregnancy at four to six weeks (Hegar, 1985, Read et al., 2007). However, many years before, Harkness & Harkness (1959) documented that distensibility of rat cervical tissue increased dramatically starting mid-gestation between days 11 and 12, again indicative of a softening to the cervical structure (Harkness and Harkness, 1959). Cervical softening is classified as the first measurable decline in the tensile strength or tissue compliance compared with non-pregnant. Digital cervical examination in women and biomechanical studies in mice have indicated that softening initiates in the first trimester of pregnancy in women and by day 12 of a 19 day gestation in mice (Leppert, 1995, Read et al., 2007, Timmons et al., 2010).

The softening phase is different from the remodelling stages that occur closer to term, as it is a relatively slow and incremental process which occurs in a progesterone-rich environment. Despite the progressive increase in compliance, tissue competence is preserved. Changes in tissue compliance during softening are proposed to be facilitated by changes in the composition or structure of the extracellular matrix (ECM) in humans and rats (Liggins, 1978, Leppert, 1995). This is supported by the observations that cervical incompetence is increased in women with inherited defects in collagen and elastin synthesis or assembly such as Ehlers-Danlos and Marfan syndromes (Meijboom et al., 2006). In addition, mice deficient in the ECM protein, thrombospondin 2, have altered collagen fibril morphology and premature cervical softening (Kokenyesi et al., 2004).

Cervical ripening at the end of gestation is a more accelerated stage defined by maximal loss of tissue compliance and integrity. Ripening is characterised by an increase in hyaluronan content, weakening of the collagen matrix, increased collagen solubility (Hillier and Wallis, 1982, Granstrom et al., 1989), changes in the distribution of inflammatory cells, increased tissue growth and hydration and loss of tensile strength (Uldbjerg et al., 1983, Straach et al., 2005, Timmons et al., 2010). Ripening takes place within a week or two preceding birth in women, or in the hours preceding birth in mice. Following delivery, the final stage of remodelling, known as postpartum repair, allows recovery of tissue integrity and competency. Each phase of remodelling is coordinated within a unique endocrine environment affecting epithelial, stromal, immune and endothelial cell function as well as the composition and structure of the ECM (Timmons et al., 2010).

### 1.5.3 Cervical architecture: The extracellular matrix

The predominant molecules of the cervical extracellular matrix are type 1 (70%) and type 3 (30%) collagen (Kleissl et al., 1978), with a small amount of type 4 collagen at the basement membrane (Minamoto et al., 1987). Intercalated among the collagen molecules are glycosaminoglycans (Fumagalli et al., 2012), proteoglycans, elastin, and various gylcoproteins such as fibronectins. There is also a cellular portion of the extracellular matrix consisting of smooth muscle, epithelium, fibroblasts and blood vessels. The relative ratio of smooth muscle to connective tissue is not uniformly distributed throughout the cervix. The upper cervical portion closest to the myometrium has lower connective tissue ratio compared to the lower distal portion of the cervix (Ludmir and Sehdev, 2000). Cervical remodelling, transitioning from non-pregnant to late pregnant cervix, is greatly facilitated by the reorganisation of the extracellular matrix.

#### *Collagen*

Collagen is the most important component of the extracellular matrix as it determines the tensile strength of the fibrous connective tissue (Read et al., 2007, Word et al., 2007, Timmons et al., 2010, Mahendroo, 2012). In its natural helical state, collagen proteins are rigid and essentially non-extensible. Synthesis of stable collagen triple helices requires vast co-translational and post-transitional modifications. Once arranged as a triple helix, the collagen can then be cross-linked into fibrils, fibres and bundles. Collagen fibres must be at least 20 μm in length to maintain tensile strength, and the process of cross-linking further enhances this tensile strength (Aspden, 1988). When cross-linked, collagen is less accessible to collagenases and proteases that act to degrade the collagen fibres. In the non-pregnant cervix, collagen bundles are densely and irregularly packed.

Throughout pregnancy, collagen is actively synthesised and continuously remodelled by collagenases, which are secreted from both cervical cells and neutrophils. Collagen is broken down by collagenases both intracellularly, to remove structurally defective pro-collagen to prevent the formation of weak structural collagen and extracellularly, to slowly weaken (soften) the collagen matrix to allow delivery of the fetus (Junqueira et al., 1980, Uldbjerg et al., 1983, Ludmir and Sehdev, 2000).

Even by the end of the first trimester, the collagen bundles become less compactly assembled, resulting in an overall decrease in the collagen concentration. However, with smooth muscle cells and elastic tissue, the collagen fibres align in a certain direction parallel to each other. Therefore, the cervix feels softer than the non-pregnant cervix, but is still able to maintain the pregnancy *in utero* (Ludmir and Sehdev, 2000). As the pregnancy progresses closer to term, there is a further decrease in the overall concentration of collagen. Cervical cells secrete decorin, a small molecular weight proteoglycan that coats collagen fibrils. The levels of decorin rise both in late pregnancy and in labour. When the ratio of decorin to collagen increases, it is likely to cause a dispersal of collagen fibrils leading to disorganisation of the collagen fibres (Rechberger and Woessner, 1993). The concentration of collagen therefore decreases as a consequence of this relative “dilution” of the collagen as it is dispersed and remodelled into fine fibres. Hyaluronic acid, a glycosaminoglycan, is secreted by fibroblasts and has a high affinity for water molecules. As collagen fibres disperse, hyaluronic acid levels increase in cervical cells, along with the volume of water (Ludmir and Sehdev, 2000).

As summarised above, the properties of collagen are influenced by changes in synthesis, posttranslational modifications, assembly of fibres and degradation of fibres. Current understanding confirms that changes in collagen structure precede cervical softening and contribute to the progressive decline in the tensile strength of the cervix. Maximal tensile strength diminishment occurs at birth and is rapidly regained in the postpartum period (Timmons et al., 2010, Akins et al., 2011). It is believed that the structural reorganisation of collagen by the end of gestation allows access of proteases to active sites allowing more effective removal of less mature collagen. The upregulation of collagen assembly genes in the postpartum period are considered to promptly replenish mature collagen in the matrix resulting in a marginal overall change in total collagen content. The relative contribution of collagen degradation versus structural reorganisation remains controversial, and further investigations will be required to clarify this inconsistency (Timmons et al., 2010).

***Elastic component***

Elastin fibres provide recoil to tissues that undergo repeated stretch. Along with collagen, elastin is another important component of the extracellular matrix of the uterine cervix. These fibres are located in defined regions of the stromal matrix and comprise 0.9–2.4% of the total amount of connective tissue, without a substantial change in content over the course of pregnancy. They are organised parallel to and between collagen fibres and assemble in bands of 20-30 μm thickness (Leppert et al., 1983, Leppert et al., 1986). These thin sheets are capable of being stretched in any direction. Elastin allows the uterus to retain the fetus during gestation, but with mechanical stress, the elastin component can distend to twice its length to allow the cervix to dilate for parturition.

The importance of elastin fibres in facilitating reversible extensibility or elasticity is suggested by the reduction in elastin fibre content in women with cervical insufficiency. In biopsies from patients with clinically evident incompetent cervices, histologic evaluation reveals both a decrease in elastin and abnormal architecture (Leppert et al., 1987). The elastin fibres appear broken and fragmented compared to samples from women with full-term pregnancies that revealed elastin oriented in a band-like manner (Leppert et al., 1987).

***Cellular components of the cervix***

Smooth muscle cells and fibroblasts make up the cellular component of the human uterine cervix (Leppert, 1995). Early in gestation, turnover of both smooth muscle and fibroblasts is initiated and the cervix undergoes hyperplasia as these cells proliferate. As pregnancy advances, the cells go from a proliferative phase to a quiescent phase in which physiologic cell death occurs and decorin becomes up-regulated. Decorin then further suppresses cell proliferation, which accounts for further increases in decorin levels; a process that helps to disperse collagen fibres (De Luca et al., 1996, Ludmir and Sehdev, 2000). This disorganisation of collagen then aids in an influx of water and aids in increasing the ability of the cervix to distend. Regulation of cell death can be affected in multiple ways, including secretion of hormones and cytokines. The pattern of physiologic cell death appears to be controlled precisely during the various stages of cervical remodelling. Physiologic cell death induces invasion of the cervical stroma by neutrophils and macrophages. These cells then induce the release of collagenases and elastase from cervical stromal cells to contribute to cervical remodelling (Ludmir and Sehdev, 2000).

### *Matricellular proteins*

Matricellular proteins are not considered to be structural components of the extracellular matrix themselves, but they modulate the functions of structural proteins such as collagen as well as cell functions through interactions with cell surface receptors, proteases, and growth factors. Matricellular proteins include SPARC (secreted protein acidic and rich in cysteine), thrombospondin 1, thrombospondin 2 and tenascin C which modulate interactions of cells with the extracellular matrix during development, remodelling and wound healing (Midwood et al., 2004, Timmons et al., 2010, Akins et al., 2011). Transcription of tenascin C, thrombospondin 1, thrombospondin 2 and fibrillin is increased several-fold in the postpartum cervix which validates their described roles in wound healing and tissue repair. In summary, matricellular proteins are expressed and regulated during cervical remodeling, but their specific function in this process remains to be elucidated (Timmons et al., 2010).

### 1.5.4 Mechanisms controlling cervical ripening prior to labour onset

Animal studies have provided a working understanding of cervical remodelling, but much of the proposed model remains to be tested experimentally in humans. In summary, cervical remodelling is the result of a series of complex and properly timed biochemical processes that consequently lead to the rearrangement and realignment of the collagen molecules, decreased collagen fibre strength and diminished tensile strength of the ECM. Softening is characterised by increased collagen turnover and reduced collagen crosslinking. As mature, crosslinked collagen is depleted from the matrix, it is replenished with the less mature collagen resulting in a progressive decline in tissue stiffness (House et al., 2009, Akins et al., 2011). Associated with changes in the ECM is the localisation of leukocytes to the subepithelial region, along with increased proliferation and an increase in the surveillance capability of epithelia via expression of repair and barrier maintenance factors. These changes take place in a low oestrogen and high progesterone environment (Timmons et al., 2010). The shift to the accelerated stage of cervical ripening is mediated by a decline in progesterone synthesis, increased cervical progesterone metabolism and increased synthesis of estradiol and relaxin. The ongoing processes initiated during the softening phase are then joined during ripening by increased vascularisation, a change in glycosaminoglycan (GAG) composition and alteration in tissue hydration which together result in increased tissue volume. The best understood GAG change is an increase in hyaluronan, which facilitates further disorganisation of collagen fibres and provides increased viscoelasticity to the cervix. The maximal loss of tissue tensile strength might result from disruption of stable high MW hyaluronan crosslinked to versican owing to increased metabolism of both GAGs.

Disruption of these crosslinks might culminate in loss of integrity, allowing maximal dilation during labour upon initiation of uterine contractions. Changes in barrier properties of the cervical epithelia via changes in expression of tight junction, aquaporin and gap junction proteins might also accompany this phase of remodelling (Timmons et al., 2010, Mahendroo, 2012).

The structural changes in ECM components have been linked to a cervical stromal inflammatory response (Dubicke et al., 2010). During cervical ripening there is an influx of neutrophils, eosinophils, mast cells, and macrophages into the cervical stroma (Timmons et al., 2010, Word et al., 2007, Read et al., 2007). There is also an increase in the enzyme PTGS2 associated with cervical ripening, which leads to a local increase of prostaglandin E2 (PGE2) in the cervix. PGE2 in turn stimulates the release of interleukin IL–8 increasing chemotaxis for neutrophils, which is associated with collagenase activity promoting collagen degradation. There is an increase in the activity of matrix metalloproteinases 2 and 9, enzymes that degrade extracellular matrix proteins. Cervical collagenase (also called matrix metalloproteinase 1) and elastase also increase (Stygar et al., 2002, Read et al., 2007, Word et al., 2007, Timmons et al., 2010). The trigger for these changes to the morphology of the cervix is considered to be linked to the increased concentration of PTGS2, endogenous cytokine and prostaglandin synthesis, and decrease in functional progesterone receptor, which all occur as a result of the activation for the onset of labour. Increasing oestrogen levels also lead to an increased collagenase activity, cervical cell apoptosis, and eosinophil infiltration in the cervix (Word et al., 2007, Read et al., 2007).

The nitric oxide synthase (NOS)/nitric oxide (NO) system has been postulated to have a regulatory role in the process of cervical ripening (Ledingham et al., 2000, Tornblom et al., 2005). Gene expression of endothelial inducible NOS is significantly higher in cervical tissues from women in labour compared to unripe cervices (Tornblom et al., 2005). In animal studies increased cervical NO is associated with an increase in metalloproteinase activity, cellular apoptosis in the cervix, and glycosaminoglycan synthesis in the cervix. In a rat model, the administration of a nitric oxide synthase inhibitor (L-nitro-arginine methylester) was able to block cervical ripening, whereas the direct application of a NO donor (sodium nitroprusside) to the cervix induced cervical ripening (Calder, 1998, Chwalisz and Garfield, 1998, Buhimschi et al., 1996).

There is much controversy surrounding the theory that activation of immune cells is required for physiological cervical ripening at term and some groups who work mainly with rodent models, openly oppose the concept (Hirsch et al., 2006, Timmons and Mahendroo, 2006, Gonzalez et al., 2009, Timmons et al., 2009, Mahendroo, 2012). These groups suggest that during ripening there is an influx of monocytes into the cervix that are dependent on the loss of progesterone function. In addition, resident macrophages and neutrophils are present in the cervix at this time. Despite the presence of these leukocytes, mRNA expression of proinflammatory genes such as IL-1$\alpha$, IL-6, TNF, CXCL1, PTGS1, and PTGS2 are believed not to be induced during ripening though some are increased shortly after postpartum. Furthermore, depletion of neutrophils has no effect on timing of parturition and myeloperoxidase activity, a marker of functional neutrophils, is not measurable until postpartum. These data suggest that immune cells are present but not activated during rodent cervical ripening, thus suggesting that physiological ripening is not mediated by an inflammatory cascade (Mahendroo, 2012).

However, some theories still propose a potential role for inflammatory mediators in human cervical ripening, particularly in relation to preterm labour; gene expression of proinflammatory genes such as IL-1$\alpha$ and IL-1$\beta$ are higher in cervical biopsies from women in labour compared to unripe cervical tissues (Dubicke et al., 2010). Monocytes which invade the cervical stroma either prior to birth, during labour or shortly postpartum are differentiated to produce macrophages with two diverse phenotypes, M1 and M2 (Timmons et al., 2010). M1 macrophages are activated by pro-inflammatory mediators such as LPS and IFN$\gamma$ and express pro-inflammatory cytokines such as IL-6, IL-12, and TNF (Dalton et al., 1993, Gordon, 2003, Mosser, 2003, Gordon and Martinez, 2010). M2 macrophages are activated by IL-4 and IL-13 and produce anti-inflammatory cytokines such as IL-10, IL-1 receptor antagonist and TGF$\beta$ (Stein et al., 1992, Doherty et al., 1993, Song et al., 2000, Mosser, 2003). The activation of M1 macrophages protect the reproductive tract from the threat of microbial invasion, and generate pro-inflammatory molecules which are important for the postpartum clearance of cervical extracellular matrix molecules. Alternatively, M2 macrophages prevent over-activation of the M1-mediated inflammatory process and instead promote repair of the cervix back to the non-pregnant state (Timmons et al., 2009, Timmons et al., 2010). Postpartum repair is characterised by a significant increase in transcription of genes involved in matrix repair (e.g. matricellular proteins, collagen assembly) and epithelial barrier function (Hassan et al., 2009, Timmons et al., 2010).

In summary, cervical remodelling (inclusive of softening and ripening) is a dynamic, progressive process resulting in realignment of collagen, degradation of collagen cross-linking due to proteolytic enzymes and dilation of the cervix resulting from these processes plus uterine contractions. This is a complicated series of events in which many things occur both simultaneously and sequentially. Cervical repair then occurs postpartum so that a successful pregnancy can occur again in the future. If the timing of these complex cervical changes is not tightly controlled, a delay in delivery post term or preterm delivery can result, or it can even result in an impairment of spontaneous vaginal delivery once labour has initiated (Ludmir and Sehdev,2000).

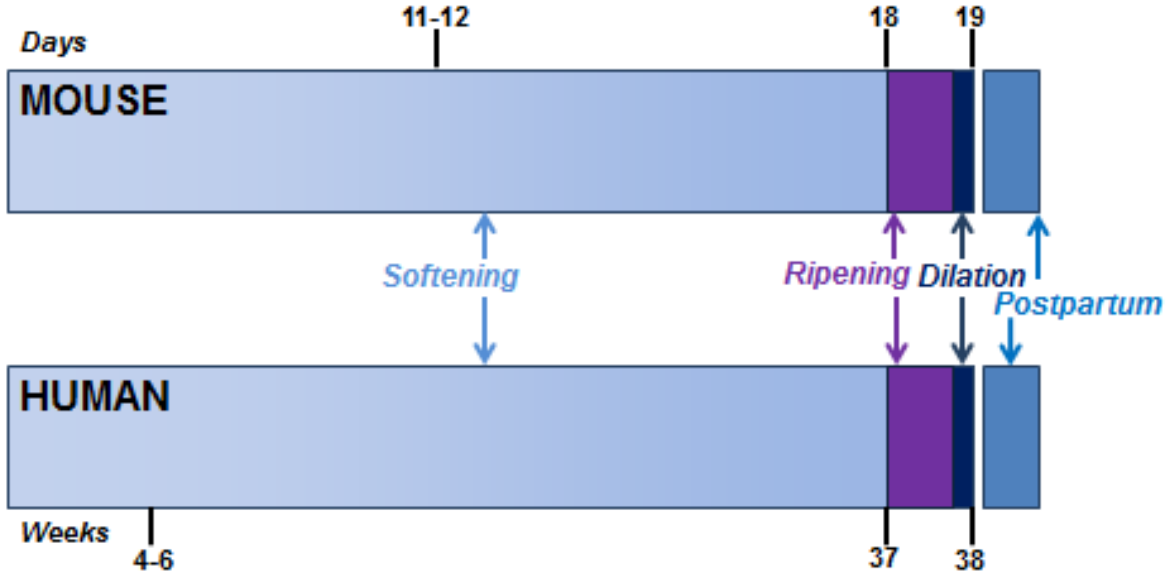


**Figure 1.8 Representative schematic of the stages of cervical remodelling**

The changes in cervical physiology during human and mouse gestation can be divided into distinct, overlapping phases: softening, ripening/dilation, and postpartum repair. (Information for the mouse was adapted from: Cervical remodelling during pregnancy and parturition: molecular characterisation of the softening phase in mice (Read et al., 2007).

## 1.6 The Myometrium in Pregnancy and Labour

### 1.6.1 Structure of the uterus

Myometrial function in pregnant ageing mice was investigated as part of this thesis; this following section describes the activation of the myometrium for labour. The human uterus is located between the cervix and the fallopian tubes. It compromises a single chamber. The myometrium, the major tissue component of the uterus, is located between the endometrium and the perimetrium (Figure 1.9). The myometrium is composed of predominantly smooth muscle and extracellular matrix. Knowledge of the exact number, or relative proportion, of smooth muscle fibres that exist in normal myometrium, is limited (Sweeney et al., 2013). However, research into the microanatomy of the human term-pregnant myometrium has indicated there are clearly defined structural elements, which include densely packed sheets and cylindrical bundles of myocytes (Young and Hession, 1999).

The structure of the human myometrium is composed of three layers: the supravascular, the vascular and the subvascular. The outermost supravascular layer is predominantly a longitudinal arrangement of smooth muscle cells that are arranged in interconnecting bundles of 10 to 50 partially overlapping cells and set in a matrix of collagenous connective tissue. The middle vascular layer is thick and consists of an interlacing mesh of muscle fibres interspersed with blood vessels. The innermost subvascular layer is adjacent to the endometrium and is predominantly a circular arrangement of muscular fibres running perpendicular to the long axis of the uterus; this layer runs clockwise and counter-clockwise in a spiral (Noe et al., 1999, Schünke et al., 2010, Blackburn, 2012).

Mice have a duplex uterine structure, consisting of two uterine horns that join together at the uterine body (Figure 1.9). Each uterine horn has a myometrial smooth muscle layer. The mouse myometrial structure is similar to that of human myometrium composing of two layers: an outer longitudinal layer of smooth muscle fibres and a thicker inner circular muscle layer; the two layers are separated by loose, highly vascular connective tissue (Brody and Cunha, 1989, Treuting and Dintzis, 2012).

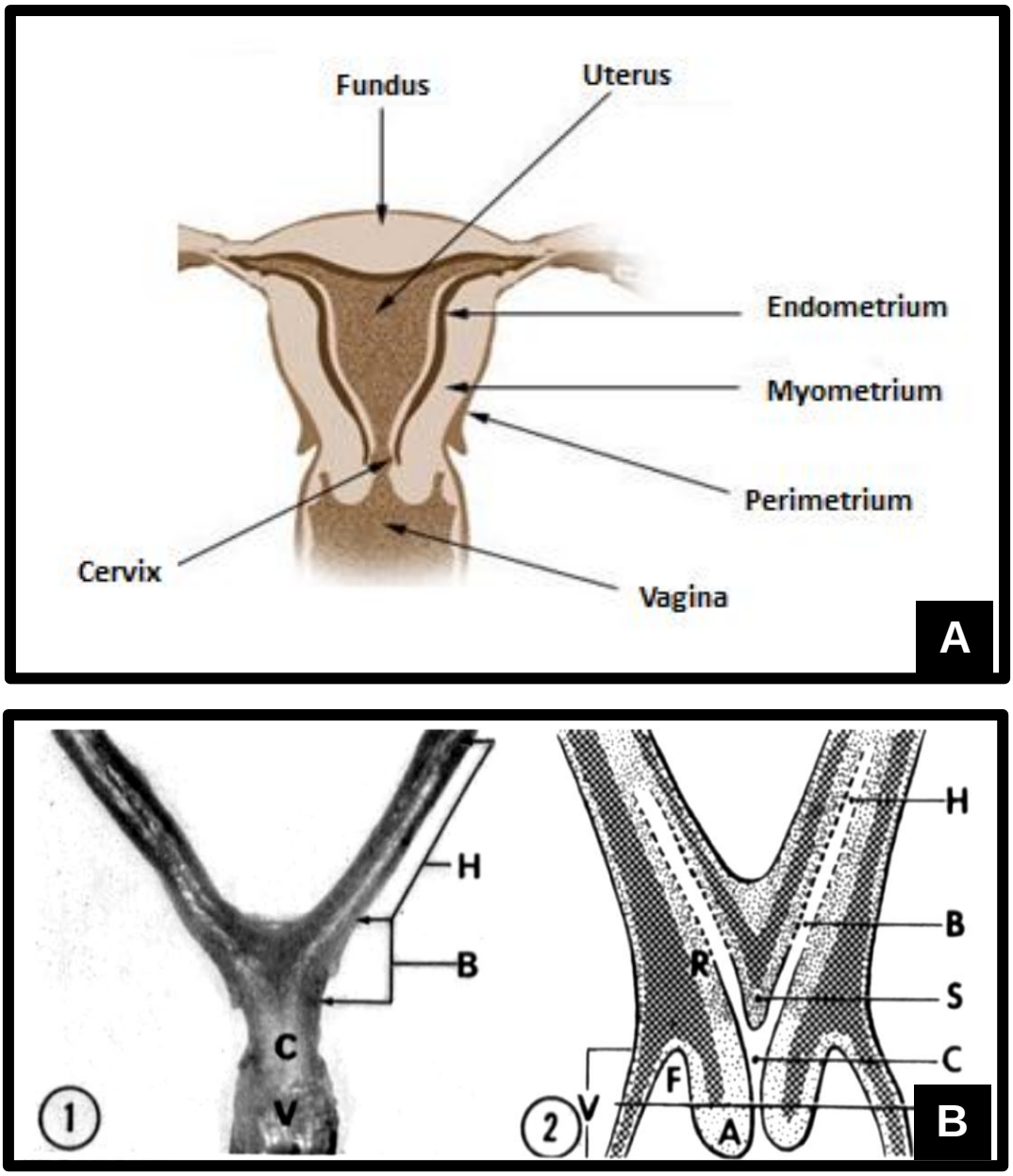


**Figure 1.9 Schematic frontal section through human and mouse uterine structures**
**A:** Human uterus; figure from http://medicalterms.info/anatomy/Uterine-Wall/
The human uterus compromises of one uterine chamber and cervix. The uterine wall is made up of three layers: the endometrium, the myometrium (smooth muscle layer), and the perimetrium. **B:** Mouse uterine horns; figure from: A study of the uterine cervix of the mouse (Leppi, 1964). **1.** The mouse reproductive tract compromises of two uterine horns (H) that join to form the body of the uterus (B), the cervix (C) and vagina (V) (x 4 magnification). **2.** Representative diagram showing the lumen of each uterine horn (H) are continuous with those of the uterine corpus (B). Each uterine horn is made up of an outer layer of longitudinal muscle and a thicker inner layer of circular smooth muscle, as represented by crosshatching. (V) vagina, (F) vaginal fornices, (C) cervix, (A) cervical and vaginal stroma, (R) stroma of the uterine horns, (S) septum.

### 1.6.2 Myometrial function in menstruation and menopause

The non-pregnant uterus exhibits contractile activity during menstruation and can be responsible for the dysmenorrhea. The uterus exhibits two known patterns of myometrial contraction during the menstrual cycle. The first has been termed “focal and sporadic bulging of the myometrium” (Togashi, 2007), which frequently involves the entire layer of the myometrium. These contractions are sustained and last for several minutes. The second pattern: “uterine peristalsis", initiates rhythmic ‘wave-like’ subtle contractions, which are likely to be responsible for the shedding of the subendometrial myometrium, and required for the transport of spermatozoa from the external *os* of the cervix into the fallopian tubes (Kunz and Leyendecker, 2002).

Concentrations of the female steroid hormones alternate during the menstrual cycle and influence the pattern of myometrial activity in both human and animal models. These hormones also control levels of ATP and other metabolites required for contraction and can influence uterine excitability. Recordings of uterine pressures in the non-gravid uterus, as well as MR imaging have shown that the pattern of myometrial activity, such as the direction of contraction propagation throughout the uterus varies with the different phases of the menstrual cycle. Antegrade contractions, which are contractions propagating from the fundus towards the cervical end of the uterus, favour forward emptying or discharge of the uterine content such as menstrual blood, whilst cervico-fundal contractions aid in sperm transport (Arrowsmith et al., 2012).

The menopause is marked with a gradual decline in hormonal secretion from the ovaries, to the point when the ovaries cease to function, and there is a characteristic loss of regular menstruation and eventual permanent cessation of menses (Burger et al., 2008). Contrary to the assumption that uterine activity ceases following the menopause, rhythmical myometrial contractions have been seen by ultrasound examination in postmenopausal women and low levels of spontaneous activity have been reported in strips from human post-menopausal myometrium *in vitro* (de Vries et al., 1990, Domali et al., 2001, Arrowsmith et al., 2012). In conclusion, the uterus is a dynamic organ which functions throughout a lifetime, but changes accordingly with advancing age.

### 1.6.3 Myometrial contraction and activation at labour onset

For the majority of pregnancy, the uterus demonstrates limited contractile activity (quiescence), with sporadic, low amplitude and arrhythmic contractions. During this state, the contractile function of the myometrial smooth muscle is considered to be suppressed by the down regulation of contractile associated proteins (CAPs) such as gap junctions proteins, uterotonin receptors, PTGS2 and elements of calcium signalling, and/or the upregualtion of pro-quiescence pathways (Norwitz et al., 1999, Bernal, 2001, Lopez Bernal, 2003, Smith et al., 2007, Smith, 2007, Kamel, 2010).

In the human myometrium, the resting membrane potential has been shown to increase as term approaches (Parkington et al., 1999). The reasons for this change are not entirely known, but a decrease in specific potassium ($K^+$) channel populations is likely to play a key role (Khan et al., 2001). The switch to a more positive potential renders the cell closer to the threshold for an action potential, which will be elicited by spontaneous and/or agonist-meditated myometrial depolarisation. Membrane depolarisation leads to the opening of voltage dependent L-type calcium channels and to a lesser extent, calcium release from intracellular stores. The subsequent rise in intracellular calcium mediates formation of calcium-calmodulin complexes and leads to

activation of myosin light chain kinase and phosphorylation of the myosin light chain allowing cross-bridge cycling and hence contraction (Tribe et al., 2000, Tribe, 2001).

The uterotonins that lead to contraction are primarily prostaglandins and oxytocin. In humans, augmented expression of $IP_3$-coupled prostaglandin receptors (Slater et al., 2006, Astle et al., 2007) is seen along with an increase in oxytocin receptor (OXTR) numbers. The increase in OXTR expression is also likely to be activated by a rise in circulating and local tissue production of oxytocin. Furthermore, the action potentials are more effectively propagated throughout the myometrial syncytium close to term, via enhanced intercellular connections. This is demonstrated by an increase in expression of connexin-43 (Cx43, a component of gap junctions). Expression at term of both OXTR and Cx43 are believed to be augmented by uterine stretch (Ou et al., 1997, Ou et al., 1998).

Some of these changes, including downregulation of specific potassium channels (Knock et al., 2001, Khan et al., 2001) and the expression and formation of gap junctions (Di et al., 2001) are considered to be mediated by the rising concentrations of circulating oestrogen. Unlike other species where a decrease in progesterone precedes labour, levels of circulating progesterone remain elevated in humans, but recent research suggests that a switch in the myometrial progesterone receptor A/B isoform ratio leads to 'functional' progesterone withdrawal, which may be a trigger in the switch from uterine quiescence to active contractions (Mesiano et al., 2002, Tan et al., 2012, Mesiano et al., 2011). In addition, suppression of PRB is paralleled with increased NF-κB activation. NF-κB activity in myometrium is not only important to antagonizes the relaxatory effects of progesterone, but is also considered to upregulate expression of contraction-associated proteins such as PTGS2, and other pro-inflammatory mediators, including TNF, and IL-1β that are associated with the onset of labour (Khanjani et al., 2011, Cookson and Chapman, 2010). An up-regulation of all these cellular systems prior to labour onset ensures that the uterus is primed to respond to uterotonins and contract forcefully at the time of parturition.

***Uterine Activation via contraction-associated proteins***

The myometrial switch from a quiescent state during pregnancy to a muscle that is spontaneously active and sensitive to endogenous uterotonins during labour is termed "uterine activation". One of the primary theories for this myometrial activation proposes that it is a result of coordinated up-regulation of genes for CAPs, which may be regulated by a common mechanism (Cook et al., 2000, Tribe, 2001). CAPs include OXTR, PTGS2, Cx43 prostaglandin $F_{2\alpha}$ ($PGF_{2\alpha}$) receptor and heat shock proteins 70 and 90. The evidence for a role for CAPs in parturition originates from both human and animal studies reporting that significant increases in CAPs are associated with labour at term. In both humans and rodents, a significant increase in myometrial $PGF_{2\alpha}$ receptor mRNA expression is associated with labour at term and myometrial OXTR density increases significantly before parturition in every model in which it has been studied, including the human. Expression of OXTR and Cx43 has also been shown to increase with labour onset, possibly as a result of steroid hormone changes and uterine stretch (Garfield et al., 1977, Ou et al., 1997, Brodt-Eppley and Myatt, 1998, Brodt-Eppley and Myatt, 1999, Cook et al., 2000). Once activated, the myometrium is able to respond to stimulants such as oxytocin and prostaglandins. Prostaglandins have both direct and indirect effects on myometrial contractility; they stimulate myometrial contractions, further increase uterine sensitivity to uterotonic agents, synchronise myometrial contractions and alter hormone synthesis (Cook et al., 2000).

### *Uterine Myocyte Excitability*

The development of powerful myometrial contractions requires increased excitability of the myocytes, and increased connectivity between them. The excitability of the myometrium is governed by the myocyte resting membrane potential which is determined by opposing inward ($Na^+$, $Ca^{2+}$) and outward ($K^+$, $Cl^-$) ionic fluxes (Tribe, 2001). Before the initiation of labour, the myocyte maintains a relatively high interior electronegativity, which lowers the likelihood of depolarisation and contraction. The resting membrane potential is created by the ATPase-driven sodium-potassium pump, which transports out three sodium ions for every two potassium ions that enter the cell (Smith, 2007). Open potassium channels permit potassium ions to leave the cell along the concentration gradient, further increasing the intracellular electronegativity. The myocytes of the uterus are maintained in a relaxed state by a variety of factors that increase intracellular cyclic AMP (cAMP). The increase in cAMP activates protein kinase A, which promotes phosphodiesterase activity and dephosphorylation of myosin light-chain kinase, required to drive uterine contractions (Sanborn, 2000, Smith, 2007).

The resting membrane potential gradually becomes more depolarised as term approaches. At onset of labour, depolarisation occurs when PGF2$\alpha$ and oxytocin bind to cell-surface receptors, thus promoting the opening of ligand-regulated calcium channels. Activation of these receptors also triggers the release of calcium ions from sarcoplasmic reticulum stores. As the calcium begins to enter the cell, the drop in electronegativity stimulates the opening of large numbers of voltage-regulated calcium channels, resulting in a rapid movement of calcium ions into the cell and, subsequently, depolarisation (Tribe et al., 2000).

In a detailed study by Parkington *et al.* (1999), the resting membrane potential was shown to increase from around –70 mV at 29 weeks to –55 mV at term and during labour. These changes were associated with an increased frequency of contractions *in vitro* (Parkington et al., 1999, Tribe, 2001, Smith, 2007). This emphasises the importance of increased excitability of the myocytes for successful myometrial contractions.

***The expression of the gap junction protein connexin-43 in the myometrium is necessary for parturition***

The development of myocyte synchrony is a critical aspect of myometrial activity at labour. As parturition advances, there is increasing synchronisation of the electrical activity of the uterus (Eswaran et al., 2004, Smith, 2007). At the cellular level, this synchrony is achieved by electrical conduction through connecting myofibrils, which transmit the electrical activity to nearby muscle fibres. The activated myocytes produce prostaglandins, which act in a paracrine manner to depolarise neighbouring myocytes. This process leads to a wave of activity as multiple myocytes are recruited into the contraction (Smith, 2007).

The connectivity of myocytes that allow them to function together is promoted by gap junction connections between adjacent myocytes created by multimers of Cx43. There is an increased synthesis of the Cx43 protein that forms gap junctions at term parturition (Doring et al., 2006). Gap junctions are considered to allow the flow of current, calcium ions and small molecules (<1000 D molecular weight) between adjacent myocytes (Smith et al., 2007, Smith, 2007). The importance of Cx43 to synchronise myometrial cells and generate successful uterine contractility for parturition has been demonstrated by a study of genetically altered mice, where Cx43 deficient mice exhibited delayed parturition (Doring et al., 2006, Ratajczak and Muglia, 2008).

***Contraction of the Myometrium***

Myometrial contractions in all species arise from spontaneous action potentials due to an unstable membrane potential of the myocytes, which is likely to reflect differing ion channel expressions or biophysical profiles. Spontaneous action potentials permit the entry of calcium ions from the extracellular space, which are essential for contractile activation (Mitchell and Taggart, 2009). Actin filaments in association with myosin are essential for muscle contraction. Serine 19 on the regulatory light chains of myosin must be phosphorylated in order to achieve a significant interaction between myosin and actin (Wray et al., 2001, Wray, 2007). Myosin light chain kinase (MLCK), a serine/threonine protein kinase, enables this phosphorylation. Myocyte action potentials cause a rise in intracellular calcium ions, these bind to calmodulin which subsequently activates MLCK. Activated MLCK promotes the phosphorylation of the regulatory 20-kDa myosin light chains ($MLC_{20}$), which then initiates actin–myosin ATPase on the myosin heavy chains. The ATPase yields energy to drive the sliding of myosin over the actin filaments (cross-bridge cycling) creating the movement that establishes myometrial contraction (Moore and Bernal, 2001, Wray, 2007).

There are two key sources for the increase in intracellular calcium ions: entry across the surface membrane through voltage-gated L-type $Ca^{2+}$ channels and/or release from the sarcoplasmic reticulum (SR). The primary source of calcium ions for contraction in the myometrium are from the action potential-mediated depolarisation and consequent opening of L-type $Ca^{2+}$ channels (Matthew et al., 2004). If L-type channels are blocked or MLCK is inhibited, contractions are obliterated, underlining the importance of the $Ca^{2+}$–calmodulin–MLCK pathway for uterine contractility (Wray, 2007). There is considered to be minimal contribution of calcium ions released from uterine SR calcium stores consequent to G protein-mediated phospholipase C (PLC) hydrolysis of membrane phosphatidylinositol 4,5- bisphosphate ($PIP_2$), inositol 1,4,5-trisphosphate ($IP_3$) generation and binding to $IP_3$ receptors to release stored calcium ions into the cytoplasm (Wray, 2007).

However, there are mixed opinions regarding the contribution of the calcium ions released from these stores to the activation of myometrial contraction (Taggart and Wray, 1998, Tribe et al., 2000, Noble et al., 2009). Muscle relaxation occurs when the action potential ceases, intracellular calcium concentrations fall back to basal levels, and the myosin light chain is dephosphorylated by myosin light chain phosphatase (MLCP) (Sanborn et al., 2005).

## 1.7 Current Understanding of Maternal Age in Relation to Parturition

### 1.7.1 Timing of birth

Overall, this topic has been poorly researched. There has been very little detailed research into the impact of maternal age and delayed parturition; although clinical studies suggest they are risk factors for induction (an indication of failure to go into labour) and post-date pregnancies as mentioned in section 1.2. Assessment of the fetal HPA and hormonal cascades during human pregnancy would be technically challenging as it is difficult to investigate pregnancy experimentally in humans. As a first step, the influence of maternal age on pregnancy duration and maternal and fetal hormonal profiles could be investigated in pregnant animals.

To my knowledge, the only work to have been published investigating reproductive ageing in female C57BL/6J mice was carried out by Holinka *et al*., between 1977-1979 (Holinka and Finch, 1977, Holinka et al., 1978, Holinka et al., 1979). They reported that gestation was extended during ageing in previously parous C57BL/6J mice from 18.6 days at 3-7 months (age at which authors defined as reproductively fertile) to 20.8 days at 11-12 months (age at which authors defined as reproductively aged) (Holinka et al., 1978). They also found that plasma progesterone, measured by radioimmunoassay, decreased sharply after day 16 of gestation in 3-7 month old mice, whereas the rate of decrease in 11-12 month old mice was 55% less than in the younger group. In 3-7 months old mice, pre-parturitional progesterone levels were

inversely correlated ($p<0.05$) with the number of viable pups on day 18, whereas such a correlation ($p<0.05$) persisted from days 19-22 in the older mice. In 11-12 month old mice, gestation length was inversely correlated with litter size; no significant correlation was found in the younger group. They concluded that a decline of progesterone is generally considered necessary for parturition in rodents; therefore the retarded decrease of progesterone in 11-12-month-old mice is likely to be a major factor in their prolonged gestation (Holinka et al., 1978). Holinka *et al.*, also found average litter size decreased with age in previously parous mice from 7.8 pups in 3-7 month old mothers to 4.6 pups in 11-12 month old mothers; as well as mortality at birth being increased with gestation length in 11-12 month old mice (Holinka et al., 1978).

Holinka *et al.* (1979) went on to examine the relationships between plasma progesterone and the number of viable embryos and resorptions in aged C57BL/6J mice to elucidate the possible mechanisms contributing to the loss of fertility during ageing. In mice aged 3-7 months and 11-12 months, the older mice had 12% fewer implantation sites on days 6-10, $p<0.001$. Major losses of viable embryos occurred after day 13 in older mice, primarily because the average resorption frequency doubled ($p<0.001$). In 6% of the older mice, all conceptuses underwent resorption, which was rarely found in younger mice. They also reported that total uterine weight was less throughout pregnancy in the older mice. However, when uterine weight was normalized to viable fetuses, there were no differences between the age groups from day 10 to term. The increase in plasma progesterone values between days 1-6 were less in older mice with a significant deficit of 40% on day 4, $p<0.05$. However, no correlation was found between plasma progesterone and the number of viable fetuses or resorption sites during days 11-15 (Holinka et al., 1979).

These studies by Holinka and colleagues give some background to the impact of maternal age on the timing and success of parturition in previously parous mice at their very extreme limit of reproductive viability; however, it still remains unclear how maternal age impacts on nulliparous mice at initial stages of reproductive ageing.

### 1.7.2 Cervical ripening

Similarly, there is limited data relating to the disruption of cervical ripening as a consequence of advanced maternal age, particularly in rodents under controlled experimental conditions. A retrospective, cohort study carried out by Malamed *et al.* (2010) compared all women admitted for pre-induction cervical ripening and failed to respond to PGE2 with a randomly selected control group of women who underwent successful pre-induction cervical ripening with PGE2. They looked at 122 women in the study group and 366 in the control group. A comparison between the two groups revealed that maternal age above 30 years (OR = 2.7, 95% CI: 1.3 to 5.6) was an independent and significant predictor of cervical ripening failure with PGE2 (Melamed et al., 2010). This study suggests that there may be an abnormal regulation in the timing of the cervical ripening, or may result from unique molecular mechanisms in advanced maternal age mothers, which means that they were unable to ripen even with PGE2 administration. Similar findings are highlighted by a study which aimed to determine risk factors for failure of labour to progress. Sheiner *et al.* (2002), published that maternal age greater than 35 years was one of the independent risk factors for failure of labour to progress during the first stage (OR = 3.0, 95% CI: 2.6 to 3.6), indicating that mothers of advanced maternal age experience a greater risk of failed cervical dilation in labour (Sheiner et al., 2002).

### 1.7.3 Myometrial contractility

Advanced maternal age women have significantly more complications of pregnancy and parturition and have an increased risk of Caesarean section as previously discussed in section 1.2; however, the reason behind this remains unclear. The association of the increased incidence of clinical complications observed as maternal age increases is paralleled by evidence that ageing adversely effects uterine function. At present, there are no animal data published investigating the effect of ageing on myometrial activity, but to my knowledge, there are two human studies. Smith *et al.* (2008) have shown that there is a linear relationship between the age of the mother and the risk of Caesarean delivery, operative vaginal birth and long duration of labour. Older age in first pregnancy was associated with both an increased risk of Caesarean section and increased duration of labour. Moreover, the need for operative vaginal deliveries was also higher in women of advanced age and these findings were shown not to be explained by comorbidities such as obesity or gestational diabetes. In this study, they measured the function of human myometrium in relation to age by using a standard organ bath system. Spontaneous contractile activity was quantified and also assessed for coupling as can be seen in Figure 1.10. Coupling was defined as the presence of two or more distinct peaks before the return to baseline, which is generally associated with dysfunctional labour *in vivo* (Smith et al., 2008). They found that spontaneous contraction of isolated myometrium strips declined with advancing maternal age, and that there was a 93% increase in the chance of developing coupling with a five year increase in age. Both clinical and scientific data would indicate a decline in myometrium function with advancing maternal age (Smith et al., 2008). However, the data for spontaneous contractile activity in this study is presenting only as the ratio of the mean integral tension during spontaneous contractile activity and the mean integral tension under in the presence of 50 mM potassium, making the data difficult to compare to other uterine contraction studies where more information such as force and frequency of spontaneous contractions, as well as the mean integral tension of spontaneous contractions alone are also provided.

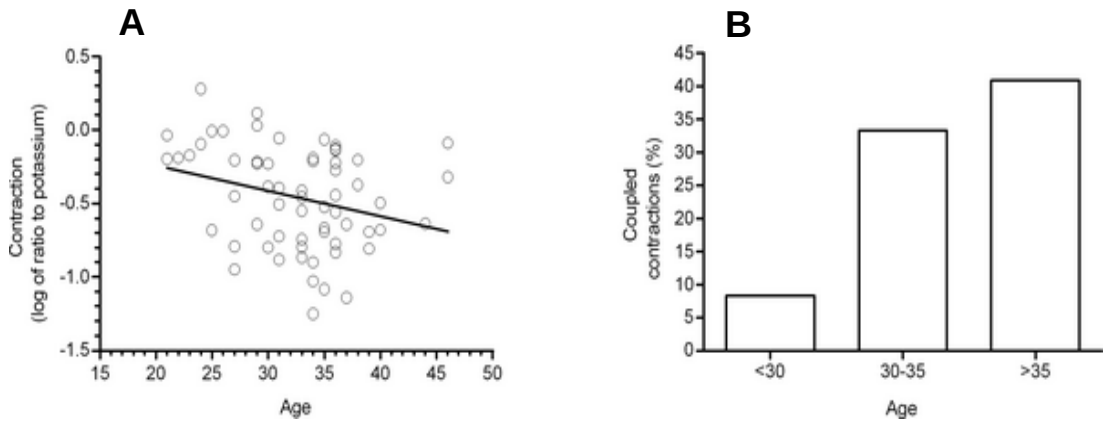


**Figure 1.10 *Ex vivo* human myometrial contractility in relation to maternal age**
**A:** Mean spontaneous contractile activity (quantified as contraction units) of isolated strips of myometrium obtained from women (n=62) at the time of planned Caesarean section in relation to the age of the donor. **B:** The proportion of spontaneous contractions that were multiphasic in relation to maternal age (n=62, 181 samples). Figure from: The effect of delaying childbirth on primary cesarean section rates (Smith et al., 2008).

It has been proposed that the myometrium is less effective or less responsive to uterotonic agents such as oxytocin or prostaglandins with increasing maternal age (Greenberg et al., 2007). This theory is supported by Main *et al.* (2000), who indicated an increasing need for oxytocin-augmentation in women of older age and suggested that this effect of ageing was a gradual and continuous process (Main et al., 2000). In a recent study published by Arrowsmith *et al.* (2012), they examined myometrial contractility in over 100 women, aged 25–72 (both pregnant and non-pregnant). Myometrial function in relation to age was measured using a standard organ bath system; myometrial tissues were examined within 12 hours of biopsy excision, and allowed to equilibrate for two hours to generate stable spontaneous contractions. Spontaneous contractile activity was quantified in the presence and absence of oxytocin, to provide evidence to support the theory described by Main *et al.* (2000) and Greenberg *et al.* (2007). Arrowsmith *et al.* (2012) reported a significant decrease in spontaneous contractility seen with increase in age; however this is reported only for myometrium in non-pregnant state.

In pregnant myometrium, they found a wide range of contractile ability between pregnant women and little evidence for decreased spontaneous activity between the ages of 25–40, as shown in Figure 1.11. It is important to note here that the age range included for the non-pregnant myometrial samples is much wider (25–72 years) than for the pregnant myometrial samples, so a direct comparison cannot be drawn between the two cohorts. Authors also report a decline in responses to oxytocin (10 nM; expressed as a percentage increase in integral of force compared to control) with increasing maternal age (Arrowsmith et al., 2012). However, statistical analyses provided do not support this statement.

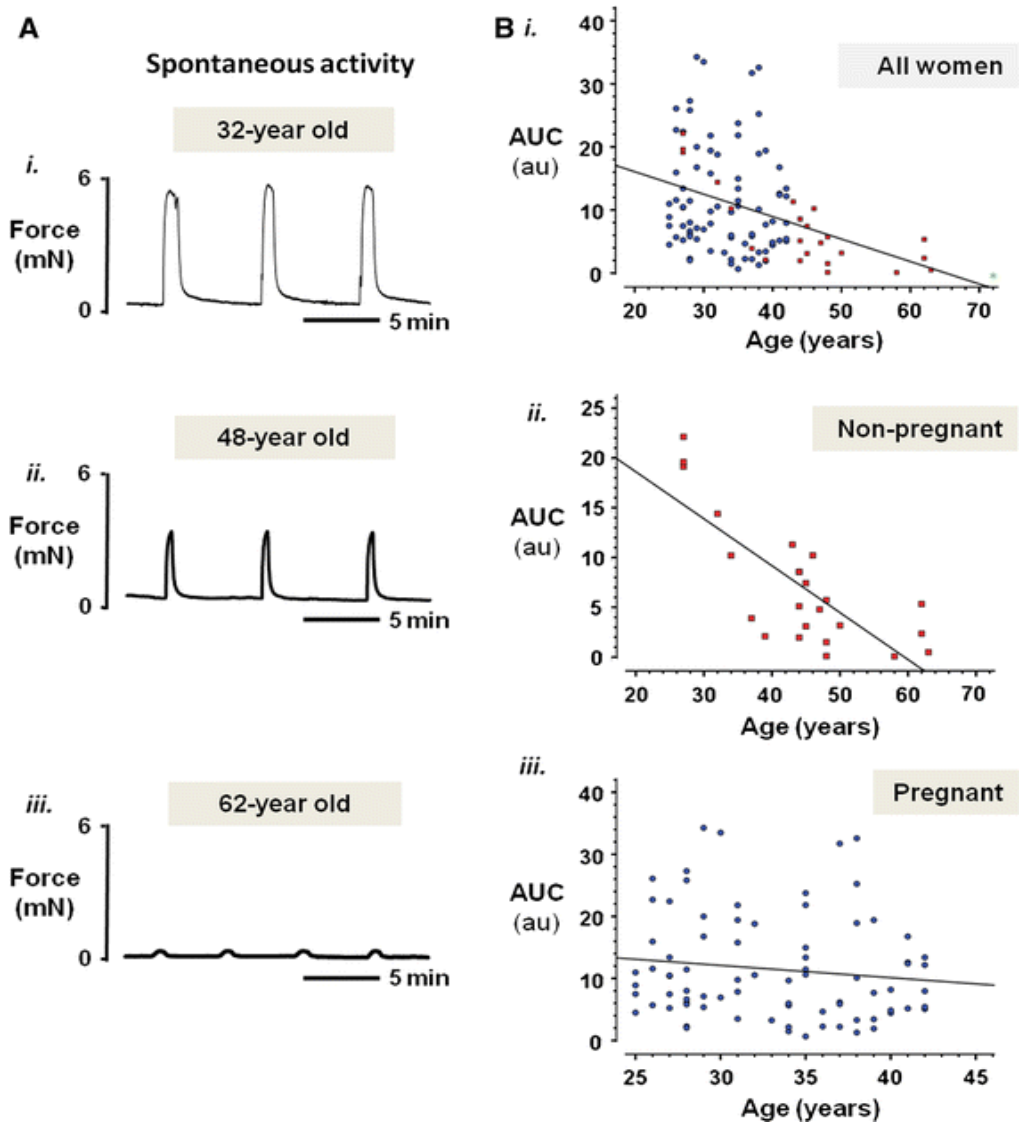


**Figure 1.11 Myometrial contractility in relation to maternal age**

**A:** Representative traces of isometric recordings of spontaneously contracting myometrial strips obtained from a (i) 32-year old, (ii) 48-year old and (iii) 62-year old woman undergoing hysterectomy. **B:** Plots of spontaneous contractile activity [quantified as area under the contraction curve, (AUC, in arbitary units, au)] of strips of pregnant and/or non-pregnant myometrium obtained from women undergoing planned Caesarean section delivery or hysterectomy respectively, against age. Spearman's rank test found a significant negative correlation between integral of force and age (i; combined data, r = -0.379, p< 0.01, n = 104). (ii, iii) Plots of non-pregnant and preg-nant women separately. A significant negative correlation between integral of force and age was found for non-pregnant women alone (ii; r = -0.529, p = 0.008, n = 24). In contrast, no significant correlation was found for pregnant women (iii; n = 80). Pregnant women are denoted by blue circles, non-pregnant women are denoted by red squares. Figure from: What do we know about what happens to myometrial function as women age? (Arrowsmith et al., 2012).

## 1.8 Study Hypotheses and Objectives

In summary, review of the literature indicates there is a need to investigate the reasons why older women aged 35 years and above, exhibit a higher incidence of complications in pregnancy and labour. Experimental evidence is sparse and there is no clear understanding of how physiological processes are impaired as women age. A more detailed understanding of the mechanistic impacts of ageing on labour could ultimately influence the clinical management of these women.

The overarching goal of this study was to determine whether advanced maternal age has a detrimental impact on uterine and/or cervical function at the end of gestation. There are several hypotheses to be explored due to the complexity of the hormonal processes of the timing of parturition that trigger the initiation of cervical ripening and myometrial activation. It is technically and ethically difficult to fully explore these mechanisms in pregnant women, and as a result a mouse model of maternal ageing in pregnancy was used in an attempt to dissect out the contribution of each factor on parturition independently and in combination.

***Hypotheses***

1. The timing/initiation of labour will be disrupted and prolonged in older mothers, as a consequence of delayed parturition signals.
2. The physiological preparation and consequent ripening of the cervix will be delayed in older mothers, contributing to the possible delay in parturition.
3. The physiological activation of myometrium at term will be delayed in older mothers, contributing to the possible delay in parturition.
4. The ability of the myometrium to contract at term will deteriorate in older mothers as a result of a reduction in the number of functional myometrial mitochondria, resulting in reduced ATP generation and energy availability for effective uterine contractions during labour.

***Specific objectives***

1. To validate the methodology used within this thesis.
2. To demonstrate that advanced maternal age in mice impacts on gestation length and parturition duration.
3. To assess the impact of maternal age on gene/protein expression in myometrium and cervix from non-pregnant and pregnant mice.
4. To determine whether age induced alterations in the gene/protein expression in the myometrium/cervix or mitochondrial function translate into disruptions in spontaneous and agonist-induced myometrial contractility and cervical tensile strength (a measure of cervical softening) *in vitro*.
5. To determine mitochondrial copy number and function in myometrium from non-pregnant and pregnant mice of different ages.

# Chapter 2

## Materials and Methods

# Chapter 2 : Materials and Methods

## 2.1 Animals

### 2.1.1 Mouse model of advanced maternal age

The “Breeding Strategies for Maintaining Colonies of Laboratory Mice” manual compiled by the Jackson Laboratory (USA), states that female laboratory mice typically become sexually mature between five and eight weeks of age. When referring to reproductive life span, this manual states that a female laboratory mouse can breed up to approximately seven to eight months post sexual maturity (Lambert, 2009). Nelson and colleagues (1982, 1984) published some fundamental work on the oestrous cycle in ageing C57BL/6J mice. They confirmed that cycle frequency was initially low (Phase I) in mice under the age of three months, due to prolonged cycle durations and late-starting cycles. Phase II, when mice were three to five months old, was when cycle frequency peaked; this typically lasted between seven to ten months. Thereafter cycle frequency declined steadily, known as Phase III. They found that the average age of cessation of cycling was varied, but usually occurred between eleven and sixteen months of age. During the peak cycling period in phase II, the average cycle lengths were four days, but these became progressively longer by nine months of age. (Nelson et al., 1982, Felicio et al., 1984). This evidence suggest that peak reproductive ability begins to decline after nine months of age and can completely cease as early as eleven months of age in C57BL/6J mice.

Considering the work by Nelson and colleagues, and in collaboration with Charles River (Charles River Laboratories, UK), it was decided that virgin C57BL/6J mice at eight months of age would suitably model nulliparous advanced maternal age (definition of advanced maternal age in women indicates pregnancy at any age above thirty five years (Bewley et al., 2009)). In this strain of mouse, it was evident that pregnancy success was already lowered at this age, since a total number of fifty females would need to be mated in order to achieve ten estimated pregnancies in the mice. This is a considerably lower pregnancy success rate than that seen with younger C57BL/6J females. A control group, at three months of age was used to

model when cycle frequency firsts peaks (Nelson et al., 1982, Felicio et al., 1984) assuming this to be a period when reproduction ability would be at a maximum. Finally, to determine the degree to reproductive decline seen with age in this particular strain, a mid-group at five months of age was also used for some experimental techniques (stated within individual results chapters where applicable). The age three, five and eight months are indicative of the age when mice were mated rather than age at the end of gestation. All mice were maintained under controlled conditions (25°C, 12-hour light/dark cycle), and fed a standard chow diet. Females (all ages) were mated with C57BL/6J males approximately three to four months of age (Charles River Laboratories, UK). Conception was determined by the presence of a vaginal plug (day 0 of gestation). All animals were treated in accordance with The Animals (Scientific Procedures) Act 1986 guidelines.

### 2.1.2 Age matched non- pregnant controls

Where appropriate, experimental techniques were repeated with age matched (three, five and eight month old) non-pregnant female mice. To control for changes to uterine smooth muscle during the mouse oestrous cycle, all tissue was collected when mice were in the oestrous stage of their cycle.

***Determination of non-pregnant mouse oestrous cycle:***

All C57BL/6J mice were sourced from Charles River, and allowed to acclimatise to their new environment for one week after which daily vaginal smearing commenced. Vaginal smearing was carried out at the same time every day (between the hours of 10.00-11.30AM). Each mouse was held securely using the scruffing technique, while the vagina was flushed with $H_2O$ using a thin-ended Pasteur pipette (SLS, UK). The flushed fluid droplet was expelled onto a microscope slide and examined under a light microscope (Olympus, UK), so that the cells could be characterised. The oestrous stage was confirmed by the presence of large cornified epithelial cells with very few or no visible nuclei; an example is shown in Figure 2.1.

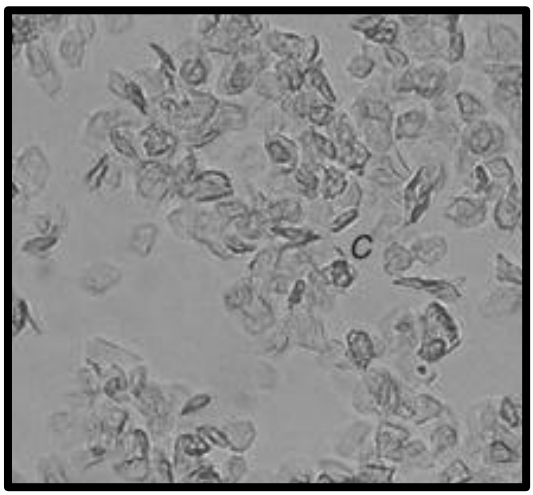


**Figure 2.1 Unstained vaginal secretion from mouse (oestrus stage), with anucleated cornified epithelial cells**
Figure from: Assessing reproductive status/stages in mice (Caligioni, 2009).

### 2.1.3 Mouse serum and tissue collection

On day 18 of gestation, time mated pregnant mice were killed by cervical dislocation, in accordance with Schedule 1 of UK Home Office guidelines. Immediately after mice were confirmed dead, approximately 500 μl of blood was collected into a 2 ml round bottomed microcentrifuge tube (Eppendorf, Germany) from each mouse by cardiac puncture. Each microcentrifuge tube was incubated in an upright position at room temperature for 30 minutes to allow clotting, after which it was spun in a centrifuge for 10 minutes at 13000 x *g* to separate serum. The supernatant (serum) was carefully aspirated at room temperature, aliquote into a cryogenic vial (Sigma-Aldrich, UK) and stored at −80°C until required for serum progesterone measurements.

Once blood had been collected, uterine horns, cervices and bladders were carefully dissected from each mousse. Placenta and fetuses were removed from uterine tissue, and fetuses were immersed in ice-cold PBS. After dissection, uterine, cervical and bladder tissues were either immediately snap frozen in liquid nitrogen for deoxyribonucleic acid (DNA) extraction and protein isolation, placed into RNAlater (Ambion, Warrington, UK) according to manufacturer's recommendations for ribonucleic acid (RNA) extraction and then stored at −80°C (RNAlater is an aqueous, non-toxic tissue storage reagent that rapidly permeates tissue inactivating RNAase activity to prevent breakdown of RNA, its composition and formulation is proprietary information), or placed straight into ice-cold, phosphate-buffered saline (PBS; Sigma-Aldrich, UK) for isometric tension recording. Cervical biopsies taken for histological analysis were fixed by overnight immersion in 10% (v/v) formal saline solution (Formaldehyde solution 10% v/v in 0.9% NaCl solution; Fisher Scientific, UK), after which they were embedded in paraffin (see section 2.8.1 for further details). Non-pregnant mice were confirmed to be at oestrous stage of their cycle, after which uterine and cervical tissue were collected in the same way as described above for pregnant mice.

For all planned experiments, tissue were collected from aged late pregnant and non-pregnant mice (eight month old, n = 6-10), compared to young late pregnant and non-pregnant mice (three month old, n = 6-10), and where applicable mid-age late pregnant and non-pregnant mice (five month old, n = 6-10).

## 2.2 RNA and DNA Extraction

### 2.2.1 RNA extraction from mouse uterine and bladder tissue

Total RNA was extracted from uterine and bladder tissues (bladder tissues for microarray studies-section 2.4) using the RNeasy Kit from Qiagen (Qiagen, UK). The use of guanidinium isothiocyanate in RNA extraction was first mentioned by Ullrich *et al.* in 1977 (Ullrich et al., 1977). This method was laborious, so it was modified to a single step technique, known as guanidinium thiocyanate-phenol-chloroform extraction as described by Chomczynski and Sacchi in 1987 (Chomczynski and Sacchi, 1987). These conventional methods have since been modified further, to use solid-phase nucleic acid purification. Most commercial extraction kits such as the RNeasy kit use solid-phase nucleic acid purification (Tan and Yiap, 2009). This technique allows rapid, efficient RNA isolation compared to conventional methods, and also prevents problems that are associated with liquid-liquid extraction such as incomplete phase separation (Esser et al., 2005).

Solid-phase purification is normally performed by using a spin column, operated under centrifugal force, and use either silica matrices, glass particles, diatomaceous earth, or anion-exchange carriers as the solid support. Four key steps involved in solid-phase extraction are cell lysis, nucleic acids adsorption, washing, and elution (Tan and Yiap, 2009). With the silica matrix RNeasy kit, samples are first lysed and homogenized in the presence of a highly denaturing guanidine-thiocyanate–containing buffer in the presence of beta-mercaptoethanol, which separates rRNA from ribosomal proteins and immediately inactivates RNases by reducing disulphide bonds and destroying the

native conformation required for enzyme functionality; this ensures purification of intact RNA. Ethanol is then added to the lysate to create conditions that promote selective binding of RNA to the RNeasy membrane, since such solid phase systems will absorb nucleic acid in the extraction process dependent on the high salt content and pH of the binding buffer. The sample is then applied to the RNeasy Mini spin column. Total RNA binds to the membrane, and contaminant biomolecules such as carbohydrates, proteins, and fatty acids are efficiently washed away in the presence of a stringent washing buffer containing a guanidine salt and ethanol. Finally, a mild washing buffer (composition of which is proprietary) removes traces of salts which are still on the column due to buffers used earlier in the protocol, allowing elution of high-quality RNA in RNase-free water. The absorption process is based on the following principle: hydrogen-binding interaction with a hydrophilic matrix under chaotropic conditions; other solid-phase purification techniques rely on ionic exchange under aqueous conditions by means of an anion exchanger and affinity and size exclusion mechanisms (Tan and Yiap, 2009).

Once extracted, the integrity of the RNA is determined by two methods. The first is calculated by spectrophotometric absorbance at 260 nm. This reflects nucleic acid concentration so that one unit of optical density reflects 40 µg RNA/ml sample analysed (Wilson and Walker, 2010). In addition to this, the 260/280 nm ratio is also calculated; this value indicates any contamination from DNA/protein that may be present. A typical value for good quality RNA is usually ≥1.8 (Wilson and Walker, 2010, Wilkinson, 2000), considering a ratio of ~2 is generally accepted as “pure” RNA (Manchester, 1996). This method remains the most economical and commercial method of RNA quality analysis. However, it is important to note that the accuracy of the 260/280 nm absorbance method has been questioned, as a value of 1.8 could correspond to only 40 % RNA, with the remainder accounted for by protein (Bustin and Nolan, 2004).

The second technique uses gel electrophoresis to determine the integrity of ribosomal RNA (18S and 28S) (Fleige and Pfaffl, 2006). It measures ribosomal RNA bands on a partial denaturing agarose gel. The RNA is heated prior to loading as this disrupts the secondary structures, allowing RNA migration (Wilson and Walker, 2010). Migration of RNA along an agarose gel in an electric field is a result of the negative charge on competent nucleic acids from their negatively charged phosphate groups (Wilkinson, 2000). The magnitude of the overall negative charge of each RNA is proportional to its size. The RNA is separated on the gel moving towards the anode at a rate inversely proportional to its size. A solution of RNA of known molecular masses is included on each occasion in order to allow the molecular weights of RNA subsequently detected to be determined by comparison. Once the RNA has been separated, they can be visualised using UV light as long as the gel has been prior stained with SYBR Safe stain (Invitrogen, UK), which attaches onto the RNA and is excited by the light.

RNA is unstable due to the ubiquitous presence of RNases which are enzymes present in blood, all tissues, as well as most bacteria and fungi in the environment; therefore, RNA extraction relies on good laboratory technique and RNase-free technique (Tan and Yiap, 2009). In order to minimise the risks of contamination and degradation of RNA, the environment and reagents had to be ribonuclease-free; all solutions and equipment were autoclaved. Several measures were taken to achieve and maintain this including the use of Milli-Q treated water, treatment of tips and eppendorff tubes while wearing gloves and the use of the laminar flow cabinet to set up reactions. Moreover, all samples are maintained on ice throughout and aliquots of RNA containing solutions are prepared at the time of extraction to minimise the requirement of repeated freezing and thawing, which is known to lead to RNA degradation (Wilson and Walker, 2010).

### 2.2.2 RNA extraction protocol

Total RNA was extracted from ~ 30 mg of tissue, which was added to 600 μl of guanidine-thiocyanate–containing RLT lysis buffer (RNeasy mini kit, Qiagen, UK) in a 2 ml RNAse-free round bottomed microcentrifuge tube (Eppendorf, Germany). The sample was then homogenised using a TissueLyser (Qiagen, UK; 2 minutes at 25 Hz using two 5 mm steal beads) until the tissue had been visibly broken down. RNA was extracted from the lysate using the RNeasy mini kit (Qiagen, UK) as per manufacturer's recommendations. Since RNA is susceptible to degradation by enzyme-induced hydrolysis, gloves were worn. Both gloves and work spaces were sprayed with TriGene disinfectant (Medichem International, UK). At the end of RNeasy protocol, the extracted RNA was eluted in 30 μl of RNase/DNase free water (Qiagen, UK).

The RNA concentrations from these extractions were determined by spectrophotometric analysis (Wilson and Walker, 2010). Aliquots of each sample (1.5 μl) were used and spectrophotometric absorbance measured using a NanoDrop® spectrophotometer (NanoDrop® ND-1000 Spectrophotometer, Nanodrop Technologies, Labtech, UK). The absorbance at 260 nm relative to Milli-Q water alone was measured. In addition, the absorbance of each sample at 280 nm was measured. This allowed the calculation of the ratio of optical density of the samples at 260:280 nm. Spectrophotometric absorbencies at 260 nm reflect nucleic acids, whereas that at 280 nm reflects protein contaminants. A ratio ≥ 1.8 is regarded as satisfactory (Wilson and Walker, 2010). RNA concentrations are automatically calculated using the absorbance at 260 nm using the software (Nano D2000) with the spectrophotometer, where one unit of optical density reflects 40 μg RNA/ml.

*RNA concentration of the stock extraction (µg/µl) =*

$$\frac{\text{(Optical density at 260 nm x 40 µg/ml) x (mls of sample)}}{\text{Original stock volume added (µl)}}$$

Once quantified, each RNA sample was stored at - 80°C until required.

### 2.2.3 Agarose gel electrophoresis of RNA

A 2% agarose gel was made and used to run the RNA samples, as a test of integrity. High resolution agarose (2 g; Sigma-Aldrich, UK) was dissolved in 100 ml 0.5 × tris-borate EDTA/H2O (TBE) (diluted from 10 x TBE stock; Sigma-Aldrich, UK) by melting at 80- 100$^{o}$C for about two minutes until the agarose was fully dissolved. SYBR safe DNA gel stain (10 µl; Invitrogen, UK) was added to the 100 ml of melted agarose and then quickly poured into a level horizontal gel tank containing an appropriate size comb inserted, allowing wells to form. After around 45 minutes, once the gel had set, the comb was removed and the gel covered with 1 x TBE. Prior to loading, 1-3 µg of the RNA samples were mixed together with 8 µl of RNA loading dye (2 x RNA loading dye supplied with RNA ladder, Fermentas, UK) and heated at 65$^{o}$C for 10 minutes to disrupt the secondary structures. These samples were then loaded alongside a RNA marker (RiboRuler High Range RNA Ladder Ready-to-Use, 200 to 6000 bases, Fermentas, UK) to be used as a size comparison. Electrophoresis was then performed at a constant 100 V for approximately 2 hours. RNA was then visualised using the Gel Logic 2200 Pro Imaging System and Carestream Molecular Imaging software (Carestream Health, USA). The size and quality of RNA (28S and 18S) was then estimated by comparison to the RNA ladder.

### 2.2.4 cDNA Synthesis

Extracted RNA, 1 µg was added to a tube containing 1 µl (250 ng) random primers (Promega, UK), 1 µl 10 mM dNTP mix (Promega, UK) and RNase/DNase free water (Qiagen, UK) was added to give a final volume of 13 µl. Contents were briefly centrifuged (30 seconds at 13000 x *g*) after which the mixture was heated to 65$^{o}$C for five minutes before standing for one minute on ice. Contents were briefly centrifuged (30 seconds at 13000 *x g*) again and then 4 µl of First-strand buffer (Invitrogen, UK), 1 µl of 0.1M DTT (Invitrogen, UK), 1 µl (20 international units) of RNAsin, an RNase inhibitor (Promega, UK) and 200 international units SuperScript III (Invitrogen, UK) were added.

The contents of the tube were mixed by gentle pipetting after which, the tube was incubated for 5 minutes at 25$^{o}$C to enhance binding of the random hexamers to the template RNA, then heated to 50$^{o}$C for 60 minutes to allow cDNA synthesis and finally to 70$^{o}$C for 15 minutes to inactivate the reaction. RNase/DNase free water was added to give a final volume of 80µl. cDNA concentration (ng/µl) for each sample was quantified using the NanoDrop ND-1000 spectrophotometer (Nanodrop Technologies, Labtech, UK), and then each sample was diluted to 100 ng/µl using RNase/DNase free water (Qiagen, UK) if necessary. All cDNA samples were stored at -80$^{o}$C until required for quantitative real time PCR (qPCR).

### 2.2.5 DNA extraction from mouse uterine tissue

Total genomic DNA was extracted from uterine tissues using the ReliaPrep gDNA Purification kit (Promega, UK). The very first DNA isolation was performed by a Swiss physician, Friedrich Miescher in 1869 (Dahm, 2005). Since then, numerous methods have been developed; currently, they are divided into solution-based or column-based protocols. Most of these protocols have been developed into commercial kits that ease the DNA extraction process (Tan and Yiap, 2009). The ReliaPrep gDNA Purification kit used for this thesis employs a column-based protocol, following a four-step method:

1. Effectively disrupting or homogenizing the starting material to release the DNA.

2. Binding the DNA to the ReliaPrep™ Binding Column.

3. Removing impurities with wash solution.

4. Eluting the purified DNA.

No ethanol is used in the purification protocol, eliminating downstream problems caused by ethanol carryover.

The principle of such silica/cellulose column based purification is based on the high affinity of the negatively charged DNA backbone towards the positively charged silica particles (Esser et al., 2006). Sodium plays a role as a cation bridge that attracts the negatively charged oxygen in the phosphate backbone of nucleic acid. Sodium cations break the hydrogen bonds between the hydrogen in water and the negatively charged oxygen ions in silica under high salt conditions (pH ≤ 7) (Tan and Yiap, 2009). The DNA is tightly bound, and extensive washing removes all contamination. The purified DNA molecules can be eluted under low ionic strength (pH ≥ 7) by using ultra-pure 18 MOhm RNase/DNase water.

Once extracted, the DNA yield can be assessed using similar methods to that used for RNA yield analysis: absorbance (optical density), and agarose gel electrophoresis.

The most common technique to determine DNA yield and purity is absorbance, using a NanoDrop® spectrophotometer. Absorbance readings are performed at 260 nm (A260) where DNA absorbs light most strongly, and the number generated allows one to estimate the concentration of the solution. To ensure the numbers are useful, the A260 reading should be between 0.1–1.0 (Adams, 2003). However, DNA is not the only molecule that can absorb UV light at 260 nm. RNA also has a great absorbance at 260 nm, and the aromatic amino acids present in protein absorb at 280 nm, therefore if both contaminants are present in the DNA solution, they will contribute to the total measurement at 260 nm, meaning that the DNA quantity may be overestimated (Adams, 2003).

To evaluate DNA purity by spectrophotometry, the most common purity calculation is determining the ratio of the absorbance at 260 nm divided by the reading at 280 nm. Good-quality DNA will have an A260/A280 ratio of 1.7–2.0 (Teare et al., 1997). Strong absorbance around 230 nm can indicate that organic compounds or chaotropic salts are present in the purified DNA. A ratio of 260 nm to 230nm can help evaluate the level of salt residue in the purified DNA; the lower the ratio, the greater the amount of thiocyanate salt present. A reading at 320nm will indicate if there is turbidity in the DNA solution, indicating possible contamination. Therefore, taking a spectrum of readings from 230nm to 320nm is most informative (Wilfinger et al., 1997).

DNA concentration can be estimated by adjusting the A260 measurement for turbidity (measured by absorbance at 320 nm; A320), multiplying by the dilution factor, and using the relationship that an A260 of 1.0 = 50µg/ml pure DNA (Manchester, 1995).

*DNA concentration of the stock extraction (µg/µl) =*

(A260 reading – A320 reading) × dilution factor × 50 µg/ml

Agarose gel electrophoresis of the purified DNA reduces the issues associated with absorbance readings. As already described for RNA extraction in section 2.2.3, DNA samples intercalating with a DNA dye (6x DNA loading dye; Fermentas, UK) along with appropriately sized DNA ladder (50 bp ladder, Invitrogen, UK) can be run on a partial denaturing agarose gel stained with SYBR Safe stain (Invitrogen, UK). The negatively charged DNA backbone migrates toward the anode. Since small DNA fragments migrate faster, the DNA is separated by size. Any RNA, nucleotides and protein in the sample migrate at different rates compared to the DNA so the band(s) containing the DNA will be distinct (Wilson and Walker, 2010). Concentration and yield can be determined after gel electrophoresis is completed by comparing the sample DNA intensity to that of a DNA quantitation standard on the ladder.

### 2.2.6 DNA extraction protocol

Total genomic DNA was extracted from ~ 25 mg of tissue. Tissue was minced using a sterile scalpel (Swann Morton, UK) and added to 160 µl of PBS (Sigma-Aldrich, UK) in a 2 ml RNAse-free round bottomed microcentrifuge tube (Eppendorf, Germany), both were briefly mixed by vortex. The sample was then homogenised using a TissueLyser (Qiagen, UK; two minutes at 25 Hz using two 5 mm steal beads) until the tissue had been visibly broken down. DNA was extracted from the lysate using the ReliaPrep gDNA Purification kit (Promega, UK) as per manufacturer's recommendations. At the end of ReliaPrep gDNA Purification protocol, the extracted DNA was eluted in 100 µl of RNase/DNase free water (Qiagen, UK). Samples were quantified to give a DNA concentration in ng/µl and were checked for DNA integrity, using the NanoDrop ND-1000 spectrophotometer (Nanodrop Technologies, Labtech, UK). The absorbance of each sample at 260 nm and 280 nm relative to RNase/DNase free water alone was measured. This allowed the calculation of a ratio of optical density of samples at 260:280 nm. A ratio between 1.7-2.0 was regarded as satisfactory. Once quantified, each DNA sample was diluted to 50 ng/µl in a total volume of 100 µl using RNase/DNase free water (Qiagen, UK), and then placed in a bath sonicator (Pulsatron 55; Kerry Ultrasonics Ltd., UK) for ten minutes to shear the DNA and minimise dilution bias. Samples were then stored at - 20°C until required for quantitative real time PCR (qPCR).

## 2.3 Polymerase Chain Reaction (PCR)

Absolute quantification of unknown samples using qPCR requires a standard curve generated from serial dilutions of cDNA (of known quantities) amplified using the primers for the gene of interest.

### 2.3.1 Oligonucleotide primers

Primers required qPCR were designed using Universal Probe Library Assay Design Centre, Roche Applied Science (https:// www.roche-applied-science.com). Where possible, primers were designed ensuring that the sequences were overlapping exon-intron boundaries and amplified a product of ~ 100 base pairs (bp) in size. All oligonucleotides were purchased from Eurofins MWG Operon, Germany. Once delivered, primers were re-suspended with the appropriate volume of RNase/DNase free water (Qiagen, UK) as directed by manufacturer to give a stock concentration of 100 μM. Table 2.1 shows the forward and reverse primer sequences for all primers used for qPCR gene expression experiments.

**Table 2.1 Oligonucleotide primer sequences**

| Primer | Accession Number | Sequences |
|---|---|---|
| **mouse GAPDH** (glyceraldehyde-3-phosphate dehydrogenase) | NM_001001303 | **Forward primer:** 5'-TTGATGGCAACAATCTCCAC-3' **Reverse primer:** 5'-CGTCCCGTAGACAAAATGGT-3 |
| **mouse β2M** (beta-2 microglobulin) | NM_009735 | **Forward primer:** 5'-TTCAGTATGTTCGGCTTCCC-3' **Reverse primer:** 5'-TGGTGCTTGTCTCACTGACC-3' |
| **mouse β- actin** | NM_007393 | **Forward primer:** 5'-ATGGAGGGGAATACAGCCC-3 ' **Reverse primer:** 5'-TTCTTTGCAGCTCCTTCGTT-3' |
| **mouse OTR** (oxytocin receptor) | NM_001081147.1 | **Forward primer:** 5'-GTGCAGATGTGGAGCGTCT-3' **Reverse primer:** 5'-GTTGAGGCTGGCCAAGAG-3' |
| **mouse Cx43** (connexin 43) | X61576.1 | **Forward primer:** 5'-GTGCCGGCTTCACTTTCA-3' **Reverse primer:** 5'-GGAGTAGGCTTGGACCTTGTC-3' |
| **Mouse PTGS2** (Prostaglandin-endoperoxide synthase 2) | NM_011198.3 | **Forward primer:** 5'-GGGAGTCTGGAACATTGTGAA-3' **Reverse primer:** 5'-GTGCACATTGTAAGTAGGTGGACT-3' |

*F = Forward primer sequence; R = Reverse primer sequence.*

### 2.3.2 Reverse-transcriptase polymerase chain reaction (RT-PCR)

Polymerase Chain Reaction (PCR) is a technique used to amplify a single or a few copies of a selected region of DNA and multiply it across several orders of magnitude, generating thousands to millions of copies of that particular DNA sequence. Since its development in 1983 by Kary B. Mullis, PCR has revolutionised molecular biology. PCR has widespread medical and biological applications in many diverse fields including forensic science, histopathology, epidemiology, prenatal diagnostics (Baumforth et al., 1999), genetics, and gene cloning (Saiki et al., 1988).

Any region of any DNA molecule can be selected for PCR amplification provided the sequences at the borders of the selected regions are known. PCR involves two primers (single-stranded DNAs), which are complementary to opposite strands of the double stranded DNA sequence to be amplified. The use of thermostable DNA polymerase I allows the double stranded DNA to be separated and subsequently permits the primers to anneal to their respective sequences with minimal loss of enzymatic activity. The basic process of PCR is carried out over several cycles (typically 30- 35 cycles) of denaturation, hybridisation and synthesis resulting in the eventual synthesis of several hundred million copies of the desired DNA fragment.

Since many cellular decisions concerning survival, growth and differentiation are reflected in altered patterns of gene expression, the ability to quantitate transcription levels of specific genes is essential to any research into gene function. PCR is often coupled with reverse-transcription PCR. Reverse transcription polymerase chain reaction (RT-PCR) is currently the most sensitive method for the detection of low-abundance mRNA, which has often been obtained from limited tissue samples (Bustin, 2000, Bustin et al., 2005). The procedure, allows generation of complementary DNAs (cDNAs) for cloning using a reverse transcriptase enzyme; the cDNA can then be amplified by PCR. Most commonly used transcriptases are derived from avian myeloblastosis virus (AMV) or Moloney murine leukaemia virus (MMLV). Although both enzymes are routinely used, AMV reverse transcriptase has an advantage of

having its optimum temperature for reverse transcription of 42$^{o}$C, which appears to be of benefit if the RNA template has a high degree of secondary structure (Baumforth et al., 1999).

### 2.3.3 Reverse-transcriptase polymerase chain reaction (RT-PCR) optimisation

***Primer concentration optimisation:***

The thermodynamic stability of a duplexed primer/target structure differs for different primers and varies with primer concentrations (Nolan et al., 2006). Therefore, it is important to determine the concentration of both 5' and 3' primers that would result in optimal hybridization and priming. Real time quantitative PCR (qPCR) assays as detailed in section 2.3.8 were performed using differing combinations of concentrations of forward and reverse primers, as shown in Table 2.2 to determine optimum primer concentrations.

**Table 2.2 Primer concentration combinations tested to determine optimal primer concentrations**

| Forward Primer Concentration (nM) | Reverse Primer Concentration (nM) |
|---|---|
| 100 | 100 |
| 100 | 200 |
| 100 | 300 |
| 100 | 400 |
| 200 | 100 |
| 200 | 200 |
| 200 | 300 |
| 200 | 400 |
| 300 | 100 |
| 300 | 200 |
| 300 | 300 |
| 300 | 400 |
| 400 | 100 |
| 400 | 200 |
| 400 | 300 |
| 400 | 400 |

All forward and reverse primer sets were optimised to be used at 300 nM F, 300 nM R working concentrations, in a total reaction volume of 10 μl. The best primer concentrations were those that gave the lowest Ct value, the highest fold fluorescence change, and no primer dimer or non-specific amplification, as defined by Nolan et al., (Nolan et al., 2006). Melt curve analyses were performed to confirm the presence of one single product, and non-template controls were run to assess contamination. For each primer set, it was confirmed that unknowns sample quantification values fell within the dynamic range of the standard curve.

Figures 2.2 and 2.3 illustrate examples of primer validation for two of the genes examined using qPCR in this study: mouse glyceraldehyde 3-phosphate dehydrogenase (GAPDH) and mouse $\beta_2$ microglobulin ($\beta_2$M). Cut off values for efficiency and $R^2$ were 80% and 0.99 respectively (Bustin et al., 2005). The qPCR products for all genes were sequence verified and run on a gel to confirm product band size.

### 2.3.4 Reverse-transcriptase polymerase chain reaction (RT-PCR) protocol

RT-PCR amplifications were performed for all of the genes shown in Table 2.1. Each RT-PCR reaction volume contained the following: 3.5 μl of cDNA (100ng; from uterine muscle), and 0.75 μl (10 μM, 300nM final conc.) of each primer (forward and reverse; Eurofin MWG Operon, Germany), these were made up to a final reaction volume of 25 μl using 12.5 μl HotStarTaq master mix (Qiagen, UK) and 7.5 μl RNase/DNase free water (Qiagen, UK). All RT-PCR reactions were performed in a Px2 Thermal Cycler (Thermo Electron Corporation, UK). Cycling conditions used: initial activation step: 95˚C for 15 minutes; followed by 3 step cycling: denaturation 94˚C for 1 minute, annealing 60˚C for 1 minute, extension 72˚C for 2 minutes for a total of 40 cycles with a final extension at 72˚C for 10 minutes. RT-PCR products were stored at -20 ˚C until required for making qPCR standards.

# **GAPDH** (glyceraldehyde-3-phosphate dehydrogenase)

**Sequence ID:** NM_008084 **Product size:** 110bp

**Forward primer:** 5'-TTGATGGCAACAATCTCCAC-3' **Reverse primer:** 5'-CGTCCCGTAGACAAAATGGT-3

**Product sequence:** TTGATGGCAACAATCTCCACtttgccactgcaaatggcagccctggtgac caggcgcccaatacggccaaatccgttcacaccgaccttcACCATTTTGT CTACGGGACG

**Assay conditions:** Rotorgene 6000, Corbett Research

*Activation*: 95 °c for 5 min

*Cycling: (*melting 95 °c for 10 secs; combined annealing/extension 60 °c for 30 secs) x 40

*Melt*: 67-95ºC in 1ºC increments

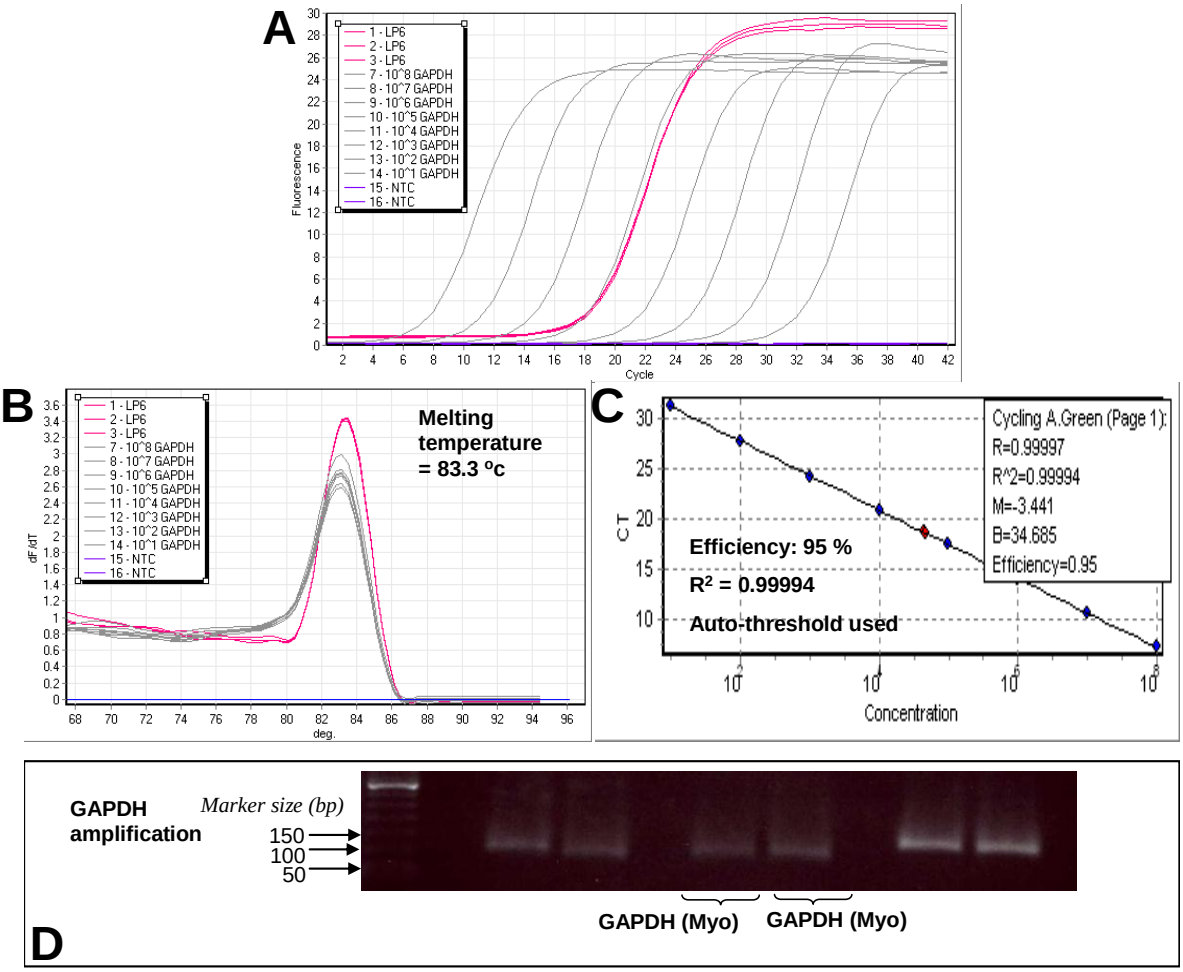


**Figure 2.2 QPCR validation data for mouse GAPDH gene**

**A:** raw fluorescence values for all samples, **B:** melt curve for all samples, **C:** generated standard curve, **D**: GAPDH qPCR amplification product shown on 2 % agarose gel; size of product is 110 bp. Pink lines shown in A and B correspond to the unknown samples isolated from myometrium from late pregnant mice (three months old, day 18 gestation), grey lines correspond to GAPDH standards, and purple lines to non-template controls.

# $\beta_2$M (beta-2 microglobulin)

**Sequence ID:** NM_009735 **Product size:** 103 bp

**Forward primer:** 5'-TTCAGTATGTTCGGCTTCCC-3' **Reverse primer:** 5'-TGGTGCTTGTCTCACTGACC-3'

**Product sequence:** TTCAGTATGTTCGGCTTCCCattctccggtgggtggcgtgagtatacttg aatttgaggggttttctggatagcatacaggccGGTCAGTGAGACAAGCA CCA

**Assay conditions:** Rotorgene 6000, Corbett Research

*Activation*: 95 °c for 5 min

*Cycling: (*melting 95 °c for 10 secs; combined annealing/extension 60 °c for 30 secs) x 40

*Melt*: 67-95ºC in 1ºC increments

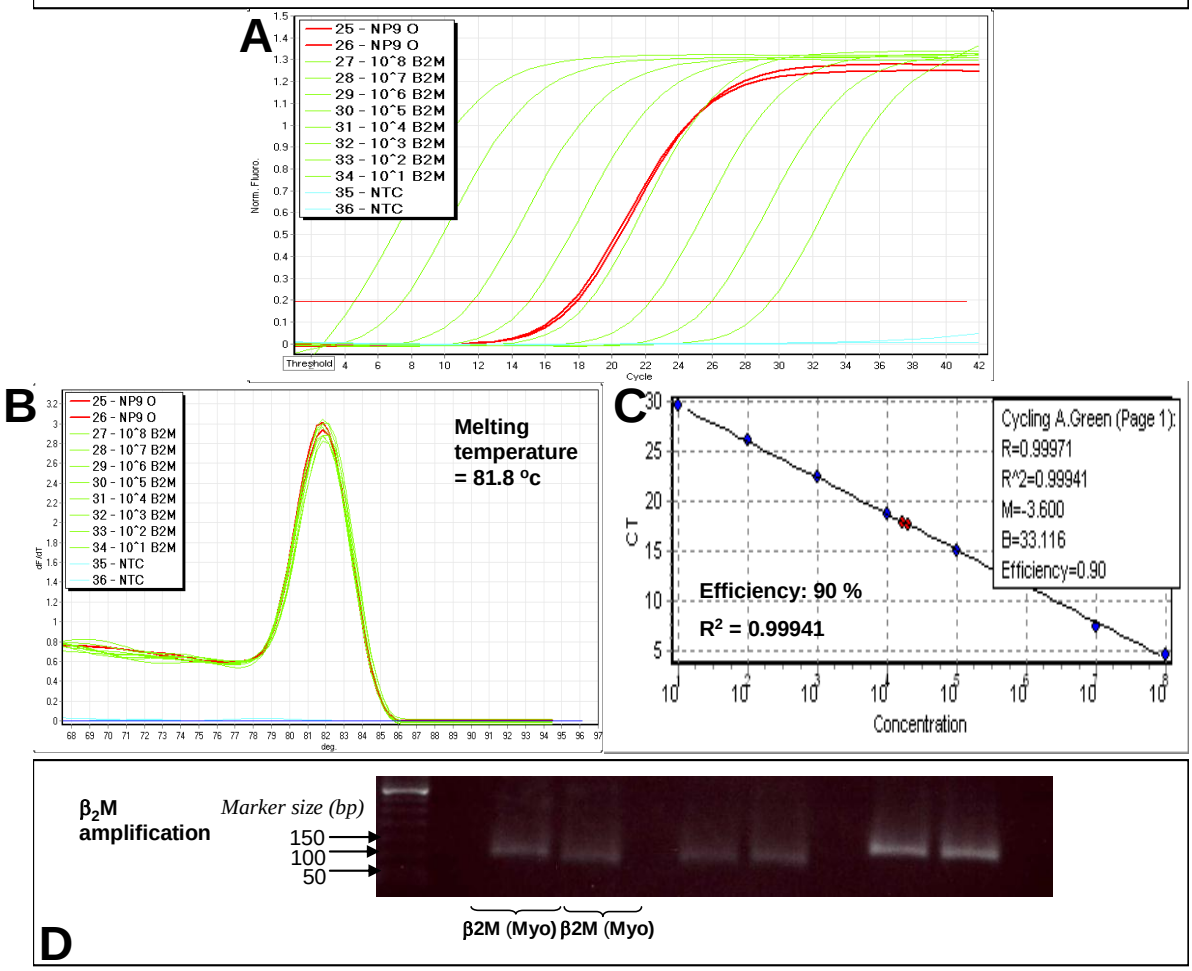


**Figure 2.3 QPCR validation data for mouse $\beta_2$M gene**

**A:** raw fluorescence values for all samples, **B:** melt curve for all samples, **C:** generated standard curve, **D:** $\beta_2$M qPCR amplification product shown on 2 % agarose gel; size of product is 103 bp. Red lines shown in A and B correspond to the unknown samples isolated from myometrium from non-pregnant mice (three months old, oestrous), green lines correspond to $\beta_2$M standards and blue lines to non-template controls.

### 2.3.5 DNA extraction from gel

The purification of DNA from agarose was first reported by Vogelstein & Gillespie (Vogelstein and Gillespie, 1979). Since then many different modifications of this original methods have been established and at present many kits are available for fast and efficient purification of DNA from agarose gels. The QIAquick gel extraction kit used for the present study combines spin-column technology with the selective binding properties of a silica membrane which absorbs the DNA in the presence of high concentrations of salt, whilst allowing contaminants to pass through; after further purification steps, DNA can then be eluted.

### 2.3.6 DNA extraction from gel protocol

RT-PCR products were run on a 2 % agarose gel in duplicates to ensure that they were of the desired size, to check for integrity, and to allow for DNA extraction from gel. High resolution agarose (2 g, Sigma-Aldrich, UK) was dissolved in 100 ml 0.5 × tris-borate EDTA/H2O (TBE) (diluted from 10 x TBE stock; Sigma-Aldrich, UK) and heated until melted; 10 µl of SYBR safe DNA gel stain (Invitrogen, UK) was added to the 100 ml of melted agarose and then quickly poured into a level horizontal gel tank containing well combs and allowed to set for 45 minutes. The samples to be run were prepared by mixing 10 µl of PCR product with 2 µl of loading buffer (6x DNA loading dye; Fermentas, UK). Once set, the well comb was removed, and the gel was submerged in 1 × TBE and loaded with the 12 µl of sample into each well. A 50 bp ladder (5 µl; Invitrogen, UK) was run at each end of the comb. The gel was then run at a constant 100 V for 1.5 hours before being imaged using the Gel Logic 2200 Pro Imaging System and Carestream Molecular Imaging software (Carestream Health, USA).

The bands of appropriate size (according to the size of the expected PCR product for each gene) were excised using a clean sharp blade on a UV transilluminator (UVP, UK). Each excised band was weighed and DNA was extracted using the QIAquick DNA extraction kit (Qiagen, UK) as per manufacturer's recommendations. The extracted DNA was eluted in 20 μl buffer EB (Elution Buffer, Qiagen, UK) and subsequently stored at -20 ˚C until required for densitometry.

### 2.3.7 Densitometry

Gel extracted DNA samples were loaded (10 μl of sample + 2 μl of loading buffer (6x DNA loading dye; Fermentas, UK) on a 2% agarose gel along with a known concentration DNA fragment ladder (MassRuler Low Range DNA ladder mix; Thermo Scientific, Germany). The samples were then size separated by running the gel at a constant 100 V for approximately one and a half hours. Once run, the gel was imaged using the Gel Logic 2200 Pro Imaging System (Carestream Health Inc., USA) and the density of each band was assessed using the Carestream Molecular Imaging software (Carestream Health, USA). The concentrations of the unknown DNA samples were calculated using their raw volume density values and comparing back to the known concentration DNA ladder. Once the DNA concentrations were calculated for each gene, serial dilutions from 1 x $10^{10}$ - $10^{1}$ copies were made as standards and stored at -80 ˚C until required for qPCR.

***Example:***

a) For a particular gene of interest, with a PCR product size of 105 bp. During densitometry, the gene of interest DNA band is closest in size to a standard of 100 bp on the DNA ladder, which is known to contain 15 ng of DNA.

For the known standard (100 bp, 15 ng DNA): the mean density of the band is measured as 33, 455 mean density units.

For the gene of interest product (105 bp, unknown DNA quantity): the mean density of the band is measured as 75, 967 mean density units.

To calculate the DNA quantity of the gene of interest band =

$\frac{100}{105} \times \frac{75{,}967 \times 15}{33{,}455}$ = 32.4 ng/ 12 μl loaded volume

= 2.7 ng/μl

b) The average molecular weight of a dNTP (assuming equal numbers of all bases A, T, G, C) = 330 Da

Since the PCR product is double stranded = 330 x 2

= 660 Da

The gene of interest PCR product is 105 bp, therefore the weight of the product

= 105 x 660

= 69, 300 Da

c) Avogadro's Constant = $6.02 \times 10^{23}$ molecules in 1 mole

1 mole = Molecular weight in grams

69, 300 g of the gene of interest PCR product = $6.02 \times 10^{23}$ molecules

Therefore, in 1ng of the gene of interest PCR product = $\frac{6.02 \times 10^{23}}{69,300 \times 10^{9}}$

$= 8.69 \times 10^{9}$ copies/ ng

From part a), there is 2.7 ng/μl PCR product in the band of interest, therefore the number of copies in 1μl of eluted PCR product from this band will be = 2.7 ng x $8.69 \times 10^{9}$ copies

$= 2.35 \times 10^{10}$ copies/ μl

Serial dilutions from $1 \times 10^{10}$ - $10^{1}$ copies can be made from this as standards.

### 2.3.8 Real time quantitative PCR (qPCR)

Real time PCR uses a signal, normally fluorescence, which increases with the increased amount of DNA formed by PCR (Bustin and Nolan, 2004). When the signal rises above a set background, it is detected. The signal normally rises in a sigmoidal way, until it reaches its plateau (Figure 2.4). During the linear increase, the signal can be compared with the signal from other samples. A standard curve with known DNA concentrations (Figure 2.5) is usually run on the same 72/100 well rotar, to compare the signal of the samples and to calculate the DNA concentrations of the unknown. The signal is normally measured at a threshold level called, cycle threshold (CT). The cycle number at which the signal crosses the CT is correlated to the initial concentration of DNA in the template (Higuchi et al., 1993).

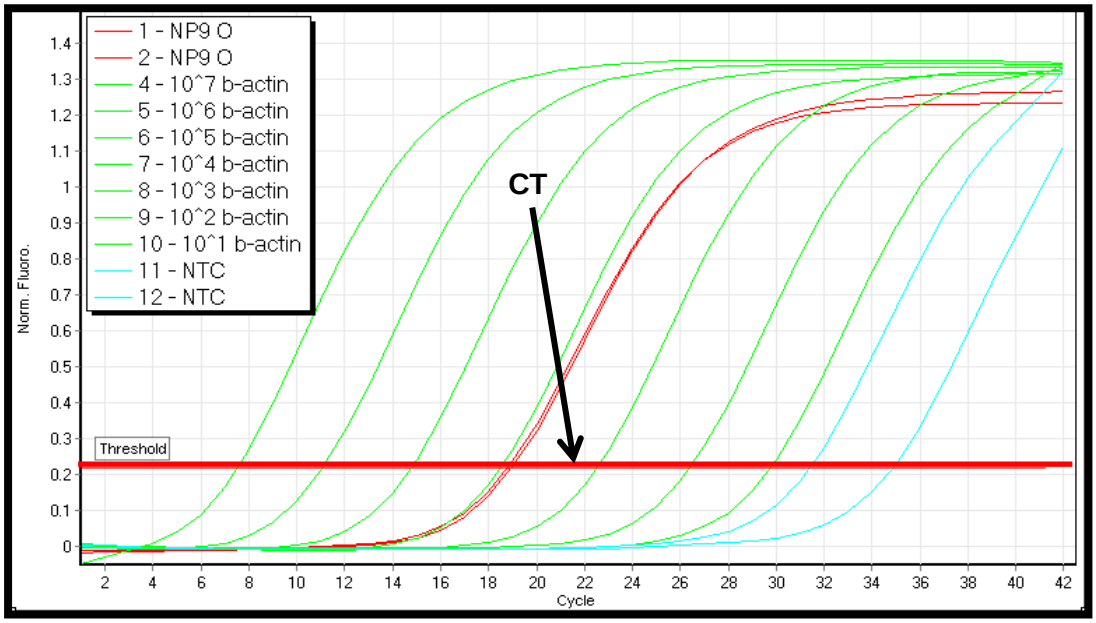


**Figure 2.4 Typical real-time PCR result showing raw fluorescence for each sample**
The cycle points (CP) is the point where the instrument (RotorGene 6000) first detects fluorescence above background noise. Green lines correspond to standards of known concentrations for the gene of interest (represented in sequential order from highest concentration of $10^7$ copies on the furthest left to lowest concentration of $10^1$ copies on the furthest right), red lines to unknown samples and blue lines to non-template controls.

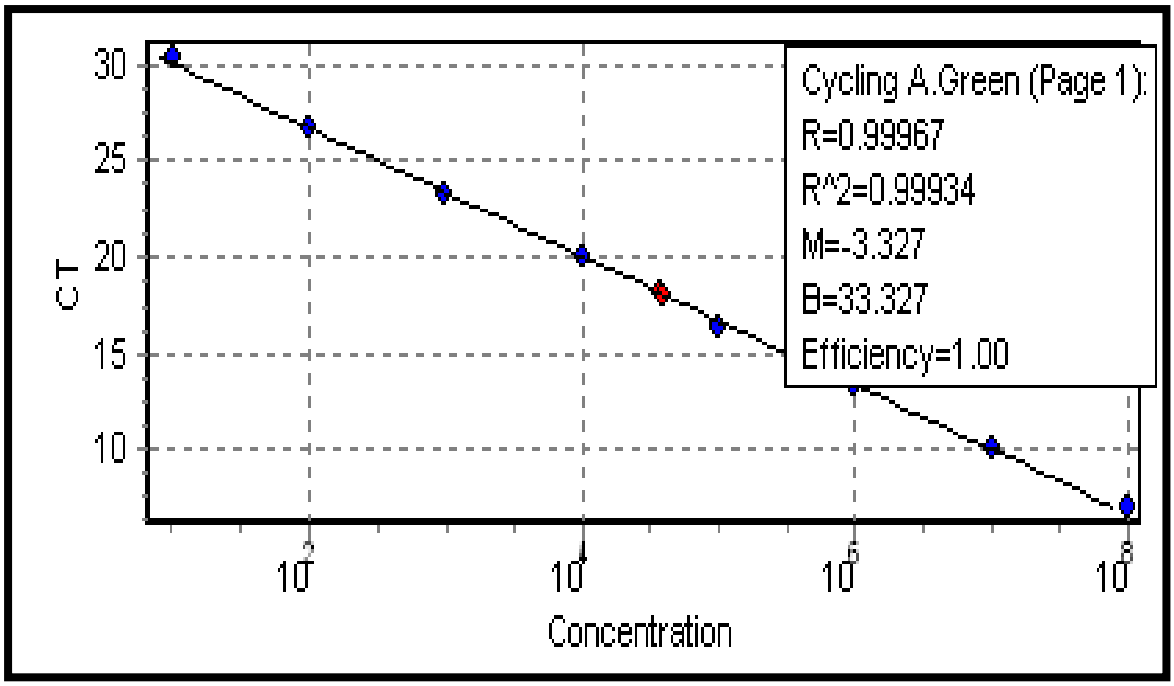


**Figure 2.5 Typical standard curve from real-time PCR**
Standard curve generated from fluorescence data, indicating the appropriate $R^2$, and efficiency (E) values (Bustin and Nolan, 2004).

DNA binding agents, like SYBR green, bind specifically to double stranded DNA; they emit a fluorescent signal when they bind to double stranded DNA. During each cycle of PCR, the amount of double stranded DNA increases with the fluorescent signal. Like with conventional PCR, the specificity of the reaction is determined entirely by its primers; however the PCR can be verified by a melting curve (Al-Robaiy et al., 2001, Ririe et al., 1997) that allows a comparison of the melting temperatures of the specific product and any suspected non-specific products (Lekanne Deprez et al., 2002). The reason for this is that different length products and products of different sequences will melt at different temperatures and will be observed as distinct peaks (Figure 2.6); therefore, a single peak should be present to confirm specificity (Bustin, 2000, Bustin and Nolan, 2004).

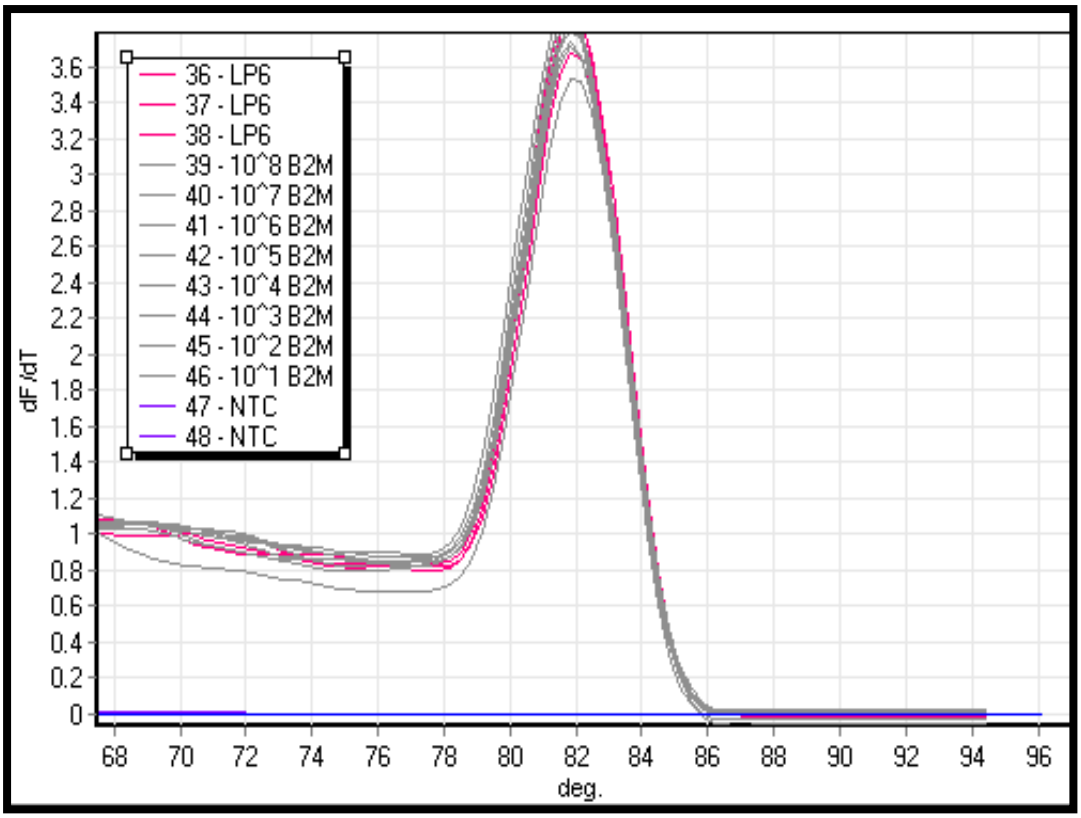


**Figure 2.6 Typical melt cure from real-time PCR**
The single peak of the melt curve indicates the specificity of the product amplified.

When comparing samples, a housekeeping gene is also used to rule out any pipetting errors and to normalise for any variation in RNA abundance between samples (Bustin, 2000). A good housekeeping gene is one that should not vary in its expression level irrespective of the disease in question/experimental conditions (Kelley et al., 1993).

### 2.3.9 Real time quantitative PCR (qPCR) protocol

Real Time qPCR was performed for the optimised primers listed in Table 2.1. A volume of 2 μl of cDNA/DNA (sections 2.2.4 or 2.2.6) was used to carry out qPCR amplifications alongside previously prepared standards from $10^8$ to $10^1$ copies using SYBR Green chemistry (QuantiFAST SYBR green; Qiagen, UK) on a RotorGene 6000 (Corbett Research, Australia). Forward and reverse primers were optimised to be used at 300 nM working concentrations, in a total reaction volume of 10 μl.

A pre-PCR cycle was run for 5 minute at 95°C followed by 42 cycles of 95°C for 10 s denaturation step, followed by 60°C for 30 s combined annealing/extension step. Melt curve analysis was performed to confirm the presence of one single product, and non-template controls were run to assess contamination. CT values and a standard curve were generated using the RotorGene software. All unknowns sample quantification values should fall within the dynamic range of the standard curve. Cut off values for efficiency and $R^2$ were 80% and 0.99 respectively. All gene qPCR products were sequence verified and run on a gel to confirm product band size.

For normalising data for the genes of interest, unknown samples were also run using reference/housekeeping genes. Quantification data for the genes of interest were expressed relative to the geometric mean of 2 or more housekeeping genes (where possible) and assessed using GeNorm software.

## 2.4 Microarray Studies of Mouse Myometrium

As described in section 2.2.2, total RNA was extracted from ~ 30 mg of myometrium and paired bladder samples collected from late pregnant (day 18 of gestation) mice. Once quantified using the NanoDrop ND-1000 spectrophotometer (Nanodrop Technologies, Labtech, UK), RNA samples were diluted to 45 ng/μl using RNase/DNase free water (Qiagen, UK). RNA samples were then passed over to the NIHR Comprehensive Biomedical Research Centre Genomics Facility (Guy's hospital, London). The Genomics Facility used the RNA samples to complete the Illumina TotalPrepTM RNA Amplification Kit (Invitrogen, UK) protocol, as per manufacturer's recommendations to make labelled cDNA. The mouseWG-6 v2.0 Expression BeadChip Kit (Illumina, UK), was then used to run the microarray. Labelled cDNA samples were detected by hybridization to 50-mer probes on the BeadChip. After washing and staining steps as per manufacturer's recommendations, BeadChips were scanned on an iScan reader (Illumina, UK).

Differential expression analysis was performed by the Genomics Facility. Comparisons were made between two ages (three month *versus* eight month old) of myometrial tissues. Myometrial expression was normalised against expression in age-matched bladder tissues. A threshold P-value of 0.05 (Diff score +/- 13) was applied to find the differentially expressed genes.

## 2.5 Infra-red Video Camera Recording of Mouse Parturition

Late pregnant (day 17 of gestation onwards) females were singly housed in cages containing bedding of white pine shavings, and minimal nesting bedding (Enviro-dri; Shepherd Speciality Papers, USA), so the view of the cameras were not obscured. Mice had access to standard chow and bottled water *ad libitum*. The light-dark cycle was maintained 12L: 12D (light 0700-1900 h). Females were monitored continuously, using infrared video cameras (600TVL Eyeball Dome; Qvis, USA) in order to accurately record from the appearance of the first pup until the completion of parturition. Cameras were connected to a Zeus Lite HDMI LX 4 Channel Full D1 Networked CCTV Recorder DVR 1TB Hard Drive (Qvis, USA), which recorded continuously for the duration of the experiment with correct time and date associated with video footage.

Following delivery, the litter size delivered per mouse was recorded and the weights of each live pup were also determined. Any pup mortality seen was also noted. Each video was examined for the precise time of birth, which was determined by the appearance and complete delivery of the first pup, this was used to determine gestation length (days). Total parturition duration (hours) was determined as the exact time between the complete delivery of the first pup to the complete delivery of the final pup.

This study was carried out for both three month old and eight month old late pregnant nulliparous females.

## 2.6 *Ex Vivo* Isometric Tension Measurements of Mouse Myometrium

Isolated tissue and organ preparations have been in use for over one hundred years, providing researchers with convenient biological models that exist without the systemic influences of the intact animal (Csapo and Goodall, 1954, Hill, 1953, Ringer, 1883, ADInstruments, 2013). Furthermore, isolated tissue preparations can generally be run in groups of two, four, or eight, and can be easily subjected to controlled changes in perfusion solution, oxygen, drugs and other factors that may affect organ function. Traditionally, such experiments have been carried out in tissue-organ baths to study *in vitro* dose response changes on isolated tissue preparations to investigate the physiology and/or pharmacology of that tissue. Tissue-organ baths are used to maintain the integrity of the tissue for several hours, in a temperature-controlled environment, while physiological measurements are performed. Typical experiments involve the addition of drugs to the organ bath, where the tissue reacts by contracting/relaxing and an isometric transducer is used to measure force generated by the tissue (Radnoti, 2010, ADInstruments, 2013).

To measure muscular activity, the organ, muscle strip or ring is attached by wire, silk or cotton suture to a force transducer which converts the force generated by the muscle into an electrical signal that can then be detected on a chart recorder or a computer based data acquisition system. The muscle is usually pre-loaded with a weight or pre-stretched using a tissue tensioner or micrometer. The suture attaching the muscle to the transducer should not touch the bath walls and should be in line with the transducer. The force transducer makes an isometric measurement, where the muscle length remains constant as force changes. Isometric measurements are measured as grams (g) or millinewtons (mN) (Dillon and Murphy, 1982, Radnoti, 2010); these force measurements can be converted to stress measurements, allowing the researcher to control for the differences caused by the size of the preparation and its effect on force output (Radnoti, 2010, Herlihy and Murphy, 1973).

Muscles have an optimal length where contraction produces a maximum active force. Maximum force usually occurs at the natural length of the muscle and is termed optimal length. The length-tension relation was first studied in uterine muscle by Csapo & Goodall in 1954 (Csapo and Goodall, 1954). They confirmed that that maximum force was developed at the 'resting length', a length determined by applying a series of slight stretches to the isolated muscle and taking as the resting length the last length before any significant resting tension was developed.

### 2.6.1 *Ex vivo* isometric tension optimisation

***Measurement of length-tension properties of non-pregnant mouse myometrium***

An adapted method as published by (Wu et al., 2008) was used.

Mouse uterine horns were cut longitudinally down the midline, and the endometrium gently removed with a cotton bud. Small myometrial muscle strips (4-5 mm in length) were dissected from each of the horns and tied at each end with thread and mounted in a standard 10 ml organ bath chamber (ADInstruments, UK). One tissue end was tied to a fixed hook, and the other to a tension transducer linked to a micrometer allowing for manual stretch of the tissue. The tissue bath contained physiological saline solution (PSS; 119 mM NaCl, 4.7 mM KCl, 1.17 mM $MgSO_4$, 25 mM $NaHCO_3$, 1.18 mM $KH_2PO_4$, 0.025 mM ethylenediaminetetraacetic acid (EDTA), 6.0 mM glucose, 2.5 M $CaCl_2$; pH 7.4) at 37°C that was bubbled with a 95% air-5% $CO_2$ mixture (BOC Gases, UK). Myometrium strips were initially held at slack length (the length at which any further 0.25 mm incremental stretch of the tissue noticeably changed passive tension), equilibrated for 30 minutes at this initial length and then stimulated with high $K^+$ solution (PSS with 60 mmM KCl substituted for NaCl) for five minutes. After washout and a further ten minutes equilibration in PSS, the tissues were stretched by 1mm (approximately 1.20–1.25-fold beyond initial length). After ten minutes equilibration at this new length, the tissues were again stimulated with high $K^+$ solution

for five minutes and subsequently returned to PSS. The active tension in response to the high $K^+$ was noted just before returning to PSS. This procedure was repeated at several tissue lengths to allow construction of an active length–tension curve. All data were recorded and analysed using LabChart 6 software (ADInstruments Limited, UK). Data for each strip was expressed as a percentage of the maximum active tension recorded; collated data was then averaged to construct the length-tension curve, as can be seen in Figure 2.7.

This experiment was repeated without the stimulation with high $K^+$ solution, but with stretching of the myometrium strips alone. The passive tension was noted just before stretching of the tissue by a further 1mm increment. This procedure was repeated at several tissue lengths to allow construction of a passive length–tension curve. Data were expressed as absolute force per cross sectional area ($mN/cm^2$), as can be seen in Figure 2.8.

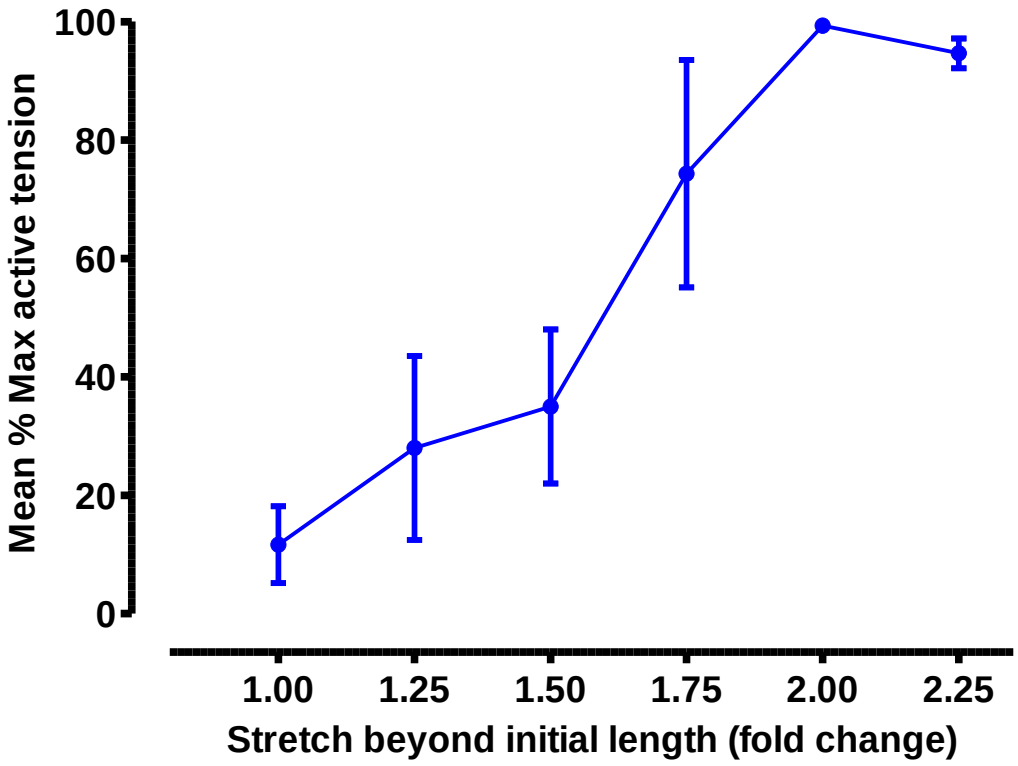


**Figure 2.7 The active (high $K^+$PSS stimulation) length-tension curve for myometrium from three month old non-pregnant mice**

Mean active tension (±SD) was normalised to the peak in active tension (100%) and the stretch was normalised to a slack length of 1.0 (n = 16 tissue strips from n = 4 mice). Where error bars are not apparent, bars lies within symbol.

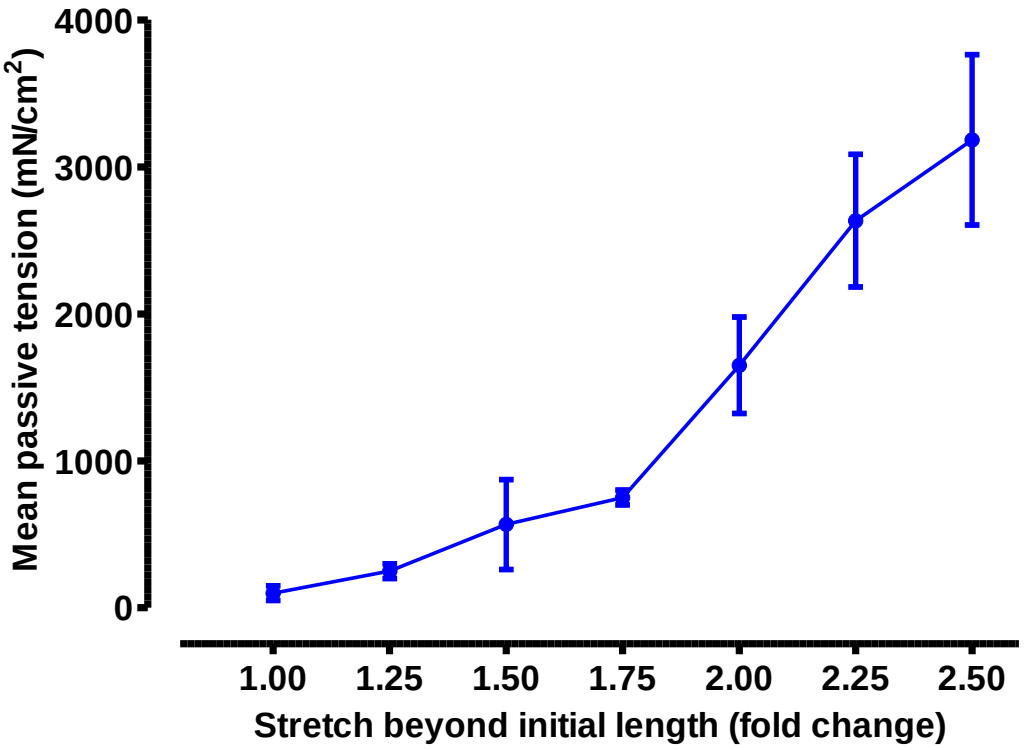


**Figure 2.8 The passive length-tension curve for myometrium from three month old non-pregnant mice**

Mean passive tension (±SD) was expressed as absolute force per cross sectional area (mM/cm$^2$), and the stretch was normalised to a slack length of 1.0 (n = 16 tissue strips from n = 4 mice).

Figure 2.7 shows the mean maximum active tension was generated when myometrial strips were stretched to 2-fold of their original/slack length. Figure 2.8 shows that at a 2- fold stretch beyond initial length, the myometrial strips are held under a mean passive force of approximately 1600 mN/cm$^2$. Taking this into consideration, it was calculated that ideal resting tension for myometrial tissue strips (5 x 2 x 2 mm dimensions) in future experiments should be 32 mN (3.26 g). However, the software (LabChart 6, ADInstruments Limited, UK) used to record data, was pre-set to grams rather than millinewtons settings, therefore a resting tension of 3 grams/29.4 mN was used for all subsequent myometrial isometric tension experiments.

### 2.6.2 *Ex vivo* isometric tension protocol

Mouse uterine horns from non-pregnant females in oestrous or late pregnant (day 18) (section 2.1.3) were cut longitudinally down the midline in non-pregnant uterine horns or along the axis of placental attachment in pregnant horns, and the endometrium gently removed with a cotton bud. Small myometrial muscle strips (5 x 2 x 2 mm dimensions) were dissected from each of the horns and tied at each end with cotton thread and mounted in a standard 10 ml organ bath chamber (Panlab 8 Chamber Organ Bath System; ADInstruments, UK). One tissue end was tied to a fixed hook, and the other to a tension transducer linked to a micrometer allowing for manual stretch of the tissue. The tissue bath contained PSS (section 2.6.1) at 37°C that was bubbled with a 95% air-5% $CO_2$ mixture (BOC Gases, UK). Myometrium strips were put under 29 mN (x2 slack length; as determined by optimisation studies) of resting tension and left to equilibrate for 45 minutes to allow spontaneous contractions with a stable baseline to develop. Contractions were recorded for a 10 minute baseline period, prior to recording spontaneous contractile activity (one hour minimum duration of recording), and response to the contractile agonists oxytocin ($10^{-12}$-$10^{-7}$ M oxytocin concentration response curve; Syntocinon; Alliance Pharmaceuticals, UK).

Maximal contractile capacity of each myometrial tissue strip in response to high $K^+$ solution (section 2.6.1; duration of 5 minutes) was measured at the end of spontaneous contractile activity experiments.

All data were recorded and analysed using LabChart 6 software (ADInstruments Limited, UK). Contractile periods were assessed using mean integral tension (MIT), which is the sum of the contraction integrals divided by the duration of the period assessed. Contraction force was measured as the mean height of contractions in the period assessed. To confirm that any observed differences in contractile activity were not due bias in dissecting the myometrial strips or their relative weights, measurements were normalised to cross sectional area of strips. The frequency of contractions were calculated as number of contractions per second, and the duration of contraction was calculated as the time in seconds between the start and end of an individual contraction, measured at 50% of the peak amplitude.

## 2.7 *Ex Vivo* Tensile Strength Measurements of Mouse Cervix

The cervix is a metabolically active organ in pregnancy composed primarily of fibroblasts and to a lesser extent smooth muscle cells. These cells secrete an extracellular matrix (ECM) rich in fibrillar collagen, elastin, proteoglycans, and hyaluronan (Leppert, 1995). During pregnancy, the cervix remains closed and firm in order to prevent passage of an immature infant through the birth canal (Mahendroo, 2012). However, near term, the cervix is extensively remodelled, making it more distensible in order to open sufficiently facilitating safe passage of the fetus at parturition. In 1895, Hegar first described 'softening' of the lower uterine segment in association with human pregnancy at four to six weeks (Read et al., 2007).

Cervical softening can be defined as a change in the biomechanical properties of the cervix when compared with the non-pregnant cervix and is characterized by a progressive decrease in tissue stiffness without loss of tensile strength (Leppert and Yu, 1994). Physiologic softening of the rat cervix was first shown by Harkness & Harkness in 1959 who noted that distensibility of cervical tissue increased dramatically starting mid-gestation between days 11 and 12 (Harkness and Harkness, 1959). Harkness and Harkness isolated cervices from pregnant rats and the tissues were distended between two cylindrical steel rods, both of which were inserted through the cervical canal. The apparatus used is summarised in Figure 2.9. The rods were arranged parallel one above the other, going through the cervical canal (X). The lower rod (r1) was fixed and immovable and the other rod (r2) was fixed to a movable stirrup on which force could be exerted to pull the two rods apart. The stirrup (S) holding the upper rod (r2), was attached above to a stainless-steel rod (r3), which went vertically upwards through a cylindrical channel (c) 5 cm long, in a sheet of Perspex. Two cotton threads (a, b) were attached to the upper end of the rod, one (b) going over a Perspex wheel (w) to a pan (p) on which weights could be placed, the other (a) going up vertically to the short arm of a light spring-loaded lever (e) which gave a magnification

of x 3.0 or x 4.5. Lever (e) had a writing point on a drum, to enable recordings of relative force.

The excised cervix was placed in position, immersed in Ringer-Locke's solution. With the two rods as close together as their mountings would allow, a zero line was marked round the drum. The apparatus was then released with no load on the pan. Under these conditions a small constant force of approximately 2 g was exerted on the upper rod, this force representing the effect caused by the upper rod and its mounting being immersed in an aqueous medium. This small force was applied for approximately one minute. Subsequently, a load was placed on the pan and left there, the effect on the tissue was recorded on the drum. The load was increased in steps of 25 g every 15 seconds until the tissue ruptured (Harkness and Harkness, 1959).

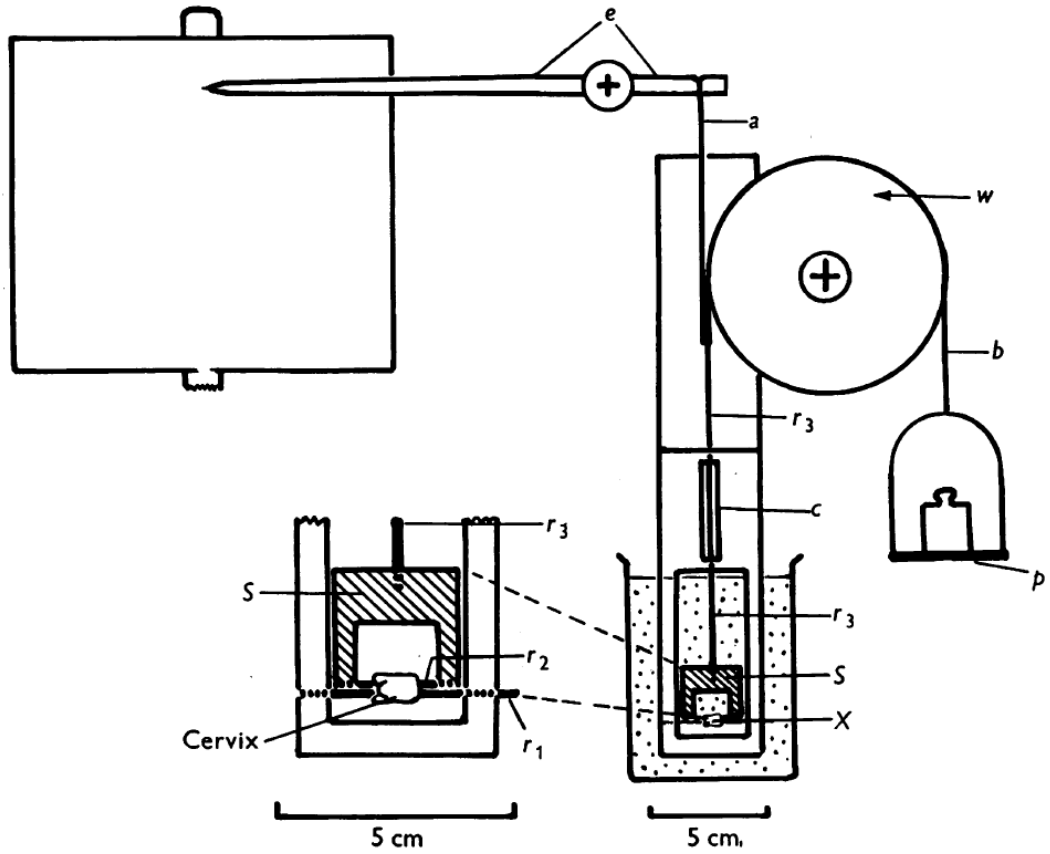


**Figure 2.9 Diagram of the apparatus used by Harkness and Harkness for stretching of pregnant rat cervical tissues**

Figure from: Changes in the physical properties of the uterine cervix of the rat during pregnancy (Harkness and Harkness, 1959)

Following on from these initial cervical tissue biomechanics studies, the methodology has been adapted further by Read *et al*., 2007 (Read et al., 2007), these authors carried out tensile distensibility and maximum stretch of isolated mouse cervical tissues. Instead of rods, they have mounted the excised cervix by means of two pins inserted through the cervical canal. One pin was attached to a calibrated mechanical drive and the other pin to a force transducer. Tissues were incubated in a water-jacketed bath containing PSS (NaCl (120.5 mM), KCl (4.8 mM), $MgCl_2$ (1.2 mM), $CaCl_2$ (1.6 mM), $NaH_2PO_4$ (1.2 mM), $NaHCO_3$ (20.4 mM), dextrose (10 mM), and pyruvate (1.0 mM), pH 7.4 at 37 $^oC$) bubbled with 95% $O_2$/5% $CO_2$. Baseline cervical dilatation (resting diameter of cervical canal) was quantified by determining the difference in cervical diameter at 0 (pins juxtaposed with no tension) and the inner cervical diameter at the initiation of tension as the pins were separated. Thereafter, the inner diameter of the cervix was increased isometrically in 0.5 mm increments at two minute intervals. The amount of force required to distend the cervix and the tension exerted by the stretched tissue were recorded. The diameter was increased until either forces exerted by the tissue reached a plateau or the tissue tore (Read et al., 2007).

### 2.7.1 Ex vivo tensile strength measurements of mouse cervix protocol

The method used was adapted from a previous report (Read et al., 2007). Whole intact mouse cervices from non-pregnant females in oestrous or late pregnant (day 18) (section 2.1.3) were isolated and dissected at the utero-cervical junction (beneath the uterine bifurcation). Each cervix was further dissected *ex vivo* to remove all vaginal tissue. Two pieces of cotton thread were passed through the cervical canal/lumen of the isolated cervix using a clean needle and a loop was tied for each piece of thread around the cervix (Figure 2.10). Each cervical preparation was mounted in a standard 10 ml organ bath chamber (Panlab 8 Chamber Organ Bath System; ADInstruments, UK). One thread loop was tied to a fixed hook, and the other to a tension transducer linked to a micrometer allowing for manual stretch of the tissue. The tissue bath contained PSS (section 2.6.1) at 37°C that was bubbled with a 95% air-5% $CO_2$ mixture (BOC Gases, UK). Cervical tissues were initially held at slack length (at which any further 0.25 mm incremental stretch of the tissue noticeably changed passive tension), and were allowed to equilibrate for 15 minutes. During this equilibration period, the inner diameter of each cervix (resting diameter of cervical os/ the baseline cervical dilatation) was taken to be at 0 mm stretch. Thereafter, the inner diameter of the cervix was stretched isometrically in 1 mm increments at two minute intervals. This increase in cervical diameter stretch was continued until either the forces exerted by the tissue reached a plateau or in very rare cases where the tissue snapped or tore. The amount of force required to distend the cervix and the tension exerted by the stretched tissue were acquired and analysed using Lab Chart 6 software (ADInstruments Limited, UK). Force was plotted as a function of cervical diameter. The slope of the linear portion of these force–strain curves were measured as an index of tissue stiffness and elasticity.

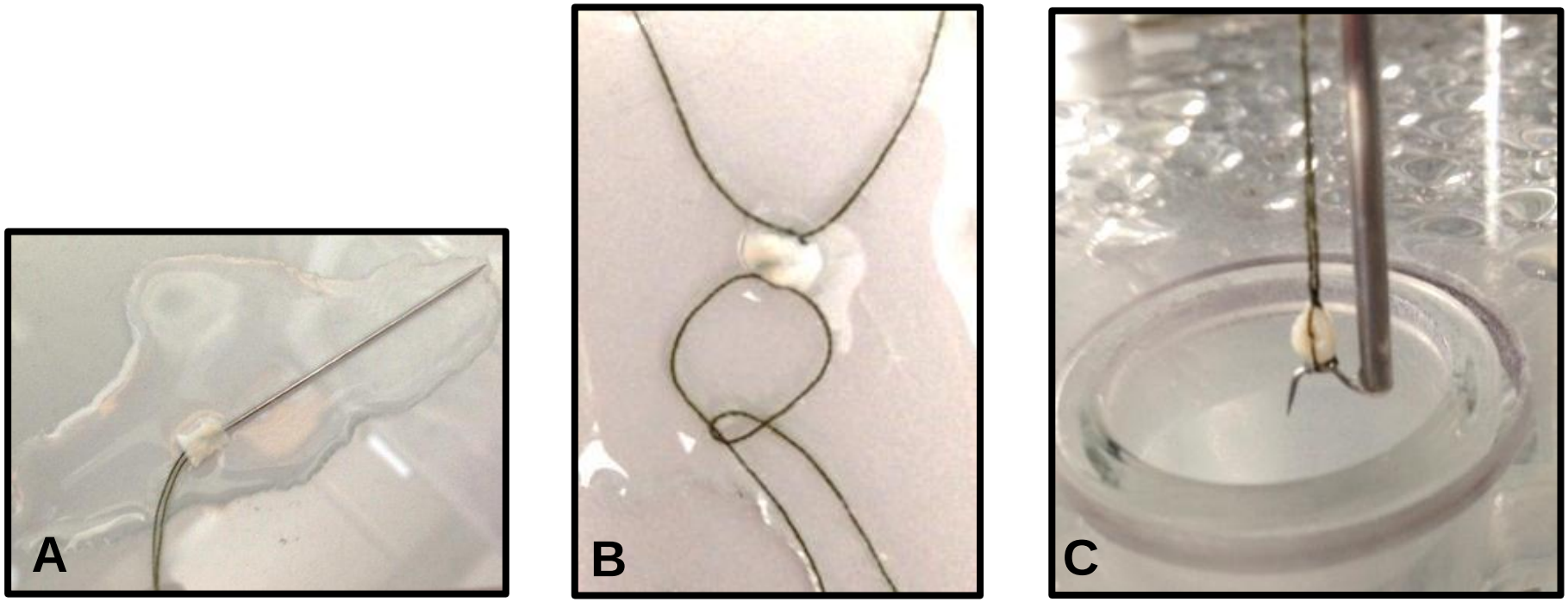


**Figure 2.10 Images to show how cervical tissues were mounted into in a standard 10 ml organ bath chamber**
**A:** Two pieces of cotton thread were passed through the cervical canal/lumen of the isolated cervix using a clean needle, **B:** a loose loop was tied for each piece of thread around the cervix, **C:** loops of thread were used to mount cervical preparation in a standard 10 ml organ bath chamber.

## 2.8 Histological Studies in Mouse Cervix

### 2.8.1 Tissue processing

Tissue processing is central to successful immunohistochemistry; fixatives are used to ensure preservation of tissue architecture and cell morphology. Prompt and adequate fixation is essential, especially in immunological studies, where fixation is imperative to ensure the adequacy of the specimen and target antigens. Inappropriate or prolonged fixation may significantly diminish the antibody binding capability.

The most common combination used for successful antigen retrieval is formalin-fixed paraffin-embedded tissue sections, as these have been shown to provide excellent morphological detail and resolution (MacIntyre, 2001, Montero, 2003, Werner et al., 2000). Formaldehyde is usually a 10% solution, usually in neutral phosphate buffer or saline (Montero, 2003). It has been demonstrated in a kinetic study of formaldehyde binding to tissue, that if the dimension of the tissue specimen is under the 2-3 mm prescribed, at least for one of the dimensions, 24 hours will be enough for good fixation (Helander, 1994).

### 2.8.2 Tissue processing protocol

Each whole intact cervical sample was fixed after overnight immersion in 10% (v/v) formal saline solution (Formaldehyde solution 10% v/v in 0.9% NaCl solution; Fisher Scientific, UK), as stated in section 2.1.3. The samples were then placed into plastic cassettes (Histosette cassettes; VWR International Ltd, UK) in a longitudinal orientation. The sample cassettes were washed in three consecutive 45 minutes washes in PBS (Sigma-Aldrich, UK), after which they were transferred to 70% ethanol ready to be processed. Processing was completed overnight using an automated tissue processor (TP1020 tissue processor; Leica Biosystems, UK). Table 2.3 outlines the series of washes that were undertaken.

**Table 2.3 Protocol used to process mouse cervical tissues in the automated tissue processor**
(TP1020 tissue processor; Leica Biosystems)

| Reagent | Time (minutes) |
|---|---|
| 70% Ethanol | 120 |
| 80% Ethanol | 120 |
| 90% Ethanol | 120 |
| 100% Ethanol | 120 |
| 100% Ethanol | 120 |
| Xylene | 120 |
| Xylene | 120 |
| Xylene | 120 |
| Wax | 120 |
| Wax | 120 |

Immediately after processing, the samples were was embedded using a wax embedding console system (EG1150 heated paraffin embedding module; Leica Biosystems, UK). Individual cervical sample wax blocks were allowed to set, and then stored in a cool environment until required for sectioning. A sledge rotary microtome (RM2135 rotary microtome; Leica Biosystems, UK) was used to cut 5-10 μm longitudinal sections of the cervical sample wax blocks; sections were allowed to dry onto SuperFrost Plus slides (VWR International Ltd, UK) using a slide drying bench set to 30°C (MH6616; Electrothermal, UK). Slides were then kept overnight in an oven set to 37°C, to allow sections to completely dry onto slides ready to be stained.

### 2.8.3 Masson's trichrome staining

Trichrome stains are primarily used for distinguishing collagen in connective and muscle tissues (Williams and Wilkins, 1977). Historically, the first trichrome system has been credited to Mallory (Lillie, 1940, Sheehan and Hrapchak, 1980). Subsequent modifications to this staining system were introduced by Masson and Gomori (Lillie, 1940, Gomori, 1950). In general, trichrome stains consist of nuclear, collagenous and cytoplasmic dyes. For the purpose of this study, a Masson's trichrome Kit (Sigma Aldrich, UK) was used, for which the procedure is based on the work of Masson as modified by Lillie (Williams and Wilkins, 1973) using aniline blue as a collagen stain instead of a green dye. Tissue sections were treated with Bouin's solution to intensify the final collagen stain colouration. Nuclei were stained with Weigert's iron hematoxylin, and cytoplasm and muscle stained with Beibrich scarlet-acid fuchsin. Rinsing in acetic acid after staining reduces the shades of colour making them more delicate and transparent (Gomori, 1950).

### 2.8.4 Masson's trichrome staining protocol

Cervical sections were stained using a Masson's Trichrome Kit (Accustain® Trichrome stains (Masson); Sigma-Aldrich, UK), to allow identification of structures and detect presence of collagen. Tissue section slides, including a positive control slide (Trichrome TISSUE-TROL, Sigma Aldrich, UK) were de-waxed by following the series of washes shown in table 2.4 (xylene; Sigma Aldrich, UK), after which they were penetrated in Bouin's Solution (Sigma Aldrich, UK) at room temperature overnight. Slides were washed in running tap water to remove yellow colour from sections, and then stained in Working Weigert's Iron Hematoxylin Solution (Sigma Aldrich, UK) for five minutes, followed by another five minute wash in running tap water. Slides were rinsed in deionized water, and then stained in Biebrich Scarlet-Acid Fucshin solution (Sigma Aldrich, UK) for five minutes, followed by another deionized water wash. Slides were immersed in working Phosphotungstic/Phosphomolybdic Acid Solution

(Sigma Aldrich, UK), and then immediately transferred to Aniline Blue Solution (Sigma Aldrich, UK); five minutes immersion in both. Acetic acid, 1% was used to wash all slides (two minutes duration) after which they were rinsed in deionized water, and dehydrated through a series of washes in alcohol, and cleared in xylene washes as summarised in Table 2.5. Immediately after dehydration, 1–2 drops of permanent mounting medium DPX (Sigma-Aldrich, UK) were added onto each section, and covered with a glass coverslip, ready to be observed by light microscopy. Following Masson's trichrome protocol, nuclei were stained black, cytoplasm and muscle fibres were stained red and collagen was stained blue in each tissue section.

Images of Masson's trichrome stained cervical tissue sections were taken using AZ100 multizoom microscope and NIS-Elements version 4.0 software (Nikon Instruments Europe, UK); images were taken at x10 magnification of original. Collagen content in each cervical section was expressed as the area of blue stain (collagen stain) calculated as a percentage of total section area (binary units) measured using NIS-Elements Version 4.0 software (Nikon Instruments Europe, UK). To avoid bias during analysis, images were assigned numbers so that experimental conditions of the sections were unknown.

### 2.8.5 Immunohistochemical labelling

Immunohistochemistry is the localisation of antigens in tissue sections by the use of labelled antibodies as specific reagents through antigen-antibody interactions that are visualized by a marker such as fluorescent dye, enzyme, radioactive element or colloidal gold. Albert H. Coons and his colleagues (Coons and Kaplan, 1950, Coons et al., 1955) were the first to label antibodies with a fluorescent dye, and used it to identify antigens within tissue sections. With the expansion and development of immunohistochemistry, enzyme labels have been introduced such as horseradish peroxidase (Kiernan, 2000, Stevens and Lowe, 2005) and alkaline phosphatase (Mason and Sammons, 1978).

### 2.8.6 Identification of optimal primary antibody dilution

In order to ensure that the optimum primary antibody (anti-MMP2 ab37150; Abcam, UK) dilution was used in subsequent experiments, a dilution series of 1:100 to 1:1000 was first conducted (Figure 2.12); these were set around the manufacturers' recommendations. One section for each dilution was then stained (method described in section 2.8.7) and viewed under a light microscope to establish the optimum dilution. Optimum dilution is one that produces good staining, with the majority of positive staining lost when the next more diluted antibody is used (Stevens and Lowe, 2005, Ross and Pawlina, 2003) (Figure 2.11).

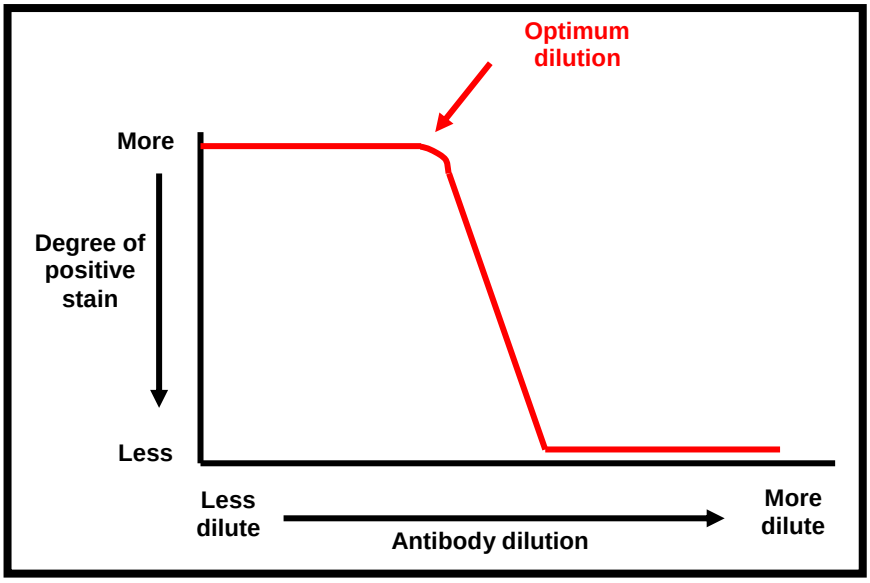


**Figure 2.11 Graph illustrating how the optimum primary antibody dilution was established**
Figure from Dr Hiten Mistry (2008).

Images of primary antibody dilutions were captured using AZ100 multizoom microscope and NIS-Elements version 4.0 software (Nikon Instruments Europe, UK) (Figure 2.12). Optimum dilution for anti-MMP2 ab37150 antibody was confirmed to be 1:500.

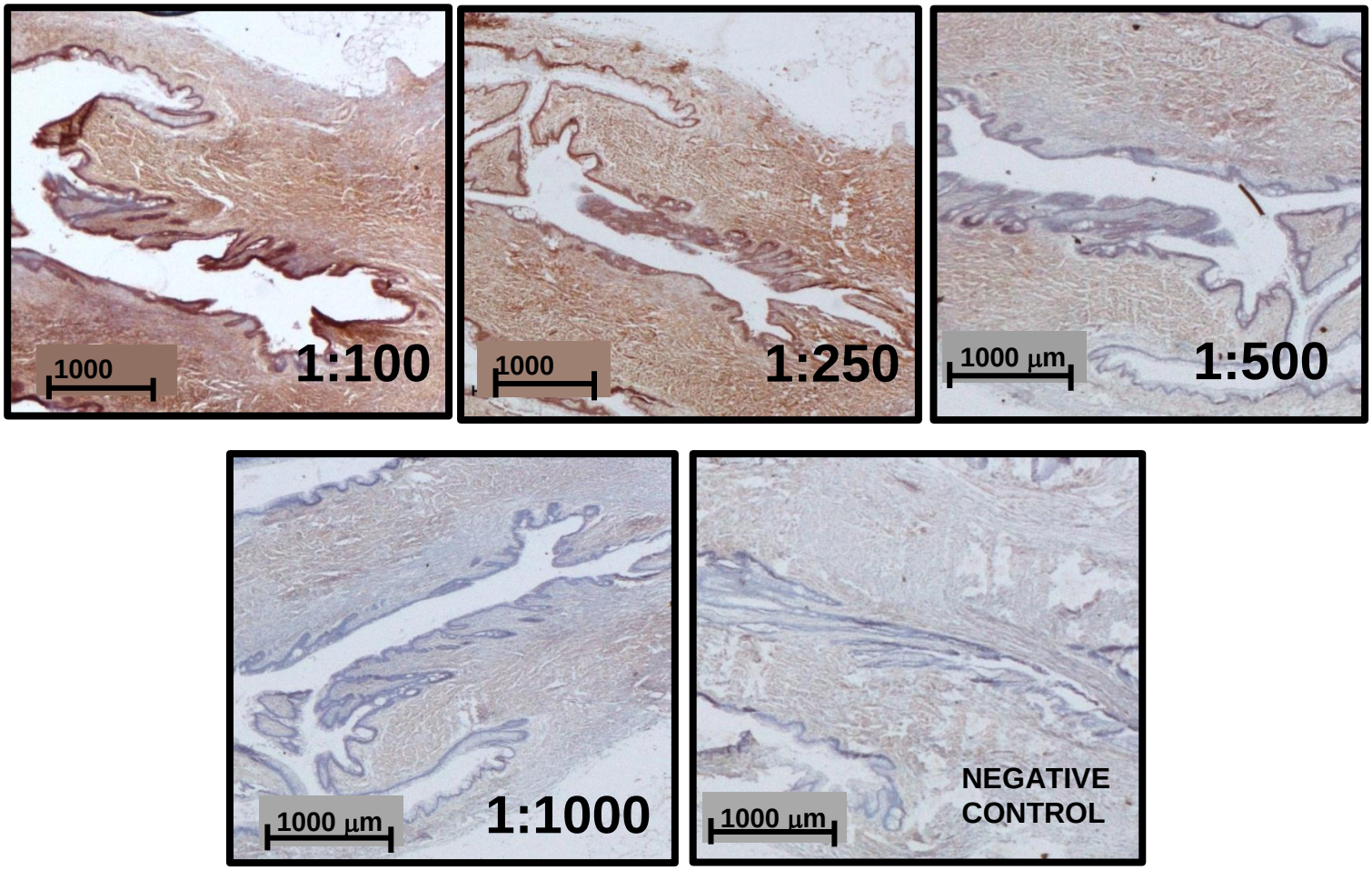


**Figure 2.12 Cervical sections from mice stained for MMP2 to identify the optimal dilution of primary antibody**
Dilution of 1:500 was selected as optimal; all sections shown at x10 magnification.

### 2.8.7 Immunohistochemical labelling protocol

The ImmunoCruz rabbit LSAB Staining System (Santa Cruz Biotechnology, Germany) was used for immunohistochemistry staining. Slides were initially de-waxed by washing sections in a number of washes as detailed in Table 2.4. After which excess liquid was aspirated from slides. Slides were then placed in a microwave-safe container and covered with a 10 mM Tris-EDTA buffer (10 mM Tris Base, 1 mM EDTA, 0.05% Tween 20, pH 8.0), and heated at highest power for ten minutes in a microwave. This heat treatment was needed to unmask antigens in the tissue sections. Slides were allowed to completely cool back down to room temperature for approximately an hour and a half, after which they were washed in deionized water three times for two minutes each on stir plate.

**Table 2.4 Protocol used to de-wax mouse cervical tissues sections**

| Reagent | Time (minutes) |
|---|---|
| Xylene | 5 |
| Xylene | 5 |
| 100% Ethanol | 5 |
| 80% Ethanol | 3 |
| 50% Ethanol | 3 |
| Deionised water | 3 |

All subsequent steps were carried out at room temperature in a humidified chamber. Endogenous peroxidase activity was quenched by incubating sections for five minutes in 1–3 drops of peroxidase block (provided in ImmunoCruz rabbit LSAB Staining kit). Slides were then rinsed with phosphate buffered saline (PBS; Sigma-Aldrich, UK), and transferred to a PBS wash for two minutes on a stir plate. Sections were then incubated for 20 minutes in 1–3 drops of serum block (provided). Primary antibody (Anti-MMP2 ab37150; Abcam, UK) was diluted in serum block (provided) to 0.5–5 µg/ml as determined by titration.

In order to ensure that the optimum primary antibody dilution was used, a dilution series was first conducted based on the manufacturer's recommendations (for example: 1: 50, 1:100, 1:250 and 1: 500); optimal dilution of 1:500 was selected for the anti-MMP2 antibody ab37150 (section 2.8.6). A border was defined around each section using a PAP pen for Immuno Staining (Sigma-Aldrich, UK), after which the diluted primary antibody was added in sufficient volume to cover each tissue section. Slides were incubated overnight in the humidified chamber at room temperature.

The following day, the slides were rinsed with PBS, and then washed in PBS twice for two minutes each on a stir plate. Sections were incubated for 30 minutes in 1–3 drops of biotinylated secondary antibody (provided). Again, the slides were rinsed with PBS, and then washed in PBS twice for 2 minutes each on a stir plate. Next, the sections were incubated for 30 minutes in 1–3 drops of HRP-streptavidin complex (provided), and again rinsed in a series of PBS washes as before. The HRP substrate was prepared as per the manufacturer's recommendations, and 1-3 drops were added to each slide. Staining was allowed to develop for ten minutes until a light brown staining was visible.

Slides were then rinsed with deionized water and transferred to a deionized water wash for two minutes on a stir plate. Slides were counterstained in Gill's formulation number 2 Hematoxylin (Sigma-Aldrich, UK) for five seconds, and then immediately washed with several changes of deionized $H_2O$. Brief destaining of Hematoxylin was carried out by dipping the slides in 0.5 % acid alcohol (0.25 ml Hydrochloric acid in 50 ml of 70% ethanol) for 1- 2 seconds, followed by a wash with tap water. Sections were then dehydrated in a number of washes as detailed in Table 2.5. Immediately after dehydration, 1–2 drops of permanent mounting medium DPX (Sigma-Aldrich, UK) were added onto each section, and covered with glass coverslip, ready to be observed by light microscopy.

**Table 2.5 Protocol used for dehydration of mouse cervical tissues sections**

| Reagent | Time (minutes) |
|---|---|
| 50% Ethanol | 3 |
| 80% Ethanol | 3 |
| 100% Ethanol | 5 |
| Xylene | 5 |
| Xylene | 5 |

Images of immunohistochemical labelled cervical tissue sections were taken using AZ100 multizoom microscope and NIS-Elements version 4.0 software (Nikon Instruments Europe, UK); images were taken at x10 magnification of original. Brown staining was quantified using ImageScope (Aperio Technologies Ltd, UK). The total percentage of positive labelled cells per x10 magnification field was determined using the 'positive pixel count' function. Results were then expressed as 'positivity' which takes into account both the number of positive pixels and the intensity of staining. To avoid bias during analysis, images were assigned numbers so that experimental conditions of the sections were unknown.

## 2.9 Mitochondrial DNA Copy Number in Mouse Myometrium

Mitochondria are double membrane organelles located in the cytosol of most eukaryotic cells. They are responsible for maintaining cellular energy balance, specifically by carrying out oxidative phosphorylation (OXPHOS) energy production to produce adenosine-5'-triphosphate (ATP). The majority of mitochondrial proteins are encoded by nuclear DNA. However, mitochondria possess their own genome consisting of a circular duplex molecule, approximately 16569 base pairs long encoding 37 genes, 13 of which code for components of the electron transport chain, and the remainder code for 2 rRNAs and 22 tRNAs essential for mitochondrial polypeptide synthesis (Rothfuss et al., 2010, Malik and Czajka, 2012). Mitochondrial protein content has been shown to be tissue specific and can vary between 500 to over 1000 proteins in different studies (Taylor et al., 2003, Johnson et al., 2007, Malik and Czajka, 2012, Smith et al., 2012a). The number of mitochondria in a cell varies depending on the specific energetic requirements of the cell, and can also depend on factors such as the stage in the cell cycle, the environment and redox balance of the cell, the stage of differentiation, and a number of cell signalling mechanisms (Rodriguez-Enriquez et al., 2009, Michel et al., 2012).

Various methods have been developed to measure mitochondrial biogenesis and mass, such as staining with MitoTracker dyes and transmission electron and fluorescent microscopy have been used to visualise mitochondria in cells (Rodriguez-Enriquez et al., 2009, Barbieri et al., 2011). Another approach includes measurement of mitochondrial enzyme activities in tissue lysates (Cerqueira et al., 2011), which is described further in section 2.10. Oxygen consumption can also be measured to quantify the respiratory function of mitochondria (Lehman et al., 2000, Fernandez-Vizarra et al., 2011). In recent years it has become more popular to measure mitochondrial DNA content as an index of mitochondrial content. As mitochondria contain DNA distinct from the nuclear genomic DNA, a convenient way to measure mitochondrial DNA content in a cell is to measure mitochondrial versus nuclear

genome ratio, termed Mt/N (Malik et al., 2011) otherwise known as mitochondrial “copy number”. The amount of mitochondrial DNA in a cell could provide a major regulatory point in mitochondrial activity, as the transcription of mitochondrial genes is proportional to their copy number (Hock and Kralli, 2009, Williams, 1986). This approach involves isolation of genomic DNA from cells or tissues of choice, and the use of qPCR to quantify a mitochondrial and a nuclear gene (Malik and Czajka, 2012).

### 2.9.1 Mitochondrial DNA content in mouse myometrium protocol

Genomic DNA was extracted from mouse myometrium from non-pregnant females in oestrous and late pregnant (day 18) mice (as described in section 2.2.6). Real Time qPCR (as described in section 2.3.9) was performed for the primers listed in Table 2.6. Primer sequences were acquired from Dr Afshan Malik’s group (Diabetes & Nutritional Sciences Division, King’s College London, UK), who have identified unique regions in the mouse mitochondrial sequence which are not duplicated in the nuclear genome. These sequences are yet to be published. Data were expressed as Mt/N ratio: the qPCR derived copy number for the mouse mitochondrial genome relative to the mouse beta-2 microglobulin copy number.

**Table 2.6 Oligonucleotide primer sequences used to determine mitochondrial copy number**

| Primer | Sequences |
|---|---|
| **mouse mitochondrion complete genome**<br><br>(Accession number: NC_005089.1) | **Forward primer:**<br>5'-CTAGAAACCCCGAAACCAAA -3'<br>**Reverse primer:**<br>5'-CCAGCTATCACCAAGCTCGT-3' |
| **mouse β2M** (beta-2 microglobulin)<br><br>(Accession number: NC_000068.8) | **Forward primer:**<br>5'-ATGGGAAGCCGAACATACTG-3'<br>**Reverse primer:**<br>5'-CAGTCTCAGTGGGGGTGAAT-3' |

*F= Forward primer sequence; R = Reverse primer sequence.*

## 2.10 Mitochondrial Electron Transport Chain Enzymatic Activities in Mouse Myometrium

The mitochondrial electron transport chain, compromising four mitochondrial complexes and an ATP synthase complex, pumps protons into the mitochondrial intermembrane space. This builds up a proton gradient which can be used by ATP synthase to produce ATP by oxidative phosphorylation (Figure 2.13). ATP is then transported to the region(s) of the cell it is required and broken down to ADP, releasing usable energy (Cox and Nelson, 2008).

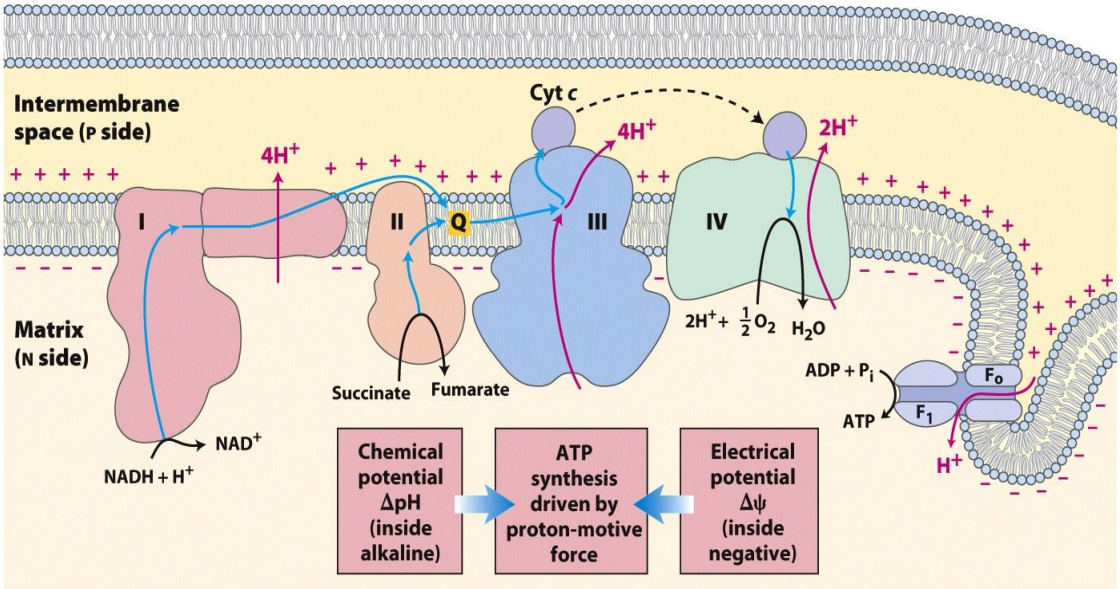


**Figure 2.13 Mitochondrial oxidative phosphorylation**
Within the mitochondria, electrons from NADH and other oxidized substrates pass through a chain of carriers/complexes arranged asymmetrically in the inner membrane. Electron flow coupled with proton transfer across the membrane, producing both a chemical gradient (ΔpH) and an electrical gradient ($\Delta\psi$). The inner mitochondrial membrane is impermeable to protons; protons can re-enter the matrix only through proton-specific channels ($F_o$). The proton-motive force that drives protons back into the matrix provides the energy for ATP synthesis, catalyzed by the $F_1$ complex associated with $F_o$ (ATP synthase complex). Figure from: Lehninger Principles of Biochemistry, Fifth Edition (Cox and Nelson, 2008).

Reactive oxygen species are normal by-products of the mitochondrial electron transport chain. ROS progressively damage the components of mitochondria, inducing the dysfunction of the electron transport chain (oxidative phosphorylation) and increased ROS production through a vicious cycle, ultimately leading to cellular dysfunction and ageing (Lagouge and Larsson, 2013). Oxidative phosphorylation in myometrial tissues was measured as part of this thesis, since it was hypothesized that tissues from older mice compared to younger would exhibit ROS-induced dysfunction of the electron transport chain that would consequently result in reduced ATP generation and energy availability for effective uterine contractions during labour.

The assay used in this study evaluates the maximal activity of three of the enzyme complexes preceding ATP synthase of the mitochondrial electron transport chain complex enzymes. This assay was carried out using snap frozen tissues collected over a two year time span. ATP synthase and ATP production cannot be measured after freezing as this disrupts the membrane and no membrane potential can build up for ATP production. This method was developed at the National Hospital for Neurology and Neurosurgery (University College London) for the analyses of biopsies from patients considered to be suffering from mitochondrial based disorders. The major strength of this assay is that it directly measures mitochondrial enzyme activity and does not rely on indirect markers.

***The principle of measuring citrate synthase activity:***

Citrate synthase [EC 2.3.3.1] is a pacemaker enzyme in the Krebs cycle. It is nuclear encoded and synthesized on cytoplasmic ribosomes, but transported into and localized in the mitochondrial matrix. Citrate synthase is therefore used as a quantitative marker enzyme for intact mitochondria (Holloszy et al., 1970, Williams et al., 1986, Hood et al., 1989), although this role of citrate synthase has been questioned in age related studies (Marin-Garcia et al., 1998). Proliferation of mitochondria in pathological studies is

usually associated with an increase in citrate synthase activity per cell, but citrate synthase activity in a specific tissue is frequently constant when expressed per mitochondrial protein. Mitochondrial respiration whether cellular or tissue, can therefore be expressed per citrate synthase activity for specific applications (Kuznetsov et al., 2002, Hutter et al., 2004, Renner et al., 2003).

The principle of this assay is that it catalyses the condensation of oxaloacetate and acetyl-CoA to form citryl-CoA and free Coenzyme A. The activity of citrate synthase is measured by the reaction of free CoA with DTNB at an absorbance of 412 nm (Shepherd and Garland, 1969, Kuznetsov et al., 2010). This assay is routinely used as an index of mitochondrial content.

Oxaloacetate + Acetyl CoA ⟶ Citrate + Coenzyme A

Coenzyme A + DTNB ⟶ DTNB-CoA (absorbs at 412 nm)

***The principle of measuring complex I activity:***

Complex I, NADH: ubiquinone oxidoreductase [EC 1.6.5.3] is the first complex in oxidative phosphorylation. It is the entry point for electrons into the respiratory chain by oxidation of NADH and transport of electrons to coenzyme-$Q_{10}$. Complex I also has proton-transporting activity over the inner mitochondrial membrane to the intermembrane space. The most commonly used technique for measuring complex I is a spectrophotometric assay measuring rotenone-sensitive NADH oxidations at 340 nm in tissue homogenate. Complex I is sensitive to different pathologies, particularly to oxidative stress, which is involved in ageing, ischemia-reperfusion injury, and anoxia/reoxygenation (Kuznetsov and Gnaiger, 2010, Rouslin, 1983, Rouslin and Millard, 1981, Rouslin and Ranganathan, 1983).

Complex I catalyses the oxidation of NADH. Electrons are transferred from NADH through complex I to ubiquinone-1 ($CoQ_1$) as an electron acceptor, which is reduced to ubiquinol. Complex I activity is measured as the rotenone-sensitive decrease in NADH at 340 nm to its non-absorbing oxidised form $NAD^+$ (Hatefi and Stiggall, 1978).

NADH + $H^+$ + ubiquinone-1 ($CoQ_1$) ⟶ $NAD^+$ + dihydroubiquinone-1 ($CoQH_2$)

***The principle of measuring complex II activity:***

Complex II, succinate-ubiquinone oxidoreductase [EC 1.3.5.1], is the only membrane-bound enzyme in the Kreb's cycle and is the second complex of the mitochondrial electron transport system. It catalyses electron transfer from succinate to the electron carrier, ubiquinone, but unlike the other four complexes it is not a proton pump. Succinate is oxidised to fumerate and ubiquinone is reduced to ubiquinol. Ubiquinol is utilized by complex III in the respiratory chain and fumarate is necessary to maintain the Kreb's cycle (Cecchini, 2003, Sun et al., 2005, Gnaiger, 2011).

Succinate + ubiquinone (Q) ⟶ Fumarate + ubiquinol (QH2)

In this reaction, succinate oxidation by complex II reduces decylubiquinone which spontaneously transfers its electrons to the dye DCPIP (2,6-diclorophenolindophenol). The change (usually decrease) in absorbance is measured at 600 nM.

Ubiquinol (QH2) + DCPIP ⟶ ubiquinone (Q) + DCPIPH2

***The principle of measuring complex III activity:***

Complex III, Ubiquinone- cytochrome c- oxidoreductase [EC 1.10.2.2] is the third enzyme complex of the mitochondrial electron transport chain. Complex III transfers two electrons from ubiquinol to ferricytochrome c and translocates four protons per pair of electrons transported into the intermembrane space (two from ubiquinol and two from the mitochondrial matrix). The function of complex III is crucial for the activity of the entire electron transport chain, since complex III can be rate-limiting in mitochondria activity (Krahenbuhl et al., 1994).

Complex III activity is measured by monitoring the reduction of cytochrome c when reduced decylubiquinone is used as a substrate and complexes I and IV activities are blocked by specific inhibitors (Krahenbuhl et al., 1994). The change in absorbance at 550 nm is measured. KCN is used to inhibit complex I by blocking electron transfer from NADH, via complex I to ubiquinone, thereby assuring that all reduction of cytochrome c is via complex II. KCN also inhibits complex IV, ensuring that there is no re-oxidation of cytochrome c. The specificity of this assay is determined by measuring the absence or presence of antimycin A, a specific inhibitor of complex III activity. The activity of complex III is measured by following the increase in the absorbance at 550 nm that corresponds to the reduction of cytochrome c. Complex III activity is then determined by the difference of the slopes before and after the addition of antimycin A.

Ubiquinol—cytochrome-c oxidoreductase catalyzes the chemical reaction:

Decylubiquinol +2 ferri-($Fe^{3+}$) cytochrome c $\rightarrow$ quinone +2 ferro-($Fe^{2+}$)cytochrome c

Oxidized cytochrome c $\rightarrow$ reduced cytochrome c

### 2.10.1 Mitochondrial electron transport chain enzyme activity protocol

Experiments were carried out during a laboratory visit to Joseph Fourier University, Grenoble, France. Experimental protocols adopted were those that were routinely used within the laboratory by Dr Luc Demaison and Dr Evangelia Mourmoura (Mourmoura et al., 2011).

***Uterine muscle sample preparation***

Non-pregnant (oestrous) and late pregnant (day 18) uterine tissues were dissected and immediately snap frozen in liquid nitrogen as described in section 2.1.3. Uterine samples (50 mg) were homogenised in 1:9 (w/v) 100 mM potassium phosphate ($K_2HPO_4 \cdot 3 \cdot H_2O$) buffer; pH adjusted to 7.4 using 100 mM potassium dihydrogen phosphate ($KH_2PO_4$) buffer. Homogenisation was carried out at 4°C in 2 ml RNAse-free round bottomed microcentrifuge tubes (Eppendorf, Germany), using a TissueLyser (Qiagen, UK; 2 minutes at 30Hz using two 5mm steal beads) until the tissue had been visibly broken down. The homogenates were centrifuged (1,500×g, 5 min, 4°C), and the resulting supernatants were stored at −80°C until determination of the various enzymatic activities.

***Measurement of enzymatic activities***

Enzymatic activities of the NADH-ubiquinone oxydo-reductase (complex I), succinate-ubiquinone oxydo-reductase (complex II), ubiquinol cytochrome c reductase (complex III) and citrate synthase were assayed using a spectrophotometer (Uvikon 941; Kontron Instruments, UK) in cuvettes containing 1 ml final volumes.

NADH-ubiquinone oxydo-reductase, complex I activity was determined spectrophotometrically by measuring the depletion of NADH at 340 nm in the presence of decylubiquinone. For each test sample, a 1 ml cuvette was placed into the spectrophotometer, and the reaction medium (pH 7.4) was made up by adding 47.5 nM potassium phosphate ($K_2HPO_4 \cdot 3 \cdot H_2O$) buffer, bovine serum-albumin (3.75 mg/ml), 0.1 mM NADH and 0.1 mM decylubiquinone to the cuvette. The reaction was initiated by adding 5 μl of 1: 200 diluted sample to the cuvette. The change in absorbance at 37°C was measured for two minutes, after which absorbance reading was stopped, and 10 μM rotenone was added to the cuvette. The change in absorbance was measured again for two minutes to evaluate the specific and nonspecific activities of complex I.

Succinate-ubiquinone oxydo-reductase, Complex II activity was again determined spectrophotometrically in the presence of succinate by measuring the disappearance of dichloro-inophenol (DCIP). In this reaction, oxidation of succinate by complex II causes reduction of decylubiquinone which spontaneously transfers its electrons to DCIP. For each test sample, a 1 ml cuvette was placed into the spectrophotometer. The reaction medium (pH 7.4) was made up by adding 45.4 mM potassium phosphate ($K_2HPO_4 \cdot 3 \cdot H_2O$) buffer, bovine serum-albumin (2.5 mg/ml), 9.3 μM antimycin A, 5 μM rotenone, 100 μM DCIP, 30 mM succinate, and 10 μl of 1: 200 diluted sample to the cuvette. The reaction mixture was stirred at 37°C inside the spectrophotometer for ten minutes, after which the reaction was initiated by addition of 50 μM decylubiquinone. The change in absorbance was then measured at 600 nM for five minutes.

Ubiquinol cytochrome c reductase, Complex III activity was spectrophotometrically determined for each test sample by measuring the depletion of cytochrome c when decylubiquinol was used as substrate and complexes I and IV were blocked by specific inhibitors. The change in absorbance at 550 nm was first evaluated at 30°C for one min in the presence of 90.7 mM potassium phosphate buffer (pH 7.4), 50 µM EDTA, bovine serum-albumin (1 mg/ml), 1 mM KCN, 100 µM oxidized cytochrome c, 0.11 mM decylubiquinol and 5 µl of 1: 200 diluted sample in order to evaluate total activity. Then the non-specific activity was measured for two minutes with the addition of antimycin A (5 µg/ ml) to the cuvette. Complex III activity was then calculated by subtraction of this non-specific activity.

Finally, citrate synthase activity was also measured spectrophotometrically. Citrate synthase catalyses the condensation of oxaloacetate and acetyl-CoA to form citryl-CoA and free Coenzyme A. Citrate synthase activity was measured for each test sample by the reaction of free Coenzyme A with DTNB at 412 nm. The reaction medium was made up by the addition of 84.5 mM Tris-Triton (Tris/0.1% [v/v] Triton) buffer (pH 8), 150 mM DTNB, 250 mM Acetyl CoA, and 5 µl 1: 200 diluted sample into a 1 ml cuvette placed into the spectrophotometer. The change in absorbance at 37°C was measured for two minutes, after which the reading was stopped, and 500 µM oxaloacetate was added to the cuvette. The absorbance was measured for a further two minutes. The difference in absorbance values before and after oxaloacetate was calculated to determine citrate synthase activity.

Protein content in each of the sample homogenates was determined by a commercially modified Lowry method (DC Protein Assay; Bio-Rad, UK) as per manufacturer's recommendations. The activities of the electron transport chain complexes were expressed in units per mg of homogenate protein content.

## 2.11 Statistical Analysis

### *Power calculations*

Power calculations were carried out for each study based on published data. Animal numbers were calculated to give a minimum of 80% power to detect a minimum of 20% difference between groups at the $p<0.05$ level.

### *Statistical tests*

For most analyses, data were tested for normal/ Gaussian distribution using the D'Agostino-Pearson omnibus normality test before running further parametric statistical analyses (as recommended by GraphPad Prism version 5.0; GraphPad Software, USA). Parametric statistical analyses such as Student's *t*-test and one-way analysis of variance (ANOVA) assume that the data being analysed follows a normal distribution (Ghasemi and Zahediasl, 2012). It was therefore important to test whether my data were normally distributed before confirming that Student's *t*-test and ANOVA were the most appropriate tests to identify statistical differences. GraphPad Prism version 5.0 offers three normal distribution tests, of which it highly recommends the D'Agostino-Pearson omnibus normality test. At first, this test computes the skewness (how symmetrical the distribution is) and kurtosis (whether the shape of the data distribution matches the Gaussian distribution) to quantify how far from Gaussian the distribution is. It then calculates how far each of these values differs from the value expected with a normal distribution, in order to compute a single p value from the sum of these discrepancies (D'Agostino et al., 1990). Student's *t*-test was used to assess data between two groups, and one-way analysis of variance (ANOVA) followed by all pairwise multiple comparison (Tukey's test) when comparing three or more groups. Data were expressed as mean ± standard error of the mean (SEM) and $p < 0.05$ was considered significant; 'n' refers to the number of animals per test group. Linear

regression analyses were carried out using Stata version 11.2 (StataCorp, College Station, USA), $p<0.05$ was considered significant. Specific details of any other statistical tests used are given within the relevant results chapters.

# Chapter 3

## Timing of Parturition in Mice of Advancing Reproductive Age

# Chapter 3 : Timing of Parturition in Mice of Advancing Reproductive Age

## 3.1 Introduction

As detailed in Chapter 1, the average maternal age of primiparous mothers in developed countries has risen steadily over the last decade, with women over the age of 35 comprising a significant proportion of the pregnant population (Bewley et al., 2009). Such trends are reflected by a simultaneous rise in the reported incidence of complications in pregnancy and during labour, which include miscarriage, stillbirth, preterm labour as well as post-term inductions, increased Caesarean section and instrumental delivery rates, failure to progress in labour, and postpartum haemorrhage (Gilbert et al., 1999, Ecker et al., 2001, Ziadeh and Yahaya, 2001, Tough et al., 2006, Jahromi and Husseini, 2008, Smith et al., 2008, Chan and Lao, 2008, Bewley et al., 2009, Ludford et al., 2012, Karabulut et al., 2013, Khalil et al., 2013). It raises the question as to how maternal age impacts on reproductive physiological processes, particularly in relation to parturition.

In animal studies of reproductive ageing, an increased length of gestation has been reported in a variety of species including goat, cow, sheep, hamster, rat and mouse (Asdell, 1929, Brakel et al., 1952, Terrill and Hazel, 1947, Soderwall et al., 1960, Moore, 1963, Holinka et al., 1978). Some have also reported an association of increased fetal mortality with prolonged gestation in rodents (Kroc et al., 1959, Moore, 1963, Holinka et al., 1978). However there is very limited information available about the impact of ageing in relation to parturition in mice, particularly in the C57BL/6 strain.

The prime objective for this part of my thesis was to validate the use of an aged primiparous pregnant mouse model by demonstrating that it successfully reflects the human situation with regard to increased gestation and length of labour.

Mice make convenient models for experimentation since they have a short gestation duration of 19 days compared to that of approximately 280 days in humans. However, there are distinct differences between human and mouse reproductive physiology which may limit the extent to which these models can provide meaningful evidence regarding the physiological mechanisms of human gestation. As detailed in Chapter 1, humans have a single chamber uterus whereas mice have two uterine horns. Mice also have a larger litter size of six to ten pups on average compared to a single fetus in most human pregnancies (Mitchell and Taggart, 2009, Ratajczak et al., 2010). The most important drawback of a mouse model of human parturition is that humans and mice regulate the production of progesterone differently. In humans, the initial site of progesterone production during gestation is the corpus luteum. However, five to six weeks after conception, the placenta is the major source of progesterone thereafter (Mitchell and Taggart, 2009). In mice, the corpora lutea are responsible for progesterone production throughout gestation, and their luteolysis induces a rapid fall in maternal progesterone concentrations triggering the onset of labour; however this is not consistent with the triggers for the onset of labour in humans (Ratajczak et al., 2010). It is also important to note that average life span of C57BL/6 mice is less than two years (Storer, 1966), whereas humans can live in excess of 80 years old, with an estimated maximum life span of 120 years (Ruiz-Torres and Beier, 2005) suggesting that the ageing processes between the two species may differ. Although there are limitations for the use of a mouse model to represent human parturition, it is technically difficult to obtain myometrial and cervical samples from women of advanced maternal age that do not have any confounding factors such as high BMI associate with them. Therefore it is difficult to fully explore the mechanisms of how maternal age impacts on reproductive physiological processes, particularly in relation to parturition in humans highlighting the need for an animal model.

## 3.2 Methods

Full descriptions and details of the methods used are described in Chapter 2, section 2.5. The age of mice as indicated within this chapter relate to the age of the dam at conception. The precise time of birth, marking the end of gestation, was determined by the appearance and complete delivery of the first pup. The precise duration of parturition was measured as the exact difference in time between the complete delivery of the first pup and the complete delivery of the last pup. Both time of first birth and duration of parturition were determined by either direct observation or by examination of video footage. Gestation length was counted as the number of days between conception and complete delivery of the first pup. Each pup (both live and stillborn) delivered per mouse was individually weighed within 6 hours after completion of parturition.

All data within this chapter were found to be normally distributed using the D'Agostino-Pearson omnibus normality test (GraphPad Prism version 5.0; GraphPad Software, USA) unless otherwise stated. Student's *t*-test was used to assess data between the two groups. Data were expressed as mean ± standard error of the mean (SEM) and $p<0.05$ was considered significant; 'n' refers to the number of animals per sample group. Linear regression analysis was carried out using Stata version 11.2 (StataCorp, USA).

## 3.3 Results

### 3.3.1 Determination of gestation length by continuous infra-red video recording and direct observation

An increased length of gestation of 20.1 ± 0.2 days was recorded in the older pregnant (eight month old) mice (n = 6), compared to 19.1 ± 0.1 days in younger pregnant (three month old) mice (n = 8, $p<0.001$) (Figure 3.1). Overall, 66.6% of the 8 month old mice had a gestation of 20 days, and 25% of mice in this group failed to maintain pregnancy to term (Table 3.1).

**Table 3.1 Individual gestation lengths between C57BL/6J mice aged three months versus eight months**

| Mouse ID | Gestation length (Days) | % Mothers that exhibited spontaneous labour |
|---|---|---|
| 3 month (1) | 19.1 | |
| 3 month (2) | 19.1 | |
| 3 month (3) | 19.1 | |
| 3 month (4) | 19.1 | |
| 3 month (5) | 19.4 | |
| 3 month (6) | 18.5 | |
| 3 month (7) | 19.1 | |
| 3 month (8) | 18.9 | **100%** (n = 8 of 8) |
| | | |
| 8 month (1) | 20.4 | |
| 8 month (2) | 20.3 | |
| 8 month (3) | 19.5 | |
| 8 month (4) | 19.5 | |
| 8 month (5) | 20.1 | |
| 8 month (6) | 20.7 | |
| 8 month (7) | Failed to maintain pregnancy | |
| 8 month (8) | Failed to maintain pregnancy | **75%** (n = 6 of 8) |

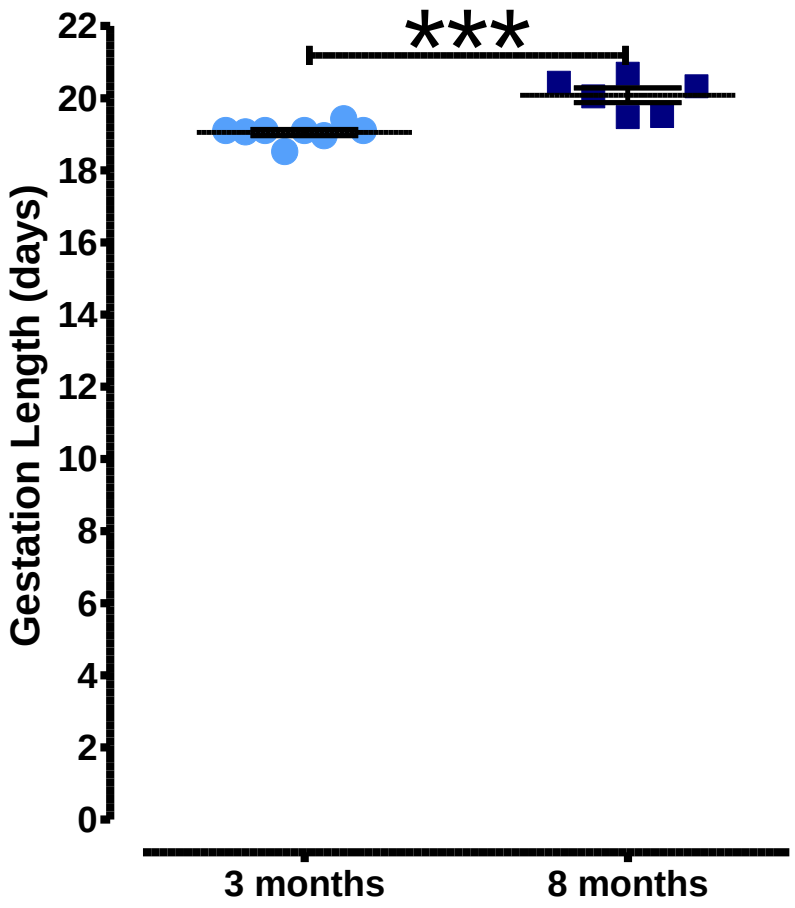


**Figure 3.1 Eight month old pregnant mice have a longer gestation length than three month old pregnant mice**

Scatter graph presenting individual gestation lengths in three month old (n = 8, light blue circles) and eight month old (n = 6, dark blue squares) pregnant mice. Gestation was significantly longer in eight month old mice, *** $p<0.001$, Student's t-test. Horizontal bars indicate means, and error bars indicate ± SEM. Gestations with similar lengths are shown as off-centered overlapping points.

### 3.3.2 Duration of parturition as a function of maternal age

Direct observation combined with infrared video recording indicated that pregnant mice of both age groups exhibited common behavioural signs prior to and during labour; these included whole body quivering, grooming of vaginal area, and repeated cycles of standing on hind legs followed by stretching out rear body in a lordosis-like movement. Figure 3.2 shows some still images captured from the video recording to illustrate common labour behaviours.

Labour duration was influenced by reproductive age; eight month old pregnant mice had a significantly longer mean duration of parturition (3.7 ± 0.3 hours, n = 6) compared to 1.0 ± 0.2 hours exhibited by the three month old group (n = 8, $p<0.001$) (Figure 3.3). Parturition in older mice was prolonged by approximately 2.7 hours (162 minutes) on average compared to younger mothers.

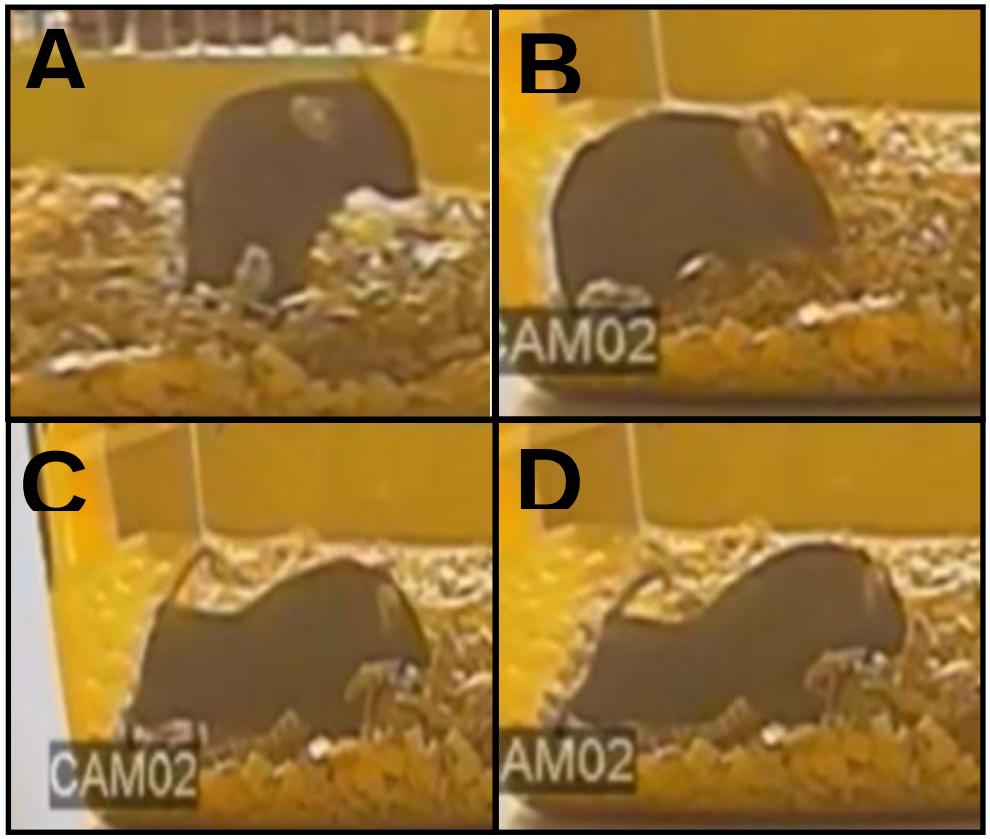


**Figure 3.2 Representative images from continuous infrared video recording showing common movements displayed prior to and during labour**
**A:** standing on hind legs; **B-D:** stretching out rear body in a lordosis-like posture. All mice (of both ages) displayed repeated signs of A-D whilst in labour.

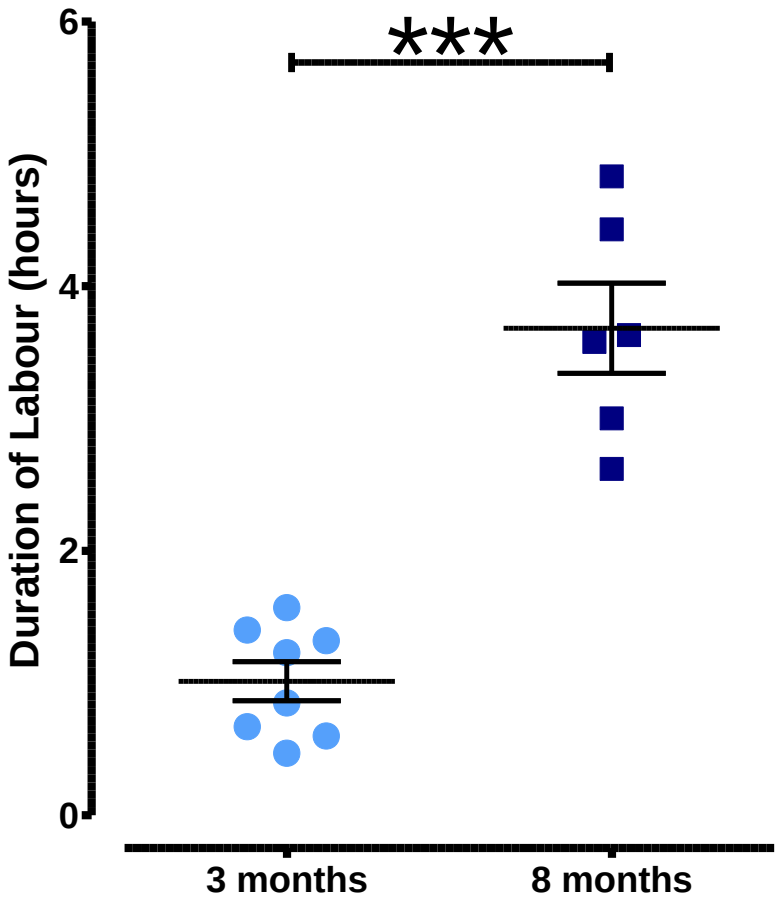


**Figure 3.3 Eight month old pregnant mice have a longer duration of labour than three month old pregnant mice**

Scatter graph presenting individual labour durations in three month old (n = 8, light blue circles) and eight month old (n = 6, dark blue squares) pregnant mice. Parturition was significantly longer in older eight month old mice, *** $p<0.001$, Student's t-test. Horizontal bars indicate means, and error bars indicate ±SEM.

### 3.3.3 Litter size as a function of maternal age

The number of pups (live and stillborn) delivered per mother was influenced by reproductive age; eight month old pregnant mice (n = 6) had a significantly reduced mean litter size of 4.8 ± 0.9 pups compared to 7.5 ± 0.2 pups delivered by the three month old mothers (n = 8, $p<0.01$) (Table 3.3, Figure 3.4). Litter size in older mothers was reduced by 36% compared to younger mothers. As shown in Table 3.2, 50% of the mothers in the eight month old group delivered stillborn pups, whereas none of the younger mothers did so.

**Table 3.2 Individual litter sizes born to C57BL/6J mice of maternal ages three month old versus eight month old**

| Mouse ID | Litter size (Days) | % Mothers that delivered stillborn pups |
|---|---|---|
| 3 month (1) | 8 | |
| 3 month (2) | 8 | |
| 3 month (3) | 7 | |
| 3 month (4) | 7 | |
| 3 month (5) | 7 | |
| 3 month (6) | 7 | |
| 3 month (7) | 8 | |
| 3 month (8) | 8 | **0%** (n= 0 of 8) |
| | | |
| 8 month (1) | 1 | |
| 8 month (2) | 4 (1 still born) | |
| 8 month (3) | 7 (1 still born) | |
| 8 month (4) | 7 | |
| 8 month (5) | 5 | |
| 8 month (6) | 5 (1 still born) | |
| 8 month (7) | Failed to maintain pregnancy | |
| 8 month (8) | Failed to maintain pregnancy | **50%** (n= 3 of 6) |

As highlighted in Table 3.2, two of the eight month old mice failed to deliver by day 22. All mice, regardless of age group, were confirmed pregnant on day 15 of gestation, but by day 22 the two older mice had intrauterine fetal loss and fetal resorption, as determined by uterine dissection. Taking this into account, four of the total eight (50%) older pregnant mice experienced some degree of fetal loss; no fetal loss was evident in the younger pregnant mice.

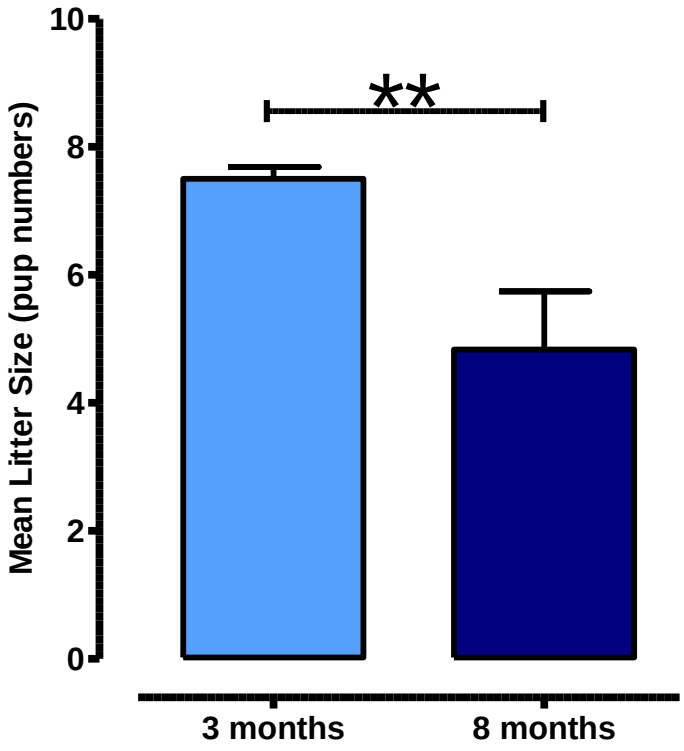


**Figure 3.4 Eight month old pregnant mice have a reduced litter size compared to three month old pregnant mice**

Bar graph illustrating litter size for three month old (n = 8) and eight month old (n = 6) pregnant mice. Litter size was significantly reduced in older eight month old mice, ** $p<0.01$, Student's t-test. Data expressed as mean ± SEM.

### 3.3.4 Pup weight as a function of maternal age

Reproductive age had no effect on the mean pup weight of the litter. There was no significant difference between the mean pup weight delivered by older pregnant mice: 1.59 ± 0.07 g (n = 29, from n = 6 mice) compared to 1.54 ± 0.04 g delivered by the younger mice (n = 60, from n = 8 mice) (Figure 3.5).

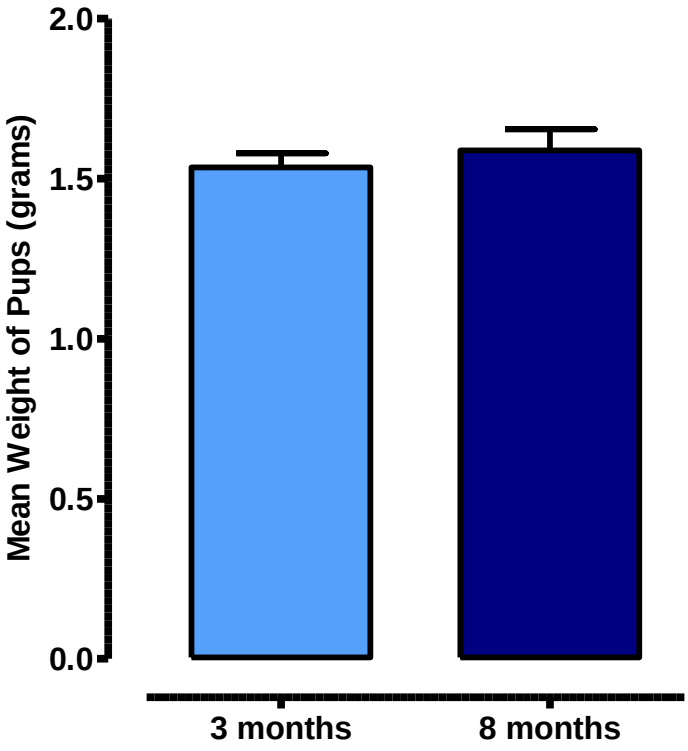


**Figure 3.5 Mean pup weight delivered by three month old pregnant mice was similar to that of eight month old pregnant mice**

Bar graph presenting mean pup weight delivered by three month old pregnant mice (n = 60, from n = 8 mice) and eight month old pregnant mice (n = 29, from n = 6 mice). Statistical comparison was non-significant, Student's t-test. Data expressed as mean ± SEM.

### 3.3.5 Length of gestation as a function of maternal age and/or litter size

Linear regression analyses were carried out to determine whether the prolongation of gestation in older mice could be explained not only by an influence of maternal age but also mechanistically because of a reduction in litter size in this group. The impact of older maternal age on gestation length was 1.03 days (95% CI: 0.59 to 1.47; $p<0.001$), which remained significant after adjustment for litter size, the effect of maternal age on gestation length, was 0.64 days (95% CI: 0.12 to 1.16; $p<0.05$). This result indicates that 62% of the increase in gestation length in older mice is due to maternal age (Figure 3.6).

Conversely, the impact of increasing litter size by one pup would reduce gestation length by 0.26 days (95% CI: -0.38 to -0.14; $p<0.001$), but after adjustment for maternal age the impact of increasing litter size by one pup was a reduction in gestation length by 0.15 days (95% CI: -0.28 to -0.01; $p <0.05$) (Figure 3.6).

A final linear regression showed there was no significant interaction between maternal age at conception and litter size on the control of gestation length.

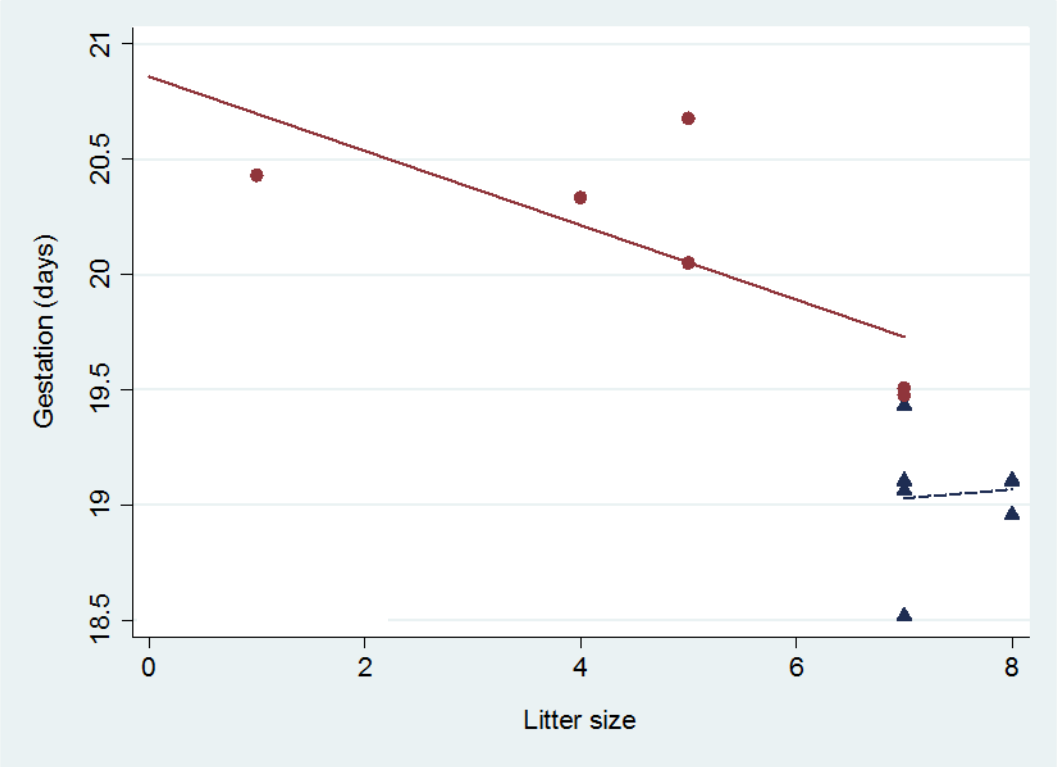


**Figure 3.6 Gestation length in C57BL/6J mice as a function of maternal age and litter size**
Scatter plot illustrating the relationship between gestation length and litter size in three month old (n = 8, dark blue triangles) and eight month old (n = 6, red circles) pregnant mice. Gestation length is prolonged with older maternal age, and with smaller litter size; however, there is no significant interaction between maternal age and litter size on the control of gestation length; linear regression analysis.

### 3.3.6 Duration of parturition as a function of maternal age and/or litter size

Further linear regression analyses were carried out to determine whether the prolonged duration of labour in older mice could be explained not only by an influence of maternal age but also mechanistically because of a reduction of litter size in this group. The impact of maternal age on labour duration was 2.67 hours (95% CI: 1.93 to 3.41; $p<0.001$); after adjustment for litter size, the effect of maternal age on labour duration was 1.77 hours (95% CI: 1.14 to 2.39; $p<0.001$). These data indicate that 66% of the increase in labour duration in older mice is due to maternal age (Figure 3.7).

Conversely, the impact of increasing litter size by one pup would reduce labour duration by 0.65 hours (95% CI: -0.89 to -0.42; $p<0.001$); this remained significant after adjustment for maternal age, the impact of increasing litter size by one pup was a reduction in labour duration by 0.34 hours (95% CI: -0.50 to -0.18; $p<0.001$) (Figure 3.7).

A final linear regression found no significant interaction between maternal age at conception and litter size on the control of labour duration.

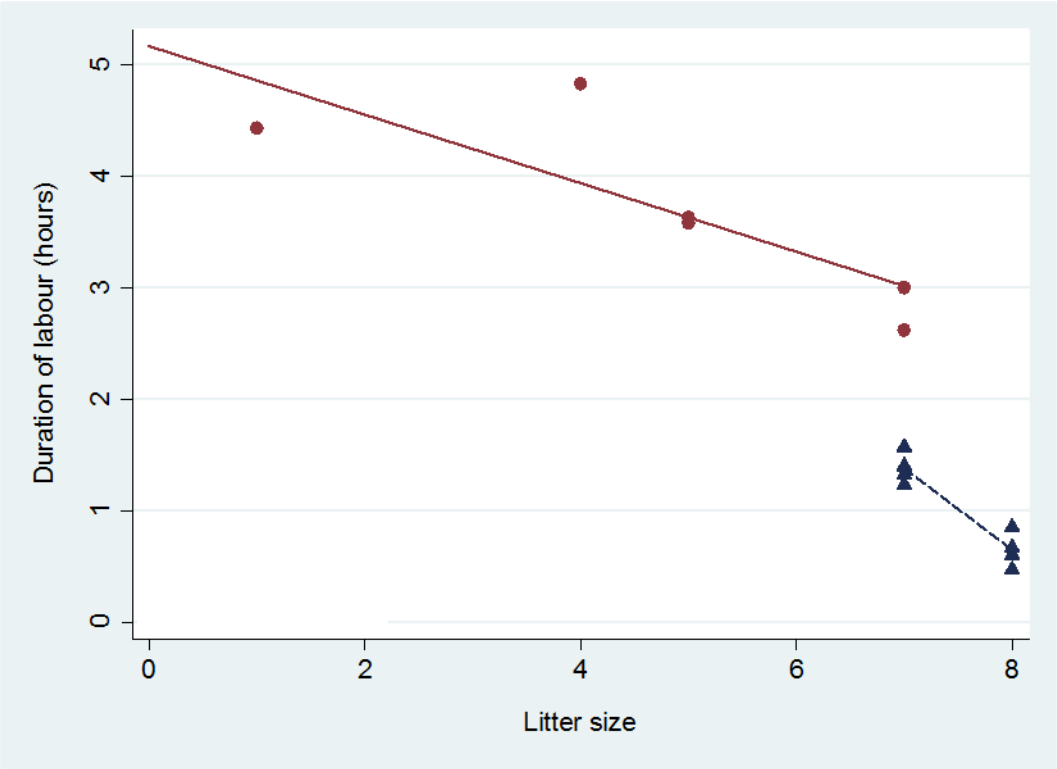


**Figure 3.7 Labour duration in C57BL/6J mice as a function of maternal age and litter size**
Scatter plot illustrating the relationship between duration of labour and litter size in three month old (n = 8, dark blue triangles) and eight month old (n = 6, red circles) pregnant mice. Labour duration is prolonged with older maternal age, and with smaller litter size; however, there is no significant interaction between maternal age and litter size on the control of labour duration; linear regression analysis.

## 3.4 Discussion

This study which focused on the impact of maternal age (at conception) on gestation length indicates that older mice are more likely to have prolonged pregnancies and longer labours compared to younger mice. Pregnancy in older mice is also associated with a reduced litter size and increased number of failed pregnancies/still births. This study supports the use of three month and eight month old pregnant C57BL/6J mice as a useful model of reproductive ageing in relation to parturition, and is also the first study to demonstrate that an aged primiparous C57BL/6J pregnant mouse model can successfully reflect increased gestation and length of labour as seen in humans.

Observations of gestation length, accurately recorded by infra-red recording and/or direct observation in C57BL/6J mice, clearly demonstrated that pregnancy duration is significantly prolonged by 1.03 days or 5% of a normal 19 day gestation in older eight month old primiparous mice. This observation confirms data from a series of historic studies and some more recent reviews that also report a marked increase in gestation length seen with advancing maternal age across various species including C57BL/6J mice and humans (Asdell, 1929, Brakel et al., 1952, Terrill and Hazel, 1947, Soderwall et al., 1960, Moore, 1963, Holinka et al., 1978, Silk et al., 1993, Jolly et al., 2000, Roos et al., 2010). The only known study to report prolonged gestation in aged C57BL/6J mice used the direct observation method and proven breeders up to the age of 11 to 12 months. They reported a gestation increase of 2.2 days in these aged mice (Holinka et al., 1978). The present study provides novel data showing that the length of gestation in primiparous C57BL/6J mice is prolonged from the age of eight months, confirming that reproductive ageing in this strain of mice begins at eight months of age.

Labour duration was also significantly lengthened by 3.6 fold in older mice compared to the younger age group; previous studies have not examined this in any detail in other animal species, including C57BL/6J mice. The novel use of infra-red video recording greatly facilitated data collection, as can be seen by the representative images extracted from 80 hours of video. The methodology employed in this study is similar to that previously published (Brown et al., 2009), but the combined use of video recording and direct observation where possible allowed for identification of behavioural labour signs and therefore accurate determination of pregnancy length (to delivery of first pup) and the duration of labour, which are rarely reported in the literature. As far as can be ascertained, this is the first study to confirm that labour duration in first pregnancies is increased with age in C57BL/6J mice.

The present study identified a negative relationship between reproductive age at conception and resultant litter size at term. Older mice delivered smaller litters and had a greater incidence of stillbirth. Additionally, a small number of older (eight month old) mice failed to deliver by 22 days of gestation and this was most likely due to pup resorption. A reduction in litter size in older animals has been reported previously across various species including C57BL/6J mice (Soderwall et al., 1960, Finn, 1963, Holinka et al., 1978, Holinka et al., 1979, Lopes et al., 2009, Monclus et al., 2011, Kong et al., 2012). Increased rates of resorption of conceptuses, intrauterine fetal deaths as well as stillbirth rate have also been reported in various studies of ageing rodents (Talbert, 1971, Holinka et al., 1979, Niggeschulze and Kast, 1994, Akiyama et al., 2006, Lopes et al., 2009, Kong et al., 2012).

Similarly, this present study identified a general negative relationship between litter size and gestation, independent of age, which confirms reported observations by others across many species including C57BL/6J mice (Biggers et al., 1963, McLaren and Michie, 1963, Holinka et al., 1978, Rydhmer et al., 2008). There is little/no published data as far as can be ascertained relating to litter sizes in first pregnancies of reproductively aged C57BL/6J mice, the strain used in the current study. The relative contribution of maternal age and litter size to gestation length and labour duration were statistically explored further and found that there is a contribution of both. However, the influence of maternal age on both gestation and labour was greater than litter size. There was no interaction between maternal age and litter size, suggesting that these factors affect the process of parturition via independent mechanisms.

An inverse relationship between fetal weight and litter size has been discussed by many authors (Biggers et al., 1963, Romero et al., 1992a, Damgaard et al., 2003, Freetly and Leymaster, 2004, Ishikawa et al., 2006, Akdag et al., 2009, Murray et al., 2010), however in this present study there was no significant relationship found between mean pup weights and litter size, and likewise between pup weights of older and younger mothers. This may be a consequence of the relatively smaller sample size used in the present study compared to others.

Data obtained in the current study is in agreement with both existing reproductive models of ageing in animals and published observations on reproductive ageing in humans. The length of labour and risk of prolonged labour has been reported to increase with increasing maternal age in humans (Greenberg et al., 2007). In this human study, older nulliparous and multiparous women were found to have a higher risk of experiencing prolonged second stage of labour than did younger women, with an odds ratio of 3.90 for nulliparous women who were older than 39 years old, compared with women who were younger than 20 years old (95% CI, 2.70-5.62). Stillbirth and fetal loss are also common risk factors for mothers of advanced maternal

age; a recent study by Haavaldsen *et al*. (2010) found women older than 40 years of age had the highest risk of fetal death throughout pregnancy, particularly in term- and post-term pregnancies (Haavaldsen et al., 2010). Another study reported the relative risk of stillbirth at 37-41 weeks of gestation was 1.88 (95% CI, 1.64-2.16) for women aged 40 years or over compared to women aged under 35 years (Reddy et al., 2006).

There are a number of possible explanations for the maternal age related prolonged gestation length, but all still require further investigation. The most likely is a delay in the initiation of progesterone withdrawal, which is essential for the onset of parturition in rodents (Weiss, 2000). Theoretically, the onset of progesterone withdrawal may either be delayed or the decline in circulating progesterone concentrations less rapid in older mice compared to younger mice. Luteolysis, the structural and functional degradation of the corpus luteum driven by the release of prostaglandin F2$\alpha$ from the endometrium (Mitchell and Taggart, 2009), induces the necessary fall in maternal progesterone concentrations in mice before labour. A disruption in this pathway could alter the timing of luteolysis and hence cause a delay in progesterone decline in older mice. However, the earliest significant decline in murine corpus luteum function has been reported to occur at 10 to 11 months of age (Harman and Talbert, 1970), so may not be as relevant to the 8 month old mice model used in this study. Interestingly, Harman and Talbert reported that pregnant mice aged 12 to 13 months old mice had no recognisable corpus lutea or implantation sites.

Luteolysis in the cow is believed to be caused by a pulsatile release of prostaglandin F2$\alpha$ from the uterus with a positive feedback mechanism between endometrial prostaglandin F2$\alpha$ and luteal oxytocin; luteal oxytocin has a physiologic role in the promotion of luteolysis (Shirasuna et al., 2007). Based on this theory, luteal oxytocin may also be involved in the control of murine luteolysis. Therefore, one can postulate that oxytocin release from the corpus luteum in older mothers may also be delayed or impaired, preventing successful luteolysis.

In the present study, an attempt was made to obtain terminal blood samples from all mice to determine serum progesterone concentrations immediately postpartum. However, many of the samples obtained were of insufficient volume, which resulted in an inadequate sample size available for analysis. Also, terminal samples would not have been fully informative, as the majority of mice had gone into labour at this point. Ideally, to accurately measure the exact rate of maternal serum progesterone decline and determine whether this changes with maternal age in C57BL/6J mice, it would be more valuable to take serial blood samples from pregnant mice throughout pregnancy. This in itself would be likely to cause stress to the animals which is commonly associated with increased fetal loss and premature delivery. To overcome this, a pilot study could be carried out whereby bleeding takes place every other day from day 13 (or even day 15) of gestation onwards. Alternatively, a cross sectional study might be more appropriate. Animals would be sacrificed at a range of gestations in both age groups. This approach would also allow accurate assessment of implantations sites and identify at which gestations fetal loss/resorption occurs.

The reduction in litter size in older mothers in this study supports well-established data from both humans and rodent models that indicate that viability decreases with an increase in maternal age (Khalil et al., 2013, Nagaoka et al., 2011, Qiao et al., 2013, Kermath and Gore, 2012, Kong et al., 2012). Possible causes for fetal loss in older mothers in this study can be a result of reproductive senescence changes such as oocyte depletion and poor oocyte quality in aged ovaries resulting in the development of fewer and/or non-viable fetuses (Liu et al., 2013). Decreased litter size is directly related to an increase in the number of defective blastocysts (as a consequence of abnormal embryonic development patterns) available for implantation. These observations suggest that pre- and peri-implantation failures may account for the decline in reproductive capacity displayed by aged mice (Day et al., 1991). Additionally, the reduction in litter size in older mothers could be explained by the failure of the aged uterus to maintain embryonic development (Talbert, 1971, Holinka

et al., 1979, Kong et al., 2012). An increase in collagen has been reported in the uterus of female rodents as a function of age, which is proposed to play an important role in the decline in embryonic survival. Increased collagen content is thought to mechanistically interfere with uterine vascularisation, which is required for successful implantation and embryonic survival (Biggers et al., 1962, Mulholland and Jones, 1993, Kong et al., 2012).

Uterine stretch studies in multiple pregnancies in humans and rodents have implicated that there is a stretch-induced increase in the expression of oxytocin receptor, cytokines and gap junctions, such as connexin-43 in the myometrium, that trigger the development of co-ordinated uterine contractions at the onset of labour (Ou et al., 1997, Lyall et al., 2002, Turton et al., 2013). This stretch induced myometrial activation in rodents is thought to occur under low progesterone levels. Therefore, if progesterone withdrawal is unaffected in the older mice in this study, the delay in the onset of labour and the increased duration of labour could be a result of reduced uterine stretch (due to fewer fetuses), meaning that the myometrium is not stretch-activated for co-ordinated contractions.

In summary, the primiparous eight month old pregnant mouse was found to successfully reflect some of the key risk factors seen in pregnancies in older women such as delayed onset of parturition, prolonged duration of labour as well as greater risk of fetal loss. In the following results chapters the myometrial expression of contractile associated proteins that are necessary for the onset of uterine contractions at labour and the ability of the myometrium to contact (both spontaneous and agonist induced) will be investigated in the older pregnant mouse model. In addition, common markers of cervical ripening such as collagen degradation and the degree of cervical softening at term will be determined.

These data will aim to determine whether there is a myometrial and/or cervical function disruption in the older eight month old mothers, which may be hindering the onset of labour.

### *Study limitations and future work*

Although the present study successfully validated a novel primiparous mouse model of reproductive ageing, further work may help to strengthen the model. As mentioned above, the primary limitation to this study is that terminal blood samples were not collected for the entire sample set. It would be advantageous to repeat this study and collect blood samples from day 13 of gestation onwards, to track maternal progesterone levels over late gestation. This would give a better understanding of whether the delayed onset of labour in older primiparous mice is caused by a sustained elevation of maternal serum progesterone or via other mechanisms. Since a quarter of the older mothers experienced intra-uterine fetal loss and did not labour, it would also be valuable when repeating this study to use a larger sample size. Implantation sites were not examined; however, if done so, it would have given a better understanding of the degree of reproductive ageing in eight month old pregnant mice.

### *Conclusions*

The outcome of this study adds to the existing data pertaining to reproductive ageing in mice and confirms that both gestation and parturition are prolonged in a primparous mouse model of maternal ageing, as well as deterioration in reproductive capacity reflected by a decline in litter size. The mouse model mimics characteristics of the problems associated with ageing in humans and is a suitable model to further assess the mechanisms responsible for the age induced changes demonstrated in this study.

# Chapter 4

## Alterations in Cervical Remodelling as a Consequence of Reproductive Ageing in Mice

# Chapter 4 : Alterations in Cervical Remodelling as a Consequence of Reproductive Ageing in Mice

## 4.1 Introduction

As detailed in Chapter 1, cervical remodelling towards the end of pregnancy in mice can be divided into four stages: softening, ripening, dilation and postpartum repair (Word et al., 2007, Leppert, 1995, Timmons et al., 2010). Cervical softening, the first stage, is defined as a change in the biomechanical properties of the cervix, specifically a measurable decline in tissue tensile strength when compared with the non-pregnant cervix and is characterised by a progressive decrease in tissue stiffness without loss of tensile strength (Leppert and Yu, 1994). The ability of the cervix to soften yet remain resistant to forces exerted upon it involves a dual mechanism in which there is an increase in the size of the cervix along with maintained stiffness of the cervical wall (Read et al., 2007). The “strength” of cervical extracellular matrix is determined by the content and organisation of collagen. Cervical softening is associated with disorganisation of the collagen network (House et al., 2009). Final cervical ripening precedes the biomechanical dilation of the cervix during parturition. Increased collagenases have been observed in the cervix during ripening, which degrade collagen and contribute to the reorganisation of the extracellular matrix before parturition. Gelatinases such as MMP2 and MMP9 have been reported to cleave and consequently activate pro-collagenases and also target denatured collagen IV, and hence have been indicated to play a role in the cervical ripening process (Stygar et al., 2002, Mahendroo, 2012).

Since proper cervical function is essential for successful parturition to occur, the prime objective for this part of the thesis was to determine whether cervical softening, collagen content and expression of MMP2 were altered in aged eight month old primiparous pregnant mice and conclude whether the physiological preparation of cervical tissue for labour was impaired and thus delayed in these mice.

## 4.2 Methods

Full descriptions and details of the methods are described in Chapter 2, sections 2.7 and 2.8. In summary, *ex vivo* tensile strength measurements of the cervix were used to assess cervical canal distension in three, five and eight month old non-pregnant and late pregnant mice. Tension generated at the limit at which no further distension of the cervical canal could be achieved was recorded as maximum tension of the cervical tissues (understood as another measurement of cervical biomechanical properties). Collagen was detected by Masson's trichrome blue staining and MMP2 expression was detected by immunohistochemical staining in cervical tissues from non-pregnant and late pregnant mice of all ages. All non-pregnant cervical tissues were collected when mice were in oestrous stage of their reproductive cycle and all late pregnant cervical tissues on day 18 of gestation. The age of late pregnant mice (three, five and eight months) as indicated within this chapter relates to the age of dams at conception.

All data within this chapter were found to be normally distributed using the D'Agostino-Pearson omnibus normality test (GraphPad Prism version 5.0; GraphPad Software, USA), unless otherwise stated. Student's *t*-test was used to assess data between two groups and one-way analysis of variance (ANOVA) followed by all pairwise multiple comparison (Tukey's test) was used when comparing three or more groups. Data were expressed as mean ± standard error of the mean (SEM), and $p<0.05$ was considered significant; 'n' refers to the number of animals per sample group.

## 4.3 Results

### 4.3.1 Biomechanical assessment of cervical softening

*Ex vivo* tensile strength measurements in isolated cervices demonstrated that maximal distension (increase in cervical canal diameter) was significantly greater in mice of all ages in the late pregnant state compared to non-pregnant, implicating that some degree of cervical softening had occurred in all groups by day 18 of gestation (Figures 4.1 and 4.2). The maximal distension achieved by late pregnant cervical tissues compared to age matched non-pregnant tissues was 2.59, 2.88 and 1.82 fold higher for three, five and eight month old mice respectively ($n = 6\text{-}9$, $p<0.0001$ for all) (Figure 4.2). There was no significant difference between maximal distension obtained in tissues from non-pregnant mice aged three and five months of age, however there was a 1.72 fold increase in cervical distension in tissues from eight month old non-pregnant mice ($10.6 \pm 0.2$ mm, $n = 8$) compared to the three month old group ($6.2 \pm 0.2$ mm, $n = 6$, $p<0.001$), and a 1.70 fold increase compared to the five month old non-pregnant group ($6.3 \pm 0.2$ mm, $n = 8$, $p<0.001$) (Figure 4.2). In late pregnant mice, cervical tissues from eight month old mice demonstrated a 1.21 fold increase in maximal cervical distension ($19.3 \pm 0.4$ mm, $n = 6$) compared to the three month old late pregnant group ($16.0 \pm 0.5$ mm, $n = 9$, $p<0.001$), and there was a 1.13 fold increase in tissues from five month old mice ($18.0 \pm 0.3$ mm, $n = 6$) compared to the three month group ($p<0.01$) (Figure 4.2).

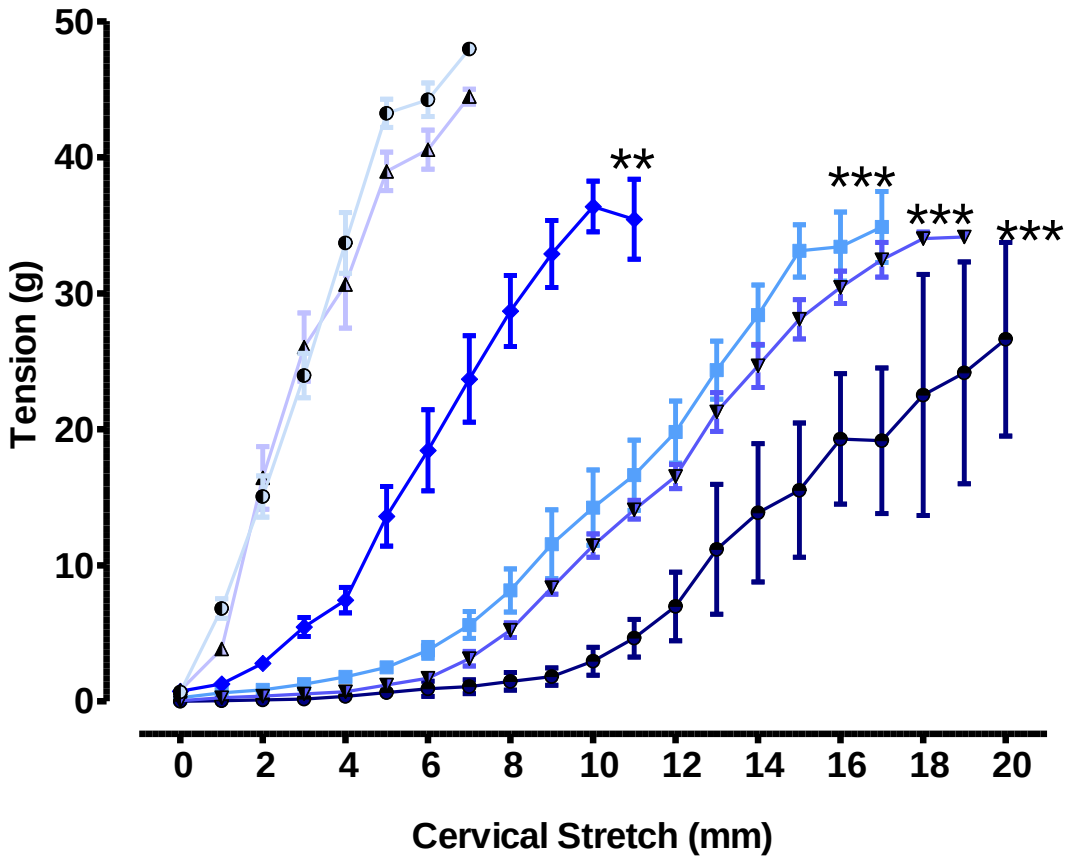


**Figure 4.1 The impact of age on cervical distension induced by stretch in non-pregnant and late pregnant tissues**

Tension generated by the cervix is plotted as a function of incremental stretch of the cervical canal diameter as stress-strain curves. Tissues obtained from non-pregnant three month (n = 6, black/light blue circles), five month (n = 8, black/light purple triangles), and eight month (n = 8, blue diamonds) old mice, as well as late pregnant three month (n = 9, light blue squares), five month (n = 6, black/ blue inverted triangles), and eight month (n = 6, black/dark blue circles) old mice. Summary measure means were significantly different between non-pregnant mice aged three months compared to eight months, and five months compared to eight months (** $p<0.01$), as well as non-pregnant compared to late pregnant mice of all three age groups (*** $p<0.001$); ANOVA followed by all pairwise multiple comparison Tukey's test. Data expressed as mean ±SEM.

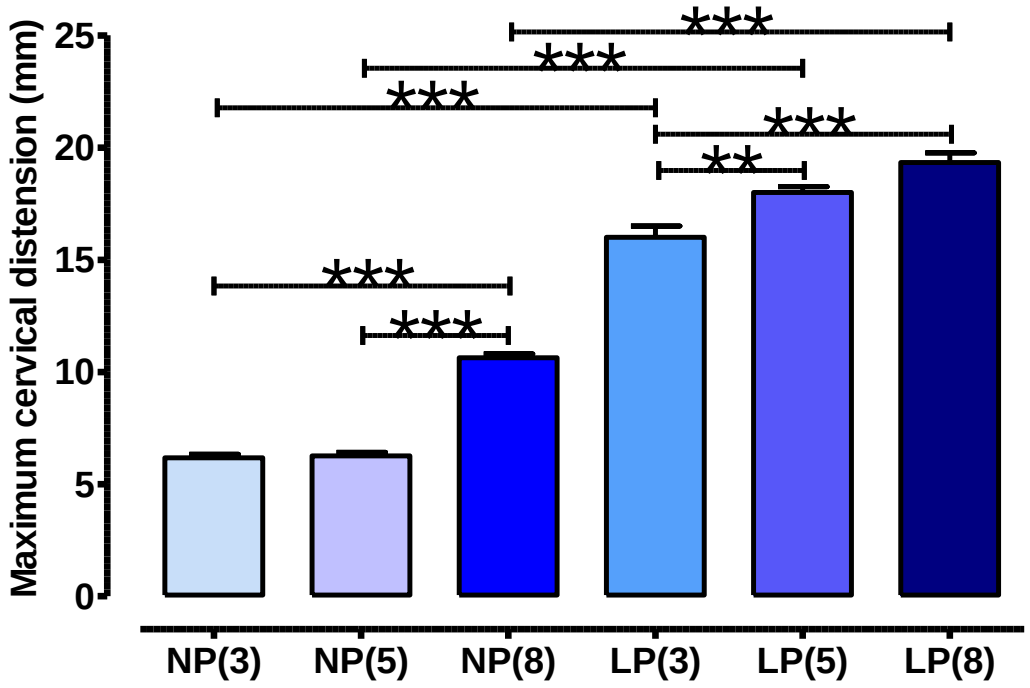


**Figure 4.2 Maximum distension of cervical canal is enhanced in older eight month old mice both in non-pregnant and late pregnant states compared to younger age group**

Cervices from non-pregnant three month [NP(3), n = 6], five month [NP(5), n = 8], and eight month [NP(8), n = 8] old mice, as well as late pregnant three month [LP(3), n = 9], five month [LP(5), n = 6], and eight month [LP(8), n = 6] old mice were distended until no further stretch of the cervical canal was possible. Transition from non-pregnant to pregnant state, significantly increased maximal cervical distension in all three age groups, *** $p<0.001$. Advance in age from three to eight months, and five to eight months in non-pregnant mice, and from three to five to eight months in late pregnant mice also significantly increased maximal cervical distension, ** $p<0.01$ and *** $p<0.001$; ANOVA followed by all pairwise multiple comparison Tukey's test. Data expressed as mean ±SEM maximal cervical stretch/distension.

Maximal tension of cervical tissues was significantly reduced by a factor of 0.78 in late pregnant mice of three months of age (34.2 ± 2.3 g, n = 9) compared to age matched non-pregnant cervical tissues (44.0 ± 1.0 g, n = 6, $p<0.05$). Similarly, maximal tension was significantly reduced in cervical tissues from five month old late pregnant mice (32.5 ± 1.5 g, n = 6) by a factor of 0.79 compared to cervices from non-pregnant mice of five months of age (41.1 ± 1.6 g, n = 8, $p<0.05$) (Figure 4.3). This difference was not apparent in tissues taken from eight month old mice. There was no age-specific change in maximal tension developed in cervical tissues taken from non-pregnant mice (three, five and eight month age groups). Likewise, the maximal tension values developed in cervical tissues taken from three, five and eight month old late pregnant mice were similar, again displaying no age induced effect (Figure 4.3).

Cervical stiffness was determined as the slope of cervical distension stress-strain curves as demonstrated in Figure 4.1. Cervical stiffness was significantly reduced in mice of all ages in the late pregnant state compared to non-pregnant by a factor of 0.32, 0.27 and 0.49 for three, five and eight month old mice respectively (n = 6-9, $p<0.0001$ for all) (Figure 4.4). There was no significant difference in cervical stiffness between tissues from non-pregnant mice aged three and five months of age, however there was a decline by a factor of 0.48 between the three (7.1 ± 0.2 g/mm, n = 6) and eight (3.4 ± 0.2 g/mm, n = 8, $p<0.001$) month old non-pregnant groups, and a factor of 0.5 between the five (6.584± 0.2 g/mm, n = 8) and eight month old non-pregnant groups ($p<0.001$) (Figure 4.4). There was no difference in cervical stiffness measured between all ages of late pregnant mice.

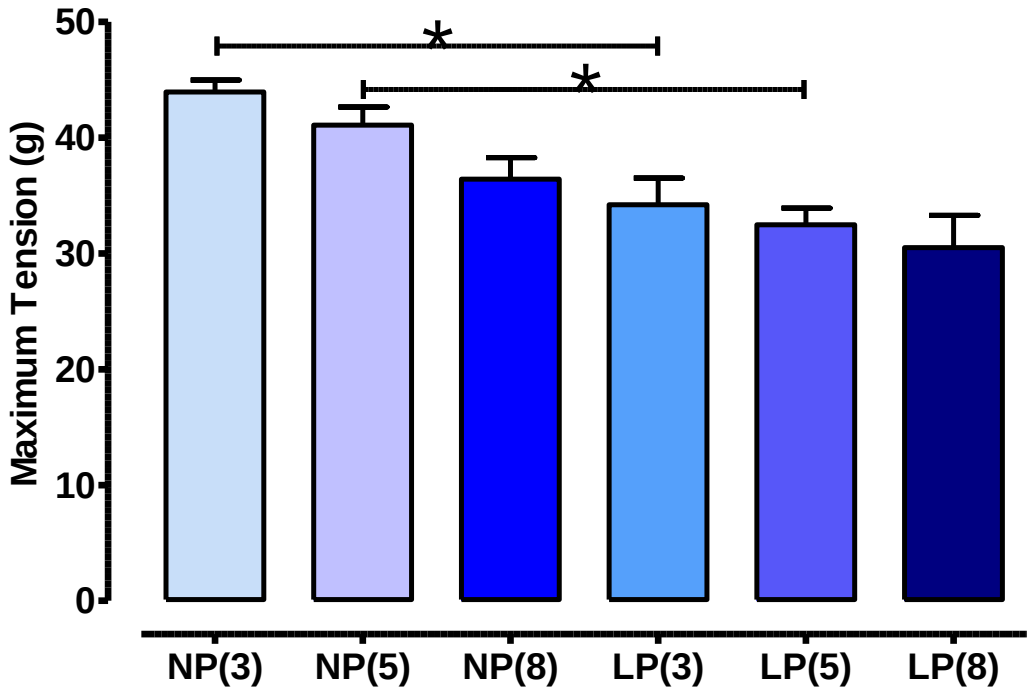


**Figure 4.3 Maximum cervical tension is reduced in late pregnant mice of three and five months of age compared to age matched non-pregnant mice**

Cervices from non-pregnant three month [NP(3), n = 6], five month [NP(5), n = 8], and eight month [NP(8), n = 8] old mice, as well as late pregnant three month [LP(3), n = 9], five month [LP(5), n = 6], and eight month [LP(8), n = 6] old mice were distended via the cervical canal until no further increase in tension was generated by cervical tissues. Transition from non-pregnant to pregnant state significantly reduced maximal cervical tension in three and five month old mice, *$p<0.05$; however this was not apparent in eight month old mice; ANOVA followed by all pairwise multiple comparison Tukey's test. Data expressed as mean ± SEM maximum tension generated at maximal cervical stretch.

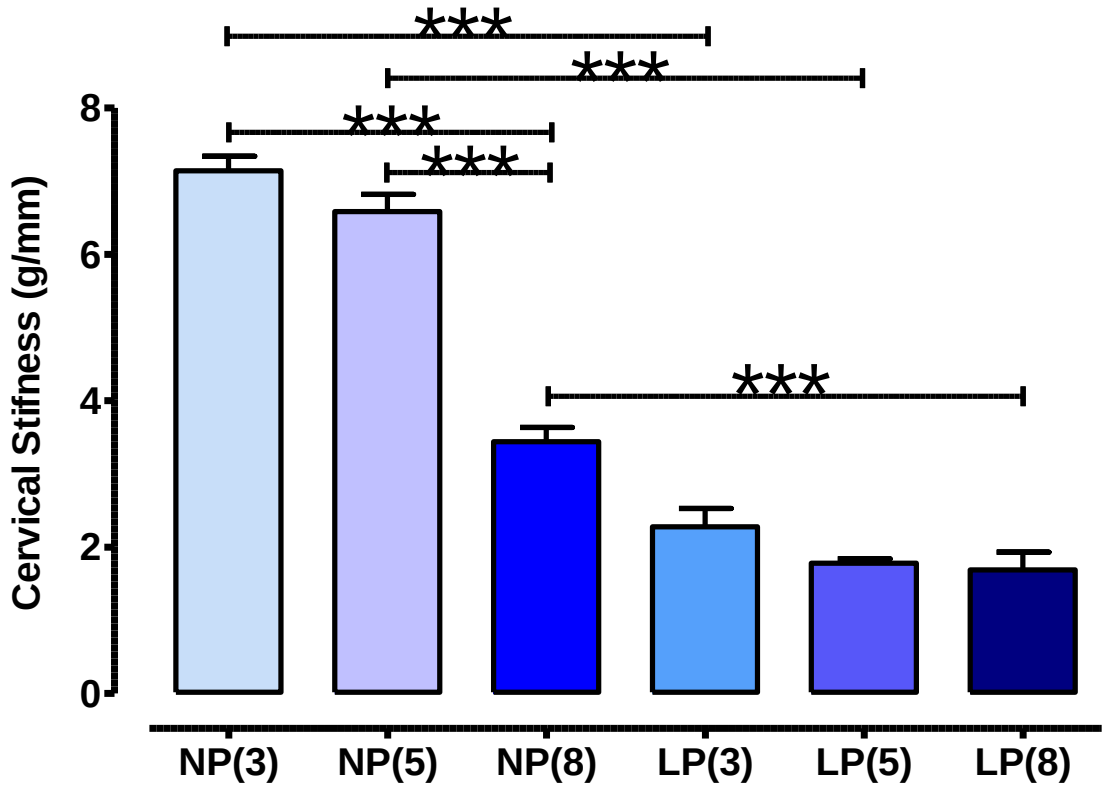


**Figure 4.4 Cervical stiffness is reduced in tissues from late pregnant mice of three, five and eight months of age compared to age matched non-pregnant mice**

Bar graph presenting cervical stiffness as determined by the slope of cervical distension stress-strain curves. Tissues obtained from non-pregnant three month [NP(3), n = 6], five month [NP(5), n = 8], and eight month [NP(8), n = 8] old mice, as well as late pregnant three month [LP(3), n = 9], five month [LP(5), n = 6], and eight month [LP(8), n = 6] old mice. Transition from non-pregnant to pregnant state, significantly reduced cervical stiffness in three, five and eight month old mice, ***$p<0.001$. Advance in age from three to eight months and five to eight months in non-pregnant mice also significantly reduced cervical stiffness *** $p<0.001$, however advance in age did not change cervical stiffness in tissues from late pregnant mice; ANOVA followed by all pairwise multiple comparison Tukey's test. Data expressed as mean ± SEM cervical stiffness.

### 4.3.2 Determination of collagen proportion in cervical tissues

Representative images of Masson's trichrome blue-stained collagen in cervical tissues from non-pregnant and late pregnant mice of three, five and eight months of age are shown in Figures 4.5, 4.6 and 4.7. The proportion of Masson's trichrome blue staining (expressed as a percentage of the total cervical area) was not significantly altered between the three age groups in both the non-pregnant and late pregnant cervical tissues (Figure 4.8). For both non-pregnant and late pregnant mice, the greatest mean collagen content was detected in tissues from eight month old mice, but these differences did not reach significance ($p = 0.197$). Non-pregnant cervical tissues from all ages exhibited a high proportion of blue stained collagen, which was noticeably the most prominent tissue component (Figures 4.5, 4.6 and 4.7). The transition from non-pregnant to late pregnancy in all mice significantly deteriorated the collagen content in cervical tissues (Figure 4.8). The collagen content percentage decline in late pregnant cervices compared to non-pregnant was -28 % in three month old mice (63.0 ± 4.2 reduced to 34.6 ± 3.5 %, $p<0.001$), -29 % in five month old mice (64.1 ± 3.4 reduced to 34.9 ± 1.7 %, $p<0.001$), and -32 % for eight month old mice (69.8 ± 2.4 reduced to 37.8 ± 2.1 %, $p<0.001$); $n = 6$ for all groups. These data were also evident by the weaker and more sparse blue staining seen in images of cervical tissues from late pregnant compared to non-pregnant mice.

Although not quantified in this present study, it was observed that smooth muscle cells (stained red) appeared to form tight bundles within the collagen and along the edges of the cervix in non-pregnant tissues of all ages. This tight bundling of smooth muscle appeared disrupted along with collagen in late pregnant cervical tissues (Figures 4.5, 4.6 and 4.7).

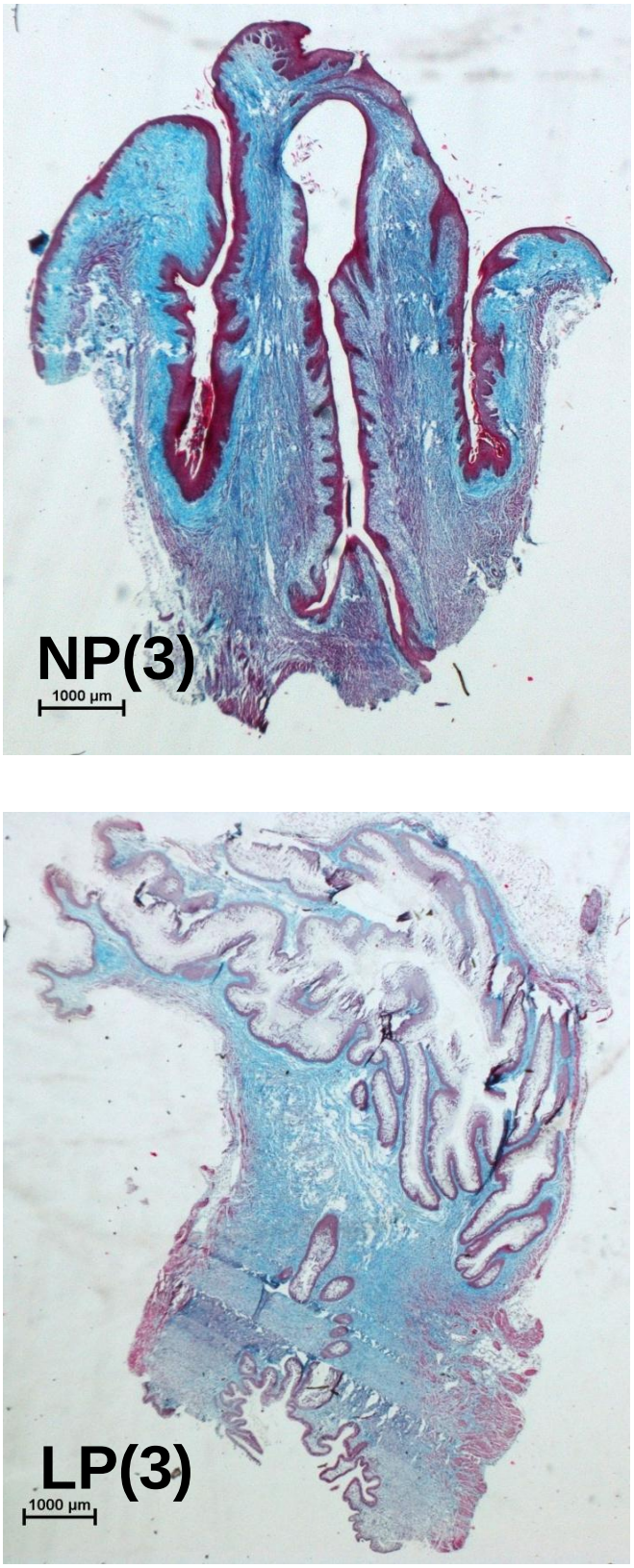


**Figure 4.5 Representative images of Masson's trichrome staining of collagen in cervical tissues from three month old non-pregnant (NP) and late pregnant (LP) mice**

Masson's trichrome staining for collagen (blue) and smooth muscle (red) in cervical tissues obtained from non-pregnant three month old [NP(3)], and late pregnant three month old [LP(3)] mice. Collagen localisation is predominantly in the extracellular matrix in both NP(3) and LP(3) images, however the collagen staining is more sparse in the LP(3) cervix. Original magnification x10.

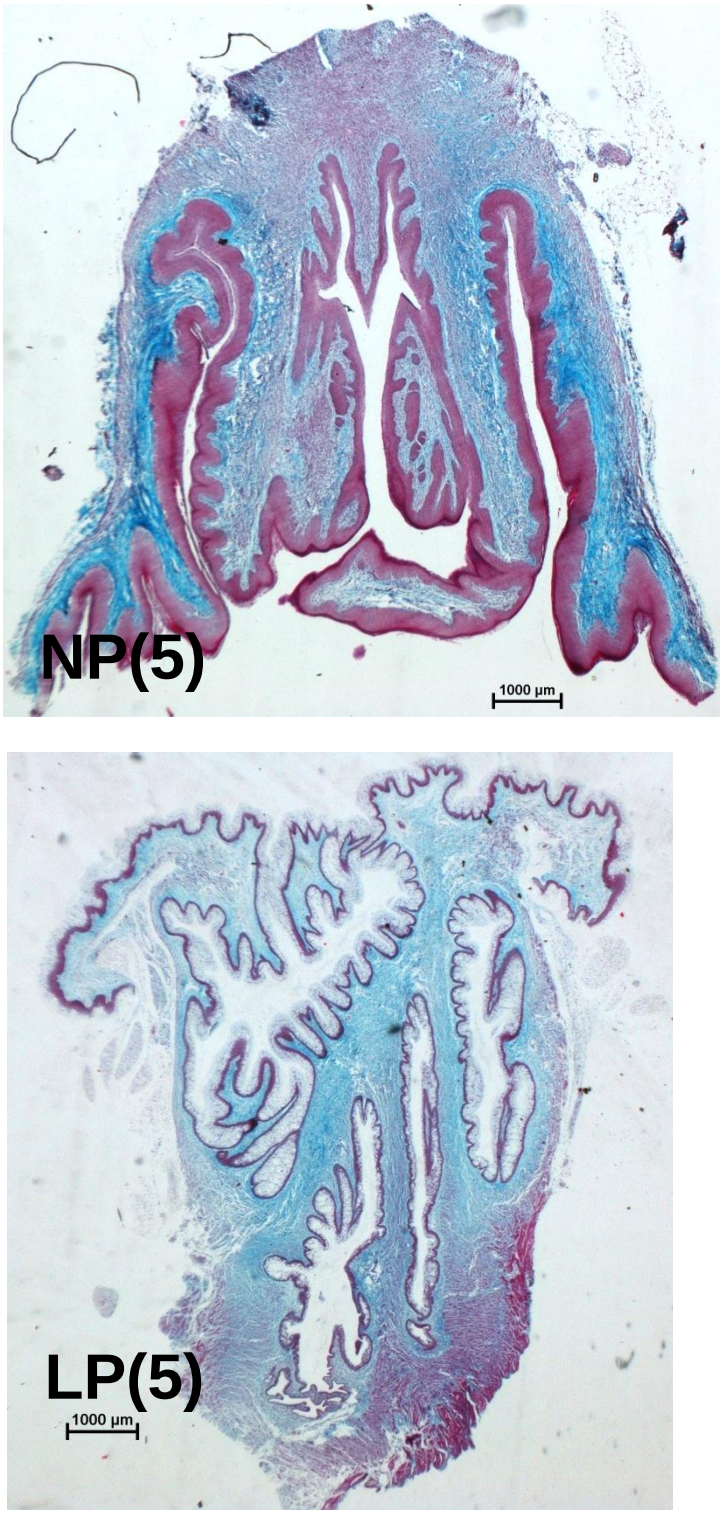


**Figure 4.6 Representative images of Masson's trichrome staining of collagen in cervical tissues from five month old non-pregnant (NP) and late pregnant (LP) mice**

Masson's trichrome staining for collagen (blue) and smooth muscle (red) in cervical tissues obtained from non-pregnant five month old [NP(5)], and late pregnant five month old [LP(5)] mice. Collagen localisation is predominantly in the extracellular matrix in both NP(5) and LP(5) images, however the collagen staining appears less intense in the LP(5) cervix. Original magnification x10.

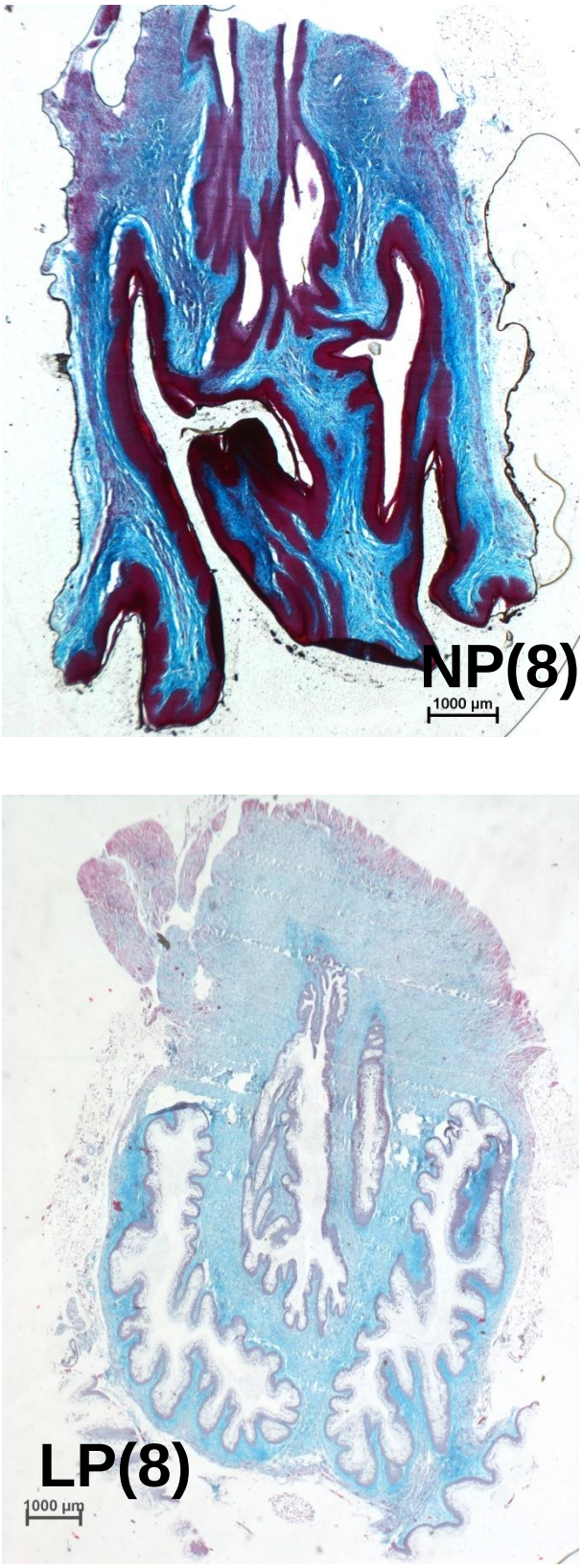


**Figure 4.7 Representative images of Masson's trichrome staining of collagen in cervical tissues from eight month old non-pregnant (NP) and late pregnant (LP) mice**
Masson's trichrome staining for collagen (blue) and smooth muscle (red) in cervical tissues obtained from non-pregnant eight month old [NP(8)], and late pregnant eight month old [LP(8)] mice. Collagen localisation is predominantly in the extracellular matrix in both NP(8) and LP(8) images, however the collagen and smooth muscle staining is noticeably weaker in the LP(8) cervix. Original magnification x10.

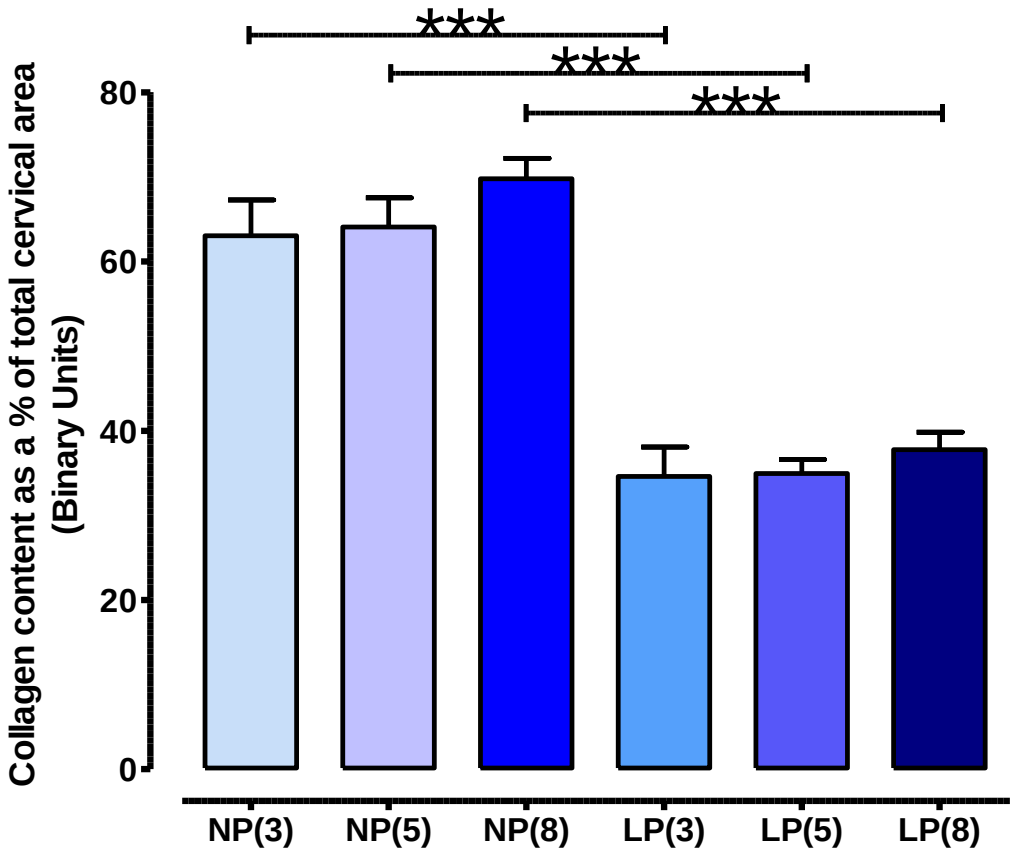


**Figure 4.8 Collagen content is lower in cervical tissues from late pregnant mice compared to non-pregnant mice as determined by Masson's trichrome stain for collagen**

Bar graph presenting percentage of collagen content in cervical tissues obtained from non-pregnant three month [NP(3), n = 6], five month [NP(5), n = 6] and eight month [NP(8), n = 6] old mice, as well as late pregnant three month [LP(3), n = 6], five month [LP(5), n = 6], and eight month [LP(8), n = 6] old mice. Transition from non-pregnant to pregnant state, significantly reduced cervical collagen content in three, five and eight month old mice, ***$p<0.001$. It appears that advancing age correlates with marginally greater collagen content in both non-pregnant and late pregnant tissues, but this did not reach significance; ANOVA followed by all pairwise multiple comparison Tukey's test. Data expressed as mean ± SEM content expressed as a percentage of total cervical area.

### 4.3.3 Expression of MMP2 in cervical tissues

MMP2 expression was detected by immunohistochemical brown staining predominantly in the epithelium and stromal matrix in all cervical tissues from non-pregnant three, five, and eight month old mice, as well as late pregnant three, five, and eight month old mice (Figures 4.9, 4.10 and 4.11). MMP2 protein expression, quantified by mean ± SEM arbitrary units of positivity, was not significantly altered between the three age groups in both non-pregnant and late pregnant cervical tissues (Figure 4.12). In both non-pregnant and late pregnant mice, a greater degree of MMP2 expression was found in tissues from eight month old mice, but this did not reach significance. Comparison of MMP2 staining in cervical tissue from age matched non-pregnant and late pregnant mice suggested that MMP2 expression was generally higher in non-pregnant mice (Figure 4.12), but this again did not reach significance. These data are also suggested by the stronger brown staining seen in images of non-pregnant cervical tissues compared to late pregnant.

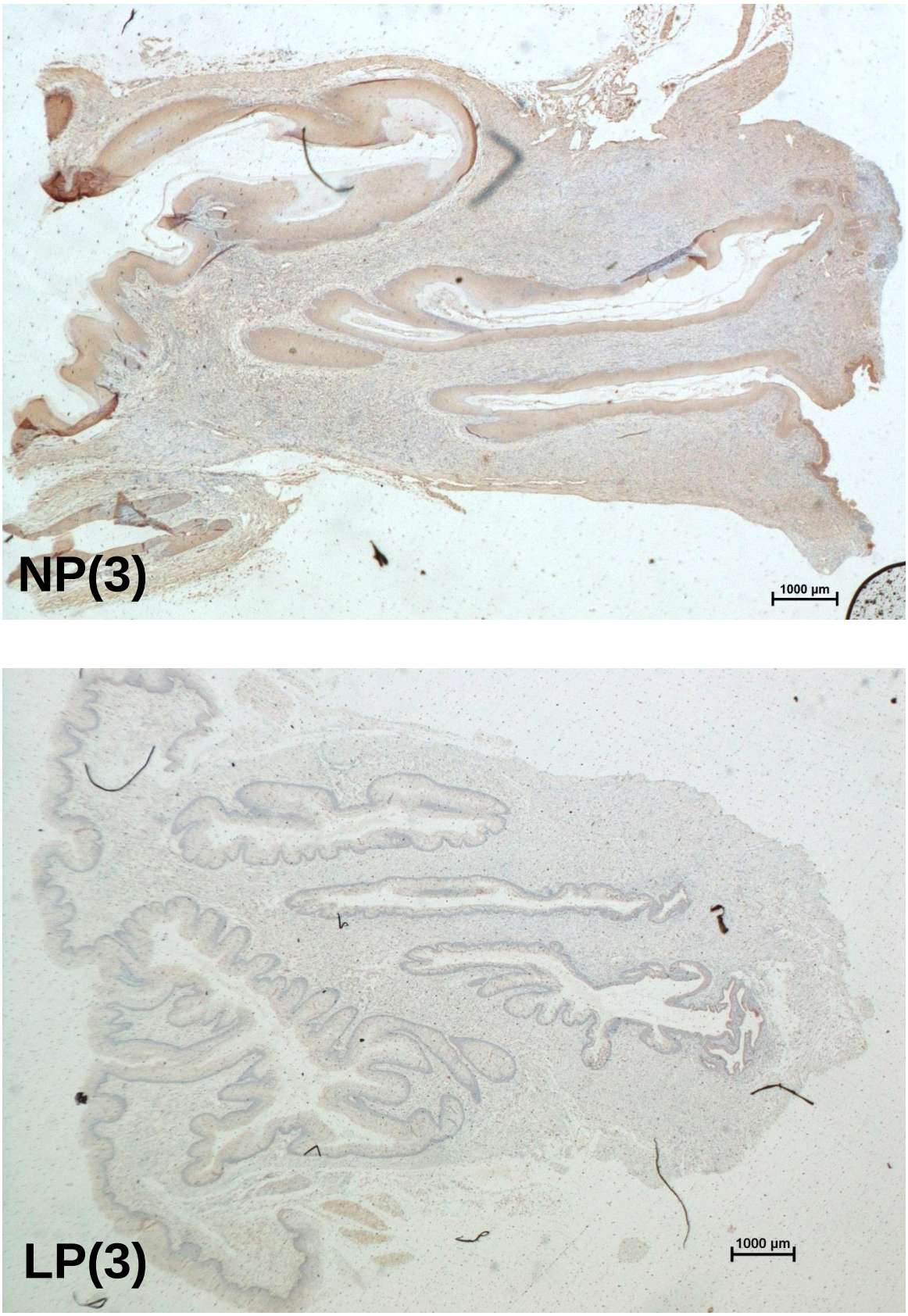


**Figure 4.9 Representative images of immunohistochemical staining of MMP2 in cervical tissues from three month old non-pregnant (NP) and late pregnant (LP) mice**

Cervical tissues obtained from non-pregnant three month old [NP(3)], and late pregnant three month old [LP(3)] mice. MMP2 localisation as defined by the brown staining can be found in the columnar and squamous epithelium and stroma in NP(3) but this is greatly reduced in the LP(3) image. Original magnification x10.

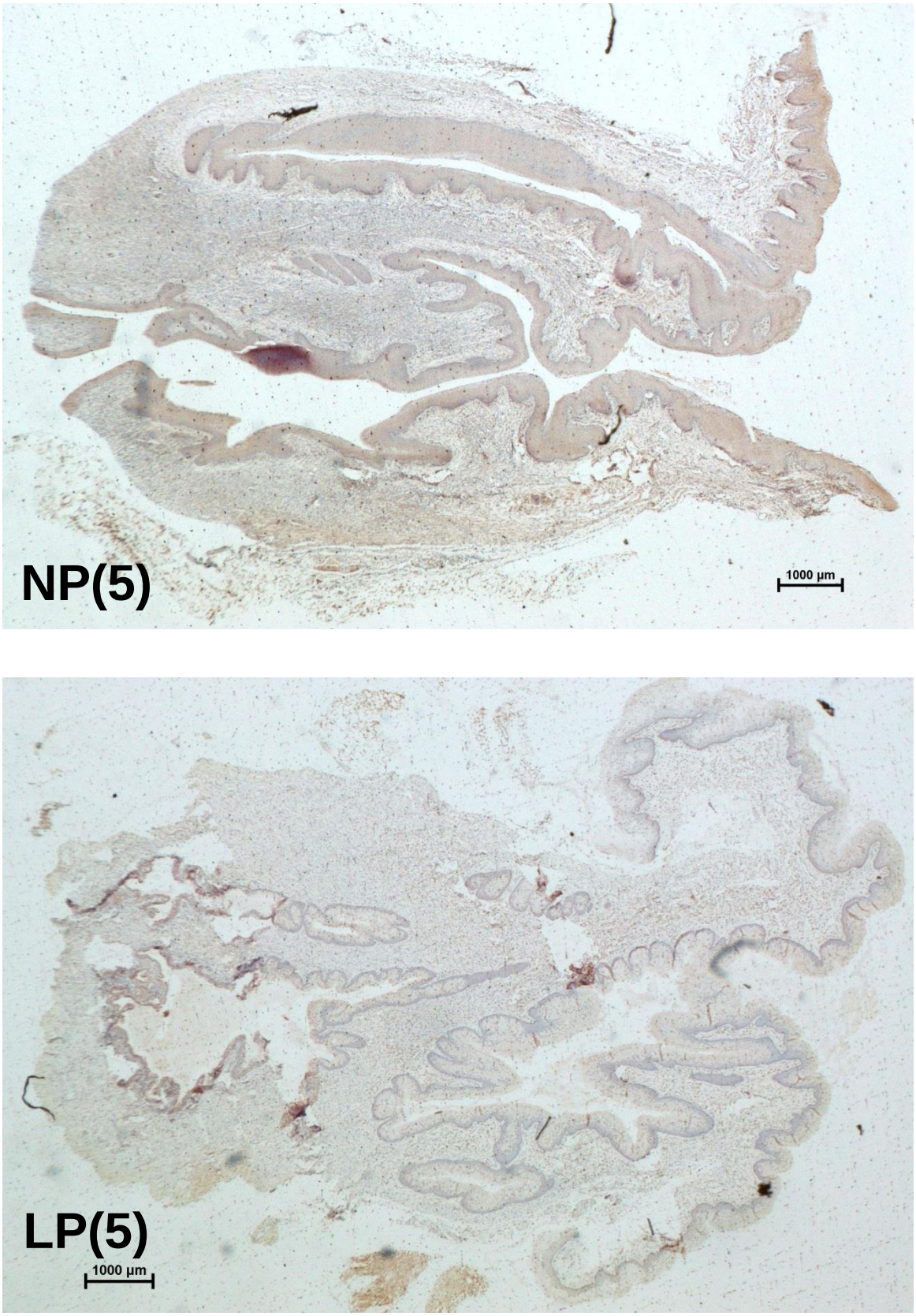


**Figure 4.10 Representative images of immunohistochemical staining of MMP2 in cervical tissues from five month old non-pregnant (NP) and late pregnant (LP) mice**

Cervical tissues obtained from non-pregnant five month old [NP(5)], and late pregnant five month old [LP(5)] mice. MMP2 localisation as defined by the brown staining can be found in the columnar and squamous epithelium and stroma in NP(5) but to a lesser degree in the LP(5) image. Original magnification x10.

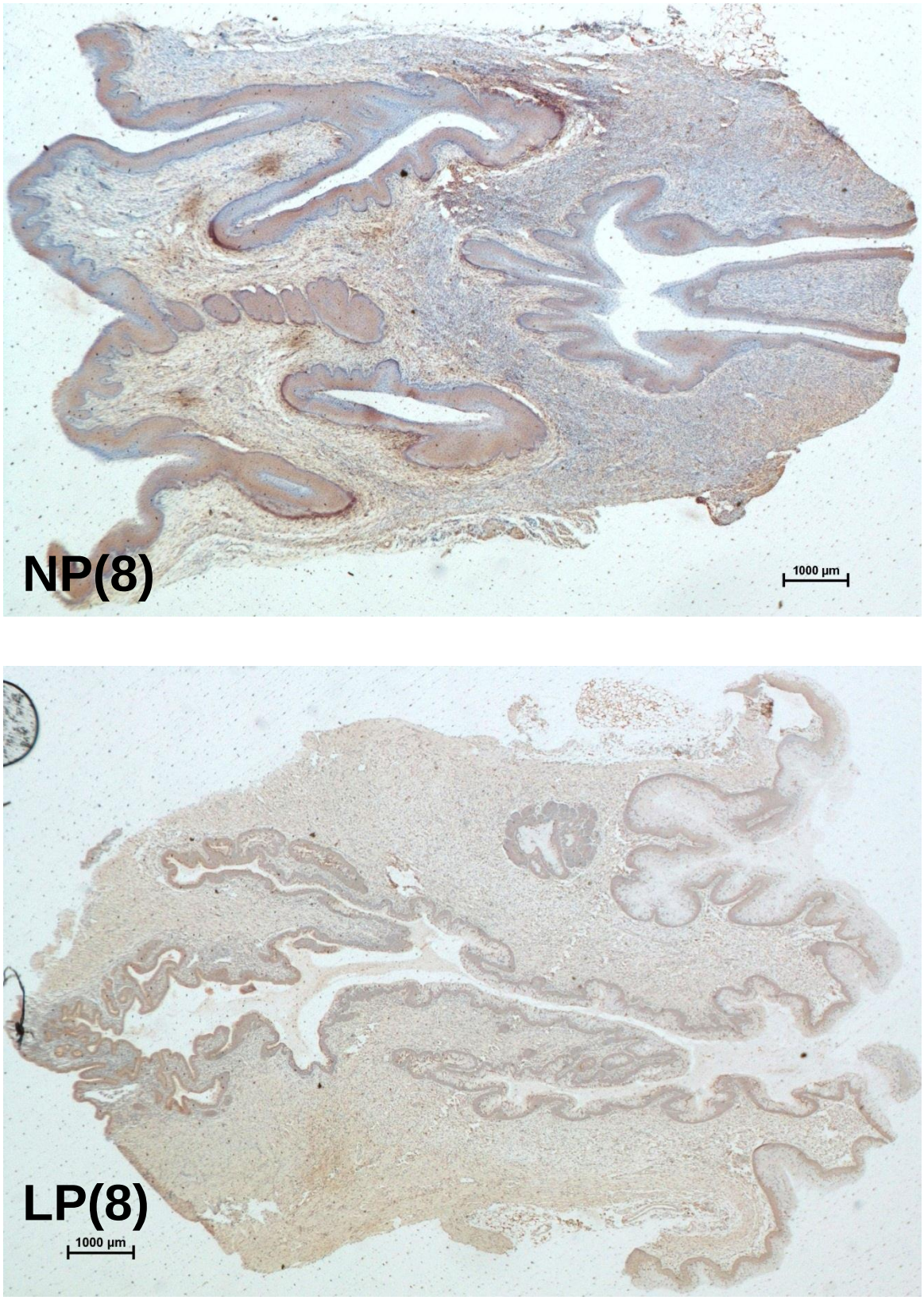


**Figure 4.11 Representative images of immunohistochemical staining of MMP2 in cervical tissues from eight month old non-pregnant (NP) and late pregnant (LP) mice**

Cervical tissues obtained from non-pregnant eight month old [NP(8)], and late pregnant eight month old [LP(8)] mice. MMP2 localisation as defined by the strong brown staining can be found in the columnar and squamous epithelium and stroma in both NP(8) and LP(8) images. Original magnification x10.

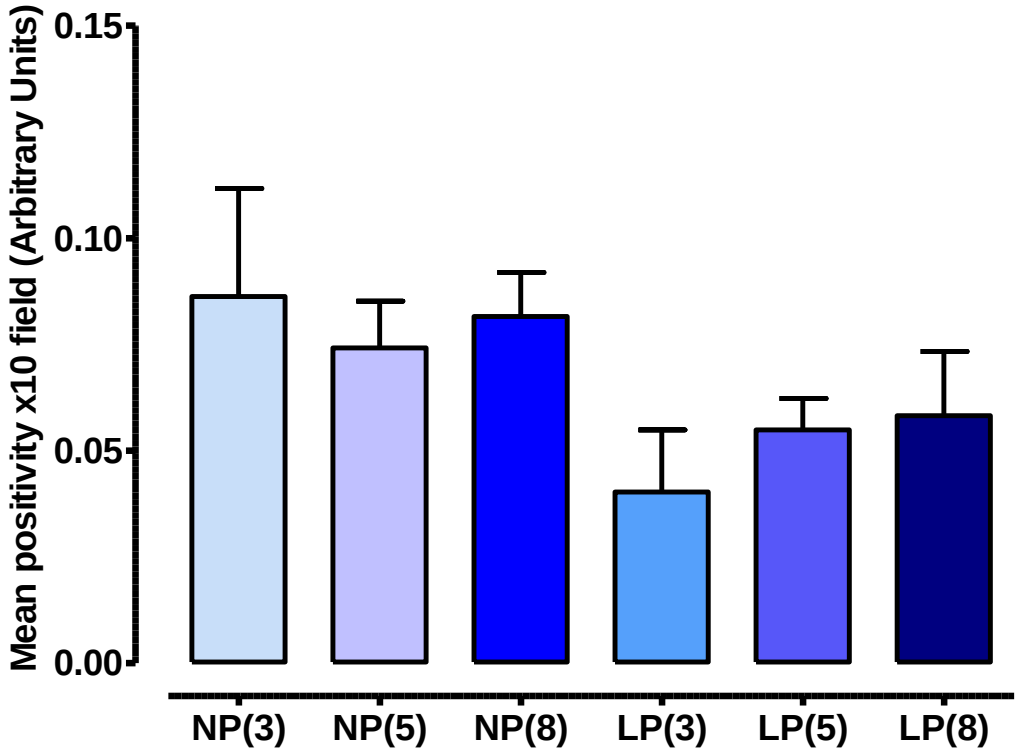


**Figure 4.12 Expression of MMP2 is not significantly altered by the effect of age in cervical tissues from both non-pregnant and late pregnant mice**

Bar graph presenting expression of MMP2 in cervical tissues obtained from non-pregnant three month [NP(3), n = 6], five month [NP(5), n = 6] and eight month [NP(8), n = 6] old mice, as well as late pregnant three month [LP(3), n = 6], five month [LP(5), n = 6], and eight month [LP(8), n = 6] old mice. Comparisons across all groups did not reach significance; ANOVA followed by all pairwise multiple comparison Tukey's test. Data expressed as mean ±SEM arbitrary positivity score.

## 4.4 Discussion

This study reports a generalised preservation of both cervical biomechanical properties as well as relative collagen content in cervices from non-pregnant mice compared to late pregnant mice. The functional properties of cervices from non-pregnant animals declined at eight months as distensibility increased and cervical stiffness reduced. An impact of age was also detectable in tissues from primiparous late pregnant mice, but the magnitude of this effect was suppressed in comparison and limited to a change in distensibility. It seems unlikely, therefore, that age-induced changes in cervical properties will have a major impact on the progress of labour in this model.

The direct comparison of cervical structure and function in tissues from non-pregnant and younger pregnant mice clearly demonstrated that in late pregnancy, cervices were more distensible, developed less tension in response to stretch and exhibited reduced stiffness compared to those from non-pregnant animals. This change was associated with an approximate two fold reduction in cervical tissue collagen content, but not MMP2 expression, in pregnancy. These data complement the existing body of literature in rodents related to cervical remodelling (Harkness and Harkness, 1959, Read et al., 2007, Word et al., 2007). They reported an incremental decline in tissue stiffness from day 12 of gestation onwards reaching a maximum decrease at the time of birth (Harkness and Harkness, 1959, Read et al., 2007, Vargis et al., 2012).

In the present study, collagen content or proportion of Masson's trichrome blue stained collagen was reduced in all late pregnant cervical tissues compared to age-matched non-pregnant tissues, which fits the common understanding that either collagen is degraded or there is an alteration in collagen structure during cervical softening, resulting in an overall reduced collagen proportion in the cervix. A recent study published by Vargis *et al*., (2012) reported similar findings in Masson's trichrome stained histological studies of pregnant mouse cervical tissues.

They examined samples from multiple time points (non-pregnant, gestation days 4–19, and one day postpartum) throughout pregnancy. They reported that non-pregnant, early pregnant and postpartum cervical tissues exhibited a dense blue stained collagen network, which was noticeably the most prominent tissue component, but by the end of gestation on day 19, the dense collagen network appeared to become disorganized and sparse (Vargis et al., 2012). The loss of dense blue staining representative of collagen was also seen between non-pregnant and late pregnant cervical samples in this study

As far as can be determined, there has been little or no previous assessment of cervical biomechanical properties in rodents of different ages. The studies highlighted above compared cervical properties of non-pregnant and pregnant adults and did not specifically address the issue of reproductive age at conception. Most stated using "adult" animals and only Read *et al*., (2007) reported an age range of three- six months for the adults in their pregnancy group. In the non-pregnant state, tissue compliance was mainly compromised in cervical tissues taken from eight month old mice. This appears to mirror the generalised age-associated changes reported for other collagen rich tissues and organs such as skin and bone (Baroni Edo et al., 2012, Quan et al., 2010, Varani et al., 2006, Wang et al., 2002). However, there wasn't a significant change in collagen content in cervices from older mice. This may be because the approach was only semi-quantitative or that the changes in distensibility and stiffness precede any visually detectable changes in collagen content. Extending the study to include groups of mice beyond the reproductive age span (e.g. >12 months) would confirm this. Similarly additional assays for determining collagen content could be employed.

In late pregnancy, there are less apparent age-induced differences in cervical biomechanical properties. Indeed, the tissues from eight month old pregnant mice only display enhanced distensibility and not reduced stiffness compared to tissue from three and five month old pregnant animals. There is also not a loss of collagen content or activation of MMP2. The age effects seen in non-pregnant animals are most likely masked by the considerable changes induced by pregnancy itself, which include enhanced distensibility and reduced cervical stiffness/ collagen content. Given the similarity of cervical change induced by age and pregnancy, it is unlikely that the impact of advancing maternal age on the cervix plays a key role in delaying parturition in older mice.

To definitively confirm this, experiments would need to also take into account the delayed parturition of approximately 24 hours in the eight month old mice. All cervices were harvested on day 18 of gestation for this part of the study (protocol decided prior to analysing the data for gestation length). It may have been more appropriate to use cervices taken on day 19 for the eight month group as in normal pregnancy the peak of cervical change occurs just before parturition (Read et al., 2007, Timmons et al., 2010).

As for non-pregnant mice, there was no significant change in collagen or MMP2 content associated with ageing in pregnant animals which may have been related to the limited age span that could be used in this pregnancy focussed study. The literature reporting age-induced alterations in pregnant cervix collagen content is sparse, but there has been one study in punch biopsies of human cervix from non-pregnant women. The mean collagen concentration (62.2 +/- 6.6%) was found to increase with age (0.5% per year, $r = 0.45$, $p = 0.003$). Normalized maximum stiffness also increased with age ($r = 0.32$, $p = 0.017$), whereas no change in collagen tensile strength with respect to age was found (Oxlund et al., 2010). These results demonstrate that collagen contributes to cervical tissue tensile strength and age should be considered a confounding factor.

Current data in the field support the theory that changes in collagen processing, assembly and structure contribute to the progressive alterations in tensile strength of the cervix through pregnancy (Akins et al., 2011, Timmons et al., 2010, Mahendroo, 2012). Although this present study examined relative collagen content, further investigations could provide a more detailed understanding of how collagen structure and/or concentration are altered throughout gestation and by age. Increased collagen solubility in late pregnant cervix compared with non-pregnant has been reported (House et al., 2009, Read et al., 2007, Timmons et al., 2010). Collagen that is soluble in acetic acid and pepsin reflects newly synthesized collagen or collagen that is less organised. In addition, total cervical collagen content can be determined; methods described by Read *et al*. (2007). Concentration of collagen can then be more accurately determined by dividing the total collagen (mg) by the wet weight (mg) of the tissue. Polarized light microscopy and transmission electron microscopy have also proven useful methods to visualise and quantify collagen organisation and microstructure in the cervix (Clark et al., 2006) and would be an ideal technique to examine collagen organization in the late pregnant cervix directly.

Decline in expression/enzymatic activity of lysyl oxidase and lysyl hydroxylase have also been reported in the pregnant mouse cervix; these catalyse the formation of strong collagen crosslinks. Loss of this activity could be responsible in part for early changes in collagen structure resulting in an increase in collagen solubility. Expression of three genes that encode lysyl hydroxylase (Plod1, -2, and -3) can be measured by qPCR throughout gestation to gain an understanding of any potential loss of collagen crosslinks which could contribute to increased collagen solubility and disorganisation during the softening phase (Akins et al., 2011).

MMPs were examined in this study because they participate in cervical remodelling by aiding the degradation of the network of collagen fibres and thus increase the distensibility required for delivery (Choi et al., 2009, Stygar et al., 2002, van Engelen et al., 2008) and it was surprising that no change in expression was noted in late pregnancy. Previously, immunohistochemistry and qPCR studies have confirmed that cervical columnar epithelial cells are capable of synthesizing MMP2 at term in mice. However, this requires low progesterone concentrations and is thought to be triggered as a consequence of progesterone withdrawal and local cervical progesterone metabolism at term in mouse parturition (Gonzalez et al., 2011). Similarly, proteins localised by immunohistochemistry and mRNA levels of MMP2 were found to be increased in the human cervix at term pregnancy compared with the non-pregnant state (Stygar et al., 2002).

In both mice and humans, MMP2 is thought to play a key role in cervical remodelling during the ripening phase rather than the softening. This may explain why there were no significant differences seen between MMP2 expression in non-pregnant and late pregnant cervical tissues in the current study. Mouse cervical ripening usually occurs within 24 hours prior to parturition (Read et al., 2007), therefore since cervical tissues were collected on day 18 of gestation, this time point may not have captured the initiation of the cervical ripening phase, particularly in relation to the eight month old group of mice.

***Study limitations and future work***

Cervical remodelling is a complex mechanism which involves numerous interlinked pathways and steps, eventually resulting in maximal loss of tissue compliance and integrity to facilitate cervical dilation at parturition (Timmons et al., 2010, Mahendroo, 2012). With time permitting, there are many more technical approaches that could have provided valuable supplementary data. One of the key experiments, as mentioned above would be to quantify collagen solubility and collagen concentrations in cervical samples. To directly measure enzymatic activity of MMP2 in cervical tissues, gelatin zymography would be a key approach for future work (Kelly et al., 2004). Alternatively, the gene and/or protein expression of MMP 8 and 9 as well as ADAMTS1 (a distintegrin-like and metalloproteinase with thrombospondin type 1 motif) could have been assessed as these are also proteases important in the breakdown of ECM molecules such as collagen and proteoglycans (Holt et al., 2011). Gene expression profiles using qPCR of components of the ECM architecture such as proteoglycans (e.g. versican, decorin, and biglycan) and matricellular proteins (tenascins, thrombospondins, and SPARC protein) which modulate matrix organisation and consequently tissue strength would assist in building up the complex picture of the cervical softening processes in the pregnant and ageing cervix (Akins et al., 2011). Finally, it has been reported that the amount of smooth muscle appears to increase in cervical insufficiency (House et al., 2009); increased smooth muscle content more than likely results in a reduction in cervical rigidity. Therefore, in addition to collagen, quantification of Masson's trichrome red stained smooth muscle as a percentage of total cervical area would have been useful to identify any possible age-related alterations.

The fundamental limitation to this current study would be that cervical tissues were collected on day 18 of gestation. An extension of this study would be to collect cervical tissues on gestation day 19 and possibly day 20 for the older eight month old mice in order to capture tissues in the ripening phase. This would determine whether there are

any age-related changes that occur specifically to cervical ripening. Since cervical softening initiates on day 12 of gestation, it would also be of interest to repeat this experiment and examine cervical tissues on day 12, 15, 18 and 19/20 of gestation, which would identify whether there is a shift in timing of cervical softening and ripening onset in older primiparous mice. Another key limiting factor is that cervical ripening occurs when progesterone levels have dropped nearing the onset of parturition (Mahendroo, 2012). Therefore, as for results regarding timing of parturition in older primparous mice, it would also have been beneficial in this study to know the serum progesterone profiles in late gestation in these mice.

***Conclusions***

Pregnancy induces a significant decrease in cervical tensile strength in preparation for labour. There is a limited impact of age on cervical function in pregnancy although at eight months there appears to be a change in distensibility. Further studies are required to determine whether this difference is further enhanced at the onset of parturition, since cervical remodelling in the ripening phase continues to takes place in the hours before labour.

# Chapter 5

## Alterations in Myometrial Function as a Consequence of Reproductive Ageing in Mice

# Chapter 5 : Alterations in Myometrial Function as a Consequence of Reproductive Ageing in Mice.

## 5.1 Introduction

As discussed in Chapter 1, for the majority of pregnancy, the uterus demonstrates limited contractile activity (quiescence), with sporadic, low amplitude and arrhythmic contractions. During this state, the contractile function of the myometrial smooth muscle is thought to be suppressed by the upregualtion of pro-quiescence pathways such as NF-κB and the down-regulation of contractile associated proteins (CAPs) including the oxytocin receptor (OXTR), prostaglandin-endoperoxide synthase 2 (PTGS2, also known as prostaglandin G/H synthase and cyclooxygenase 2), and the gap junction protein connexin-43 (Cx43). Uterine activation, the myometrial switch from a quiescent state to a muscle that is spontaneously active and sensitive to endogenous uterotonins during labour, is an essential step in the onset of parturition. Significant increases in CAPs are associated with uterine activation at term in both humans and animals, which support the theory for a role for CAPs in the control of parturition onset (Ou et al., 1997, Ou et al., 1998, Norwitz et al., 1999, Bernal, 2001, Lopez Bernal, 2003, Smith, 2007, Smith et al., 2007, Shynlova et al., 2009).

There are a plethora of studies examining the effect of maternal age on oocyte number and function as well as the success of IVF; however the function of the myometrium and how it may be altered with advancing age has not been studied in detail. The current study has looked at the expression of CAPs, spontaneous contractile activity, as well as agonist-induced contractile responses in the myometrium in an attempt to elucidate if an impairment in the coordinated up-regulation of CAP genes, has a negative impact on the physiological preparation and hence the function of the myometrium at the end of gestation in primiparous mice.

## 5.2 Methods

Full descriptions and details of the methods are described in Chapter 2, sections 2.3, 2.4, and 2.6. All non-pregnant myometrial tissues were collected when mice were in oestrous stage of their reproductive cycle and all late pregnant myometrium on day 18 of gestation. The age of late pregnant mice as indicated within this chapter relate to their age at conception.

Genome-wide, age-induced changes in uterine gene expression (normalised against paired bladder expression) were studied using mouseWG-6 v2.0 Expression BeadChip microarrays (Illumina, UK) in late pregnancy of three month old versus eight month old mice. Differential expression analysis was carried out using the differential expression module and Student's t-test was used for calculating the statistical significance between groups. Benjamini and Hochberg multiple testing correction was applied to adjust p-values (Benjamini and Hochberg, 1995). Differentially expressed genes were identified based on the adjusted p-value <0.05 (Diff Score >= ±13). In addition, gene expression profiles of PTGS2, Cx43 and OXTR measured by qPCR were examined in non-pregnant and late pregnant myometrium from three, five and eight month old mice. Data for qPCR were expressed relative to the geometric mean of the most stable housekeeping genes β-2 microglobulin (β2M), glyceraldehyde 3-phosphate dehydrogenase (GAPDH), and β-actin as determined by GeNorm software (Vandesompele et al., 2002).

Spontaneous and oxytocin augmented contractile activity were examined in non-pregnant and late pregnant myometrium from three, five and eight month old mice using isometric tension recordings. To confirm that any observed differences in contractile activity were not due to bias in dissecting the myometrial strips or their relative weights, measurements were normalised to the cross-sectional area of each strip.

In order to analyse the contractile response of late pregnant myometrium to oxytocin, the mean integral tension (MIT) generated under increasing oxytocin concentrations (from $10^{-12}$ to $10^{-7}$ M) were represented as percentages of the baseline spontaneous activity. For each strip, the concentration response was calculated as the rate of change per tenfold increase in concentration by linear regression (Matthews et al., 1990); first using all concentrations, and then using only higher concentrations ($10^{-9}$ to $10^{-7}$ M), where graphical evidence suggested a change in slope. Linear regression of the dose response on animal age (three, five and eight months) with a Random-effects GLS (generalised least squares) model (Swamy and Arora, 1972) was used. The 96 strips by the 24 animals were grouped, allowing robust standard errors (Arellano, 1987). Differences between the age groups were estimated with 95% confidence intervals. Linear regression analysis was carried out using Stata version 11.2 (StataCorp, USA).

All other data within this chapter were found to be normally distributed using the D'Agostino-Pearson omnibus normality test (GraphPad Prism version 5.0, GraphPad Software, USA). Student's *t*-test was used to assess data between two groups and one-way analysis of variance (ANOVA) followed by all pairwise multiple comparison (Tukey's test) when comparing three or more groups. Data were expressed as mean ± standard error of the mean (SEM) and $p<0.05$ was considered significant; 'n' refers to the number of animals per sample group unless stated otherwise.

## 5.3 Results

### 5.3.1 Microarray analysis of late pregnant myometrial gene expression

Microarray analysis was unable to identify any differentially expressed genes between three month and eight month old late pregnant myometrium with the differential score cut-off >= ±13. Although significance was not reached, genes with the highest and lowest difference scores as identified in this study are shown in Tables 5.1 and 5.2 respectively.

### 5.3.2 Contractile-associated protein gene expression analysis in late pregnant myometrium

Expression of PTGS2 mRNA determined by qPCR was low in non-pregnant and late pregnant myometrium. There were no significant age-induced differences in expression in myometrium from non-pregnant or late pregnant mice. Although PTGS2 copy number was higher in late pregnant myometrium from mice of all ages, the differences again were not significant (three month old non-pregnant vs. late pregnant, $p = 0.597$, $n = 8$ for both groups; five month old non-pregnant vs. late pregnant, $p = 0.673$, $n = 8$ for both groups; eight month old non-pregnant vs. late pregnant, $p = 0.699$, $n = 8$ for both groups; Figure 5.1).

**Table 5.1 Microarray identification of genes with the highest differential expression scores between three (LP3) and eight (LP8) month old late pregnant mouse myometrium corrected for expression in paired bladder tissue**

| Gene | LP(3) Mean Expression Signal | LP(8) Mean Expression Signal | Differential Expression Score | LP(8)/LP(3) fold change |
|---|---|---|---|---|
| Peroxisome biogenesis factor 26 (Pex26) | 169.8 | 267.3 | 1.884 | 1.574 |
| Matrin 3 (Matr3) | 4930.6 | 5735.4 | 1.884 | 1.163 |
| Ctdsp2 protein (LOC100046500) | 129.2 | 234 | 1.884 | 1.811 |
| RIKEN cDNA E130102H24(E130102H24Rik) | 171.7 | 236.6 | 1.884 | 1.378 |
| Dynactin 1 (Dctn1) | 113.1 | 217 | 1.872 | 1.919 |
| Component of Sp100-rs (Csprs) | 107.8 | 231.8 | 1.789 | 2.150 |
| Tetraspanin 7 (Tspan7) | 392.9 | 480.2 | 1.779 | 1.222 |
| Indolethylamine N-methyltransferase (Inmt) | 2661.3 | 7672.2 | 1.565 | 2.883 |
| Homeo box D4 (Hoxd4) | 221.7 | 346 | 1.565 | 1.561 |
| RAS-like, family 11, member A (Rasl11a) | 93.4 | 162.2 | 1.565 | 1.737 |

No significant differentially expressed genes were identified.

**Table 5.2 Microarray identification of genes with the lowest differential expression scores between three (LP3) and eight (LP8) month old late pregnant mouse myometrium corrected for expression in paired bladder tissue**

| Gene | LP(3) Mean Expression Signal | LP(8) Mean Expression Signal | Differential Expression Score | LP(8)/LP(3) fold change |
|---|---|---|---|---|
| Kidney androgen regulated protein | 7152.3 | 2464 | -1.884 | 0.344 |
| Ig heavy chain V region 3 precursor (LOC637785) | 411 | 115.3 | -1.884 | 0.281 |
| Monoclonal antibody BBK-2 heavy chain (LOC677643) | 608.4 | 190.8 | -1.884 | 0.314 |
| Immunoglobulin kappa-chain (LOC100047162) | 1998.9 | 757.3 | - 1.872 | 0.379 |
| Ig kappa chain V-V region MPC11 precursor (LOC637227) | 1354.8 | 439.5 | -1.872 | 0.324 |
| Ribosomal protein S16 (Rps16) | 13798.8 | 11190.8 | -1.872 | 0.811 |
| Immunoglobulin heavy chain (J558 family) (Igh-VJ558) | 12961.4 | 5303.1 | -1.831 | 0.409 |
| Leucine rich repeat containing 26 (Lrrc26) | 302.2 | 129.9 | -1.779 | 0.430 |
| Serine (or cysteine) peptidase inhibitor, clade B (ovalbumin), member 11 (Serpinb11) | 412.4 | 115.4 | -1.779 | 0.280 |
| Light chain of the monoclonal antibody MST2 (LOC100046793) | 564.2 | 166.7 | -1.672 | 0.295 |

No significant differentially expressed genes were identified.

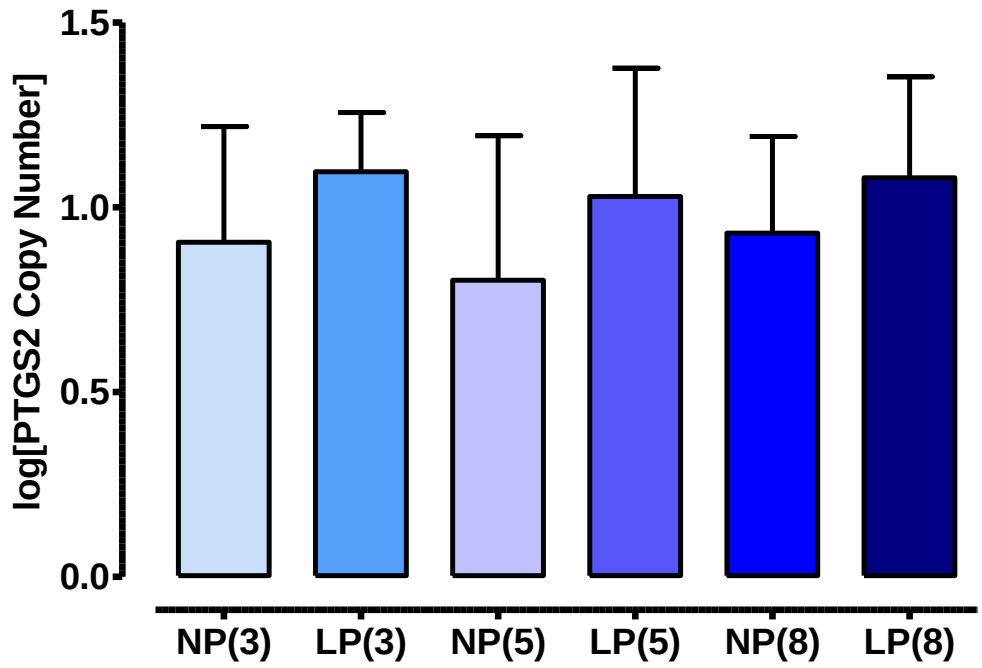


**Figure 5.1 Expression of prostaglandin-endoperoxide synthase 2 mRNA in non-pregnant and late pregnant mouse myometrium**

Bar graph presenting mRNA expression of prostaglandin-endoperoxide synthase 2 in myometrium from non-pregnant three month old (NP(3), n = 8) late pregnant three month old (LP(3), n = 8), non-pregnant five month old (NP(5), n = 8), late pregnant five month old (LP(5), n = 8) non-pregnant eight month old (NP(8), n = 8) and late pregnant eight month old (LP(8), n = 8) mice. Data expressed as log geometric mean of copy number ± SEM normalised to housekeeping genes β2M and GAPDH. All statistical comparisons across all groups were non-significant; ANOVA followed by all pairwise multiple comparison Tukey's test.

Expression of Cx43 mRNA was extremely low in non-pregnant myometrium from three, five and eight month old mice. However, late pregnancy appeared to be associated with a significant upregulation of expression in tissues from mice of all ages (fold change of 6.16, 9.12 and 8.17 for three, five and eight month old mice respectively compared to non-pregnant tissues; $p<0.001$, $n = 8$ for all groups)(Figure 5.2). Cx43 expression was lower in late pregnant myometrium from eight month old mice ($4.18 \pm 0.03$ log[Cx43 copy number]) compared with three month old mice ($4.40 \pm 0.03$; $p<0.01$, $n = 8$ for both groups). However there were no other age-induced, statistically different expression levels across groups.

Late pregnancy was also associated with a significant upregulation of oxytocin receptor (OXTR) mRNA expression in all ages of mice, when compared with non-pregnant myometrium. OXTR copy number was low in non-pregnant tissues but was increased by a fold change of 2.1 in three month old ($p<0.001$, $n = 8$ for both groups), 2.4 in five month old ($p<0.001$, $n = 8$ for both groups), and 1.8 in eight month old ($p<0.01$, $n = 8$ for both groups) late pregnant myometrium (Figure 5.3). Similar to Cx43 expression, there was reduced myometrial expression of OXTR in older (eight months) late pregnant mice ($2.67 \pm 0.19$ log[OXTR copy number]) compared to younger mice (three months; $2.11 \pm 0.12$, $p<0.05$, $n = 8$ for both groups). No significant difference in OXTR expression was found between three vs. five months, and five vs. eight months old mice.

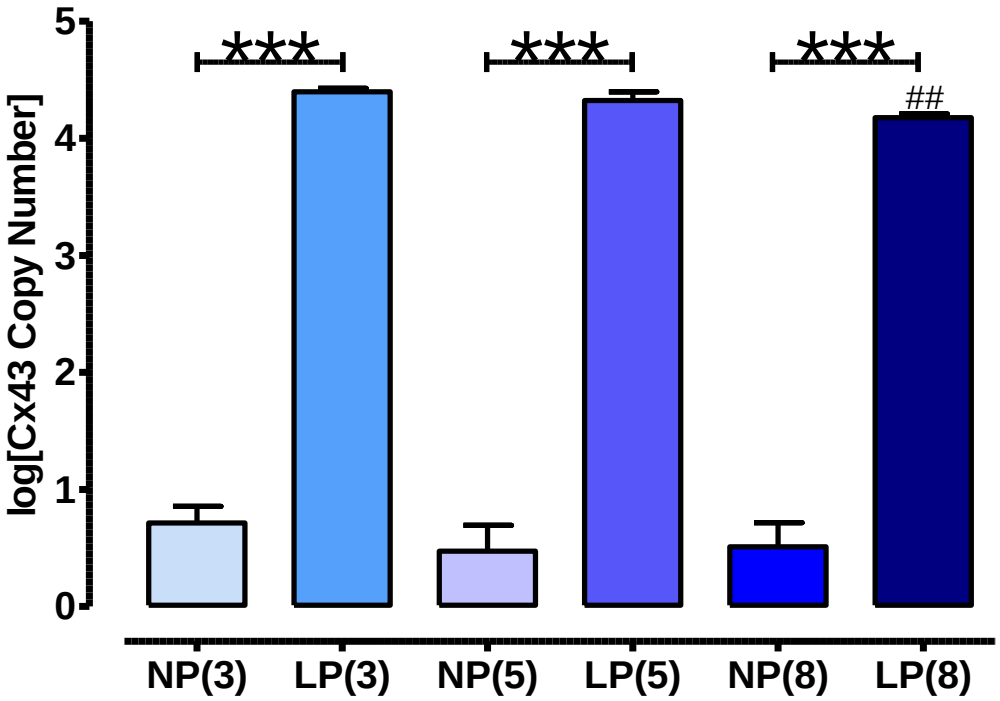


**Figure 5.2 Expression of connexin-43 mRNA increases in myometrium from late pregnant mice compared to non-pregnant mice**

Bar graph illustrating expression of connexin-43 in myometrium from non-pregnant three month old (NP(3), n = 8) late pregnant three month old (LP(3), n = 8), non-pregnant five month old (NP(5), n = 8), late pregnant five month old (LP(5), n = 8) non-pregnant eight month old (NP(8), n = 8) and late pregnant eight month old (LP(8), n = 8) mice. Data expressed as log geometric mean of copy number ± SEM normalised to housekeeping genes β2M and GAPDH. Expression of connexin-43 was significantly increased in late pregnant myometrium of all age groups compared to non-pregnant, ***p<0.001, and significantly lower in late pregnant myometrium from eight month old mice compared to late pregnant three month old, ##p<0.01; ANOVA followed by all pairwise multiple comparison Tukey's test.

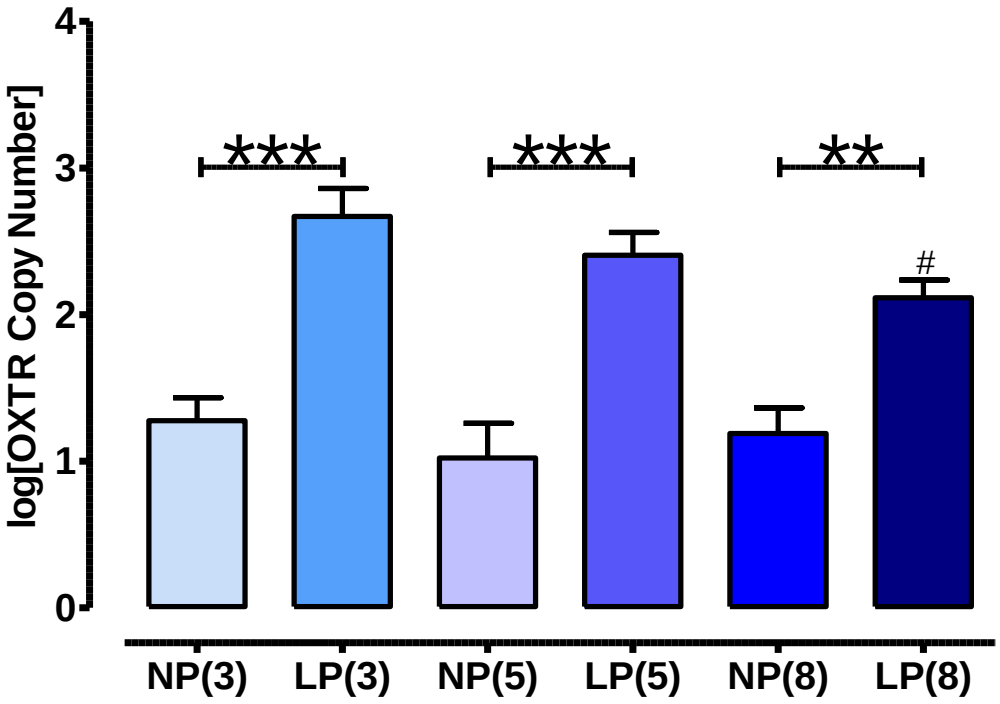


**Figure 5.3 Expression of oxytocin receptor mRNA increases in myometrium from late pregnant mice compared to non-pregnant mice**

Bar graph presenting expression of oxytocin receptor in myometrium from non-pregnant three month old (NP(3), n = 8) late pregnant three month old (LP(3), n = 8), non-pregnant five month old (NP(5), n = 8), late pregnant five month old (LP(5), n = 8) non-pregnant eight month old (NP(8), n = 8) and late pregnant eight month old (LP(8), n = 8) mice. Data expressed as log geometric mean of copy number ± SEM normalised to housekeeping genes β2M and GAPDH. Expression of oxytocin receptor was significantly increased in late pregnant myometrium of all age groups compared to non-pregnant; ***p<0.001, **p<0.01, and significantly lower in late pregnant myometrium from eight month old mice compared to late pregnant three month old, #p<0.05; ANOVA followed by all pairwise multiple comparison Tukey's test.

### 5.3.3 Spontaneous contractile activity of non-pregnant and late pregnant myometrium

The mean integral tension (MIT) of spontaneous myometrial contractions was significantly higher in all late pregnant mice compared to non-pregnant mice of all age groups ($p<0.001$, $p<0.05$, n = 32 tissue strips from n = 8 mice for each group) (Figure 5.4). The spontaneous contractile activity was similar between all age groups in both non-pregnant and late pregnant cohorts. Although the mean integral tension values were numerically lower in myometrium from eight month compared to three month old mice in both non-pregnant and late pregnant cohorts, the differences were not significant (non-pregnant three month old vs. eight month old, $p= 0.7755$, n = 32 tissue strips from n = 8 mice for each group; late pregnant three month old vs. eight month old, $p= 0.0511$, n = 32 tissue strips from n = 8 mice for each group) (Figure 5.4).

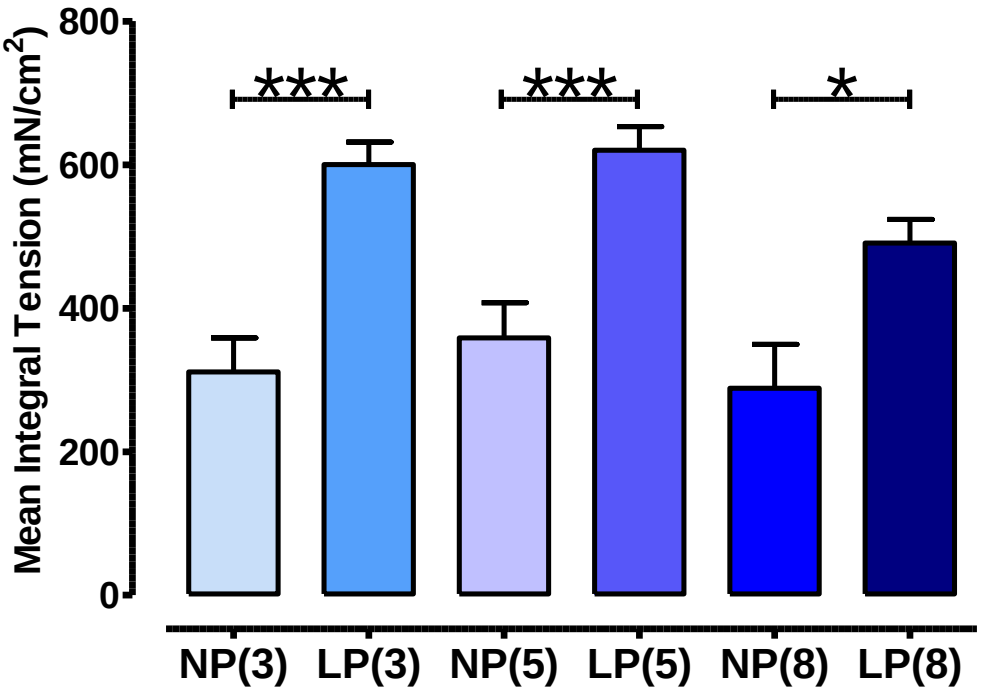


**Figure 5.4 Spontaneous contractile activity is greater in myometrium from late pregnant mice compared to non-pregnant mice**

Bar graph presenting spontaneous contractile activity in myometrium from non-pregnant three month old (NP(3), n = 32 strips from n = 8) late pregnant three month old (LP(3), n = 32 strips from n = 8), non-pregnant five month old (NP(5), n = 32 strips from n = 8), late pregnant five month old (LP(5), n = 32 strips from n = 8) non-pregnant eight month old (NP(8), n = 32 strips from n = 8) and late pregnant eight month old (LP(8), n = 32 strips from n = 8) mice. Data expressed as mean integral tension ± SEM. Mean integral tension was significantly higher in late pregnant myometrium compared to non-pregnant across all age groups, ***p<0.001,*p<0.05; ANOVA followed by all pairwise multiple comparison Tukey's test.

The maximal contractile capacity, expressed as mean peak amplitude induced by $K^+$ PSS (40 mM), was significantly increased in myometrium from late pregnant mice compared to tissues form non-pregnant mice in all three age categories; $p<0.01$, $p<0.05$, n = 32 tissue strips from n = 8 mice for each group (Figure 5.5). High $K^+$-induced contraction amplitudes were similar in myometrium from all non-pregnant age groups. In late pregnant mouse myometrium, there was a trend towards an age-associated reduction in high $K^+$ induced contraction amplitude, but this was not significant; p = 0.071 (Figure 5.5).

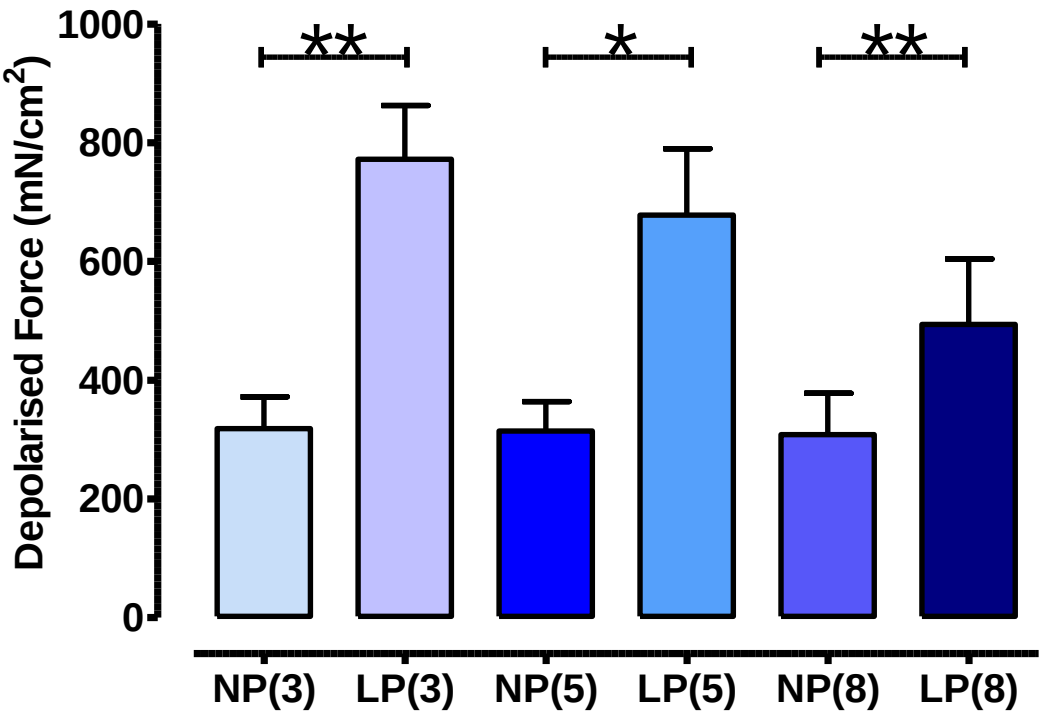


**Figure 5.5 Contraction amplitude under high $K^+$ is greater in myometrium from late pregnant mice compared to non-pregnant mice**

Bar graph presenting force amplitude under high $K^+$ in myometrium from non-pregnant three month old (NP(3), n = 32 strips from n = 8) late pregnant three month old (LP(3), n = 32 strips from n = 8), non-pregnant five month old (NP(5), n = 32 strips from n = 8), late pregnant five month old (LP(5), n = 32 strips from n = 8) non-pregnant eight month old (NP(8), n = 32 strips from n = 8) and late pregnant eight month old (LP(8), n = 32 strips from n = 8) mice. Data expressed as mean depolarised contraction amplitude ± SEM. Amplitude was significantly higher in late pregnant myometrium compared to non-pregnant across all age groups, **p<0.01,*p<0.05; ANOVA followed by all pairwise multiple comparison Tukey's test.

The frequency and duration of spontaneous contractions in myometrium from non-pregnant mice was similar regardless of age (data not shown). In contrast, spontaneous contractions were twice as frequent in myometrium from late pregnant older eight month old mice (0.05 Hz, n = 32 tissue strips from n = 8 mice) compared to three month old mice (0.03 Hz, $p<0.05$, n = 32 tissue strips from n = 8 mice). However, statistical comparisons between late pregnant groups (three vs. five months and five vs. eight months) were non-significant (Figure 5.6 C).

In tandem with contraction frequency, the duration of contractions in tissues from late pregnant mice aged eight months was reduced by – 36 % and – 41 % compared with five month old (31.7 to 20.2 seconds) and three month old (34.2 to 20.2 seconds) myometrium respectively, $p<0.01$ for both, n = 32 tissue strips from n = 8 mice for all groups. No statistical difference was identified between mean contraction duration of myometrium from three vs. five month old mice (Figure 5.6 D).

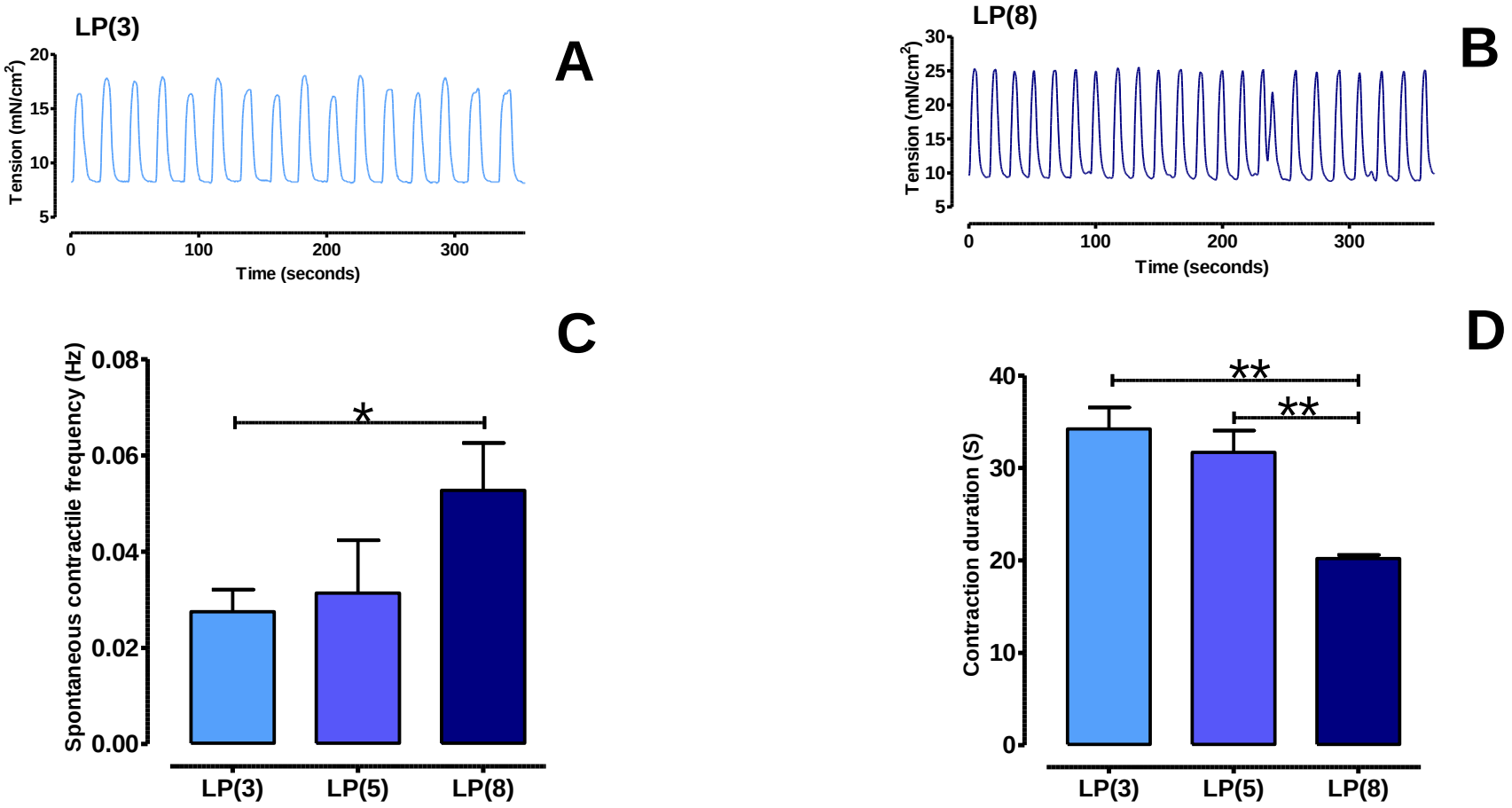


**Figure 5.6 Effect of maternal age on the frequency and duration of spontaneous contractions in late pregnant mouse myometrium *in vitro***

**A:** Representative trace showing spontaneous myometrial contractions from late pregnant three month old mouse, LP(3); **B:** Representative trace showing spontaneous myometrial contractions from late pregnant eight month old mouse, LP(8); **C:** Spontaneous myometrial contraction frequency was significantly greater in late pregnant eight month old mice, LP(8) *p<0.05; **D:** Myometrial spontaneous contraction duration was significantly shorter in late pregnant eight month old mice,**p<0.01; ANOVA followed by all pairwise multiple comparison Tukey's test. All data expressed as mean ± SEM.

### 5.3.4 Effect of oxytocin on spontaneous contractions of non-pregnant and late pregnant myometrium

In non-pregnant mice, application of oxytocin ($10^{-12}$-$10^{-7}$ M) did not significantly augment contractile activity in spontaneously contracting myometrium *in vitro*. Although, mean integral tension appeared numerically greater after the addition of oxytocin, this increase was not statistically different to baseline spontaneous contractile activity. All statistical comparisons across all age groups were also non-significant, n = 32 tissue strips from n = 8 mice for all groups (Figure 5.7). There does not appear to be an influence of maternal age on oxytocin-induced contractile activity in non-pregnant myometrium.

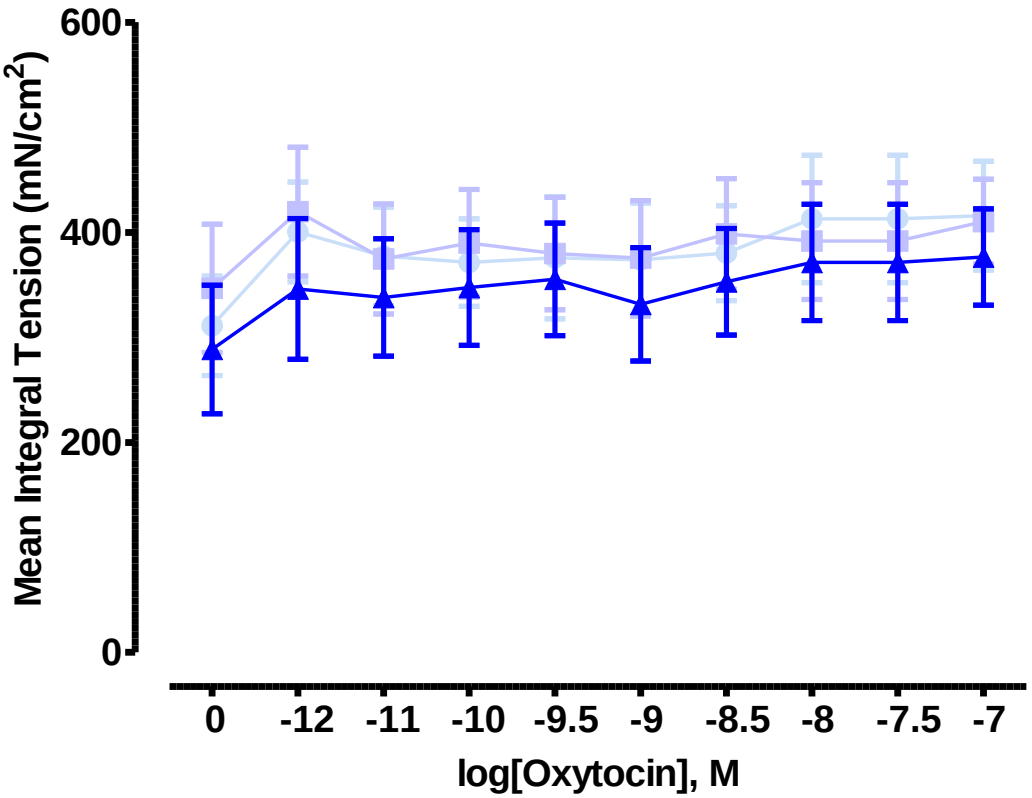


**Figure 5.7 Effect of oxytocin ($10^{-12}$-$10^{-7}$ M) on the contractile activity in myometrial tissues taken from non-pregnant mice at different ages**

Line graph illustrating the effect of oxytocin ($10^{-12}$-$10^{-7}$ M) on contractile activity in myometrium from non-pregnant three month old (NP(3), n = 32 strips from n = 8, light purple squares), non-pregnant five month old (NP(5), n = 32 strips from n = 8, light blue circles), and non-pregnant eight month old (NP(8), n = 32 strips from n = 8, dark blue triangles) mice. Data expressed as mean integral tension ± SEM normalised to cross-sectional area of myometrial strips. All statistical comparisons across all groups were non-significant; linear regression analysis. *The label "0" on the x-axis relates to spontaneous contractile activity before application of oxytocin.*

The application of oxytocin at concentrations $10^{-12}$-$10^{-7}$ M appeared to augment contractile activity (MIT) compared to baseline spontaneous contractile activity in late pregnant myometrium from mice in all age groups (Figure 5.8). It was not possible to formally test this to obtain $EC_{50}$ and $E_{max}$ values as the response was not sigmoidal. However, the slope of the response across the concentration range could be analysed. Using this approach, a significant difference in the contractile activity was detected related to maternal age, particularly at higher oxytocin concentrations. Overall, the slope of the response was lower in the five month old mice (mean difference: -7.29, 95% CI: -12.31 to -2.28, $p<0.01$) and eight month mice (mean difference: -7.63, 95% CI: -13.92 to -1.35, $p<0.05$) compared to three month old mice (actual slope 27.95, 95% CI: 23.41 to 32.49). In the higher concentration range ($10^{-9}$ to $10^{-7}$ M), the mean slope differences were even greater for both the five month old mice (-12.77, 95% CI: -25.24 to -0.29, $p<0.05$) and the three month old mice (-17.22, 95% CI: -31.94 to -2.51, $p<0.05$), compared to the slope of the three month old mice (actual slope 39.22, 95% CI: 27.20 to 51.24).

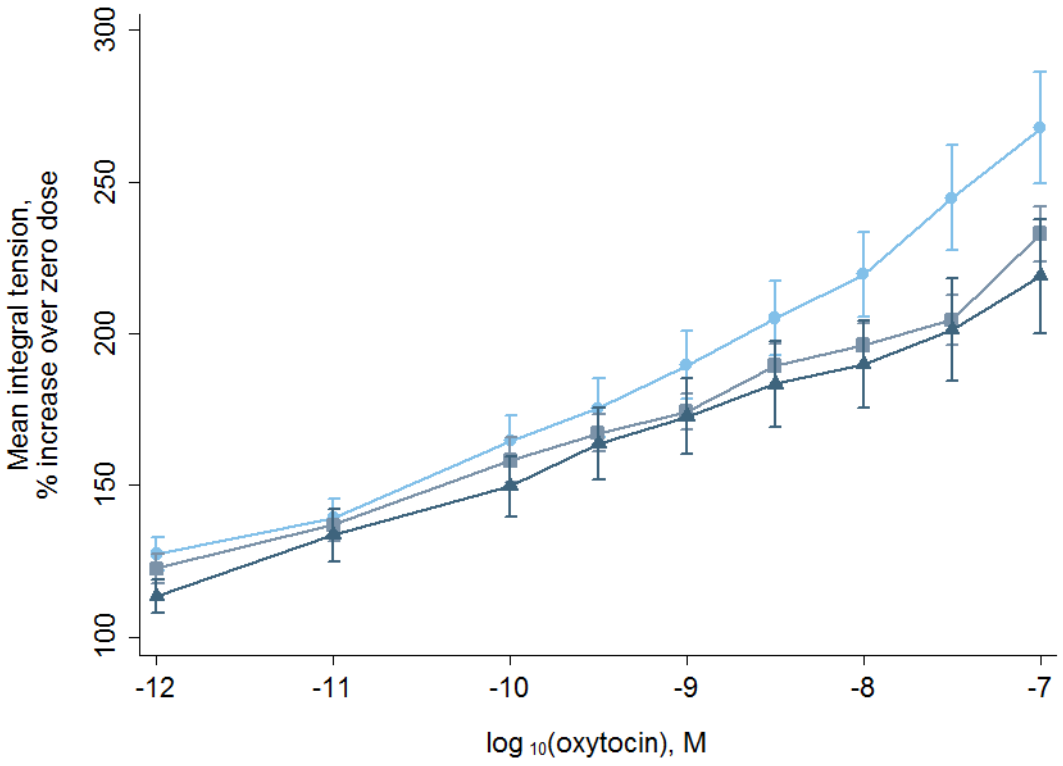


**Figure 5.8 Effect of oxytocin ($10^{-12}$-$10^{-7}$ M) on the contractile activity in myometrial tissues taken from late pregnant mice at different ages**

Line graph illustrating the effect of oxytocin ($10^{-12}$-$10^{-7}$ M) on contractile activity in myometrium from late pregnant three month old (LP(3), n = 32 strips from n = 8, light blue circles), late pregnant five month old (LP(5), n = 32 strips from n = 8, mid-blue squares), and late pregnant eight month old (LP(8), n = 32 strips from n = 8, dark blue triangles) mice. Data expressed as mean integral tension expressed as a percentage increase of the baseline spontaneous activity ± SEM. Application of oxytocin at concentrations $10^{-12}$ - $10^{-7}$ M were able to augment mean integral tension in myometrium from mice of all ages; linear regression analysis. *The label "0" on the x-axis relates to spontaneous contractile activity before application of oxytocin.*

## 5.4 Discussion

The aim of this study was to ascertain whether there is an inherent decrease in contractile function associated with increasing maternal age and if this is sufficient to explain the prolongation of pregnancy in older mice. Whilst the microarray analysis was limited in usefulness, mRNA expression of two key CAPs, Cx43 and OXTR, was slightly reduced in the older group of mice. There was an associated alteration in contractile frequency and duration in myometrium from eight month old pregnant mice and although this was not reflected in a reduced MIT, it does represent less effective contractile activity. All of the changes related to age were specific to the pregnant state; very little difference in mRNA expression or contractile parameters were detected in non-pregnant animals of different age.

The mouse genome-wide microarray was undertaken in order to identify new candidate genes, in addition to known contraction and pregnancy associated genes, which may be altered by age in pregnant mouse uterus. Unfortunately, the results failed to identify any upregulation or downregulation of significant genes in mouse uterus for eight month compared to three month old mice. This may have been for several reasons. Firstly, following advice from the bioinformatician involved, paired samples from bladder were run simultaneously with uterine tissues. This was to identify uterine specific gene regulation by 'subtracting' general ageing effects on smooth muscle. Given this approach, it is not surprising that only a limited number of uterine genes were found to be altered with age, albeit not significantly. With hindsight, it may have been more useful to look at the uterus without adjustment for similar changes in the bladder. Small fold changes in a variety of genes have been presented in the results, but the functional significance of these in the uterus are unknown. Review of the literature relating to these genes did not identify any particular function

that might be relevant to the regulation of uterine contraction apart from perhaps, RASl11a member of the small GTPase protein family and dynactin.

Of the three candidate genes assessed by qPCR, only Cx43 and OXTR were upregulated in late pregnancy compared to the non-pregnant state, which is similar to other studies in both mice and humans (Chow and Lye, 1994, Ou et al., 1997, Ou et al., 1998, Wathes et al., 1999, Cook et al., 2000, Liedman et al., 2009). However, there was a small but significant suppression of this pregnancy-induced response in myometrium from older mice, which has not been reported in the literature. The functional impact of this change is hard to definitively elucidate as there is still relatively high expression levels in older animals and undoubtedly, assuming that mRNA levels translate to an increase in protein, there would be sufficient Cx43 to aid gap junction formation to promote uterine contractions. However, if this small decrease in mRNA is physiologically relevant, then a reduction in gap junction number could result in limited conduction of electrical activity in the uterus resulting in shortened and less effective contractions.

Similarly, the dramatic increase in expression of OXTR in late pregnancy is thought to be a key priming event promoting the switch from quiescent to contractile activity when endogenous oxytocin is produced during labour (Kimura et al., 2013). Although OXTR expression was greatly upregulated in late pregnant myometrial tissues from older mice, there was a small reduction in expression when compared to myometrium from younger mice. As for Cx43, it is difficult to predict that this would be functionally relevant, however consideration of the data discussed below would strongly suggest that myometrium from older mice may be less responsive to oxytocin due to a reduction in OXTR expression.

Taken together, these data could suggest that ageing in primiparous mice suppresses the late pregnancy rise in contraction associated proteins leading to altered contractility. There may be other contributing factors, however, that cannot be disregarded. For example, a fall in maternal plasma progesterone and/or a reduction in myometrial stretch at term can activate Cx43 and OXTR expression in rat and human studies (Ou et al., 1997, Ou et al., 1998, Lyall et al., 2002, Terzidou et al., 2005). Since myometrial tissues were taken on day 18 of gestation, and parturition in older mice was delayed by one day (as shown in Chapter 3), it is possible that a delayed fall in maternal plasma progesterone may be responsible for this slight change in Cx43 and OXTR expression. Therefore, it would be beneficial to repeat this study using myometrial tissues collected on day 19 of gestation in older primiparous mice. Since eight month old mice had reduced litter sizes, there may have also been less mechanical stretch of the myometrium at term in these animals which could also contribute to the reduction in CAPs gene expression in older mice at term. There is also a need to confirm protein expression levels of these important CAP genes in tissues from late pregnant mice of different ages.

There is copious evidence to support the role for prostaglandins and PGHS1 and 2 in mouse pregnancy. PGHS1 derived prostaglandins are thought to be important during uterine preparation for implantation (Reese et al., 1999). Uterine expression of PGHS2, another key CAP, has been reported to be induced at labour in mice and humans, suggesting the involvement of PGHS2 in producing uterotonic prostaglandins during parturition (Slater et al., 1999, Tsuboi et al., 2000, Tsuboi et al., 2003, Renthal et al., 2013). Interestingly, expression of PTGS2 in this study was not induced by pregnancy or indeed regulated by age. This might be explained by the use of myometrium taken at day 18 of gestation, a day before delivery in the younger mice and two days before the eight month old group. Tsuboi *et al*., (2000) reported an absence of PGHS2 mRNA upregulation in the myometrium of wild-type mice on the

day before parturition, but strong signals for PGHS2 mRNA were detected in the myometrium on the day of parturition (Tsuboi et al., 2000).

To the best of my knowledge, this is the first study to investigate the influence of age on spontaneous and oxytocin-induced myometrial contractions in primparous C57BL/6 mice. The data strongly suggest that spontaneous contractions are less effective in tissues from older mothers as they are more frequent but of shorter duration, which is likely to limit propulsive force. These data add to the limited amount of information related to contractile activity in human myometrium from older mothers. Smith *et al.* (2008), reported that there is a negative correlation between contractile activity in human myometrial tissues (quantified by calculating the ratio of the mean integral tension during spontaneous contractile activity and the mean integral tension under in the presence of 50 mM potassium) with increasing maternal age (Smith et al., 2008).

In non-pregnant mice, application of oxytocin ($10^{-12}$-$10^{-7}$ M) did not augment contractile activity in spontaneously contracting myometrium *in vitro*. OXTR mRNA expression was lower in non-pregnant tissues but was increased by an approximate two fold change in late pregnant myometrium from mice of all ages. Assuming that mRNA levels translate to an increase in protein, this data would suggest that there would be fewer oxytocin receptors present in non-pregnant myometrium compared to late pregnant, explaining why oxytocin was unable to successfully augment contractile activity in non-pregnant tissues. Supporting this assumption, many studies have shown that oxytocin receptor density in the myometrium sharply increases at the end of pregnancy in species including the rat (Kaneko et al., 1995), guinea pig (Alexandrova and Soloff, 1980), rabbit (Maggi et al., 1988), and humans (Fuchs et al., 1984).

Application of oxytocin was able to augment contractile activity in late pregnant myometrium; however, tissues from older pregnant mice were less responsive to oxytocin and appeared to require higher concentrations of oxytocin to generate equal contractile activity as myometrium from younger mice. These data are consistent with findings from a recent study that show contractile responses to oxytocin (10 nM) were reduced in myometrium from pregnant women aged 40 and above compared to myometrium from women aged 39 years and under. This study also reported that there were no age-induced alterations in spontaneous contractions seen in pregnant human myometrium at term, but frequency and duration of contractions were not assessed (Arrowsmith et al., 2012). In the present study, there was no specific age-induced decrease in contractile activity of non-pregnant mouse myometrium. In contrast, Arrowsmith and colleagues have reported a striking reduction in spontaneous contractile force in non-pregnant human myometrium from older women (post 30 years old) when compared to myometrium from non-pregnant 25-29 year olds (Arrowsmith et al., 2012).

***Future work***

The two human studies discussed above, suggest that perhaps there are age-induced changes to myometrial morphology, increased cholesterol in the myometrium of older women, and decreased expression of L-type calcium channels in the myometrium of older women which may be contributing to the age-induced change in spontaneous contractile activity (Smith et al., 2008, Arrowsmith et al., 2012). Therefore, potential future work could examine myometrial morphology, measure cholesterol concentration and expression of L-type calcium channels as well as potassium channels and whether these change with age in pregnancy. There is also an opportunity to dissect the interactions between pregnancy, age, obesity and dyslipidemia using the validated mouse model from this study.

***Conclusions***

The outcome of this study indicates that maternal age influences expression of CAPs; specifically, expression of Cx43 and OXTR in late pregnant myometrium and that spontaneous contractions and oxytocin augmented activity is altered in older mice. It can be hypothesised that longer acting, coordinated contractions are necessary for producing sufficient cumulative force for the successful expulsion of pups, hence duration of labour was found to be considerably shorter in the three month old mice compared with older eight month old mice (Chapter 3). These data suggest that myometrium from older mice on day 18 of gestation may not be fully "activated" for parturition. If this were to be translated into the human situation, it would have implications for the management of labour in older mothers and influence the debate about elective Caesarean section in this group.

# Chapter 6

## Mitochondrial Number and Function in Ageing Myometrium

# Chapter 6 : Mitochondrial Number and Function in Ageing Myometrium

## 6.1 Introduction

In the previous results chapter, there was a marked reduction in contractile potential in myometrium from older mice when compared to younger controls. The working hypothesis is that mitochondrial dysfunction may be involved in this process. The mitochondrial theory of ageing is that ageing is a consequence of mitochondrial reactive oxygen species (ROS) accumulation, which causes progressive damage to MtDNA and other mitochondrial constituents during an individual's lifetime. It is widely accepted that mitochondrial oxidative stress is a major factor in the pathophysiology of ageing in many organs, including skeletal muscle, heart, and brain. There is evidence that in these organs, mitochondrial biogenesis is deregulated, since cumulative MtDNA mutations result in dysfunction of the mitochondrial electron transport chain, causing further ROS production in mitochondria and subsequently more MtDNA mutations and decline in cellular mitochondrial mass (Lee and Wei, 2007, Wei et al., 2009, Ivanova and Yankova, 2013, Lagouge and Larsson, 2013). There is also some evidence that mitochondrial dysfunction may play a key role in age-related smooth muscle deterioration such as in the bladder and blood vessels (Lin et al., 2000, Ungvari et al., 2008). This raises the question as to whether there are similar ageing-induced alterations in mitochondrial biogenesis and/or decline in functional mitochondrial mass in the mouse myometrium, which would result in an insufficient supply of energy to drive adequate uterine contractions.

Thus, the objective of the present study was to test the hypothesis that ageing leads to a decline in mitochondrial mass as reflected by a decline in mitochondrial copy number, and a dysfunction in mitochondrial biogenesis via measurement of the enzymatic activities of the electron transport chain complexes.

## 6.2 Methods

Full descriptions and details of the methods are described in Chapter 2, sections 2.9 and 2.10. In summary, mitochondrial copy number and enzymatic activities of the mitochondrial electron transport chain complexes were measured in non-pregnant and late pregnant myometrium from three, five and eight month old mice. All non-pregnant myometrial tissues were collected when mice were in oestrous stage of their reproductive cycle and all late pregnant myometrium on day 18 of gestation. The age of late pregnant mice as indicated within this chapter relate to their age at conception.

All data within this chapter were found to be normally distributed using the D'Agostino-Pearson omnibus normality test (GraphPad Prism version 5.0; GraphPad Software, USA), unless otherwise stated. Student's *t*-test was used to assess data between two groups and one-way analysis of variance (ANOVA) followed by all pairwise multiple comparison (Tukey's test) when comparing three or more groups. Data were expressed as mean ± standard error of the mean (SEM) and $p<0.05$ was considered significant; 'n' refers to the number of animals per sample group.

## 6.3 Results

### 6.3.1 Mitochondrial DNA (MtDNA) content in myometrium.

There was a significant reduction (-26%) in MtDNA copy number as measured by Mt/N ratio in myometrium from non-pregnant eight month old mice (23.56 ± 1.59) compared with myometrium from non-pregnant three month old mice (31.75 ± 2.07 units; $p<0.05$) (Figure 6.1). Mt/N was slightly smaller (-9%) in non-pregnant myometrium from five month old mice (28.79 ± 1.78) compared with three month old myometrium, and greater (+22%) than eight month old myometrium, but these did not reach significance.

In myometrium from late pregnant mice, there was a significant reduction in Mt/N between three month old mice (48.63 ± 1.67) compared with five month (38.61 ± 1.60; -25%, $p<0.01$) and compared with eight month (28.80 ± 1.72; -41%, $p<0.001$) old mice. There was also a significant reduction (-21%) in Mt/N between late pregnant myometrium from five month and eight month old mice ($p<0.01$; Figure 6.1).

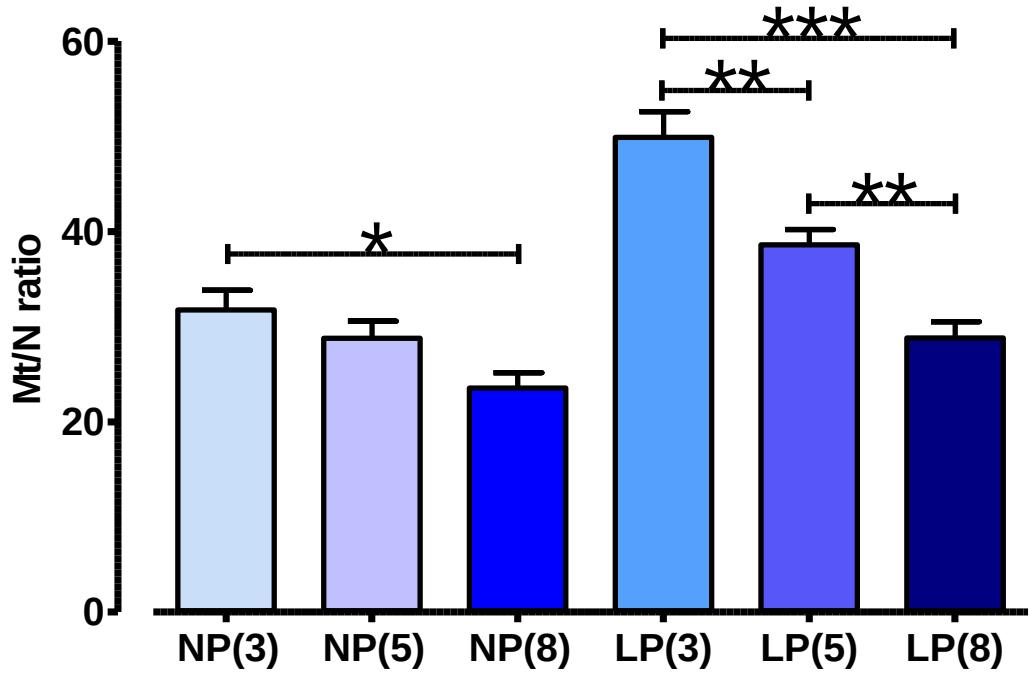


**Figure 6.1 MtDNA copy number ratio declines by the influence of maternal age in non-pregnant and late pregnant mouse myometrium**

Bar graph depicting Mt/N in myometrium from non-pregnant three month old [NP(3), n = 8], non-pregnant five month old [NP(5), n = 8] and non-pregnant eight month old [NP(8), n = 8], late pregnant three month old [LP(3), n = 8], late pregnant five month old [LP(5), n = 8] and late pregnant eight month old [LP(8), n = 8] mice. Mt/N was significantly reduced by the influence of age between NP(3) and NP(8) myometrium, * $p<0.05$, but not NP(5); Mt/N was significantly reduced by the influence of age between LP(3) and LP(8) myometrium, ***$p<0.001$, LP(3) and LP(5) myometrium, **$p<0.01$, and LP(5) and LP(8) myometrium, **$p<0.01$; ANOVA followed by all pairwise multiple comparison Tukey's test. Data expressed as mean ± SEM.

There was a significant increase in Mt/N between non-pregnant and late pregnant myometrium from three month old mice (+53%, p<0.001) and likewise between non-pregnant and late pregnant myometrium from five month old mice (+34%, p<0.01). Although there was an increase (+22%) in Mt/N between non-pregnant and late pregnant myometrium from eight month old mice, this difference did not reach significance; p = 0.052 (Figure 6.2).

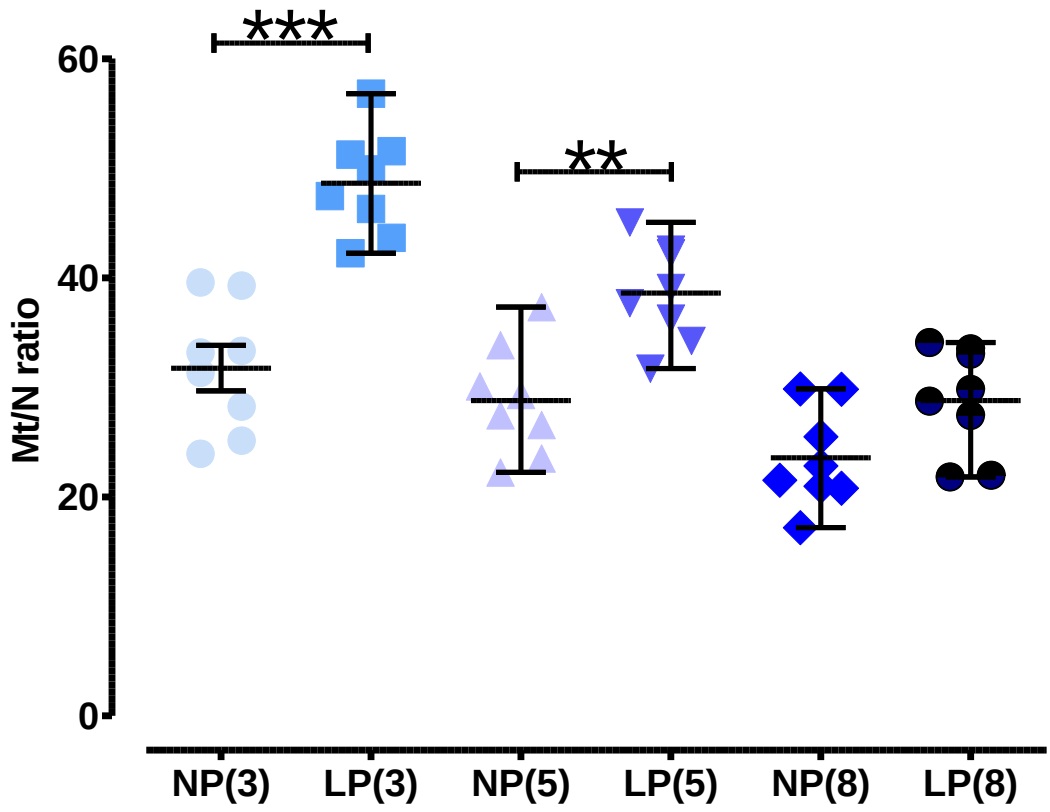


**Figure 6.2 MtDNA copy number ratio increases by the influence of pregnancy in myometrium from young mice**

Scatter graph presenting Mt/N in non-pregnant three month old [NP(3), n = 8] late pregnant three month old [LP(3), n = 8], non-pregnant five month old [NP(5), n = 8], late pregnant five month old [LP(5), n = 8] non-pregnant eight month old [NP(8), n = 8] and late pregnant eight month old [LP(8), n = 8] mice. Mt/N was significantly increased by the influence of pregnancy between NP(3) and LP(3) myometrium, ***p<0.001, and NP(5) and LP(5) myometrium, **p<0.01; ANOVA followed by all pairwise multiple comparison Tukey's test. Data expressed as mean ± SEM.

### 6.3.2 Mitochondrial electron transport chain enzyme activities in myometrium

Figure 6.3 demonstrates that citrate synthase activity in myometrial tissue protein was not significantly affected by age in neither non-pregnant (three months vs. eight months, p = 0.896, n = 8 for both groups); nor late pregnant mice (three months vs. eight months, p = 0.952, n = 8 for both groups). However for both age groups, citrate synthase enzyme activity was numerically lower in the late pregnant mouse myometrium compared to the non-pregnant state, although these differences were not significant (n = 8 for all groups; Figure 6.3).

Similarly, complex I (NADH dehydrogenase) activity in myometrial protein was not modified by age in neither non-pregnant (three month old vs. eight month old, p = 0.465, n = 8 for both groups) nor late pregnant mice (three month old vs. eight month old, p = 0.075 n = 8 for both groups) (Figure 6.4). Myometrial tissue NADH dehydrogenase activity was not significantly altered by pregnancy in either age group compared to the non-pregnant state (n = 8 for all groups; Figure 6.4).

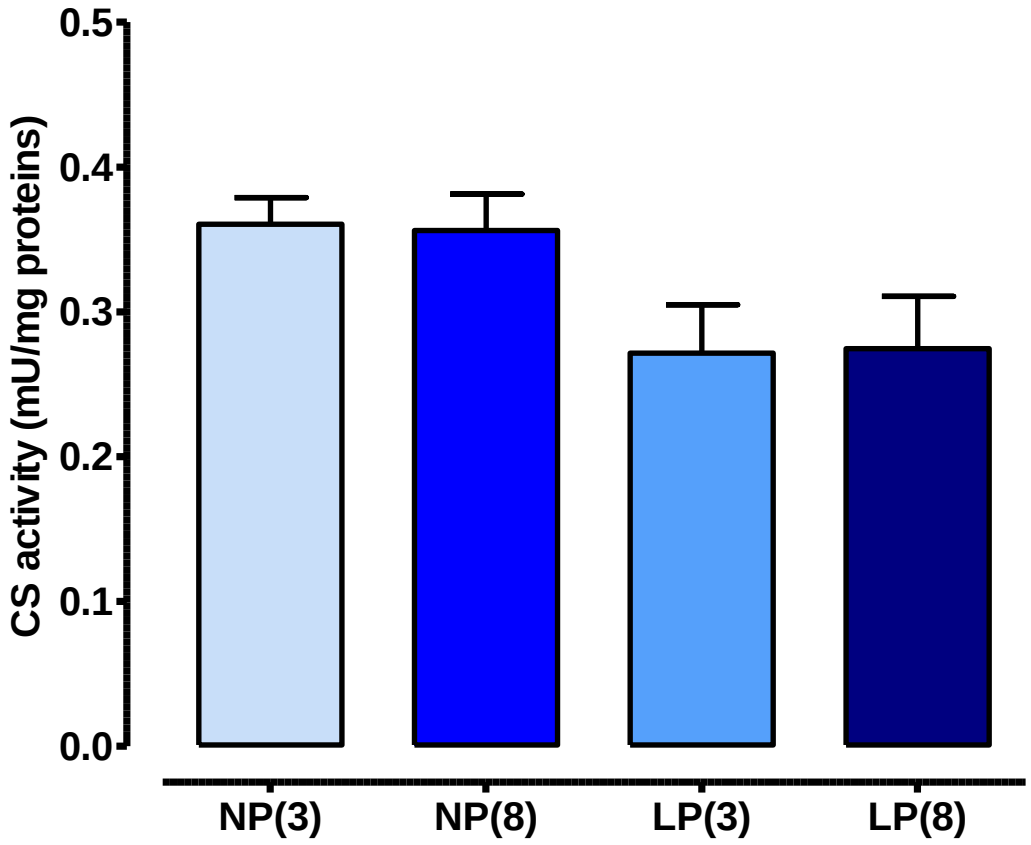


**Figure 6.3 Citrate Synthase activity is unchanged by the influence of maternal age and pregnancy in mouse myometrium**

Bar graph depicting citrate synthase enzyme activity in myometrium from non-pregnant three month old [NP(3), n = 8] late pregnant three month old [LP(3), n = 8], non-pregnant eight month old [NP(8), n = 8] and late pregnant eight month old [LP(8), n = 8] mice. Statistical comparison was non-significant; ANOVA followed by all pairwise multiple comparison Tukey's test. Data expressed as mean ± SEM.

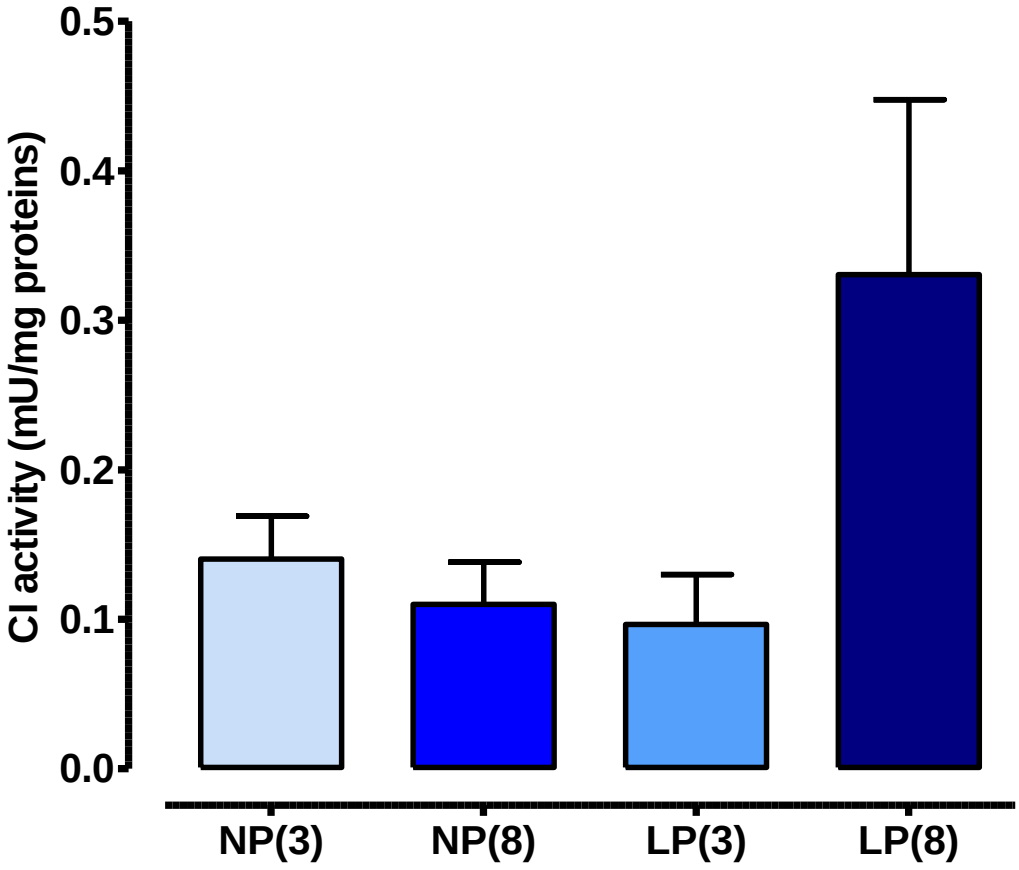


**Figure 6.4 Complex I/NADH dehydrogenase activity is unchanged by the influence of maternal age and pregnancy in mouse myometrium**

Bar graph depicting NADH dehydrogenase enzyme activity in myometrium from non-pregnant three month old [NP(3), n = 8] late pregnant three month old [LP(3), n = 8], non-pregnant eight month old [NP(8), n = 8] and late pregnant eight month old [LP(8), n = 8] mice. Statistical comparison was non-significant; ANOVA followed by all pairwise multiple comparison Tukey's test. Data expressed as mean ± SEM.

Complex II (succinate dehydrogenase) activity was not significantly altered by age in both non-pregnant (three months vs. eight months, p = 0.205, n = 8 for both groups) and late pregnant mice (three months vs. eight months, p = 0.654, n = 8 for both groups) (Figure 6.5). However, succinate dehydrogenase activity was significantly increased by pregnancy in myometrium from both three month and eight month old mice (p<0.001, p<0.01 respectively, n = 8 for all groups) (Figure 6.5). Succinate dehydrogenase was higher in myometrium from pregnant three month old (64%) and eight month old (43%) mice compared to age-matched non-pregnant controls for both groups.

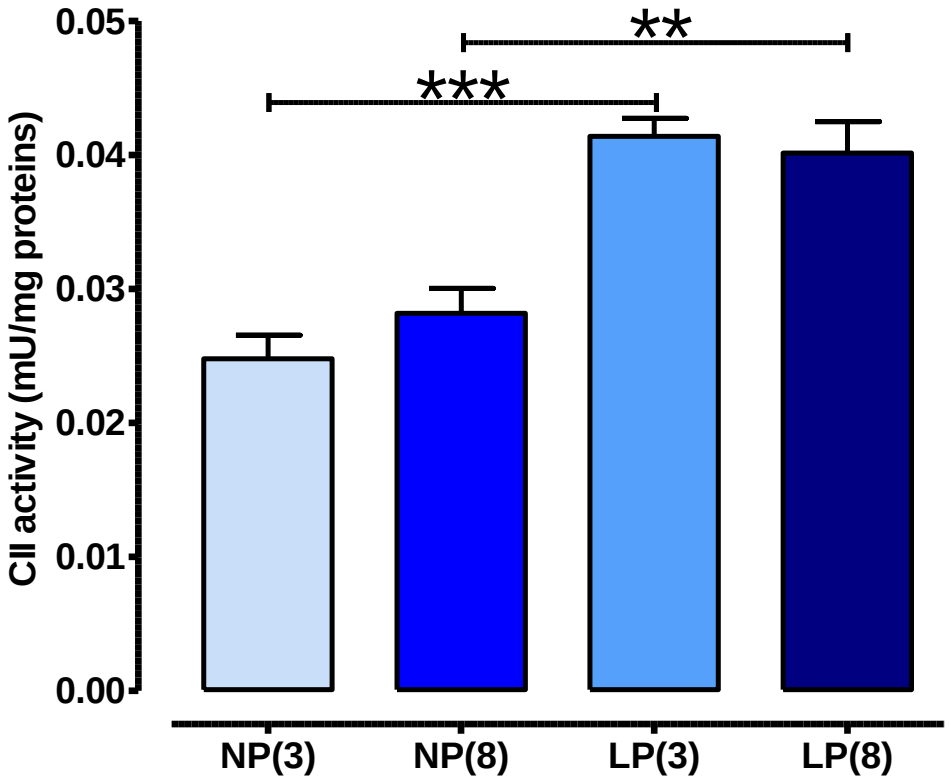


**Figure 6.5 Complex II/succinate dehydrogenase activity is unchanged by age but raised by pregnancy in mouse myometrium**

Bar graph depicting succinate dehydrogenase enzyme activity in myometrium from non-pregnant three month old [NP(3), n = 8] late pregnant three month old [LP(3), n = 8], non-pregnant eight month old [NP(8), n = 8] and late pregnant eight month old [LP(8), n = 8] mice. Transition from non-pregnant to pregnant state significantly increased succinate dehydrogenase activity in myometrium from both ages *** p<0.001, ** p<0.01; ANOVA followed by all pairwise multiple comparison Tukey's test. Data expressed as mean ± SEM.

Complex III (ubiquinol cytochrome c reductase) activity was also not significantly altered by age in non-pregnant (three months vs. eight months, p = 0.299, n = 8 for both groups) and late pregnant mice (three months vs. eight months, p = 0.399, n = 8 for both groups) (Figure 6.6). For both age groups, the enzyme activity in the myometrium was numerically higher in myometrial tissues from pregnant mice compared to the non-pregnant state but these did not reach significance (n = 8 for all groups; Figure 6.6).

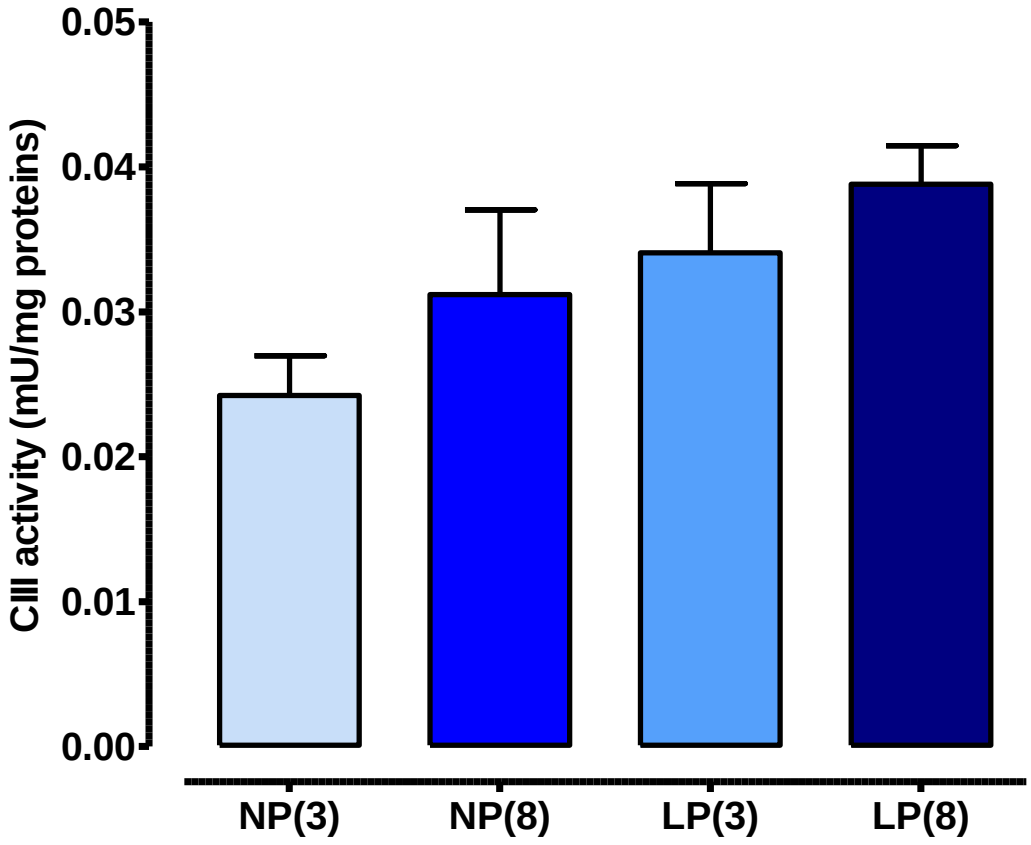


**Figure 6.6 Complex III/Ubiquinol cytochrome c reductase activity is unchanged by the influence of maternal age and pregnancy in mouse myometrium**

Bar graph presenting ubiquinol cytochrome c reductase enzyme activity in myometrium from non-pregnant three month old [NP(3), n = 8] late pregnant three month old [LP(3), n = 8], non-pregnant eight month old [NP(8), n = 8] and late pregnant eight month old [LP(8), n = 8] mice. Statistical comparison was non-significant; ANOVA followed by all pairwise multiple comparison Tukey's test. Data expressed as mean ± SEM.

## 6.4 Discussion

This study provides, as far as can be ascertained from the literature, a unique set of data assessing mitochondrial number and activity in myometrium from primiparous mice in early stages of reproductive ageing. There was a clear reduction in Mt/N seen with age in myometrial tissues from both pregnant and non-pregnant animals. Interestingly, there was a pregnancy-associated enhancement in the Mt/N in younger mice, but this difference was suppressed in older mice. In contrast, activities of mitochondrial electron transport chain enzymes NADH dehydrogenase and ubiquinol cytochrome c reductase (complexes I and III), as well as citrate synthase activity in mouse myometrium were not influenced by age or pregnancy state. Succinate dehydrogenase (complex II) activity was also unaltered by age, but was considerably increased in the pregnant state.

These data are somewhat different from the bulk of published data for other muscles, cardiac and skeletal and to some degree smooth muscle in both humans and rodents, where the process of ageing has often been associated with an alteration in the enzymatic activities of all or some of the mitochondrial electron transport chain complexes (Yen et al., 1989, Cooper et al., 1992, Torii et al., 1992, Sugiyama et al., 1993, Takasawa et al., 1993, Ojaimi et al., 1999, Kwong and Sohal, 2000, Lin et al., 2000, Short et al., 2005, Muller et al., 2010). Citrate synthase activity in skeletal muscle, as well as the activities of electron transport chain complexes II and III in cardiac muscle have been found to be significantly decreased in mature C57BL/6 male mice aged 18 months (compared to 3 months) and 25 months (compared to 2 months) respectively (Figueiredo et al., 2008, Padrao et al., 2012). Although a reduction in the activities of mitochondrial respiratory complexes is commonly reported in ageing muscles, contradictory data also exist, with some studies showing an increase in activities with age. In addition, alterations in mitochondrial respiratory complex

activities are not apparent across all tissues in aged animals. A study measuring the activities of respiratory complexes in mitochondria isolated from brain, heart, skeletal muscle, liver, and kidney of young (3.5 months), adult (12–14 months) and old (28–30 months) C57BL/6 male mice reported that complex I activity did not vary with age in any of the tissues (Kwong and Sohal, 2000); a similar finding to the present study. Changes to complex II activity differed across tissues, with no age-related alteration in the kidney and liver, an 11% increase in activity in cardiac muscle after the age of 12 months (compared to young mice) and a 30% increase in activity in skeletal muscle in aged 28-30 month old mice (compared to young). Complex III activity was reduced by 40% in brain tissues from aged 28 month old mice (compared to young mice), yet increased by 20% in skeletal muscle at the age of 28 month old (compared to young mice). Again, age-induced alterations in enzyme activity were not constant throughout all tissues, with no change in complex III activity being reported in the kidney, liver, and heart across all ages of mice (Kwong and Sohal, 2000). In summary, age-related alterations in enzyme activities of the mitochondrial electron transport chain complexes are widely reported, but there does not seem to be a uniform pattern of whether these activities are increased or decreased as a result of ageing.

The reasons for not detecting age-related changes in enzyme activities of mitochondrial electron transport complexes I-III in myometrium in the present study may be related to the ages of mice used. The three and eight month groups were selected because they were at suitably separate reproductive periods relative to the lifetime of a mouse. However, the majority of studies published to date have reported age-induced alterations in mitochondrial electron transport chain complex enzyme activities in muscles from animals far older than eight month of age. It could be proposed that although there may be some mitochondrial ROS damage by this age, it may not have reached the peak whereby it interrupts the electron transport chain function.

The present mitochondrial copy number data is interesting as it clearly shows that there is a generalised age-related reduction in copy number both in the non-pregnant and pregnant states at eight month of age. It suggests that the reduction in mitochondrial copy number precedes any change in mitochondrial complex activity. Reduced MtDNA copy number has been previously reported as a consequence of ageing in rodent and human skeletal muscle (Barazzoni et al., 2000, Short et al., 2005, Peterson et al., 2012). Barazzoni *et al.* have reported a 23 - 40% reduction in MtDNA copy number in skeletal muscle from 27 month old rats compared to rats of 6 month of age (Barazzoni et al., 2000). According to the mitochondrial theory of ageing, a decline in MtDNA, is a direct result of mitochondrial ROS accumulation which in turn causes progressive damage to MtDNA and other mitochondrial constituents. MtDNA is particularly susceptible to oxidative damage because it is near the major site of ROS production, lacks protective histones, and has weaker DNA repair mechanisms. However, there are discrepancies over mtDNA mutation frequencies and to what extent ROS production is responsible; there is increasing evidence that perhaps a majority of mutations are due to the inherent error rate of mtDNA polymerase gamma (Peterson et al., 2012).

In relation to pregnancy-induced changes in complex activity, irrespective of age, only the activity of complex II was found to be significantly increased in pregnant myometrium in this study. The acceleration of complex II enzyme activity can potentially be explained by the fundamental uterine changes essential for successful pregnancy. Physiological growth of the pregnant uterus occurs by two mechanisms: an increase in cell number (hyperplasia), and an increase in cell size (hypertrophy). Hypertrophy usually results in an increase in cell organelles, including mitochondria (Douglas et al., 1988, Shynlova et al., 2006). Since there are more mitochondria present in pregnant myometrium, as indicated by the increased MTDNA copy number ratio in young pregnant animals compared to the non-pregnant state, this may in part

explain the greater complex II enzyme activity. The impact of pregnancy on mitochondrial electron transport chain enzyme activities in myometrium appears to have only been previously studied by one other group (Geyer and Riebschläger, 1974) and whilst they only measured cytochrome c-oxidase/complex IV activity, it was also significantly increased in pregnant human and rat myometrium compared to non-pregnant myometrium (ages of human subjects were not reported; pregnant rats were 40 days of age) (Geyer and Riebschläger, 1974).

The rise in complex II activity is mirrored by a generalised rise in mitochondrial copy number in myometrium from young pregnant mice compared to young non-pregnant mice. It again suggests that in younger animals, such an increase in mitochondrial copy number is a physiological adaptation to pregnancy. These observations are also similar to data originating from human myometrium (Geyer and Riebschläger, 1974), where in addition to the increase in mitochondrial complex IV activity in pregnancy, there is also evidence of an increase in the number of mitochondria. This again is likely to be linked to pregnancy-induced hypertrophy of the myometrium (Shynlova et al., 2006).

This hypertrophic adaptation is far less apparent as the mice age within the reproductive window. This failure to increase mitochondrial copy number in older animals, particularly in pregnancy, is likely to have physiological consequences in the parturition phase of pregnancy. Indeed, the marked reduction in contractile potential in myometrium from older mice shown in the previous results chapter may be explained in part by a reduction in functional mitochondria, as reflected by the decline in Mt/N in these aged animals. The level of MtDNA in a cell could provide a major regulatory point in mitochondrial activity, as the transcription of mitochondrial genes is proportional to their copy number. Therefore, the reduction in Mt/N could potentially reflect a concurrent reduction in capacity to generate sufficient cellular energy (ATP) to drive uterine contractions.

Myometrial contractions arise from spontaneous action potentials that permit the entry of calcium ions and elevate the intracellular calcium concentration (Tribe, 2001). In addition, actin filaments in association with myosin are also essential for muscle contraction. The binding of ATP to ATPase on the myosin heavy chains catalyses the dephosphorylation of ATP to ADP yielding energy to drive the sliding of myosin over actin filaments (cross-bridge cycling) creating the movement that establishes myometrial contraction (Moore and Bernal, 2001, Wray, 2007). For these reasons intracellular calcium ion modulation and ATP availability are of importance when investigating the control of myometrial contractions.

The role of mitochondria and ATP provision in the control of uterine contractions has previously been studied in mouse myometrium (Gravina et al., 2010). Mitochondria were investigated here since they are able to take up, store and release calcium via the mitochondrial $Ca^{2+}$ uniporter (Kirichok et al., 2004), indicating that they may play an important role in uterine contraction activation through the modulation of intracellular calcium. Cumulative concentration–response experiments were performed to determine the effects of specific mitochondrial inhibiting drugs on the force of spontaneous contractions of myometrium. Response curves were determined for: carbonylcyanide-3-chlorophenylhydrazone (CCCP), a protonophore uncoupler that abolishes the mitochondrial membrane potential, and rotenone, a respiratory chain inhibitor of mitochondrial electron transport chain complex I. These agents decreased the force of contractions in a concentration-dependent manner (Gravina et al., 2010). An ATP synthase inhibitor, oligomycin had no effect over a wide concentration range for at least 30 minutes, a period over which CCCP, and rotenone markedly reduced contraction amplitude. The authors suggested that this indicated these actions did not occur through lack of ATP within the uterine cells and is consistent with the view that mitochondria can modulate intracellular $Ca^{2+}$ concentration without compromising ATP production (Davidson and Duchen, 2007). Consequently, the finding that the inhibition

of contractile force was not due to ATP depletion suggests that mitochondrial $Ca^{2+}$ handling has an independent role in determining uterine contractility (Chalmers and McCarron, 2008, Gravina et al., 2010, Gravina et al., 2011). Since mitochondria have been shown to be important regulators of contractility as well as intracellular $Ca^{2+}$; in the present study we can also hypothesise that an age-related reduction in contractile potential in the myometrium, and the concurrent reduction in MtDNA copy number could indicate that fewer mitochondria present in the myometrium would impact on the uptake/release of intracellular $Ca^{2+}$ and in turn disrupt uterine contractions.

***Study limitations and future work***

A clear limitation of this study is that only the enzyme activities of mitochondrial electron transport chain complexes I-III were measured in aged non-pregnant and pregnant myometrium. It would have been advantageous to also measure the activities of complex IV, and interactions between complexes such as NADH cytochrome c reductase (activity of complex I+III) and succinate cytochrome c reductase (activity of complex II+III), as well as complex V, ATP synthase. Knowledge of how all of these electron transport chain enzyme activities differ between three month and eight month of age in mouse myometrium may help to clarify the degree, if any, of how ageing impacts on oxidative phosphorylation and hence, mitochondrial ATP synthesis.

There are many more methods to study mitochondria, and if time and cost permitted, it would have been of interest to investigate the role of mitochondria in ageing myometrium further. Future work includes electron microscopy to study whether mitochondria exhibit common signs of ageing such as enlargement/mitochondrial swelling, matrix vacuolisation, and altered cristae (Picard et al., 2013). Staining dyes such as MitoTracker or fluorescence microscopy may be used to visualise

mitochondria in cells. This method can provide additional data to support the finding that mitochondrial numbers are reduced in myometrium from eight month old mice (Barbieri et al., 2011). Measurement of oxygen consumption using a Clarke-type $O_2$ electrode can quantify respiratory function in mitochondria, which would provide data to support the mitochondrial electron transport chain enzyme activities (Mourmoura et al., 2011). Cumulative dose response curves for CCCP, rotenone and oligomycin on pregnant myometrium can determine whether the reduction in mitochondrial copy number in older eight month old mice is exerting an effect by altering intracellular $Ca^{2+}$ concentration without compromising ATP production (Gravina et al., 2010). Oxidative stress caused by mitochondrial ROS can result in the formation of highly reactive and unstable lipid hydroperoxides (Negre-Salvayre et al., 2010). Therefore as an indicator of oxidative damage, lipid hydroperoxides can be quantified in myometrial tissues from mice of all ages (TBARS assay kit; Cayman Chemical, USA). One final study of interest would be to perform a mouse mitochondria PCR array, as sold by Qiagen (The Mouse Mitochondria RT² Profiler PCR Array System; Qiagen, UK) which profiles the expression of 84 genes involved in the biogenesis and function of mitochondria. This would help to identify any other potential biomarkers within mitochondria, which could contribute to the maternal age-induced alterations in myometrial contractility.

***Conclusions***

The influence of maternal age of eight months cannot be linked to any significant alterations in the mitochondrial electron transport chain complex activities in myometrium from non-pregnant or pregnant mice. The significant reduction in Mt/N seen in myometrium from eight month old mice can potentially influence two mitochondrial-controlled routes of uterine contractions: reduction in overall ATP synthesis or decrease in intracellular $Ca^{2+}$. Further studies are necessary to fully elucidate the role of mitochondria in ageing non-pregnant and pregnant myometrium.

# Chapter 7

## General Discussion and Future Work

# Chapter 7 : General Discussion and Future Work

Life expectancy in women has risen from 42 years of age in 1838 to 82 years of age in 2010 (Office for National Statistics for England and Wales, 2011a) and concurrent with this, there has been a trend for women to extend childbirth into their later years of fertility which has introduced the term 'advanced maternal age' to describe mothers who have babies at the age of 35 years and beyond (Kirz et al., 1985, Bewley et al., 2009, Bayrampour and Heaman, 2010). The principal aim of this thesis was to determine whether advanced maternal age has a detrimental impact on uterine and/or cervical function at the end of gestation. This thesis provides the first comprehensive study of the impact of ageing in pregnant mice and demonstrates that advancing reproductive age not only prolongs gestation, but duration of labour as well. Such delays are unlikely to be underpinned by impaired cervical softening, but more likely related to disrupted uterine activation at term. This is evidenced by a reduction in spontaneous contractile and oxytocin augmented myometrial activity in older mice coupled with reduced gene expression of contractile associated proteins. The significant reduction in MtDNA copy number ratio in myometrium from older mice could also potentially contribute to less effective contractile activity because of a reduction in overall ATP synthesis or decrease in intracellular $Ca^{2+}$. The collective data from this thesis highlight several important additional research questions that could be addressed further.

## 7.1 Is progesterone withdrawal delayed in older pregnant mice?

The initiation of progesterone withdrawal is essential for the onset of parturition in rodents (Sugimoto et al., 1997, Weiss, 2000). The data from this thesis would strongly suggest that timing of progesterone withdrawal at term in older nulliparous mice may be a key regulator in the initiation of labour. Therefore, the most pertinent question to be answered by future work is whether there is a delay in progesterone withdrawal at term in older mice that could explain the delay in parturition and related uterine activation. To accurately measure the exact rate of maternal serum progesterone decline and determine whether this changes with maternal age in C57BL/6J mice, serial blood samples from pregnant mice could be taken throughout pregnancy until day of parturition. Alternatively, to reduce stress to mice, a cross sectional study might be more appropriate, whereby mice of three and eight months of age would be sacrificed over a range of gestations in order to acquire terminal blood samples. Another key contributing factor to progesterone sensitivity would be progesterone receptor availability and turnover. To determine whether delayed parturition in older nulliparous mice may be due to greater availability of progesterone receptors compared to younger mice, immunohistochemistry can be used to determine presence and localisation of progesterone receptor isoforms in myometrial and cervical samples, and mRNA expression of progesterone receptor isoforms can be quantified using qPCR.

## 7.2 Is cervical ripening delayed as a result of reproductive ageing in mice?

The physiological alterations to the cervix in pregnancy were studied at day 18 of gestation in this thesis. At this time point it is only possible to assess cervical softening, since cervical ripening in mice occurs in the hours preceding birth (Read et al., 2007). Cervical ripening at the end of gestation may be more important than the cervical softening phase, since it is when there is maximal loss of cervical tissue compliance and integrity (Timmons et al., 2010, Mahendroo, 2012). Ripening is the most accelerated phase of cervical remodelling and occurs when maternal plasma progesterone concentrations have dropped nearing the onset of parturition (Mahendroo, 2012), again emphasizing the importance of progesterone withdrawal in the control initiation of parturition. An extension of the study described in Chapter 4, would be to repeat all experimental techniques using cervical tissues collected on gestation day 19 (for three months old mice) and 20 (for eight months old mice) in order to capture tissues in the ripening phase. This would determine whether there are any age related changes that occur specifically to cervical ripening, and whether this plays a role in the delay in parturition and prolonged labour in older mice.

## 7.3 Is spontaneous myometrial contractile activity in older mice altered by a reduction in ion channel expression?

A number of $Ca^{2+}$ and $K^+$ channels, including voltage-regulated L-type $Ca^{2+}$channels and $Ca^{2+}$-activated $K^+$ channels have been implicated in the control of myometrial membrane potential and subsequent regulation of contractions (Sanborn, 2000, Tribe, 2001, Khan et al., 2001). In ageing rodent studies, decreased expression of voltage and $Ca^{2+}$-activated $K^+$ channels have been reported in coronary smooth muscle (Marijic et al., 2001). This highlights the need to examine ion channel expression in myometrium from pregnant aged mice, since lower expression of $Ca^{2+}$ and/or $K^+$ channels could potentially contribute to the less effective spontaneous contractile activity exhibited by these older mice compared to the younger age group.

## 7.4 Is spontaneous myometrial contractile activity in older mice altered by increased body weight?

In addition, consideration of the dual impact of body mass index (BMI) and age is worth considering. In humans it is difficult to assess the impact of age alone as body mass index and maternal fat mass (kg) increases as women age (Maple-Brown et al., 2013). Ageing also results in increased in myometrial cholesterol. Both cholesterol and BMI have been shown to depress myometrial contractility (Zhang et al., 2007, Arrowsmith et al., 2012). Pharmacological addition of cholesterol to contracting strips of human and animal myometrium *in vitro* inhibits contractile activity; furthermore, human myometrial strips with high cholesterol content contract less effectively *in vitro* compared to those with lower cholesterol content (Shmygol et al., 2007, Noble et al., 2009, Arrowsmith et al., 2012). The use of animal models provide a unique opportunity to dissect out the potentially confounding factors of obesity and age *in vivo* and *in vitro* using a range of molecular and physiological techniques. For example, the

quantification of cholesterol in myometrium from pregnant older mice, would determine whether the less effective spontaneous contractility of myometrium from older mice compared to younger is a consequence of cholesterol accumulation with age. Moreover, *in vivo* studies of ageing in obese and non-obese mice using video imaging and uterine telemetry, would allow assessment of gestation and parturition length.

## 7.5 Are uterine contractions less effective in older mice due to reduced ATP synthesis or decreased intracellular $Ca^{2+}$?

A significant reduction in MtDNA copy number was exhibited in myometrium from older pregnant mice compared to younger mice in this thesis. Since mitochondria are a key site for ATP production and can also modulate intracellular $Ca^{2+}$ concentrations (Davidson and Duchen, 2007), it raises the question whether the reduction in the number of myometrial mitochondria, result in less effective uterine contractions due to a reduction in overall ATP synthesis, or by decreasing intracellular $Ca^{2+}$ concentrations. Future work would involve cumulative concentration response experiments to determine the effects of specific mitochondrial inhibitors such as carbonylcyanide-3-chlorophenylhydrazone, as well as an ATP synthase inhibitor such as oligomycin on spontaneous contractile activity of mouse myometrium (Gravina et al., 2010). There is also a need to examine the ability of aged myometrial tissues to generate prolonged contractions *in vivo* using uterine telemetry to determine whether function correlates to *in vitro* MtDNA copy number ratio in both human and mouse myometrial tissues.

## 7.6 What is the current understanding of the impact of advanced maternal age on myometrial function?

Limited data has been published on the impact of advanced maternal age on myometrial contractility *in vitro*. One study reports a negative correlation between contractile activities in myometrial tissues from pregnant women with age (Smith et al., 2008), however, the only other existing study reports that age-induced reduction in spontaneous myometrial contractions is evident only in non-pregnant human myometrium and not in pregnant myometrium (Arrowsmith et al., 2012). Preliminary data on the impact of maternal age (> 35 years of age; BMI < 30; n = 23) on spontaneous contractions in human myometrium *in vitro*, would suggest that over a period of an hour, spontaneous contractile activity is not significantly different to that of myometrium from younger women (< 25 years of age; BMI < 30; n = 12); Student's t-test. Spontaneous contractile mean integral tension is 358 ± 34.8 mN/cm$^2$ in myometrium from younger women, and 338 ± 27.1 mN/cm$^2$ in myometrium from women of advanced maternal age. It could be possible that experimental examination of short time periods of contractions may not reveal any age induced alterations in myometrial contractility, but prolonged observations, over hours or days may identify more profound contractile impairment.

In summary, the data from this thesis emphasise the physiological and cellular changes that occur with reproductive ageing, and have begun to answer some of the questions as to what mechanisms and reproductive tissues are predominantly affected by ageing. This work highlights the need for additional research in this nascent area and there is broad scope for future experimental work in both mouse models and human tissues in order to develop a more detailed understanding of the mechanistic impact of maternal ageing on labour. A more complex understanding of the relationship between age and reproductive outcomes will ultimately influence the clinical management of the burgeoning problem of advanced maternal age and pregnancy.

# Chapter 8

## References

## References


ADAMS, D. S. 2003. *In: Lab Math: A Handbook of Measurements, Calculations, and Other Quantitative Skills for Use at the Bench. Chapter 5,* New York, Cold Spring Harbor Laboratory Press.

ADINSTRUMENTS. 2013. ADinstruments. Available: http://www.adinstruments.com/solutions/research/applications/organ-bath-experiments#overview 2013].

AKDAG, F., ARSLAN, S. & DEMIR, H. 2009. The Effect of Parity and Litter Size on Birth Weight and the Effect of Birth Weight Variations on Weaning Weight and Pre-Weaning Survival in Piglet. *Journal of Animal and Veterinary Advances,* 8**,** 2133-2138.

AKINS, M. L., LUBY-PHELPS, K., BANK, R. A. & MAHENDROO, M. 2011. Cervical softening during pregnancy: regulated changes in collagen cross-linking and composition of matricellular proteins in the mouse. *Biol Reprod,* 84**,** 1053-62.

AKIYAMA, T., NAGATA, M. & AOKI, F. 2006. Inadequate histone deacetylation during oocyte meiosis causes aneuploidy and embryo death in mice. *Proc Natl Acad Sci U S A,* 103**,** 7339-44.

ALCORN, J. L., HAMMER, R. E., GRAVES, K. R., SMITH, M. E., MAIKA, S. D., MICHAEL, L. F., GAO, E., WANG, Y. & MENDELSON, C. R. 1999. Analysis of genomic regions involved in regulation of the rabbit surfactant protein A gene in transgenic mice. *Am J Physiol,* 277**,** L349-61.

ALEXANDROVA, M. & SOLOFF, M. S. 1980. Oxytocin receptors and parturition in the guinea pig. *Biol Reprod,* 22**,** 1106-11.

ALLPORT, V. C., PIEBER, D., SLATER, D. M., NEWTON, R., WHITE, J. O. & BENNETT, P. R. 2001. Human labour is associated with nuclear factor-kappaB activity which mediates cyclo-oxygenase-2 expression and is involved with the 'functional progesterone withdrawal'. *Mol Hum Reprod,* 7**,** 581-6.

ARELLANO, M. 1987. PRACTITIONERS' CORNER: Computing Robust Standard Errors for Within-groups Estimators*. *Oxford Bulletin of Economics and Statistics,* 49**,** 431-434.

ARMANIOS, M., ALDER, J. K., PARRY, E. M., KARIM, B., STRONG, M. A. & GREIDER, C. W. 2009. Short telomeres are sufficient to cause the degenerative defects associated with aging. *Am J Hum Genet,* 85**,** 823-32.

ARROWSMITH, S., ROBINSON, H., NOBLE, K. & WRAY, S. 2012. What do we know about what happens to myometrial function as women age? *J Muscle Res Cell Motil,* 33**,** 209-17.

ASDELL, S. A. 1929. Variation in the Duration of Gestation in the Goat. *The Journal of Agricultural Science,* 19**,** 382-396.

ASPDEN, R. M. 1988. The theory of fibre-reinforced composite materials applied to changes in the mechanical properties of the cervix during pregnancy. *J Theor Biol,* 130**,** 213-21.

ASTLE, S., NEWTON, R., THORNTON, S., VATISH, M. & SLATER, D. M. 2007. Expression and regulation of prostaglandin E synthase isoforms in human myometrium with labour. *Mol Hum Reprod,* 13**,** 69-75.

AYDOS, S. E., ELHAN, A. H. & TUKUN, A. 2005. Is telomere length one of the determinants of reproductive life span? *Arch Gynecol Obstet,* 272**,** 113-6.

BALABAN, R. S., NEMOTO, S. & FINKEL, T. 2005. Mitochondria, oxidants, and aging. *Cell,* 120**,** 483-95.

BALASCH, J. & GRATACOS, E. 2012. Delayed childbearing: effects on fertility and the outcome of pregnancy. *Curr Opin Obstet Gynecol,* 24**,** 187-93.

BARAZZONI, R., SHORT, K. R. & NAIR, K. S. 2000. Effects of aging on mitochondrial DNA copy number and cytochrome c oxidase gene expression in rat skeletal muscle, liver, and heart. *J Biol Chem,* 275**,** 3343-7.

BARBIERI, E., BATTISTELLI, M., CASADEI, L., VALLORANI, L., PICCOLI, G., GUESCINI, M., GIOACCHINI, A. M., POLIDORI, E., ZEPPA, S., CECCAROLI, P., STOCCHI, L., STOCCHI, V. & FALCIERI, E. 2011. Morphofunctional and Biochemical Approaches for Studying Mitochondrial Changes during Myoblasts Differentiation. *J Aging Res,* 2011**,** 845379.

BARJA, G. & HERRERO, A. 2000. Oxidative damage to mitochondrial DNA is inversely related to maximum life span in the heart and brain of mammals. *FASEB J,* 14**,** 312-8.

BARONI EDO, R., BIONDO-SIMOES MDE, L., AUERSVALD, A., AUERSVALD, L. A., MONTEMOR NETTO, M. R., ORTOLAN, M. C. & KOHLER, J. N. 2012. Influence of aging on the quality of the skin of white women: the role of collagen. *Acta Cir Bras,* 27**,** 736-40.

BASS, T. M., WEINKOVE, D., HOUTHOOFD, K., GEMS, D. & PARTRIDGE, L. 2007. Effects of resveratrol on lifespan in Drosophila melanogaster and Caenorhabditis elegans. *Mech Ageing Dev,* 128**,** 546-52.

BAUMFORTH, K. R., NELSON, P. N., DIGBY, J. E., O'NEIL, J. D. & MURRAY, P. G. 1999. Demystified ... the polymerase chain reaction. *Mol Pathol,* 52**,** 1-10.

BAUR, J. A. 2010. Resveratrol, sirtuins, and the promise of a DR mimetic. *Mech Ageing Dev,* 131**,** 261-9.

BAYLIS, D., BARTLETT, D. B., PATEL, H. P. & ROBERTS, H. C. 2013. Understanding how we age: insights into inflammaging. 2:8. Available: http://www.longevityandhealthspan.com/content/2/1/8.

BAYRAMPOUR, H. & HEAMAN, M. 2010. Advanced maternal age and the risk of cesarean birth: a systematic review. *Birth,* 37**,** 219-26.

BENJAMINI, Y. & HOCHBERG, Y. 1995. Controlling the False Discovery Rate: A Practical and Powerful Approach to Multiple Testing. *Journal of the Royal Statistical Society. Series B (Methodological),* 57**,** 289-300.

BENZIES, K., TOUGH, S., TOFFLEMIRE, K., FRICK, C., FABER, A. & NEWBURN-COOK, C. 2006. Factors influencing women's decisions about timing of motherhood. *J Obstet Gynecol Neonatal Nurs,* 35**,** 625-33.

BERNAL, A. L. 2001. Overview of current research in parturition. *Exp Physiol,* 86**,** 213-22.

BEWLEY, S., LEDGER, W. & NIKOLAOU, D. 2009. *Reproductive Ageing.,* London, The Royal College of Obstetricians and Gynaecologists.

BIGGERS, J. D., CURNOW, R. N., FINN, C. A. & MCLAREN, A. 1963. Regulation of the gestation period in mice *J Reprod Fertil,* 6**,** 125-38.

BIGGERS, J. D., FINN, C. A. & MC, L. A. 1962. Long-term reproductive performance of female mice. II. Variation of litter size with parity. *J Reprod Fertil,* 3**,** 313-30.

BLACKBURN, E. H., GREIDER, C. W. & SZOSTAK, J. W. 2006. Telomeres and telomerase: the path from maize, Tetrahymena and yeast to human cancer and aging. *Nat Med,* 12**,** 1133-8.

BLACKBURN, S. T. 2012. *Maternal, fetal, and neonatal physiology,* Philadelphia, USA, Saunders

BLASCO, M. A. 2007. Telomere length, stem cells and aging. *Nat Chem Biol,* 3**,** 640-9.

BOONEKAMP, J. J., SIMONS, M. J., HEMERIK, L. & VERHULST, S. 2013. Telomere length behaves as biomarker of somatic redundancy rather than biological age. *Aging Cell,* 12**,** 330-2.

BOSSY-WETZEL, E., BARSOUM, M. J., GODZIK, A., SCHWARZENBACHER, R. & LIPTON, S. A. 2003. Mitochondrial fission in apoptosis, neurodegeneration and aging. *Curr Opin Cell Biol,* 15**,** 706-16.

BRAKEL, W. J., RIFE, D. C. & SALISBURY, S. M. 1952. Factors Associated with the Duration of Gestation in Dairy Cattle. *Journal of dairy science,* 35**,** 179-194.

BRODT-EPPLEY, J. & MYATT, L. 1998. Changes in expression of contractile FP and relaxatory EP2 receptors in pregnant rat myometrium during late gestation, at labor, and postpartum. *Biol Reprod,* 59**,** 878-83.
BRODT-EPPLEY, J. & MYATT, L. 1999. Prostaglandin receptors in lower segment myometrium during gestation and labor. *Obstet Gynecol,* 93**,** 89-93.
BRODY, J. R. & CUNHA, G. R. 1989. Histologic, morphometric, and immunocytochemical analysis of myometrial development in rats and mice: I. Normal development. *Am J Anat,* 186**,** 1-20.
BROMBERGER, J. T., MATTHEWS, K. A., KULLER, L. H., WING, R. R., MEILAHN, E. N. & PLANTINGA, P. 1997. Prospective study of the determinants of age at menopause. *Am J Epidemiol,* 145**,** 124-33.
BROSS, T. G., ROGINA, B. & HELFAND, S. L. 2005. Behavioral, physical, and demographic changes in Drosophila populations through dietary restriction. *Aging Cell,* 4**,** 309-17.
BROWN, N., MORROW, J. D., SLAUGHTER, J. C., PARIA, B. C. & REESE, J. 2009. Restoration of on-time embryo implantation corrects the timing of parturition in cytosolic phospholipase A2 group IVA deficient mice. *Biol Reprod,* 81**,** 1131-8.
BUHIMSCHI, I., ALI, M., JAIN, V., CHWALISZ, K. & GARFIELD, R. E. 1996. Differential regulation of nitric oxide in the rat uterus and cervix during pregnancy and labour. *Hum Reprod,* 11**,** 1755-66.
BURGER, H. G., HALE, G. E., DENNERSTEIN, L. & ROBERTSON, D. M. 2008. Cycle and hormone changes during perimenopause: the key role of ovarian function. *Menopause,* 15**,** 603-12.
BURGER, J. M., BUECHEL, S. D. & KAWECKI, T. J. 2010. Dietary restriction affects lifespan but not cognitive aging in Drosophila melanogaster. *Aging Cell,* 9**,** 327-35.
BUSTIN, S. A. 2000. Absolute quantification of mRNA using real-time reverse transcription polymerase chain reaction assays. *J Mol Endocrinol,* 25**,** 169-93.
BUSTIN, S. A., BENES, V., NOLAN, T. & PFAFFL, M. W. 2005. Quantitative real-time RT-PCR--a perspective. *J Mol Endocrinol,* 34**,** 597-601.
BUSTIN, S. A. & NOLAN, T. 2004. Pitfalls of quantitative real-time reverse-transcription polymerase chain reaction. *J Biomol Tech,* 15**,** 155-66.
CALDER, A. A. 1998. Nitric oxide--another factor in cervical ripening. *Hum Reprod,* 13**,** 250-1.
CALIGIONI, C. S. 2009. Assessing reproductive status/stages in mice. *Curr Protoc Neurosci,* Appendix 4**,** Appendix 4I.
CECCHINI, G. 2003. Function and structure of complex II of the respiratory chain. *Annu Rev Biochem,* 72**,** 77-109.
CERQUEIRA, F. M., LAURINDO, F. R. & KOWALTOWSKI, A. J. 2011. Mild mitochondrial uncoupling and calorie restriction increase fasting eNOS, akt and mitochondrial biogenesis. *PLoS One,* 6**,** e18433.
CHALMERS, S. & MCCARRON, J. G. 2008. The mitochondrial membrane potential and Ca2+ oscillations in smooth muscle. *J Cell Sci,* 121**,** 75-85.
CHAN, B. C. & LAO, T. T. 1999. Influence of parity on the obstetric performance of mothers aged 40 years and above. *Hum Reprod,* 14**,** 833-7.
CHAN, B. C. & LAO, T. T. 2008. Effect of parity and advanced maternal age on obstetric outcome. *Int J Gynaecol Obstet,* 102**,** 237-41.
CHAN, D. C. 2006. Mitochondria: dynamic organelles in disease, aging, and development. *Cell,* 125**,** 1241-52.
CHANCE, B., SIES, H. & BOVERIS, A. 1979. Hydroperoxide metabolism in mammalian organs. *Physiol Rev,* 59**,** 527-605.
CHEN, Q., VAZQUEZ, E. J., MOGHADDAS, S., HOPPEL, C. L. & LESNEFSKY, E. J. 2003. Production of reactive oxygen species by mitochondria: central role of complex III. *J Biol Chem,* 278**,** 36027-31.

CHOI, S. J., JUNG, K. L., OH, S. Y., KIM, J. H. & ROH, C. R. 2009. Cervicovaginal matrix metalloproteinase-9 and cervical ripening in human term parturition. *Eur J Obstet Gynecol Reprod Biol,* 142**,** 43-7.

CHOMCZYNSKI, P. & SACCHI, N. 1987. Single-step method of RNA isolation by acid guanidinium thiocyanate-phenol-chloroform extraction. *Anal Biochem,* 162**,** 156-9.

CHOW, L. & LYE, S. J. 1994. Expression of the gap junction protein connexin-43 is increased in the human myometrium toward term and with the onset of labor. *Am J Obstet Gynecol,* 170**,** 788-95.

CHWALISZ, K. & GARFIELD, R. E. 1998. Role of nitric oxide in the uterus and cervix: implications for the management of labor. *J Perinat Med,* 26**,** 448-57.

CLARK, K., JI, H., FELTOVICH, H., JANOWSKI, J., CARROLL, C. & CHIEN, E. K. 2006. Mifepristone-induced cervical ripening: structural, biomechanical, and molecular events. *Am J Obstet Gynecol,* 194**,** 1391-8.

CONDON, J. C., JEYASURIA, P., FAUST, J. M. & MENDELSON, C. R. 2004. Surfactant protein secreted by the maturing mouse fetal lung acts as a hormone that signals the initiation of parturition. *Proc Natl Acad Sci U S A,* 101**,** 4978-83.

COOK, J. L., ZARAGOZA, D. B., SUNG, D. H. & OLSON, D. M. 2000. Expression of myometrial activation and stimulation genes in a mouse model of preterm labor: myometrial activation, stimulation, and preterm labor. *Endocrinology,* 141**,** 1718-28.

COOKSON, V. J. & CHAPMAN, N. R. 2010. NF-kappaB function in the human myometrium during pregnancy and parturition. *Histol Histopathol,* 25**,** 945-56.

COOPER, J. M., MANN, V. M. & SCHAPIRA, A. H. 1992. Analyses of mitochondrial respiratory chain function and mitochondrial DNA deletion in human skeletal muscle: effect of ageing. *J Neurol Sci,* 113**,** 91-8.

CORBI, G., CONTI, V., SCAPAGNINI, G., FILIPPELLI, A. & FERRARA, N. 2012. Role of sirtuins, calorie restriction and physical activity in aging. *Front Biosci (Elite Ed),* 4**,** 768-78.

COX, M. & NELSON, D. L. 2008. *Lehninger Principles of Biochemistry,* New York, W. H. Freeman.

CRITCHLEY H, BENNETT P & S, T. 2004. *Preterm Birth,* London, RCOG Publications.

CSAPO, A. 1956. Progesterone block. *Am J Anat,* 98**,** 273-91.

CSAPO, A. & GOODALL, M. 1954. Excitability, length tension relation and kinetics of uterine muscle contraction in relation to hormonal status. *J Physiol,* 126**,** 384-95.

D'AGOSTINO, R., BELANGER, A., D'AGOSTINO, R JR. 1990. A suggestion for using powerful and informative tests of normality. *The American Statistician*, 44 (4)**,** 316–321.

DAHM, R. 2005. Friedrich Miescher and the discovery of DNA. *Dev Biol,* 278**,** 274-88.

DALTON, D. K., PITTS-MEEK, S., KESHAV, S., FIGARI, I. S., BRADLEY, A. & STEWART, T. A. 1993. Multiple defects of immune cell function in mice with disrupted interferon-gamma genes. *Science,* 259**,** 1739-42.

DAMGAARD, L. H., RYDHMER, L., LOVENDAHL, P. & GRANDINSON, K. 2003. Genetic parameters for within-litter variation in piglet birth weight and change in within-litter variation during suckling. *J Anim Sci,* 81**,** 604-10.

DAVIDSON, S. M. & DUCHEN, M. R. 2007. Endothelial mitochondria: contributing to vascular function and disease. *Circ Res,* 100**,** 1128-41.

DAY, J. R., LAPOLT, P. S. & LU, J. K. 1991. Plasma patterns of prolactin, progesterone, and estradiol during early pregnancy in aging rats: relation to embryonic development. *Biol Reprod,* 44**,** 786-90.

DE LUCA, A., SANTRA, M., BALDI, A., GIORDANO, A. & IOZZO, R. V. 1996. Decorin-induced growth suppression is associated with up-regulation of p21, an inhibitor of cyclin-dependent kinases. *J Biol Chem,* 271**,** 18961-5.

DE VRIES, K., LYONS, E. A., BALLARD, G., LEVI, C. S. & LINDSAY, D. J. 1990. Contractions of the inner third of the myometrium. *Am J Obstet Gynecol,* 162**,** 679-82.

DI, W. L., LACHELIN, G. C., MCGARRIGLE, H. H., THOMAS, N. S. & BECKER, D. L. 2001. Oestriol and oestradiol increase cell to cell communication and connexin43 protein expression in human myometrium. *Mol Hum Reprod,* 7**,** 671-9.

DILLON, P. F. & MURPHY, R. A. 1982. Tonic force maintenance with reduced shortening velocity in arterial smooth muscle. *Am J Physiol,* 242**,** C102-8.

DOHERTY, T. M., KASTELEIN, R., MENON, S., ANDRADE, S. & COFFMAN, R. L. 1993. Modulation of murine macrophage function by IL-13. *J Immunol,* 151**,** 7151-60.

DOMALI, E., ASPRODINI, E., MOLYVDAS, P. A. & MESSINIS, I. E. 2001. In vitro effects of endothelin-1 on the contractility of myometrium obtained from pre- and postmenopausal women. *J Endocrinol,* 168**,** 153-62.

DORING, B., SHYNLOVA, O., TSUI, P., ECKARDT, D., JANSSEN-BIENHOLD, U., HOFMANN, F., FEIL, S., FEIL, R., LYE, S. J. & WILLECKE, K. 2006. Ablation of connexin43 in uterine smooth muscle cells of the mouse causes delayed parturition. *J Cell Sci,* 119**,** 1715-22.

DORMAN, J. B., ALBINDER, B., SHROYER, T. & KENYON, C. 1995. The age-1 and daf-2 genes function in a common pathway to control the lifespan of Caenorhabditis elegans. *Genetics,* 141**,** 1399-406.

DOUGLAS, A. J., CLARKE, E. W. & GOLDSPINK, D. F. 1988. Influence of mechanical stretch on growth and protein turnover of rat uterus. *Am J Physiol,* 254**,** E543-8.

DUBICKE, A., FRANSSON, E., CENTINI, G., ANDERSSON, E., BYSTROM, B., MALMSTROM, A., PETRAGLIA, F., SVERREMARK-EKSTROM, E. & EKMAN-ORDEBERG, G. 2010. Pro-inflammatory and anti-inflammatory cytokines in human preterm and term cervical ripening. *J Reprod Immunol,* 84**,** 176-85.

DUDLEY, D.J. A. & DANGERFIELD, S.S.E. 1996. Interleukin-10 (IL-10) prevents preterm birth in a mouse model of infection-mediated preterm labor. *J. Soc. Gynecol. Investig.* **3**: 67A

DUNLAP, K. A. & STORMSHAK, F. 2004. Nongenomic inhibition of oxytocin binding by progesterone in the ovine uterus. *Biol Reprod,* 70**,** 65-9.

ECKER, J. L., CHEN, K. T., COHEN, A. P., RILEY, L. E. & LIEBERMAN, E. S. 2001. Increased risk of cesarean delivery with advancing maternal age: indications and associated factors in nulliparous women. *Am J Obstet Gynecol,* 185**,** 883-7.

ESSER, K.-H., MARX, W. H. & LISOWSKY, T. 2005. Nucleic acid free matrix: regeneration of DNA binding columns. *BioTechniques,* 39**,** 270–271.

ESWARAN, H., PREISSL, H., WILSON, J. D., MURPHY, P. & LOWERY, C. L. 2004. Prediction of labor in term and preterm pregnancies using non-invasive magnetomyographic recordings of uterine contractions. *Am J Obstet Gynecol,* 190**,** 1598-602; discussion 1602-3.

FABRIZIO, P. & LONGO, V. D. 2007. The chronological life span of Saccharomyces cerevisiae. *Methods Mol Biol,* 371**,** 89-95.

FANG, X., WONG, S. & MITCHELL, B. F. 2002. Messenger RNA for progesterone receptor isoforms in the late-gestation rat uterus. *Am J Physiol Endocrinol Metab,* 283**,** E1167-72.

FATA, J. E., CHAUDHARY, V. & KHOKHA, R. 2001. Cellular turnover in the mammary gland is correlated with systemic levels of progesterone and not 17beta-estradiol during the estrous cycle. *Biol Reprod,* 65**,** 680-8.

FELICIO, L. S., NELSON, J. F. & FINCH, C. E. 1984. Longitudinal studies of estrous cyclicity in aging C57BL/6J mice: II. Cessation of cyclicity and the duration of persistent vaginal cornification. *Biol Reprod,* 31**,** 446-53.

FERNANDEZ-VIZARRA, E., ENRIQUEZ, J. A., PEREZ-MARTOS, A., MONTOYA, J. & FERNANDEZ-SILVA, P. 2011. Tissue-specific differences in mitochondrial activity and biogenesis. *Mitochondrion,* 11**,** 207-13.

FIGUEIREDO, P. A., FERREIRA, R. M., APPELL, H. J. & DUARTE, J. A. 2008. Age-induced morphological, biochemical, and functional alterations in isolated mitochondria from murine skeletal muscle. *J Gerontol A Biol Sci Med Sci,* 63**,** 350-9.

FINLEY, L. W. & HAIGIS, M. C. 2009. The coordination of nuclear and mitochondrial communication during aging and calorie restriction. *Ageing Res Rev,* 8**,** 173-88.

FINN, C. A. 1963. REPRODUCTIVE CAPACITY AND LITTER SIZE IN MICE: EFFECT OF AGE AND ENVIRONMENT. *J Reprod Fertil,* 6**,** 205-14.

FISCHER, D. P., HUTCHINSON, J. A., FARRAR, D., O'DONOVAN, P. J., WOODWARD, D. F. & MARSHALL, K. M. 2008. Loss of prostaglandin F2alpha, but not thromboxane, responsiveness in pregnant human myometrium during labour. *J Endocrinol,* 197**,** 171-9.

FITZGERALD, C., ZIMON, A. E. & JONES, E. E. 1998. Aging and reproductive potential in women. *Yale J Biol Med,* 71**,** 367-81.

FLEIGE, S. & PFAFFL, M. W. 2006. RNA integrity and the effect on the real-time qRT-PCR performance. *Mol Aspects Med,* 27**,** 126-39.

FONTANA, L., PARTRIDGE, L. & LONGO, V. D. 2010. Extending healthy life span--from yeast to humans. *Science,* 328**,** 321-6.

FRANCESCHI, C., CAPRI, M., MONTI, D., GIUNTA, S., OLIVIERI, F., SEVINI, F., PANOURGIA, M. P., INVIDIA, L., CELANI, L., SCURTI, M., CEVENINI, E., CASTELLANI, G. C. & SALVIOLI, S. 2007. Inflammaging and anti-inflammaging: a systemic perspective on aging and longevity emerged from studies in humans. *Mech Ageing Dev,* 128**,** 92-105.

FREETLY, H. C. & LEYMASTER, K. A. 2004. Relationship between litter birth weight and litter size in six breeds of sheep. *J Anim Sci,* 82**,** 612-8.

FREW, L. & STOCK, S. J. 2011. Antimicrobial peptides and pregnancy. *Reproduction,* 141**,** 725-35.

FRIEDMAN, D. B. & JOHNSON, T. E. 1988. A mutation in the age-1 gene in Caenorhabditis elegans lengthens life and reduces hermaphrodite fertility. *Genetics,* 118**,** 75-86.

FROY, O. 2011. Circadian rhythms, aging, and life span in mammals. *Physiology (Bethesda),* 26**,** 225-35.

FUCHS, A. R., FUCHS, F., HUSSLEIN, P. & SOLOFF, M. S. 1984. Oxytocin receptors in the human uterus during pregnancy and parturition. *Am J Obstet Gynecol,* 150**,** 734-41.

FUMAGALLI, M., ROSSIELLO, F., CLERICI, M., BAROZZI, S., CITTARO, D., KAPLUNOV, J. M., BUCCI, G., DOBREVA, M., MATTI, V., BEAUSEJOUR, C. M., HERBIG, U., LONGHESE, M. P. & D'ADDA DI FAGAGNA, F. 2012. Telomeric DNA damage is irreparable and causes persistent DNA-damage-response activation. *Nat Cell Biol,* 14**,** 355-65.

GARFIELD, R. E., SIMS, S. & DANIEL, E. E. 1977. Gap junctions: their presence and necessity in myometrium during parturition. *Science,* 198**,** 958-60.

GEYER, H. & RIEBSCHLÄGER, M. 1974. EFFECT OF PREGNANCY ON CYTOPLASMIC AND MITOCHONDRIAL ENZYMES IN HUMAN AND ANIMAL MYOMETRIUM. *Acta Endocrinologica,* 77**,** 368-379.

GHASEMI, A., ZAHEDIASL, S. 2012. Normality tests for statistical analysis: a guide for non-statisticians. *International journal of endocrinology and metabolism,* 10(2)**,** 486-489.

GILBERT, W. M., NESBITT, T. S. & DANIELSEN, B. 1999. Childbearing beyond age 40: pregnancy outcome in 24,032 cases. *Obstet Gynecol,* 93**,** 9-14.

GINDOFF, P. R. & JEWELEWICZ, R. 1986. Reproductive potential in the older woman. *Fertil Steril,* 46**,** 989-1001.

GIUNTA, S. 2008. Exploring the complex relations between inflammation and aging (inflamm-aging): anti-inflamm-aging remodelling of inflamm- aging, from robustness to frailty. *Inflamm Res,* 57**,** 558-63.

GNAIGER, E. 2011. Mitochondrial Pathways to Complex II, Glycerophosphate Dehydrogenase and ElectronTransferring Flavoprotein. *Mitochondrial Physiology Network* 11.09

GOLD, E. B., CRAWFORD, S. L., AVIS, N. E., CRANDALL, C. J., MATTHEWS, K. A., WAETJEN, L. E., LEE, J. S., THURSTON, R., VUGA, M. & HARLOW, S. D. 2013. Factors Related to Age at Natural Menopause: Longitudinal Analyses From SWAN. *Am J Epidemiol,* 178**,** 70-83.

GOMORI, G. 1950. A rapid one-step trichrome stain. *Am J Clin Pathol,* 20**,** 661-4.

GONCHAROVA, N. D. 2013. Stress responsiveness of the hypothalamic-pituitary-adrenal axis: age-related features of the vasopressinergic regulation. *Front Endocrinol (Lausanne),* 4**,** 26.

GONZALEZ, J. M., DONG, Z., ROMERO, R. & GIRARDI, G. 2011. Cervical remodeling/ripening at term and preterm delivery: the same mechanism initiated by different mediators and different effector cells. *PLoS One,* 6**,** e26877.

GONZALEZ, J. M., XU, H., CHAI, J., OFORI, E. & ELOVITZ, M. A. 2009. Preterm and term cervical ripening in CD1 Mice (Mus musculus): similar or divergent molecular mechanisms? *Biol Reprod,* 81**,** 1226-32.

GORDON, S. 2003. Alternative activation of macrophages. *Nat Rev Immunol,* 3**,** 23-35.

GORDON, S. & MARTINEZ, F. O. 2010. Alternative activation of macrophages: mechanism and functions. *Immunity,* 32**,** 593-604.

GORONZY, J. J. & WEYAND, C. M. 2013. Understanding immunosenescence to improve responses to vaccines. *Nat Immunol,* 14**,** 428-36.

GRAHAM, C. E. 1966. Cyclic changes in the squamo-columnar junction of the mouse cervix uteri. *Anat Rec,* 155**,** 251-60.

GRANSTROM, L., EKMAN, G., ULMSTEN, U. & MALMSTROM, A. 1989. Changes in the connective tissue of corpus and cervix uteri during ripening and labour in term pregnancy. *Br J Obstet Gynaecol,* 96**,** 1198-202.

GRAVINA, F. S., JOBLING, P., KERR, K. P., DE OLIVEIRA, R. B., PARKINGTON, H. C. & VAN HELDEN, D. F. 2011. Oxytocin depolarizes mitochondria in isolated myometrial cells. *Exp Physiol,* 96**,** 949-56.

GRAVINA, F. S., PARKINGTON, H. C., KERR, K. P., DE OLIVEIRA, R. B., JOBLING, P., COLEMAN, H. A., SANDOW, S. L., DAVIES, M. M., IMTIAZ, M. S. & VAN HELDEN, D. F. 2010. Role of mitochondria in contraction and pacemaking in the mouse uterus. *Br J Pharmacol,* 161**,** 1375-90.

GREENBERG, M. B., CHENG, Y. W., SULLIVAN, M., NORTON, M. E., HOPKINS, L. M. & CAUGHEY, A. B. 2007. Does length of labor vary by maternal age? *Am J Obstet Gynecol,* 197**,** 428 e1-7.

GUALDONI, G. A., KOVARIK, J. J., HOFER, J., DOSE, F., DOBERER, D., STEINBERGER, P., WOLZT, M. & ZLABINGER, G. J. 2013. Resveratrol enhances TNF-alpha production in human monocytes upon bacterial stimulation. *Biochim Biophys Acta*.

HAAVALDSEN, C., SARFRAZ, A. A., SAMUELSEN, S. O. & ESKILD, A. 2010. The impact of maternal age on fetal death: does length of gestation matter? *Am J Obstet Gynecol,* 203**,** 554 e1-8.
HARKNESS, M. L. & HARKNESS, R. D. 1959. Changes in the physical properties of the uterine cervix of the rat during pregnancy. *J Physiol,* 148**,** 524-47.
HARMAN, D. 1956. Aging: a theory based on free radical and radiation chemistry. *J Gerontol,* 11**,** 298-300.
HARMAN, D. 1972. The biologic clock: the mitochondria? *J Am Geriatr Soc,* 20**,** 145-7.
HARMAN, S. M. & TALBERT, G. B. 1970. The effect of maternal age on ovulation, corpora lutea of pregnancy, and implantation failure in mice. *J Reprod Fertil,* 23**,** 33-9.
HARPER, J. M., LEATHERS, C. W. & AUSTAD, S. N. 2006. Does caloric restriction extend life in wild mice? *Aging Cell,* 5**,** 441-9.
HARPER, M. E., MONEMDJOU, S., RAMSEY, J. J. & WEINDRUCH, R. 1998. Age-related increase in mitochondrial proton leak and decrease in ATP turnover reactions in mouse hepatocytes. *Am J Physiol,* 275**,** E197-206.
HARRISON, D. E., STRONG, R., SHARP, Z. D., NELSON, J. F., ASTLE, C. M., FLURKEY, K., NADON, N. L., WILKINSON, J. E., FRENKEL, K., CARTER, C. S., PAHOR, M., JAVORS, M. A., FERNANDEZ, E. & MILLER, R. A. 2009. Rapamycin fed late in life extends lifespan in genetically heterogeneous mice. *Nature,* 460**,** 392-5.
HASSAN, S. S., ROMERO, R., TARCA, A. L., NHAN-CHANG, C. L., VAISBUCH, E., EREZ, O., MITTAL, P., KUSANOVIC, J. P., MAZAKI-TOVI, S., YEO, L., DRAGHICI, S., KIM, J. S., ULDBJERG, N. & KIM, C. J. 2009. The transcriptome of cervical ripening in human pregnancy before the onset of labor at term: identification of novel molecular functions involved in this process. *J Matern Fetal Neonatal Med,* 22**,** 1183-93.
HATEFI, Y. & STIGGALL, D. L. 1978. Preparation and properties of NADH: cytochrome c oxidoreductase (complex I--III). *Methods Enzymol,* 53**,** 5-10.
HAVELOCK, J. C., KELLER, P., MULEBA, N., MAYHEW, B. A., CASEY, B. M., RAINEY, W. E. & WORD, R. A. 2005. Human myometrial gene expression before and during parturition. *Biol Reprod,* 72**,** 707-19.
HAYFLICK, L. & MOORHEAD, P. S. 1961. The serial cultivation of human diploid cell strains. *Exp Cell Res,* 25**,** 585-621.
HEFFNER, L. J. 2004. Advanced maternal age--how old is too old? *N Engl J Med,* 351**,** 1927-9.
HEGAR, A. E. L. 1985. Diagnose der fru¨hesten Schwangerschaftsperiode (German article). *Deutsche Medizinische Wochenschrift,* 21**,** 565–567.
HEKIMI, S., LAPOINTE, J. & WEN, Y. 2011. Taking a "good" look at free radicals in the aging process. *Trends Cell Biol,* 21**,** 569-76.
HERLIHY, J. T. & MURPHY, R. A. 1973. Length-tension relationship of smooth muscle of the hog carotid artery. *Circ Res,* 33**,** 275-83.
HERRERA, E., SAMPER, E., MARTIN-CABALLERO, J., FLORES, J. M., LEE, H. W. & BLASCO, M. A. 1999. Disease states associated with telomerase deficiency appear earlier in mice with short telomeres. *EMBO J,* 18**,** 2950-60.
HIGUCHI, R., FOCKLER, C., DOLLINGER, G. & WATSON, R. 1993. Kinetic PCR analysis: real-time monitoring of DNA amplification reactions. *Biotechnology (N Y),* 11**,** 1026-30.
HILL, A. V. 1953. The mechanics of active muscle. *Proc R Soc Lond B Biol Sci,* 141**,** 104-17.
HILLIER, K. & WALLIS, R. M. 1982. Collagen solubility and tensile properties of the rat uterine cervix in late pregnancy: effects of arachidonic acid and prostaglandin F 2 alpha. *J Endocrinol,* 95**,** 341-7.

HIRSCH, E., FILIPOVICH, Y. & MAHENDROO, M. 2006. Signaling via the type I IL-1 and TNF receptors is necessary for bacterially induced preterm labor in a murine model. *Am J Obstet Gynecol,* 194**,** 1334-40.
HOCK, M. B. & KRALLI, A. 2009. Transcriptional control of mitochondrial biogenesis and function. *Annu Rev Physiol,* 71**,** 177-203.
HOEIJMAKERS, J. H. 2009. DNA damage, aging, and cancer. *N Engl J Med,* 361**,** 1475-85.
HOLINKA, C. F. & FINCH, C. E. 1977. Age-related changes in the decidual response of the C57BL/6J mouse uterus. *Biol Reprod,* 16**,** 385-93.
HOLINKA, C. F., TSENG, Y. C. & FINCH, C. E. 1978. Prolonged gestation, elevated preparturitional plasma progesterone and reproductive aging in C57BL/6J mice. *Biol Reprod,* 19**,** 807-16.
HOLINKA, C. F., TSENG, Y. C. & FINCH, C. E. 1979. Reproductive aging in C57BL/6J mice: plasma progesterone, viable embryos and resorption frequency throughout pregnancy. *Biol Reprod,* 20**,** 1201-11.
HOLLOSZY, J. O., OSCAI, L. B., DON, I. J. & MOLE, P. A. 1970. Mitochondrial citric acid cycle and related enzymes: adaptive response to exercise. *Biochem Biophys Res Commun,* 40**,** 1368-73.
HOLT, R., TIMMONS, B. C., AKGUL, Y., AKINS, M. L. & MAHENDROO, M. 2011. The molecular mechanisms of cervical ripening differ between term and preterm birth. *Endocrinology,* 152**,** 1036-46.
HOOD, D. A., ZAK, R. & PETTE, D. 1989. Chronic stimulation of rat skeletal muscle induces coordinate increases in mitochondrial and nuclear mRNAs of cytochrome-c-oxidase subunits. *Eur J Biochem,* 179**,** 275-80.
HORIO, Y., HAYASHI, T., KUNO, A. & KUNIMOTO, R. 2011. Cellular and molecular effects of sirtuins in health and disease. *Clin Sci (Lond),* 121**,** 191-203.
HOUSE, M., KAPLAN, D. L. & SOCRATE, S. 2009. Relationships between mechanical properties and extracellular matrix constituents of the cervical stroma during pregnancy. *Semin Perinatol,* 33**,** 300-7.
HOVLAND, A. R., POWELL, R. L., TAKIMOTO, G. S., TUNG, L. & HORWITZ, K. B. 1998. An N-terminal inhibitory function, IF, suppresses transcription by the A-isoform but not the B-isoform of human progesterone receptors. *J Biol Chem,* 273**,** 5455-60.
HUANG, H. & MANTON, K. G. 2004. The role of oxidative damage in mitochondria during aging: a review. *Front Biosci,* 9**,** 1100-17.
HUMAN FERTILISATION AND EMBRYOLOGY AUTHORITY, 2011. Fertility Treatment in 2011. Available: http://www.hfea.gov.uk/docs/HFEA_Fertility_Trends_and_Figures_2011_-_Annual_Register_Report.pdf;
HUTTER, E., RENNER, K., PFISTER, G., STOCKL, P., JANSEN-DURR, P. & GNAIGER, E. 2004. Senescence-associated changes in respiration and oxidative phosphorylation in primary human fibroblasts. *Biochem J,* 380**,** 919-28.
ISHIKAWA, H., SEKI, R., YOKONISHI, S., YAMAUCHI, T. & YOKOYAMA, K. 2006. Relationship between fetal weight, placental growth and litter size in mice from mid- to late-gestation. *Reproductive Toxicology,* 21**,** 267-270.
ISLAM, K. N. & MENDELSON, C. R. 2002. Potential role of nuclear factor kappaB and reactive oxygen species in cAMP and cytokine regulation of surfactant protein-A gene expression in lung type II cells. *Mol Endocrinol,* 16**,** 1428-40.
IVANOVA, D. G. & YANKOVA, T. M. 2013. The free radical theory of aging in search of a strategy for increasing life span. *Folia Med (Plovdiv),* 55**,** 33-41.
JAHROMI, B. N. & HUSSEINI, Z. 2008. Pregnancy outcome at maternal age 40 and older. *Taiwan J Obstet Gynecol,* 47**,** 318-21.

JASKELIOFF, M., MULLER, F. L., PAIK, J. H., THOMAS, E., JIANG, S., ADAMS, A. C., SAHIN, E., KOST-ALIMOVA, M., PROTOPOPOV, A., CADINANOS, J., HORNER, J. W., MARATOS-FLIER, E. & DEPINHO, R. A. 2011. Telomerase reactivation reverses tissue degeneration in aged telomerase-deficient mice. *Nature,* 469**,** 102-6.

JEFFERIES, J. 2008. Fertility assumptions for the 2006-based national population projections. *Popul Trends***,** 19-27.

JIA, K., CHEN, D. & RIDDLE, D. L. 2004. The TOR pathway interacts with the insulin signaling pathway to regulate C. elegans larval development, metabolism and life span. *Development,* 131**,** 3897-906.

JOHNSON, D. T., HARRIS, R. A., FRENCH, S., BLAIR, P. V., YOU, J., BEMIS, K. G., WANG, M. & BALABAN, R. S. 2007. Tissue heterogeneity of the mammalian mitochondrial proteome. *Am J Physiol Cell Physiol,* 292**,** C689-97.

JOHNSON, S. C., RABINOVITCH, P. S. & KAEBERLEIN, M. 2013. mTOR is a key modulator of ageing and age-related disease. *Nature,* 493**,** 338-45.

JOLLY, M., SEBIRE, N., HARRIS, J., ROBINSON, S. & REGAN, L. 2000. The risks associated with pregnancy in women aged 35 years or older. *Human Reproduction,* 15**,** 2433-2437.

JUNQUEIRA, L. C., ZUGAIB, M., MONTES, G. S., TOLEDO, O. M., KRISZTAN, R. M. & SHIGIHARA, K. M. 1980. Morphologic and histochemical evidence for the occurrence of collagenolysis and for the role of neutrophilic polymorphonuclear leukocytes during cervical dilation. *Am J Obstet Gynecol,* 138**,** 273-81.

KAEBERLEIN, M., MCVEY, M. & GUARENTE, L. 1999. The SIR2/3/4 complex and SIR2 alone promote longevity in Saccharomyces cerevisiae by two different mechanisms. *Genes Dev,* 13**,** 2570-80.

KALETTA, T. & HENGARTNER, M. O. 2006. Finding function in novel targets: C. elegans as a model organism. *Nat Rev Drug Discov,* 5**,** 387-98.

KAMEL, R. M. 2010. The onset of human parturition. *Arch Gynecol Obstet,* 281**,** 975-82.

KANEKO, Y., KAWARABAYASHI, T., SUGIMORI, H. & TSUKAMOTO, T. 1995. Changes in kinetic properties of oxytocin receptors in longitudinal muscle membranes of rat uterus during gestation. *J Mol Recognit,* 8**,** 179-83.

KAPAHI, P., ZID, B. M., HARPER, T., KOSLOVER, D., SAPIN, V. & BENZER, S. 2004. Regulation of lifespan in Drosophila by modulation of genes in the TOR signaling pathway. *Curr Biol,* 14**,** 885-90.

KARABULUT, A., OZKAN, S., BOZKURT, A. I., KARAHAN, T. & KAYAN, S. 2013. Perinatal outcomes and risk factors in adolescent and advanced age pregnancies: comparison with normal reproductive age women. *J Obstet Gynaecol,* 33**,** 346-50.

KELLY, B. A., BOND, B. C. & POSTON, L. 2004. Aortic adaptation to pregnancy: elevated expression of matrix metalloproteinases-2 and -3 in rat gestation. *Mol Hum Reprod,* 10**,** 331-7.

KEMNITZ, J. W. 2011. Calorie restriction and aging in nonhuman primates. *ILAR J,* 52**,** 66-77.

KENNY, L. C., LAVENDER, T., MCNAMEE, R., O'NEILL, S. M., MILLS, T. & KHASHAN, A. S. 2013. Advanced maternal age and adverse pregnancy outcome: evidence from a large contemporary cohort. *PLoS One,* 8**,** e56583.

KERMATH, B. A. & GORE, A. C. 2012. Neuroendocrine control of the transition to reproductive senescence: lessons learned from the female rodent model. *Neuroendocrinology,* 96**,** 1-12.

KHALIL, A., SYNGELAKI, A., MAIZ, N., ZINEVICH, Y. & NICOLAIDES, K. H. 2013. Maternal age and adverse pregnancy outcomes: a cohort study. *Ultrasound Obstet Gynecol*.

KHAN-DAWOOD, F. S. 1987. In vitro conversion of pregnenolone to progesterone in human term placenta and fetal membranes before and after onset of labor. *Am J Obstet Gynecol,* 157**,** 1333-7.

KHAN, R. N., MATHAROO-BALL, B., ARULKUMARAN, S. & ASHFORD, M. L. 2001. Potassium channels in the human myometrium. *Exp Physiol,* 86**,** 255-64.

KHANJANI, S., KANDOLA, M. K., LINDSTROM, T. M., SOORANNA, S. R., MELCHIONDA, M., LEE, Y. S., TERZIDOU, V., JOHNSON, M. R. & BENNETT, P. R. 2011. NF-kappaB regulates a cassette of immune/inflammatory genes in human pregnant myometrium at term. *J Cell Mol Med,* 15**,** 809-24.

KIMURA, T., OGITA, K., KUMASAWA, K., TOMIMATSU, T. & TSUTSUI, T. 2013. Molecular analysis of parturition via oxytocin receptor expression. *Taiwan J Obstet Gynecol,* 52**,** 165-70.

KIRICHOK, Y., KRAPIVINSKY, G. & CLAPHAM, D. E. 2004. The mitochondrial calcium uniporter is a highly selective ion channel. *Nature,* 427**,** 360-4.

KIRZ, D. S., DORCHESTER, W. & FREEMAN, R. K. 1985. Advanced maternal age: the mature gravida. *Am J Obstet Gynecol,* 152**,** 7-12.

KLASS, M. R. 1977. Aging in the nematode Caenorhabditis elegans: major biological and environmental factors influencing life span. *Mech Ageing Dev,* 6**,** 413-29.

KLEISSL, H. P., VAN DER REST, M., NAFTOLIN, F., GLORIEUX, F. H. & DE LEON, A. 1978. Collagen changes in the human uterine cervix at parturition. *Am J Obstet Gynecol,* 130**,** 748-53.

KNOCK, G. A., TRIBE, R. M., HASSONI, A. A. & AARONSON, P. I. 2001. Modulation of potassium current characteristics in human myometrial smooth muscle by 17beta-estradiol and progesterone. *Biol Reprod,* 64**,** 1526-34.

KOKENYESI, R., ARMSTRONG, L. C., AGAH, A., ARTAL, R. & BORNSTEIN, P. 2004. Thrombospondin 2 deficiency in pregnant mice results in premature softening of the uterine cervix. *Biol Reprod,* 70**,** 385-90.

KONG, S., ZHANG, S., CHEN, Y., WANG, W., WANG, B., CHEN, Q., DUAN, E. & WANG, H. 2012. Determinants of uterine aging: lessons from rodent models. *Sci China Life Sci,* 55**,** 687-93.

KORFHAGEN, T. R., BRUNO, M. D., GLASSER, S. W., CIRAOLO, P. J., WHITSETT, J. A., LATTIER, D. L., WIKENHEISER, K. A. & CLARK, J. C. 1992. Murine pulmonary surfactant SP-A gene: cloning, sequence, and transcriptional activity. *Am J Physiol,* 263**,** L546-54.

KOTA, S. K., GAYATRI, K., JAMMULA, S., KOTA, S. K., KRISHNA, S. V., MEHER, L. K. & MODI, K. D. 2013. Endocrinology of parturition. *Indian J Endocrinol Metab,* 17**,** 50-9.

KRAHENBUHL, S., TALOS, C., WIESMANN, U. & HOPPEL, C. L. 1994. Development and evaluation of a spectrophotometric assay for complex III in isolated mitochondria, tissues and fibroblasts from rats and humans. *Clin Chim Acta,* 230**,** 177-87.

KROC, R. L., STEINETZ, B. G. & BEACH, V. L. 1959. The effects of estrogens, progestagens, and relaxin in pregnant and nonpregnant laboratory rodents. *Ann N Y Acad Sci,* 75**,** 942-80.

KUKAT, C., WURM, C. A., SPAHR, H., FALKENBERG, M., LARSSON, N. G. & JAKOBS, S. 2011. Super-resolution microscopy reveals that mammalian mitochondrial nucleoids have a uniform size and frequently contain a single copy of mtDNA. *Proc Natl Acad Sci U S A,* 108**,** 13534-9.

KUMARAN, S., PANNEERSELVAM, K. S., SHILA, S., SIVARAJAN, K. & PANNEERSELVAM, C. 2005. Age-associated deficit of mitochondrial oxidative phosphorylation in skeletal muscle: role of carnitine and lipoic acid. *Mol Cell Biochem,* 280**,** 83-9.

KUNZ, G. & LEYENDECKER, G. 2002. Uterine peristaltic activity during the menstrual cycle: characterization, regulation, function and dysfunction. *Reprod Biomed Online,* 4 Suppl 3**,** 5-9.

KUZNETSOV, A. V. & GNAIGER, E. 2010. Laboratory Protocol Complex I (NADH:Ubiquinone Oxidoreductase; EC 1.6.5.3) Mitochondrial Membrane Enzyme. *08.15***,** 1-8.

KUZNETSOV, A. V., LASSNIG, B. & GNAIGER, E. 2010. Laboratory Protocol Citrate Synthase Mitochondrial Marker Enzyme. *Mitochondrial Physiology Network,* 08.14**,** 1-10.

KUZNETSOV, A. V., STROBL, D., RUTTMANN, E., KONIGSRAINER, A., MARGREITER, R. & GNAIGER, E. 2002. Evaluation of mitochondrial respiratory function in small biopsies of liver. *Anal Biochem,* 305**,** 186-94.

KWONG, L. K. & SOHAL, R. S. 2000. Age-related changes in activities of mitochondrial electron transport complexes in various tissues of the mouse. *Arch Biochem Biophys,* 373**,** 16-22.

LABRIE, F. 2010. DHEA, important source of sex steroids in men and even more in women. *Prog Brain Res,* 182**,** 97-148.

LAGOUGE, M. & LARSSON, N. G. 2013. The role of mitochondrial DNA mutations and free radicals in disease and ageing. *J Intern Med,* 273**,** 529-43.

LAMBERT, R. 2009. *Breeding Strategies for Maintaining Colonies of Laboratory Mice* [Online]. USA: The Jackson Laboratory Available: http://jaxmice.jax.org/manual/breeding_strategies_manual.pdf

LAPLANTE, M. & SABATINI, D. M. 2012. mTOR Signaling. *Cold Spring Harb Perspect Biol,* 4.

LAPPAS, M. & RICE, G. E. 2007. The role and regulation of the nuclear factor kappa B signalling pathway in human labour. *Placenta,* 28**,** 543-56.

LARSSON, N. G. 2010. Somatic mitochondrial DNA mutations in mammalian aging. *Annu Rev Biochem,* 79**,** 683-706.

LAWLER, D. F., LARSON, B. T., BALLAM, J. M., SMITH, G. K., BIERY, D. N., EVANS, R. H., GREELEY, E. H., SEGRE, M., STOWE, H. D. & KEALY, R. D. 2008. Diet restriction and ageing in the dog: major observations over two decades. *Br J Nutr,* 99**,** 793-805.

LEDINGHAM, M. A., THOMSON, A. J., YOUNG, A., MACARA, L. M., GREER, I. A. & NORMAN, J. E. 2000. Changes in the expression of nitric oxide synthase in the human uterine cervix during pregnancy and parturition. *Mol Hum Reprod,* 6**,** 1041-8.

LEE, H. C. & WEI, Y. H. 2007. Oxidative stress, mitochondrial DNA mutation, and apoptosis in aging. *Exp Biol Med (Maywood),* 232**,** 592-606.

LEE, S. E., ROMERO, R., PARK, I. S., SEONG, H. S., PARK, C. W. & YOON, B. H. 2008. Amniotic fluid prostaglandin concentrations increase before the onset of spontaneous labor at term. *J Matern Fetal Neonatal Med,* 21**,** 89-94.

LEFEBVRE, D. L., PIERSANTI, M., BAI, X. H., CHEN, Z. Q. & LYE, S. J. 1995. Myometrial transcriptional regulation of the gap junction gene, connexin-43. *Reprod Fertil Dev,* 7**,** 603-11.

LEHMAN, J. J., BARGER, P. M., KOVACS, A., SAFFITZ, J. E., MEDEIROS, D. M. & KELLY, D. P. 2000. Peroxisome proliferator-activated receptor gamma coactivator-1 promotes cardiac mitochondrial biogenesis. *J Clin Invest,* 106**,** 847-56.

LEPPERT, P. C. 1995. Anatomy and physiology of cervical ripening. *Clin Obstet Gynecol,* 38**,** 267-79.

LEPPERT, P. C., CERRETA, J. M. & MANDL, I. 1986. Orientation of elastic fibers in the human cervix. *Am J Obstet Gynecol,* 155**,** 219-24.

LEPPERT, P. C., KELLER, S., CERRETA, J., HOSANNAH, Y. & MANDL, I. 1983. The content of elastin in the uterine cervix. *Arch Biochem Biophys,* 222**,** 53-8.

LEPPERT, P. C. & YU, S. Y. 1994. Apoptosis in the cervix of pregnant rats in association with cervical softening. *Gynecol Obstet Invest,* 37**,** 150-4.
LEPPERT, P. C., YU, S. Y., KELLER, S., CERRETA, J. & MANDL, I. 1987. Decreased elastic fibers and desmosine content in incompetent cervix. *Am J Obstet Gynecol,* 157**,** 1134-9.
LEPPI, T. J. 1964. A study of the uterine cervix of the mouse. *The Anatomical Record,* 150**,** 51-65.
LIEDMAN, R., HANSSON, S. R., IGIDBASHIAN, S. & AKERLUND, M. 2009. Myometrial oxytocin receptor mRNA concentrations at preterm and term delivery - the influence of external oxytocin. *Gynecol Endocrinol,* 25**,** 188-93.
LIGGINS, G. C. 1978. Ripening of the cervix. *Semin Perinatol,* 2**,** 261-71.
LIGGINS, G. C., FAIRCLOUGH, R. J., GRIEVES, S. A., KENDALL, J. Z. & KNOX, B. S. 1973. The mechanism of initiation of parturition in the ewe. *Recent Prog Horm Res,* 29**,** 111-59.
LILLIE, R. 1940. Further experiments with the Masson trichrome modification of Mallory's connective tissue stain. *Stain Technology,* 15.
LIN, A. T., HSU, T. H., YANG, C. & CHANG, L. S. 2000. Effects of aging on mitochondrial enzyme activity of rat urinary bladder. *Urol Int,* 65**,** 144-7.
LINDSTROM, T. & BENNETT, P. 2004. Transcriptional regulation of genes for enzymes of the prostaglandin biosynthetic pathway. *Prostaglandins Leukot Essent Fatty Acids,* 70**,** 115-35.
LINFORD, N. J., SCHRINER, S. E. & RABINOVITCH, P. S. 2006. Oxidative damage and aging: spotlight on mitochondria. *Cancer Res,* 66**,** 2497-9.
LIU, M., YIN, Y., YE, X., ZENG, M., ZHAO, Q., KEEFE, D. L. & LIU, L. 2013. Resveratrol protects against age-associated infertility in mice. *Hum Reprod,* 28**,** 707-17.
LOPES, F. L., FORTIER, A. L., DARRICARRERE, N., CHAN, D., ARNOLD, D. R. & TRASLER, J. M. 2009. Reproductive and epigenetic outcomes associated with aging mouse oocytes. *Hum Mol Genet,* 18**,** 2032-44.
LÓPEZ-OTÍN, C., BLASCO, M. A., PARTRIDGE, L., SERRANO, M. & KROEMER, G. 2013. The Hallmarks of Aging. *Cell,* 153**,** 1194-1217.
LOPEZ BERNAL, A. 2003. Mechanisms of labour--biochemical aspects. *BJOG,* 110 Suppl 20**,** 39-45.
LOPEZ BERNAL, A., NEWMAN, G. E., PHIZACKERLEY, P. J. & TURNBULL, A. C. 1988. Surfactant stimulates prostaglandin E production in human amnion. *Br J Obstet Gynaecol,* 95**,** 1013-7.
LORD, C. J. & ASHWORTH, A. 2012. The DNA damage response and cancer therapy. *Nature,* 481**,** 287-94.
LUDFORD, I., SCHEIL, W., TUCKER, G. & GRIVELL, R. 2012. Pregnancy outcomes for nulliparous women of advanced maternal age in South Australia, 1998-2008. *Aust N Z J Obstet Gynaecol,* 52**,** 235-41.
LUDMIR, J. & SEHDEV, H. M. 2000. Anatomy and physiology of the uterine cervix. *Clin Obstet Gynecol,* 43**,** 433-9.
LYALL, F., LYE, S., TEOH, T., COUSINS, F., MILLIGAN, G. & ROBSON, S. 2002. Expression of Gsalpha, connexin-43, connexin-26, and EP1, 3, and 4 receptors in myometrium of prelabor singleton versus multiple gestations and the effects of mechanical stretch and steroids on Gsalpha. *J Soc Gynecol Investig,* 9**,** 299-307.
MAGGI, M., GENAZZANI, A. D., GIANNINI, S., TORRISI, C., BALDI, E., DI TOMASO, M., MUNSON, P. J., RODBARD, D. & SERIO, M. 1988. Vasopressin and oxytocin receptors in vagina, myometrium, and oviduct of rabbits. *Endocrinology,* 122**,** 2970-80.

MAHENDROO, M. 2012. Cervical remodeling in term and preterm birth: insights from an animal model. *Reproduction,* 143**,** 429-38.
MAIN, D. M., MAIN, E. K. & MOORE, D. H., 2ND 2000. The relationship between maternal age and uterine dysfunction: a continuous effect throughout reproductive life. *Am J Obstet Gynecol,* 182**,** 1312-20.
MALIK, A. N. & CZAJKA, A. 2012. Is mitochondrial DNA content a potential biomarker of mitochondrial dysfunction? *Mitochondrion*.
MALIK, A. N., SHAHNI, R., RODRIGUEZ-DE-LEDESMA, A., LAFTAH, A. & CUNNINGHAM, P. 2011. Mitochondrial DNA as a non-invasive biomarker: accurate quantification using real time quantitative PCR without co-amplification of pseudogenes and dilution bias. *Biochem Biophys Res Commun,* 412**,** 1-7.
MANCHESTER, K. L. 1995. Value of A260/A280 ratios for measurement of purity of nucleic acids. *Biotechniques,* 19**,** 208-10.
MANCHESTER, K. L. 1996. Use of UV methods for measurement of protein and nucleic acid concentrations. *Biotechniques,* 20**,** 968-70.
MAPLE-BROWN, L. J., ROMAN, N. M., THOMAS, A., PRESLEY, L. H. & CATALANO, P. M. 2013. Perinatal factors relating to changes in maternal body fat in late gestation. *J Perinatol*.
MARIJIC, J., LI, Q., SONG, M., NISHIMARU, K., STEFANI, E. & TORO, L. 2001. Decreased expression of voltage- and Ca(2+)-activated K(+) channels in coronary smooth muscle during aging. *Circ Res,* 88**,** 210-6.
MARIN-GARCIA, J., ANANTHAKRISHNAN, R. & GOLDENTHAL, M. J. 1998. Human mitochondrial function during cardiac growth and development. *Mol Cell Biochem,* 179**,** 21-6.
MARKOVIC, D., VATISH, M., GU, M., SLATER, D., NEWTON, R., LEHNERT, H. & GRAMMATOPOULOS, D. K. 2007. The onset of labor alters corticotropin-releasing hormone type 1 receptor variant expression in human myometrium: putative role of interleukin-1beta. *Endocrinology,* 148**,** 3205-13.
MARTON, O., KOLTAI, E., NYAKAS, C., BAKONYI, T., ZENTENO-SAVIN, T., KUMAGAI, S., GOTO, S. & RADAK, Z. 2010. Aging and exercise affect the level of protein acetylation and SIRT1 activity in cerebellum of male rats. *Biogerontology,* 11**,** 679-86.
MATTHEW, A., SHMYGOL, A. & WRAY, S. 2004. Ca2+ entry, efflux and release in smooth muscle. *Biol Res,* 37**,** 617-24.
MATTHEWS, J. N., ALTMAN, D. G., CAMPBELL, M. J. & ROYSTON, P. 1990. Analysis of serial measurements in medical research. *BMJ,* 300**,** 230-5.
MATTISON, J. A., ROTH, G. S., BEASLEY, T. M., TILMONT, E. M., HANDY, A. M., HERBERT, R. L., LONGO, D. L., ALLISON, D. B., YOUNG, J. E., BRYANT, M., BARNARD, D., WARD, W. F., QI, W., INGRAM, D. K. & DE CABO, R. 2012. Impact of caloric restriction on health and survival in rhesus monkeys from the NIA study. *Nature,* 489**,** 318-21.
MAUL, H., MACKAY, L. & GARFIELD, R. E. 2006. Cervical ripening: biochemical, molecular, and clinical considerations. *Clin Obstet Gynecol,* 49**,** 551-63.
MBUGUA GITAU, G., LIVERSEDGE, H., GOFFEY, D., HAWTON, A., LIVERSEDGE, N. & TAYLOR, M. 2009. The influence of maternal age on the outcomes of pregnancies complicated by bleeding at less than 12 weeks. *Acta Obstet Gynecol Scand,* 88**,** 116-8.
MCCAY, C. M., CROWELL, M. F. & MAYNARD, L. A. 1989. The effect of retarded growth upon the length of life span and upon the ultimate body size. 1935. *Nutrition,* 5**,** 155-71; discussion 172.
MCCORD, J. M. & FRIDOVICH, I. 1969. Superoxide dismutase. An enzymic function for erythrocuprein (hemocuprein). *J Biol Chem,* 244**,** 6049-55.

MCLAREN, A. & MICHIE, D. 1963. Nature of the systemic effect of litter size on gestation period in mice *J Reprod Fertil,* 6**,** 139-41.
MEIJBOOM, L. J., DRENTHEN, W., PIEPER, P. G., GROENINK, M., VAN DER POST, J. A., TIMMERMANS, J., VOORS, A. A., ROOS-HESSELINK, J. W., VAN VELDHUISEN, D. J. & MULDER, B. J. 2006. Obstetric complications in Marfan syndrome. *Int J Cardiol,* 110**,** 53-9.
MELAMED, N., BEN-HAROUSH, A., KREMER, S., HOD, M. & YOGEV, Y. 2010. Failure of cervical ripening with prostaglandin-E2 can it be predicted? *J Matern Fetal Neonatal Med,* 23**,** 536-40.
MENDELSON, C. R. 2009. Minireview: fetal-maternal hormonal signaling in pregnancy and labor. *Mol Endocrinol,* 23**,** 947-54.
MENDELSON, C. R. & CONDON, J. C. 2005. New insights into the molecular endocrinology of parturition. *J Steroid Biochem Mol Biol,* 93**,** 113-9.
MERLINO, A. A., WELSH, T. N., TAN, H., YI, L. J., CANNON, V., MERCER, B. M. & MESIANO, S. 2007. Nuclear progesterone receptors in the human pregnancy myometrium: evidence that parturition involves functional progesterone withdrawal mediated by increased expression of progesterone receptor-A. *J Clin Endocrinol Metab,* 92**,** 1927-33.
MESIANO, S., CHAN, E. C., FITTER, J. T., KWEK, K., YEO, G. & SMITH, R. 2002. Progesterone withdrawal and estrogen activation in human parturition are coordinated by progesterone receptor A expression in the myometrium. *J Clin Endocrinol Metab,* 87**,** 2924-30.
MESIANO, S., WANG, Y. & NORWITZ, E. R. 2011. Progesterone receptors in the human pregnancy uterus: do they hold the key to birth timing? *Reprod Sci,* 18**,** 6-19.
MICHEL, S., WANET, A., DE PAUW, A., ROMMELAERE, G., ARNOULD, T. & RENARD, P. 2012. Crosstalk between mitochondrial (dys)function and mitochondrial abundance. *J Cell Physiol,* 227**,** 2297-310.
MIDWOOD, K. S., WILLIAMS, L. V. & SCHWARZBAUER, J. E. 2004. Tissue repair and the dynamics of the extracellular matrix. *Int J Biochem Cell Biol,* 36**,** 1031-7.
MIESSEN, K., EINSPANIER, R. & SCHOEN, J. 2012. Establishment and characterization of a differentiated epithelial cell culture model derived from the porcine cervix uteri. *BMC Vet Res,* 8**,** 31.
MIHM, M., GANGOOLY, S. & MUTTUKRISHNA, S. 2011. The normal menstrual cycle in women. *Anim Reprod Sci,* 124**,** 229-36.
MINAMOTO, T., ARAI, K., HIRAKAWA, S. & NAGAI, Y. 1987. Immunohistochemical studies on collagen types in the uterine cervix in pregnant and nonpregnant states. *Am J Obstet Gynecol,* 156**,** 138-44.
MITCHELL, B. F., CHALLIS, J. R. & LUKASH, L. 1987. Progesterone synthesis by human amnion, chorion, and decidua at term. *Am J Obstet Gynecol,* 157**,** 349-53.
MITCHELL, B. F. & TAGGART, M. J. 2009. Are animal models relevant to key aspects of human parturition? *Am J Physiol Regul Integr Comp Physiol,* 297**,** R525-45.
MITCHELL, P. 1961. Coupling of phosphorylation to electron and hydrogen transfer by a chemi-osmotic type of mechanism. *Nature,* 191**,** 144-8.
MONCLUS, R., TIULIM, J. & BLUMSTEIN, D. T. 2011. Older mothers follow conservative strategies under predator pressure: the adaptive role of maternal glucocorticoids in yellow-bellied marmots. *Horm Behav,* 60**,** 660-5.
MOORE, F. & BERNAL, A. L. 2001. Myosin light chain kinase and the onset of labour in humans. *Exp Physiol,* 86**,** 313-8.
MOORE, H. C. 1963. Intra-uterine foetal death during prolonged pregnancy in rats receiving progesterone: the effect of ovariectomy and oestrogens. *BJOG: An International Journal of Obstetrics & Gynaecology,* 70**,** 151-153.

MOSSER, D. M. 2003. The many faces of macrophage activation. *J Leukoc Biol,* 73**,** 209-12

MOURMOURA, E., LEGUEN, M., DUBOUCHAUD, H., COUTURIER, K., VITIELLO, D., LAFOND, J. L., RICHARDSON, M., LEVERVE, X. & DEMAISON, L. 2011. Middle age aggravates myocardial ischemia through surprising upholding of complex II activity, oxidative stress, and reduced coronary perfusion. *Age (Dordr),* 33**,** 321-36.

MUGLIA, L. J., BAE, D. S., BROWN, T. T., VOGT, S. K., ALVAREZ, J. G., SUNDAY, M. E. & MAJZOUB, J. A. 1999. Proliferation and differentiation defects during lung development in corticotropin-releasing hormone-deficient mice. *Am J Respir Cell Mol Biol,* 20**,** 181-8.

MULHOLLAND, J. & JONES, C. J. 1993. Characteristics of uterine aging. *Microsc Res Tech,* 25**,** 148-68.

MULLER, W. E., ECKERT, A., KURZ, C., ECKERT, G. P. & LEUNER, K. 2010. Mitochondrial dysfunction: common final pathway in brain aging and Alzheimer's disease--therapeutic aspects. *Mol Neurobiol,* 41**,** 159-71.

MURPHY, M. P. 2009. How mitochondria produce reactive oxygen species. *Biochem J,* 417**,** 1-13.

MURRAY, S. A., MORGAN, J. L., KANE, C., SHARMA, Y., HEFFNER, C. S., LAKE, J. & DONAHUE, L. R. 2010. Mouse gestation length is genetically determined. *PLoS One,* 5**,** e12418.

NAGAOKA, S. I., HODGES, C. A., ALBERTINI, D. F. & HUNT, P. A. 2011. Oocyte-specific differences in cell-cycle control create an innate susceptibility to meiotic errors. *Curr Biol,* 21**,** 651-7.

NATHANIELSZ, P. W. 1998. Comparative studies on the initiation of labor. *Eur J Obstet Gynecol Reprod Biol,* 78**,** 127-32.

NATIONAL INSTITUTE ON AGING, N. 2011. Biology of Aging. Available: http://www.nia.nih.gov/sites/default/files/biology_of_aging.pdf.

NEGRE-SALVAYRE, A., AUGE, N., AYALA, V., BASAGA, H., BOADA, J., BRENKE, R., CHAPPLE, S., COHEN, G., FEHER, J., GRUNE, T., LENGYEL, G., MANN, G. E., PAMPLONA, R., POLI, G., PORTERO-OTIN, M., RIAHI, Y., SALVAYRE, R., SASSON, S., SERRANO, J., SHAMNI, O., SIEMS, W., SIOW, R. C., WISWEDEL, I., ZARKOVIC, K. & ZARKOVIC, N. 2010. Pathological aspects of lipid peroxidation. *Free Radic Res,* 44**,** 1125-71.

NELSON, J. F., FELICIO, L. S., RANDALL, P. K., SIMS, C. & FINCH, C. E. 1982. A longitudinal study of estrous cyclicity in aging C57BL/6J mice: I. Cycle frequency, length and vaginal cytology. *Biol Reprod,* 27**,** 327-39.

NIGGESCHULZE, A. & KAST, A. 1994. Maternal age, reproduction and chromosomal aberrations in Wistar derived rats. *Lab Anim,* 28**,** 55-62.

NISSENSON, R., FLUORET, G. & HECHTER, O. 1978. Opposing effects of estradiol and progesterone on oxytocin receptors in rabbit uterus. *Proc Natl Acad Sci U S A,* 75**,** 2044-8.

NOBLE, K., MATTHEW, A., BURDYGA, T. & WRAY, S. 2009. A review of recent insights into the role of the sarcoplasmic reticulum and Ca entry in uterine smooth muscle. *Eur J Obstet Gynecol Reprod Biol,* 144 Suppl 1**,** S11-9.

NOE, M., KUNZ, G., HERBERTZ, M., MALL, G. & LEYENDECKER, G. 1999. The cyclic pattern of the immunocytochemical expression of oestrogen and progesterone receptors in human myometrial and endometrial layers: characterization of the endometrial-subendometrial unit. *Hum Reprod*, 14**,** 190-7.

NOLAN, T., HANDS, R. E. & BUSTIN, S. A. 2006. Quantification of mRNA using real-time RT-PCR. *Nat Protoc,* 1**,** 1559-82.
NORMAN, J. E. 2007. Preterm labour. Cervical function and prematurity. *Best Pract Res Clin Obstet Gynaecol,* 21**,** 791-806.
NORWITZ, E. R., ROBINSON, J. N. & CHALLIS, J. R. 1999. The control of labor. *N Engl J Med,* 341**,** 660-6.
NYBO ANDERSEN, A. M., WOHLFAHRT, J., CHRISTENS, P., OLSEN, J. & MELBYE, M. 2000. Maternal age and fetal loss: population based register linkage study. *BMJ,* 320**,** 1708-12.
OFFICE FOR NATIONAL STATISTICS FOR ENGLAND AND WALES, O. 2011a. *2010-based Period and Cohort Life Expectancy tables* [Online]. England and Wales: Office for National Statistics for England and Wales. Available: http://www.ons.gov.uk/ons/rel/lifetables/period-and-cohort-life-expectancy-tables/2010-based/p-and-c-le.html.
OFFICE FOR NATIONAL STATISTICS FOR ENGLAND AND WALES, O. 2011b. *Babies born in England and Wales had a father with an average age of 32.6 in 2011* [Online]. England and Wales: Office for National Statistics for England and Wales. Available: http://www.ons.gov.uk/ons/rel/vsob1/further-parental-characteristics--england-and-wales/2011/sty-fathers.html 2013].
OFFICE FOR NATIONAL STATISTICS FOR ENGLAND AND WALES, O. 2011c. *Live Births in England and Wales by Characteristics of Mother 1, 2011* [Online]. England and Wales: Office for National Statistics for England and Wales. Available: http://www.ons.gov.uk/ons/rel/vsob1/characteristics-of-Mother-1--england-and-wales/2011/sb-characteristics-of-mother-1.html#tab-Timing-of-childbearing 2013].
OJAIMI, J., MASTERS, C. L., OPESKIN, K., MCKELVIE, P. & BYRNE, E. 1999. Mitochondrial respiratory chain activity in the human brain as a function of age. *Mech Ageing Dev,* 111**,** 39-47.
OSORIO, F. G., BARCENA, C., SORIA-VALLES, C., RAMSAY, A. J., DE CARLOS, F., COBO, J., FUEYO, A., FREIJE, J. M. & LOPEZ-OTIN, C. 2012. Nuclear lamina defects cause ATM-dependent NF-kappaB activation and link accelerated aging to a systemic inflammatory response. *Genes Dev,* 26**,** 2311-24.
OU, C. W., CHEN, Z. Q., QI, S. & LYE, S. J. 1998. Increased expression of the rat myometrial oxytocin receptor messenger ribonucleic acid during labor requires both mechanical and hormonal signals. *Biol Reprod,* 59**,** 1055-61.
OU, C. W., ORSINO, A. & LYE, S. J. 1997. Expression of connexin-43 and connexin-26 in the rat myometrium during pregnancy and labor is differentially regulated by mechanical and hormonal signals. *Endocrinology,* 138**,** 5398-407.
OXLUND, B. S., ORTOFT, G., BRUEL, A., DANIELSEN, C. C., BOR, P., OXLUND, H. & ULDBJERG, N. 2010. Collagen concentration and biomechanical properties of samples from the lower uterine cervix in relation to age and parity in non-pregnant women. *Reprod Biol Endocrinol,* 8**,** 82.
PADRAO, A. I., FERREIRA, R., VITORINO, R., ALVES, R. M., FIGUEIREDO, P., DUARTE, J. A. & AMADO, F. 2012. Effect of lifestyle on age-related mitochondrial protein oxidation in mice cardiac muscle. *Eur J Appl Physiol,* 112**,** 1467-74.
PALM, W. & DE LANGE, T. 2008. How shelterin protects mammalian telomeres. *Annu Rev Genet,* 42**,** 301-34.
PANDEY, U. B. & NICHOLS, C. D. 2011. Human disease models in Drosophila melanogaster and the role of the fly in therapeutic drug discovery. *Pharmacol Rev,* 63**,** 411-36.
PARK, S. J., GOLDSMITH, L. T. & WEISS, G. 2002. Age-related changes in the regulation of luteinizing hormone secretion by estrogen in women. *Exp Biol Med (Maywood),* 227**,** 455-64.

PARKINGTON, H. C., TONTA, M. A., BRENNECKE, S. P. & COLEMAN, H. A. 1999. Contractile activity, membrane potential, and cytoplasmic calcium in human uterine smooth muscle in the third trimester of pregnancy and during labor. *Am J Obstet Gynecol,* 181**,** 1445-51.

PETERSON, C. M., JOHANNSEN, D. L. & RAVUSSIN, E. 2012. Skeletal muscle mitochondria and aging: a review. *J Aging Res,* 2012**,** 194821.

PHILLIPS, A. C., CARROLL, D., GALE, C. R., LORD, J. M., ARLT, W. & BATTY, G. D. 2010. Cortisol, DHEA sulphate, their ratio, and all-cause and cause-specific mortality in the Vietnam Experience Study. *Eur J Endocrinol,* 163**,** 285-92.

PICARD, M., WHITE, K. & TURNBULL, D. M. 2013. Mitochondrial morphology, topology, and membrane interactions in skeletal muscle: a quantitative three-dimensional electron microscopy study. *J Appl Physiol,* 114**,** 161-71.

PIEBER, D., ALLPORT, V. C., HILLS, F., JOHNSON, M. & BENNETT, P. R. 2001. Interactions between progesterone receptor isoforms in myometrial cells in human labour. *Mol Hum Reprod,* 7**,** 875-9.

POWERS, R. W., 3RD, KAEBERLEIN, M., CALDWELL, S. D., KENNEDY, B. K. & FIELDS, S. 2006. Extension of chronological life span in yeast by decreased TOR pathway signaling. *Genes Dev,* 20**,** 174-84.

QIAO, J., WANG, Z. B., FENG, H. L., MIAO, Y. L., WANG, Q., YU, Y., WEI, Y. C., YAN, J., WANG, W. H., SHEN, W., SUN, S. C., SCHATTEN, H. & SUN, Q. Y. 2013. The root of reduced fertility in aged women and possible therapentic options: Current status and future perspects. *Mol Aspects Med*.

QUAN, T., SHAO, Y., HE, T., VOORHEES, J. J. & FISHER, G. J. 2010. Reduced expression of connective tissue growth factor (CTGF/CCN2) mediates collagen loss in chronologically aged human skin. *J Invest Dermatol,* 130**,** 415-24.

RADNOTI. 2010. *Tissue Organ Bath Principles* [Online]. Available: http://www.radnoti.com/userfiles/File/Database/Tissue%20Organ%20Bath%20Principles.pdf 2013].

RANDO, T. A. & CHANG, H. Y. 2012. Aging, rejuvenation, and epigenetic reprogramming: resetting the aging clock. *Cell,* 148**,** 46-57.

RATAJCZAK, C. K. & MUGLIA, L. J. 2008. Insights into parturition biology from genetically altered mice. *Pediatr Res,* 64**,** 581-9.

RATAJCZAK, C. K., FAY, J. C. & MUGLIA, L. J. 2010. Preventing preterm birth: the past limitations and new potential of animal models. *Dis Model Mech,* 3**,** 407-14.

READ, C. P., WORD, R. A., RUSCHEINSKY, M. A., TIMMONS, B. C. & MAHENDROO, M. S. 2007. Cervical remodeling during pregnancy and parturition: molecular characterization of the softening phase in mice. *Reproduction,* 134**,** 327-40.

RECHBERGER, T. & WOESSNER, J. F., JR. 1993. Collagenase, its inhibitors, and decorin in the lower uterine segment in pregnant women. *Am J Obstet Gynecol,* 168**,** 1598-603.

REDDY, U. M., KO, C. W. & WILLINGER, M. 2006. Maternal age and the risk of stillbirth throughout pregnancy in the United States. *Am J Obstet Gynecol,* 195**,** 764-70.

REESE, J., BROWN, N., PARIA, B. C., MORROW, J. & DEY, S. K. 1999. COX-2 compensation in the uterus of COX-1 deficient mice during the pre-implantation period. *Mol Cell Endocrinol,* 150**,** 23-31.

RENNER, K., AMBERGER, A., KONWALINKA, G., KOFLER, R. & GNAIGER, E. 2003. Changes of mitochondrial respiration, mitochondrial content and cell size after induction of apoptosis in leukemia cells. *Biochim Biophys Acta,* 1642**,** 115-23.

RENTHAL, N. E., WILLIAMS, K. C. & MENDELSON, C. R. 2013. MicroRNAs--mediators of myometrial contractility during pregnancy and labour. *Nat Rev Endocrinol,* 9**,** 391-401.
RIBARIC, S. 2012. Diet and aging. *Oxid Med Cell Longev,* 2012**,** 741468.
RICHARDS, S. E., WANG, Y., CLAUS, S. P., LAWLER, D., KOCHHAR, S., HOLMES, E. & NICHOLSON, J. K. 2013. Metabolic phenotype modulation by caloric restriction in a lifelong dog study. *J Proteome Res,* 12**,** 3117-27.
RIGOULET, M., YOBOUE, E. D. & DEVIN, A. 2011. Mitochondrial ROS generation and its regulation: mechanisms involved in H(2)O(2) signaling. *Antioxid Redox Signal,* 14**,** 459-68.
RINGER, S. 1883. A third contribution regarding the Influence of the Inorganic Constituents of the Blood on the Ventricular Contraction. *J Physiol,* 4**,** 222-5.
RODRIGUEZ-ENRIQUEZ, S., KAI, Y., MALDONADO, E., CURRIN, R. T. & LEMASTERS, J. J. 2009. Roles of mitophagy and the mitochondrial permeability transition in remodeling of cultured rat hepatocytes. *Autophagy,* 5**,** 1099-106.
ROMERO, A., VILLAMAYOR, F., GRAU, M. T., SACRISTAN, A. & ORTIZ, J. A. 1992a. Relationship between fetal weight and litter size in rats: application to reproductive toxicology studies. *Reprod Toxicol,* 6**,** 453-6.
ROMERO, R., ESPINOZA, J., GONCALVES, L. F., KUSANOVIC, J. P., FRIEL, L. A. & NIEN, J. K. 2006. Inflammation in preterm and term labour and delivery. *Semin Fetal Neonatal Med,* 11**,** 317-26.
ROMERO, R., MAZOR, M., BRANDT, F., SEPULVEDA, W., AVILA, C., COTTON, D. B. & DINARELLO, C. A. 1992b. Interleukin-1 alpha and interleukin-1 beta in preterm and term human parturition. *Am J Reprod Immunol,* 27**,** 117-23.
ROMERO, R., MAZOR, M., SEPULVEDA, W., AVILA, C., COPELAND, D. & WILLIAMS, J. 1992c. Tumor necrosis factor in preterm and term labor. *Am J Obstet Gynecol,* 166**,** 1576-87.
ROOS, N., SAHLIN, L., EKMAN-ORDEBERG, G., KIELER, H. & STEPHANSSON, O. 2010. Maternal risk factors for postterm pregnancy and cesarean delivery following labor induction. *Acta Obstet Gynecol Scand,* 89**,** 1003-10.
ROTHFUSS, O., GASSER, T. & PATENGE, N. 2010. Analysis of differential DNA damage in the mitochondrial genome employing a semi-long run real-time PCR approach. *Nucleic Acids Res,* 38**,** e24.
ROUSLIN, W. 1983. Mitochondrial complexes I, II, III, IV, and V in myocardial ischemia and autolysis. *Am J Physiol,* 244**,** H743-8.
ROUSLIN, W. & MILLARD, R. W. 1981. Mitochondrial inner membrane enzyme defects in porcine myocardial ischemia. *Am J Physiol,* 240**,** H308-13.
ROUSLIN, W. & RANGANATHAN, S. 1983. Impaired function of mitochondrial electron transfer complex I in canine myocardial ischemia: loss of flavin mononucleotide. *J Mol Cell Cardiol,* 15**,** 537-42.
RUIZ-TORRES, A. & BEIER, W. 2005. On maximum human life span: interdisciplinary approach about its limits. *Adv Gerontol,* 16**,** 14-20.
RUSSELL, S. J. & KAHN, C. R. 2007. Endocrine regulation of ageing. *Nat Rev Mol Cell Biol,* 8**,** 681-91.
RYDHMER, L., LUNDEHEIM, N. & CANARIO, L. 2008. Genetic correlations between gestation length, piglet survival and early growth. *Livestock Science,* 115**,** 287-293.
SADOWSKY, D. W., NOVY, M. J., WITKIN, S. S. & GRAVETT, M. G. 2003. Dexamethasone or interleukin-10 blocks interleukin-1beta-induced uterine contractions in pregnant rhesus monkeys. *Am J Obstet Gynecol,* 188**,** 252-63.
SAIKI, R. K., GELFAND, D. H., STOFFEL, S., SCHARF, S. J., HIGUCHI, R., HORN, G. T., MULLIS, K. B. & ERLICH, H. A. 1988. Primer-directed enzymatic

amplification of DNA with a thermostable DNA polymerase. *Science,* 239**,** 487-91.

SALMINEN, A., KAARNIRANTA, K. & KAUPPINEN, A. 2012. Inflammaging: disturbed interplay between autophagy and inflammasomes. *Aging (Albany NY),* 4**,** 166-75.

SANBORN, B. M. 2000. Relationship of ion channel activity to control of myometrial calcium. *J Soc Gynecol Investig,* 7**,** 4-11.

SANBORN, B. M., KU, C. Y., SHLYKOV, S. & BABICH, L. 2005. Molecular signaling through G-protein-coupled receptors and the control of intracellular calcium in myometrium. *J Soc Gynecol Investig,* 12**,** 479-87.

SANCHIS-GOMAR, F., OLASO-GONZALEZ, G., CORELLA, D., GOMEZ-CABRERA, M. C. & VINA, J. 2011. Increased average longevity among the "Tour de France" cyclists. *Int J Sports Med,* 32**,** 644-7.

SASTRE, J., PALLARDO, F. V. & VINA, J. 2000. Mitochondrial oxidative stress plays a key role in aging and apoptosis. *IUBMB Life,* 49**,** 427-35.

SCHOTTELIUS, A. J., MAYO, M. W., SARTOR, R. B. & BALDWIN, A. S., JR. 1999. Interleukin-10 signaling blocks inhibitor of kappaB kinase activity and nuclear factor kappaB DNA binding. *J Biol Chem,* 274**,** 31868-74.

SCHUNKE, M., SCHULTE, E. & SCHUMACHE, U. 2010. *Atlas of Anatomy: Neck and Internal Organs.,* Stuttgart, Germany, Thieme.

SHAWI, M. & AUTEXIER, C. 2008. Telomerase, senescence and ageing. *Mech Ageing Dev,* 129**,** 3-10.

SHEEHAN & HRAPCHAK 1980. *Theory and Practice of Histotechnology,* St. Louis, (MO), USA.

SHEINER, E., LEVY, A., FEINSTEIN, U., HALLAK, M. & MAZOR, M. 2002. Risk factors and outcome of failure to progress during the first stage of labor: a population-based study. *Acta Obstet Gynecol Scand,* 81**,** 222-6.

SHEPHERD, D. & GARLAND, P. B. 1969. The kinetic properties of citrate synthase from rat liver mitochondria. *Biochem J,* 114**,** 597-610.

SHIRASUNA, K., SHIMIZU, T., HAYASHI, K. G., NAGAI, K., MATSUI, M. & MIYAMOTO, A. 2007. Positive association, in local release, of luteal oxytocin with endothelin 1 and prostaglandin F2alpha during spontaneous luteolysis in the cow: a possible intermediatory role for luteolytic cascade within the corpus luteum. *Biol Reprod,* 76**,** 965-70.

SHORT, K. R., BIGELOW, M. L., KAHL, J., SINGH, R., COENEN-SCHIMKE, J., RAGHAVAKAIMAL, S. & NAIR, K. S. 2005. Decline in skeletal muscle mitochondrial function with aging in humans. *Proc Natl Acad Sci U S A,* 102**,** 5618-23.

SHMYGOL, A., NOBLE, K. & WRAY, S. 2007. Depletion of membrane cholesterol eliminates the Ca2+-activated component of outward potassium current and decreases membrane capacitance in rat uterine myocytes. *J Physiol,* 581**,** 445-56.

SHYNLOVA, O., OLDENHOF, A., DOROGIN, A., XU, Q., MU, J., NASHMAN, N. & LYE, S. J. 2006. Myometrial apoptosis: activation of the caspase cascade in the pregnant rat myometrium at midgestation. *Biol Reprod,* 74**,** 839-49.

SHYNLOVA, O., TSUI, P., JAFFER, S. & LYE, S. J. 2009. Integration of endocrine and mechanical signals in the regulation of myometrial functions during pregnancy and labour. *Eur J Obstet Gynecol Reprod Biol,* 144 Suppl 1**,** S2-10.

SILK, J., SHORT, J., ROBERTS, J. & KUSNITZ, J. 1993. Gestation length in rhesus macaques (Macaca mulatta). *International Journal of Primatology,* 14**,** 95-104.

SLATER, D. M., ASTLE, S., WOODCOCK, N., CHIVERS, J. E., DE WIT, N. C., THORNTON, S., VATISH, M. & NEWTON, R. 2006. Anti-inflammatory and relaxatory effects of prostaglandin E2 in myometrial smooth muscle. *Mol Hum Reprod,* 12**,** 89-97.

SLATER, D. M., DENNES, W. J., CAMPA, J. S., POSTON, L. & BENNETT, P. R. 1999. Expression of cyclo-oxygenase types-1 and -2 in human myometrium throughout pregnancy. *Mol Hum Reprod,* 5**,** 880-4.

SMITH, A. C., BLACKSHAW, J. A. & ROBINSON, A. J. 2012a. MitoMiner: a data warehouse for mitochondrial proteomics data. *Nucleic Acids Res,* 40**,** D1160-7.

SMITH, G. C., CORDEAUX, Y., WHITE, I. R., PASUPATHY, D., MISSFELDER-LOBOS, H., PELL, J. P., CHARNOCK-JONES, D. S. & FLEMING, M. 2008. The effect of delaying childbirth on primary cesarean section rates. *PLoS Med,* 5**,** e144.

SMITH, R. 2007. Parturition. *N Engl J Med,* 356**,** 271-83.

SMITH, R. & NICHOLSON, R. C. 2007. Corticotrophin releasing hormone and the timing of birth. *Front Biosci,* 12**,** 912-8.

SMITH, R., PAUL, J., MAITI, K., TOLOSA, J. & MADSEN, G. 2012b. Recent advances in understanding the endocrinology of human birth. *Trends Endocrinol Metab,* 23**,** 516-23.

SMITH, R., VAN HELDEN, D., HIRST, J., ZAKAR, T., READ, M., CHAN, E. C., PALLISER, H., GRAMMATOPOULOS, D., NICHOLSON, R. & PARKINGTON, H. C. 2007. Pathological interactions with the timing of birth and uterine activation. *Aust N Z J Obstet Gynaecol,* 47**,** 430-7.

SODERWALL, A. L., KENT, H. A., JR., TURBYFILL, C. L. & BRITENBAKER, A. L. 1960. Variation in gestation length and litter size of the golden hamster, Mesocricetus auratus. *J Gerontol,* 15**,** 246-8.

SONG, E., OUYANG, N., HORBELT, M., ANTUS, B., WANG, M. & EXTON, M. S. 2000. Influence of alternatively and classically activated macrophages on fibrogenic activities of human fibroblasts. *Cell Immunol,* 204**,** 19-28.

STEIN, M., KESHAV, S., HARRIS, N. & GORDON, S. 1992. Interleukin 4 potently enhances murine macrophage mannose receptor activity: a marker of alternative immunologic macrophage activation. *J Exp Med,* 176**,** 287-92.

STORER, J. B. 1966. Longevity and gross pathology at death in 22 inbred mouse strains. *J Gerontol,* 21**,** 404-9.

STRAACH, K. J., SHELTON, J. M., RICHARDSON, J. A., HASCALL, V. C. & MAHENDROO, M. S. 2005. Regulation of hyaluronan expression during cervical ripening. *Glycobiology,* 15**,** 55-65.

STRAUB, R. H., MILLER, L. E., SCHOLMERICH, J. & ZIETZ, B. 2000. Cytokines and hormones as possible links between endocrinosenescence and immunosenescence. *J Neuroimmunol,* 109**,** 10-5.

STYGAR, D., WANG, H., VLADIC, Y. S., EKMAN, G., ERIKSSON, H. & SAHLIN, L. 2002. Increased level of matrix metalloproteinases 2 and 9 in the ripening process of the human cervix. *Biol Reprod,* 67**,** 889-94.

SUGIMOTO, Y., YAMASAKI, A., SEGI, E., TSUBOI, K., AZE, Y., NISHIMURA, T., OIDA, H., YOSHIDA, N., TANAKA, T., KATSUYAMA, M., HASUMOTO, K., MURATA, T., HIRATA, M., USHIKUBI, F., NEGISHI, M., ICHIKAWA, A. & NARUMIYA, S. 1997. Failure of parturition in mice lacking the prostaglandin F receptor. *Science,* 277**,** 681-3.

SUGIYAMA, S., TAKASAWA, M., HAYAKAWA, M. & OZAWA, T. 1993. Changes in skeletal muscle, heart and liver mitochondrial electron transport activities in rats and dogs of various ages. *Biochem Mol Biol Int,* 30**,** 937-44.

SUN, F., HUO, X., ZHAI, Y., WANG, A., XU, J., SU, D., BARTLAM, M. & RAO, Z. 2005. Crystal structure of mitochondrial respiratory membrane protein complex II. *Cell,* 121**,** 1043-57.

SWAMY, P. A. V. B. & ARORA, S. S. 1972. The exact finite sample properties of the estimators of coefficients in the error components regression models. *Econometrica,* 40**,** 261–275.

SWEENEY, E. M., CRANKSHAW, D. J., O'BRIEN, Y., DOCKERY, P. & MORRISON, J. J. 2013. Stereology of human myometrium in pregnancy: influence of maternal body mass index and age. *Am J Obstet Gynecol,* 208**,** 324 e1-6.

TAGGART, M. J. & WRAY, S. 1998. Contribution of sarcoplasmic reticular calcium to smooth muscle contractile activation: gestational dependence in isolated rat uterus. *J Physiol,* 511 ( Pt 1)**,** 133-44.

TAKASAWA, M., HAYAKAWA, M., SUGIYAMA, S., HATTORI, K., ITO, T. & OZAWA, T. 1993. Age-associated damage in mitochondrial function in rat hearts. *Exp Gerontol,* 28**,** 269-80.

TALBERT, G. B. 1971. Effect of maternal age on postimplantation reproductive failure in mice. *J Reprod Fertil,* 24**,** 449-52.

TAN, H., YI, L., ROTE, N. S., HURD, W. W. & MESIANO, S. 2012. Progesterone receptor-A and -B have opposite effects on proinflammatory gene expression in human myometrial cells: implications for progesterone actions in human pregnancy and parturition. *J Clin Endocrinol Metab,* 97**,** E719-30.

TAN, S. C. & YIAP, B. C. 2009. DNA, RNA, and protein extraction: the past and the present. *J Biomed Biotechnol,* 2009**,** 574398.

TAN, Y. F., LI, F. X., PIAO, Y. S., SUN, X. Y. & WANG, Y. L. 2003. Global gene profiling analysis of mouse uterus during the oestrous cycle. *Reproduction,* 126**,** 171-82.

TAYLOR, S. W., FAHY, E., ZHANG, B., GLENN, G. M., WARNOCK, D. E., WILEY, S., MURPHY, A. N., GAUCHER, S. P., CAPALDI, R. A., GIBSON, B. W. & GHOSH, S. S. 2003. Characterization of the human heart mitochondrial proteome. *Nat Biotechnol,* 21**,** 281-6.

TEARE, J. M., ISLAM, R., FLANAGAN, R., GALLAGHER, S., DAVIES, M. G. & GRABAU, C. 1997. Measurement of nucleic acid concentrations using the DyNA Quant and the GeneQuant. *Biotechniques,* 22**,** 1170-4.

TERRILL, C. E. & HAZEL, L. N. 1947. Length of gestation in range sheep. *Am J Vet Res,* 8**,** 66-72.

TERRONE, D. A., RINEHART, B. K., GRANGER, J. P., BARRILLEAUX, P. S., MARTIN, J. N., JR. & BENNETT, W. A. 2001. Interleukin-10 administration and bacterial endotoxin-induced preterm birth in a rat model. *Obstet Gynecol,* 98**,** 476-80.

TERZIDOU, V., SOORANNA, S. R., KIM, L. U., THORNTON, S., BENNETT, P. R. & JOHNSON, M. R. 2005. Mechanical stretch up-regulates the human oxytocin receptor in primary human uterine myocytes. *J Clin Endocrinol Metab,* 90**,** 237-46.

THOMPSON, L. 2013. *The Cervix* [Online]. TeachMeAnatomy. Available: http://teachmeanatomy.info/pelvis/female-reproductive-tract/cervix/.

TILSTRA, J. S., ROBINSON, A. R., WANG, J., GREGG, S. Q., CLAUSON, C. L., REAY, D. P., NASTO, L. A., ST CROIX, C. M., USAS, A., VO, N., HUARD, J., CLEMENS, P. R., STOLZ, D. B., GUTTRIDGE, D. C., WATKINS, S. C., GARINIS, G. A., WANG, Y., NIEDERNHOFER, L. J. & ROBBINS, P. D. 2012. NF-kappaB inhibition delays DNA damage-induced senescence and aging in mice. *J Clin Invest,* 122**,** 2601-12.

TIMMONS, B., AKINS, M. & MAHENDROO, M. 2010. Cervical remodeling during pregnancy and parturition. *Trends Endocrinol Metab,* 21**,** 353-61.

TIMMONS, B. C., FAIRHURST, A. M. & MAHENDROO, M. S. 2009. Temporal changes in myeloid cells in the cervix during pregnancy and parturition. *J Immunol,* 182**,** 2700-7.

TIMMONS, B. C. & MAHENDROO, M. S. 2006. Timing of neutrophil activation and expression of proinflammatory markers do not support a role for neutrophils in cervical ripening in the mouse. *Biol Reprod,* 74**,** 236-45.

TIMMONS, B. C., MITCHELL, S. M., GILPIN, C. & MAHENDROO, M. S. 2007. Dynamic changes in the cervical epithelial tight junction complex and differentiation occur during cervical ripening and parturition. *Endocrinology,* 148**,** 1278-87.

TISSENBAUM, H. A. & RUVKUN, G. 1998. An insulin-like signaling pathway affects both longevity and reproduction in Caenorhabditis elegans. *Genetics,* 148**,** 703-17.

TOGASHI, K. 2007. Uterine contractility evaluated on cine magnetic resonance imaging. *Ann N Y Acad Sci,* 1101**,** 62-71.

TOMAS-LOBA, A., FLORES, I., FERNANDEZ-MARCOS, P. J., CAYUELA, M. L., MARAVER, A., TEJERA, A., BORRAS, C., MATHEU, A., KLATT, P., FLORES, J. M., VINA, J., SERRANO, M. & BLASCO, M. A. 2008. Telomerase reverse transcriptase delays aging in cancer-resistant mice. *Cell,* 135**,** 609-22.

TORII, K., SUGIYAMA, S., TAKAGI, K., SATAKE, T. & OZAWA, T. 1992. Age-related decrease in respiratory muscle mitochondrial function in rats. *Am J Respir Cell Mol Biol,* 6**,** 88-92.

TORNBLOM, S. A., MAUL, H., KLIMAVICIUTE, A., GARFIELD, R. E., BYSTROM, B., MALMSTROM, A. & EKMAN-ORDEBERG, G. 2005. mRNA expression and localization of bNOS, eNOS and iNOS in human cervix at preterm and term labour. *Reprod Biol Endocrinol,* 3**,** 33.

TOUGH, S., BENZIES, K., NEWBURN-COOK, C., TOFFLEMIRE, K., FRASER-LEE, N., FABER, A. & SAUVE, R. 2006. What do women know about the risks of delayed childbearing? *Can J Public Health,* 97**,** 330-4.

TREUTING, P. & DINTZIS, S. 2012. *Comparative Anatomy and Histology: A Mouse and Human Atlas,* Oxford, UK, Academic Press.

TRIBE, R. M. 2001. Regulation of human myometrial contractility during pregnancy and labour: are calcium homeostatic pathways important? *Exp Physiol,* 86**,** 247-54.

TRIBE, R. M., MORIARTY, P. & POSTON, L. 2000. Calcium homeostatic pathways change with gestation in human myometrium. *Biol Reprod,* 63**,** 748-55.

TSUBOI, K., IWANE, A., NAKAZAWA, S., SUGIMOTO, Y. & ICHIKAWA, A. 2003. Role of prostaglandin H2 synthase 2 in murine parturition: study on ovariectomy-induced parturition in prostaglandin F receptor-deficient mice. *Biol Reprod,* 69**,** 195-201.

TSUBOI, K., SUGIMOTO, Y., IWANE, A., YAMAMOTO, K., YAMAMOTO, S. & ICHIKAWA, A. 2000. Uterine expression of prostaglandin H2 synthase in late pregnancy and during parturition in prostaglandin F receptor-deficient mice. *Endocrinology,* 141**,** 315-24.

TURTON, P., ARROWSMITH, S., PRESCOTT, J., BALLARD, C., BRICKER, L., NEILSON, J. & WRAY, S. 2013. A comparison of the contractile properties of myometrium from singleton and twin pregnancies. *PLoS One,* 8**,** e63800.

ULDBJERG, N., EKMAN, G., MALMSTROM, A., OLSSON, K. & ULMSTEN, U. 1983. Ripening of the human uterine cervix related to changes in collagen, glycosaminoglycans, and collagenolytic activity. *Am J Obstet Gynecol,* 147**,** 662-6.

ULLRICH, A., SHINE, J., CHIRGWIN, J., PICTET, R., TISCHER, E., RUTTER, W. J. & GOODMAN, H. M. 1977. Rat insulin genes: construction of plasmids containing the coding sequences. *Science,* 196**,** 1313-9.

UNGVARI, Z., LABINSKYY, N., GUPTE, S., CHANDER, P. N., EDWARDS, J. G. & CSISZAR, A. 2008. Dysregulation of mitochondrial biogenesis in vascular endothelial and smooth muscle cells of aged rats. *Am J Physiol Heart Circ Physiol,* 294**,** H2121-8.

VAN ENGELEN, E., BREEVELD-DWARKASING, V. N., TAVERNE, M. A., EVERTS, M. E., VAN DER WEIJDEN, G. C. & RUTTEN, V. P. 2008. MMP-2 expression

precedes the final ripening process of the bovine cervix. *Mol Reprod Dev,* 75**,** 1669-77.
VAN REMMEN, H. & RICHARDSON, A. 2001. Oxidative damage to mitochondria and aging. *Exp Gerontol,* 36**,** 957-68.

VANDESOMPELE, J., DE PRETER, K., PATTYN, F., POPPE, B., VAN ROY, N., DE PAEPE, A. & SPELEMAN, F. 2002. Accurate normalization of real-time quantitative RT-PCR data by geometric averaging of multiple internal control genes. *Genome Biol,* 3**,** RESEARCH0034.
VARANI, J., DAME, M. K., RITTIE, L., FLIGIEL, S. E., KANG, S., FISHER, G. J. & VOORHEES, J. J. 2006. Decreased collagen production in chronologically aged skin: roles of age-dependent alteration in fibroblast function and defective mechanical stimulation. *Am J Pathol,* 168**,** 1861-8.
VARGIS, E., BROWN, N., WILLIAMS, K., AL-HENDY, A., PARIA, B. C., REESE, J. & MAHADEVAN-JANSEN, A. 2012. Detecting biochemical changes in the rodent cervix during pregnancy using Raman spectroscopy. *Ann Biomed Eng,* 40**,** 1814-24.
VIDAEFF, A. C. & RAMIN, S. M. 2008. Potential biochemical events associated with initiation of labor. *Curr Med Chem,* 15**,** 614-9.
VINA, J., BORRAS, C. & MIQUEL, J. 2007. Theories of ageing. *IUBMB Life,* 59**,** 249-54.
VOGELSTEIN, B. & GILLESPIE, D. 1979. Preparative and analytical purification of DNA from agarose. *Proc Natl Acad Sci U S A,* 76**,** 615-9.
WALLER, K., SWAN, S. H., WINDHAM, G. C., FENSTER, L., ELKIN, E. P. & LASLEY, B. L. 1998. Use of urine biomarkers to evaluate menstrual function in healthy premenopausal women. *Am J Epidemiol,* 147**,** 1071-80.
WANG, X., SHEN, X., LI, X. & AGRAWAL, C. M. 2002. Age-related changes in the collagen network and toughness of bone. *Bone,* 31**,** 1-7.
WATHES, D. C., BORWICK, S. C., TIMMONS, P. M., LEUNG, S. T. & THORNTON, S. 1999. Oxytocin receptor expression in human term and preterm gestational tissues prior to and following the onset of labour. *J Endocrinol,* 161**,** 143-51.
WEEG, N., SHALOM-PAZ, E. & WISER, A. 2012. Age and infertility: the clinical point of view. *Minerva Ginecol,* 64**,** 477-83.
WEI, Y. H., WU, S. B., MA, Y. S. & LEE, H. C. 2009. Respiratory function decline and DNA mutation in mitochondria, oxidative stress and altered gene expression during aging. *Chang Gung Med J,* 32**,** 113-32.
WEINDRUCH, R. 1996. The retardation of aging by caloric restriction: studies in rodents and primates. *Toxicol Pathol,* 24**,** 742-5.
WEISS, G. 2000. Endocrinology of parturition. *J Clin Endocrinol Metab,* 85**,** 4421-5.
WILCOX, A. J., DUNSON, D. & BAIRD, D. D. 2000. The timing of the "fertile window" in the menstrual cycle: day specific estimates from a prospective study. *BMJ,* 321**,** 1259-62.
WILFINGER, W. W., MACKEY, K. & CHOMCZYNSKI, P. 1997. Effect of pH and ionic strength on the spectrophotometric assessment of nucleic acid purity. *Biotechniques,* 22**,** 474-6, 478-81.
WILKINSON, M. 2000. *Purification of RNA. In: Esssential Molecular Biology: a Practical Approach. 2nd Edition,* Oxford, Oxford University Press.
WILLIAMS & WILKINS 1973. *Staining Procedures (3rd ed.)* Baltimore (MD), USA.
WILLIAMS & WILKINS 1977. *HJ Conn's Biological Stains (9th ed.),* Baltimore (MD), USA.
WILLIAMS, R. S. 1986. Mitochondrial gene expression in mammalian striated muscle. Evidence that variation in gene dosage is the major regulatory event. *J Biol Chem,* 261**,** 12390-4.

WILLIAMS, R. S., SALMONS, S., NEWSHOLME, E. A., KAUFMAN, R. E. & MELLOR, J. 1986. Regulation of nuclear and mitochondrial gene expression by contractile activity in skeletal muscle. *J Biol Chem,* 261**,** 376-80.

WILSON, K. & WALKER, J. 2010. *Principles and Techniques of Biochemistry and Molecular Biology. 7th Edition,* Cambridge, Cambridge University Press.

WINCHESTER, S. K., IMAMURA, T., GROSS, G. A., MUGLIA, L. M., VOGT, S. K., WRIGHT, J., WATANABE, K., TAI, H. H. & MUGLIA, L. J. 2002. Coordinate regulation of prostaglandin metabolism for induction of parturition in mice. *Endocrinology,* 143**,** 2593-8.

WORD, R. A., LI, X. H., HNAT, M. & CARRICK, K. 2007. Dynamics of cervical remodeling during pregnancy and parturition: mechanisms and current concepts. *Semin Reprod Med,* 25**,** 69-79.

WRAY, S. 2007. Insights into the uterus. *Exp Physiol,* 92**,** 621-31.

WRAY, S., KUPITTAYANANT, S., SHMYGOL, A., SMITH, R. D. & BURDYGA, T. 2001. The physiological basis of uterine contractility: a short review. *Exp Physiol,* 86**,** 239-46.

WU, X., MORGAN, K. G., JONES, C. J., TRIBE, R. M. & TAGGART, M. J. 2008. Myometrial mechanoadaptation during pregnancy: implications for smooth muscle plasticity and remodelling. *J Cell Mol Med,* 12**,** 1360-73.

YADAV, A. K., MADAN, T. & BERNAL, A. L. 2011. Surfactant proteins A and D in pregnancy and parturition. *Front Biosci (Elite Ed),* 3**,** 291-300.

YASUDA, K., ISHII, T., SUDA, H., AKATSUKA, A., HARTMAN, P. S., GOTO, S., MIYAZAWA, M. & ISHII, N. 2006. Age-related changes of mitochondrial structure and function in Caenorhabditis elegans. *Mech Ageing Dev,* 127**,** 763-70.

YEN, T. C., CHEN, Y. S., KING, K. L., YEH, S. H. & WEI, Y. H. 1989. Liver mitochondrial respiratory functions decline with age. *Biochem Biophys Res Commun,* 165**,** 944-1003.

YOUNG, R. C. & HESSION, R. O. 1999. Three-dimensional structure of the smooth muscle in the term-pregnant human uterus. *Obstet Gynecol,* 93**,** 94-9.

YU, S. Y. & LEPPERT, P. C. 1991. *The collgenous tissues of the cervix during labor and delivery. In: The Extracellular Matrix of the Uterus, Cervix and Fetal Membranes: Synthesis, Degradation and Hormonal Regulation.,* NY, Perinatology Press.

YUAN, Y., KADIYALA, C. S., CHING, T. T., HAKIMI, P., SAHA, S., XU, H., YUAN, C., MULLANGI, V., WANG, L., FIVENSON, E., HANSON, R. W., EWING, R., HSU, A. L., MIYAGI, M. & FENG, Z. 2012. Enhanced energy metabolism contributes to the extended life span of calorie-restricted Caenorhabditis elegans. *J Biol Chem,* 287**,** 31414-26.

ZAKAR, T. & HERTELENDY, F. 2007. Progesterone withdrawal: key to parturition. *Am J Obstet Gynecol,* 196**,** 289-96.

ZENG, C., DU, Y., ALBERICO, T., SEEBERGER, J., SUN, X. & ZOU, S. 2011. Gender-specific prandial response to dietary restriction and oxidative stress in Drosophila melanogaster. *Fly (Austin),* 5**,** 174-80.

ZHANG, G., LI, J., PURKAYASTHA, S., TANG, Y., ZHANG, H., YIN, Y., LI, B., LIU, G. & CAI, D. 2013. Hypothalamic programming of systemic ageing involving IKK-beta, NF-kappaB and GnRH. *Nature,* 497**,** 211-6.

ZHANG, J., KENDRICK, A., QUENBY, S. & WRAY, S. 2007. Contractility and calcium signaling of human myometrium are profoundly affected by cholesterol manipulation: implications for labor? *Reprod Sci,* 14**,** 456-66.

ZIADEH, S. & YAHAYA, A. 2001. Pregnancy outcome at age 40 and older. *Arch Gynecol Obstet,* 265**,** 30-3.

# Appendix 1: List of Abstracts Arising from this Thesis

**Patel R**, Poston L, Tribe RM. Effect of advanced maternal age on mouse myometrial contractility and cervical distensibility at the end of gestation. *School of Medicine Graduate Showcase 2012, King's College London, UK.* March 2012. Poster presentation

**Patel R**, Poston L, Tribe RM. The impact of advanced maternal age on parturition in a pregnant mouse model*. Annual Academic Meeting in Obstetrics and Gynaecology, Royal College of Obstetricians and Gynaecologists, London, UK.* December 2012. Poster presentation, Prize for best poster.

**Patel R**, Poston L, Tribe RM. The impact of advanced maternal age on parturition success in a pregnant mouse model. *Society for Gynaecological Investigation Annual Meeting 2013, Orlando, Florida ,USA.* March 2013. Oral Presentation

**Patel R**, Poston L, Tribe RM. The impact of advanced maternal age on the initiation and progress of parturition in a pregnant mouse model. *The 37th Congress of the International Union of Physiological Sciences, Birmingham, UK*. July 2013. Poster Presentation

## Appendix 2: Training Courses and Workshops Attended

| Date Attended | Title |
|---|---|
| October 2009 | Introduction to Statistics - 5 Day Course<br>Graduate School, King's College London |
| October 2009 | Introduction to EndNote for Health and Physical Sciences<br>Graduate School, King's College London |
| December 2009 | Information Retrieval for Health<br>Graduate School, King's College London |
| January 2010 | Starting Your PhD in the Sciences<br>Graduate School, King's College London |
| April 2010 | Real Time Quantitative PCR Techniques Workshop<br>The Physiological Society, London |
| October 2010 | Microsoft Word 2007 introduction<br>Graduate School, King's College London |
| April 2011 | Women's Health student representative for the School of Medicine Graduate Showcase organising committee |
| December 2011 | Practical Statistics in Clinical Research<br>Royal College of Obstetricians and Gynaecologists, London. |
| February 2012 | Statistics Using Excel for BioScientists<br>Graduate School, King's College London |
| March 2012 | Writing Up the Thesis in the Sciences<br>Graduate School, King's College London |
| October 2012 | Biotechnology Young Enterprise Scheme 2012<br>GSK and the Stevenage Bioscience Catalyst (SBC), Stevenage. |
| February 2013 | Microsoft Word 2007 long documents for theses<br>Graduate School, King's College London |
| June 2013 | Preparing for the Viva<br>Graduate School, King's College London |